LAPPEENRANTA UNIVERSITY OF TECHNOLOGY
LUT School of Engineering Science
Degree Program of Chemical Engineering

Master's Thesis
2016

Harri Nieminen

LIQUID-PHASE ALCOHOL PROMOTED METHANOL SYNTHESIS FROM CO_2 AND H_2

Examiners: Professor Tuomas Koiranen
Docent Arto Laari

ABSTRACT

Lappeenranta University of Technology
LUT School of Engineering Science
Degree Program of Chemical Engineering

Harri Nieminen

Liquid-phase alcohol promoted methanol synthesis from CO_2 and H_2

Master's Thesis
2016

141 pages, 36 figures, 13 tables and 4 appendices

Examiners: Professor Tuomas Koiranen
Docent Arto Laari

Keywords: Methanol synthesis, alcohol promoted, chemical energy storage, CO_2 capture, hydrogen production

Methanol is an important and versatile compound with various uses as a fuel and a feedstock chemical. Methanol is also a potential chemical energy carrier. Due to the fluctuating nature of renewable energy sources such as wind or solar, storage of energy is required to balance the varying supply and demand. Excess electrical energy generated at peak periods can be stored by using the energy in the production of chemical compounds.

The conventional industrial production of methanol is based on the gas-phase synthesis from synthesis gas generated from fossil sources, primarily natural gas. Methanol can also be produced by hydrogenation of CO_2. The production of methanol from CO_2, captured from emission sources or even directly from the atmosphere, would allow sustainable production based on a nearly limitless carbon source, while helping to reduce the increasing CO_2 concentration in the atmosphere. Hydrogen for synthesis can be produced by electrolysis of water utilizing renewable electricity.

A new liquid-phase methanol synthesis process has been proposed. In this process, a conventional methanol synthesis catalyst is mixed in suspension with a liquid alcohol solvent. The alcohol acts as a catalytic solvent by enabling a new reaction route, potentially allowing the synthesis of methanol at lower temperatures and pressures compared to conventional processes.

For this thesis, the alcohol promoted liquid phase methanol synthesis process was tested at laboratory scale. Batch and semibatch reaction experiments were performed in an autoclave reactor, using a conventional Cu/ZnO catalyst and ethanol and 2-butanol as the alcoholic solvents. Experiments were performed at the pressure range of 30-60 bar and at temperatures of 160-200 °C.

The productivity of methanol was found to increase with increasing pressure and temperature. In the studied process conditions a maximum volumetric productivity of 1.9 g of methanol per liter of solvent per hour was obtained, while the maximum catalyst specific productivity was found to be 40.2 g of methanol per kg of catalyst per hour. The productivity values are low compared to both industrial synthesis and to gas-phase synthesis from CO_2. However, the reaction temperatures and pressures employed were lower compared to gas-phase processes. While the productivity is not high enough for large-scale industrial operation, the milder reaction conditions and simple operation could prove useful for small-scale operations.

A preliminary design for an alcohol promoted, liquid-phase methanol synthesis process was created using the data obtained from the experiments. The demonstration scale process was scaled to an electrolyzer unit producing 1 Nm^3 of hydrogen per hour. This Master's thesis is closely connected to LUT REFLEX-platform.

TIIVISTELMÄ

Lappeenrannan teknillinen yliopisto
LUT School of Engineering Science
Kemiantekniikan koulutusohjelma

Harri Nieminen
Metanolisynteesi hiilidioksidista ja vedystä alkoholipohjaisessa nestefaasissa

Diplomityö
2016

141 sivua, 36 kuvaa, 13 taulukkoa ja 4 liitettä

Tarkastajat: Professori Tuomas Koiranen
Dosentti Arto Laari

Avainsanat: Metanoli, metanolisynteesi, alkoholikatalyytti, kemiallinen energian varastointi, hiilidioksidin talteenotto, vedyn tuotanto

Metanoli on tärkeä yhdiste, jolla on useita käyttökohteita sekä polttoaineena että lähtöaineena kemianteollisuuden tuotteissa. Metanolia on mahdollista hyödyntää myös energian kemialliseen varastointiin. Koska uusiutuvista energialähteistä, kuten auringosta ja tuulesta, tuotetun energian määrä vaihtelee ajallisesti, on energian varastointi välttämätöntä vaihtelevan kysynnän ja tarjonnan tasaamiseksi. Huippuaikoina tuotettu sähköenergia voidaan varastoida käyttämällä energia kemiallisten yhdisteiden tuotantoon.

Perinteinen teollinen metanolin tuotanto perustuu kaasufaasissa tapahtuvaan synteesiin fossiilisista lähteistä, pääasiassa maakaasusta, tuotetusta synteesikaasusta. Metanolia voidaan vaihtoehtoisesti tuottaa hiilidioksidin hydrausreaktiolla. Päästölähteistä tai jopa suoraan ilmakehästä kaapatun hiilidioksidin hyödyntäminen metanolin tuotannossa mahdollistaisi lähes rajattomaan hiililähteeseen perustuvan kestävän tuotannon. Samalla hiilidioksidin pitoisuutta ilmakehässä voitaisiin vähentää. Vety metanolin tuotantoon voidaan tuottaa veden elektrolyysillä käyttäen uusiutuvista lähteistä tuotettua sähköä.

Uudessa, nestefaasissa tapahtuvassa metanolin synteesiprosessissa perinteinen kiinteä katalyytti sekoitetaan nestemäiseen alkoholiliuokseen. Alkoholi toimii katalyyttisenä liuottimena mahdollistaen vaihtoehtoisen reaktioreitin ja potentiaalisesti synteesin suorittamisen matalammassa lämpötilassa ja paineessa perinteisiin prosesseihin verrattuna.

Diplomityössä alkoholissa tapahtuvaa metanolin nestefaasisynteesiä tutkittiin laboratoriokokein. Panos- ja puolipanoskokeet suoritettiin autoklaavireaktorissa käyttäen perinteistä Cu/ZnO-metanolikatalyyttia sekä etanolia ja 2-butanolia liuottimina. Kokeet suoritettiin 30-60 bar paineissa sekä lämpötiloissa 160-200 °C.

Metanolin tuoton havaittiin kasvavan painetta ja lämpötilaa nostettaessa. Tuotto oli parhaimmillaan 1,9 g metanolia litraa liuotinta kohti tunnissa tutkituissa olosuhteissa. Katalyyttikohtainen tuotto oli parhaimmillaan 40,2 g metanolia kiloa katalyyttia kohti tunnissa. Tuottoarvot ovat alhaiset verrattuna teolliseen metanolisynteesiin sekä kaasufaasisynteesiin hiilidioksidista. Reaktiopaineet ja -lämpötilat olivat kuitenkin verraten alhaiset. Vaikka metanolin tuotto ei vaikuta riittävältä teollista tuotantoa ajatellen, voivat alhaisemmat paineet ja lämpötilat sekä yksinkertaisuus tehdä prosessista mielenkiintoisen pienen mittakaavan tuotantoa ajatellen.

Koetuloksia hyödyntäen suunniteltiin alustavasti prosessi, joka hyödyntää alkoholipohjaista menetelmää metanolin tuottamiseksi. Pienen mittakaavan prosessi skaalattiin elektrolyysiyksikköön, joka tuottaa 1 Nm^3 vetyä tunnissa. Diplomityö liittyy kiinteästi LUT:n REFLEX-tutkimusalustaan.

CONTENTS

Acronyms

AMP	2-amino-2-methyl-1-propanol
BET	Brunauer-Emmet-Teller (adsorption isotherm)
BWR	Boiling water reactor
CCR	Carbon capture and recycle
CCS	Carbon capture and sequestration
GCR	Gas-cooled reactor
DEA	diethanolamine
DME	Dimethyl ether
DMFC	Direct methanol fuel cell
DMT	Dimethyl terephthalate
DRIFTS	Diffuse reflectance infrared Fourier transform spectroscopy
ESA	Electric swing adsorption
FT	Fischer-Tropsch (synthesis)
H_{12}-NEC	N-ethylperhydrocarbazole
IGCC	Integrated gasification combined cycle
LUT	Lappeenranta University of Technology
MDEA	N-methyldiethanolamine
MEA	Monoethanolamine
MMA	Methyl methacrylate
MOF	Metal-organic framework
MTBE	Methyl tert-butyl ether

MTG	Methanol-to-gasoline (process)
MTO	Methanol-to-olefins (process)
NEC	N-ethylcarbazole
PEI	Poly(ethyleneimine)
PEM	Proton exchange membrane (electrolysis)
PSA	Pressure-swing adsorption
RWGS	Reverse water-gas shift (reaction)
SMR	Steam reforming of methane
SN	Stoichiometric number
SOE	Solid oxide electrolyzer
TAME	Tert-amyl methyl ether
TSA	Temperature swing adsorption
VSA	Vacuum swing adsorption
WGS	Water-gas-shift (reaction)
YSZ	Yttria stabilized zirconia

Nomenclature

A	Pre-exponential factor, bar $^{-1.89}$ · mol/s
C_{E}	Energy consumption of electrolyzer per m^3 (NTP) of hydrogen produced, kWh/m^3
c_{MeOH}	Concentration of methanol, mol/dm^3
E_a	Activation energy, kJ/mol
HHV	Higher heating value, kWh/m^3
k	Rate constant, bar$^{-1.89}$ · mol/s
m	Order of reaction
n_0	Amount of reactant at the start of reaction, mol
n_1	Amount of reactant at the end of reaction, mol
n_{i}	Amount of product *i* produced in reaction, mol
n_{MeOH}	Amount of methanol produced in reaction, mol
p_1	Total pressure at the start of reaction time, bar
p_2	Total pressure at the end of reaction time, bar
$p_{\mathrm{CO_2+H_2}}$	Combined partial pressure of carbon dioxide and hydrogen, bar
R	Gas constant, J/mol·K
r	Reaction rate, mol/s
S_{MeOH}	Selectivity of methanol, %
T	Absolute temperature, K
X	Conversion, %
ΔH	Reaction enthalpy, kJ/mol
η_{E}	Efficiency of electrolyzer system, %

LITERATURE REVIEW

1 INTRODUCTION

The subject of this work is the production of methanol from carbon dioxide. The aim is to test a new type of process utilizing a liquid phase alcohol promoted reaction for the synthesis of methanol from carbon dioxide and hydrogen. The work consists of a literature review of relevant research followed by laboratory scale reaction experiments.

The thesis is connected to the REFLEX research platform, which is focused on the production of renewable fuels and chemicals. An electrolyser unit with a hydrogen production capacity of 1 Nm^3 has been constructed at Lappeenranta University of Technology. Following the laboratory experiments, the alcohol promoted methanol synthesis process will be scaled to the electrolyser unit. A preliminary design for the process will be presented as part of this thesis.

The literature review is divided into three chapters. First, the following introduction presents the broader context of this work. The chapter establishes the relevance of methanol synthesis from CO_2 in the context of climate effects caused by excessive atmospheric CO_2. The second chapter discusses the storage of energy into chemical compounds. Alternative compounds, including methanol, will be presented and compared.

The third chapter focuses on methanol synthesis, reviewing the literature related to synthesis of methanol covering the fields of chemistry, catalysis and process and reactor design. The conventional industrial practice and new developments in the field are presented, including synthesis of methanol from CO_2. The alcohol promoted, liquid phase process is given particular focus in order to provide the information necessary for conducting the laboratory experiments.

1.1 Fossil fuels and emissions of CO_2

The widespread use of fossil fuels has been a major factor in the global rise in quality and convenience of life since the late 19th century. Global industrialization and population growth have led to increasing consumption of energy. Fossil fuels have provided a convenient and seemingly endless source of energy to match the increasing consumption. In addition to providing over 80 % of the current world energy supply [1], crude oil, natural gas and coal are important raw materials, providing various materials and products essential to the modern life.

The burning of fossil fuels at a massive scale for the production of electricity and heat and for powering transportation has led to the increase in concentration of carbon dioxide in the atmosphere. Carbon dioxide is a “green-house gas” capable of absorbing and emitting thermal radiation in the Earth’s atmosphere. The increasing concentration of carbon dioxide has been widely recognized as the main reason for the observed global climate change [2]. As of today, over 35 Gt per year of CO_2 is being emitted from human action. The atmospheric concentration of CO_2 has reached 400 ppm, compared to 280 ppm in the pre-industrial era.

Further, the available reserves of fossil fuels are limited. While discoveries of new deposits and increasing utilization of unconventional sources (such as shale oil and gas) have led to sizeable increases in known reserves [3], it is clear that extractable fossil fuels will run out in a certain time frame. Resultantly, the continuous increase in the exploitation of fossil energy sources and the resultant increasing CO_2 emissions do not seem sustainable either from the environmental or the economic standpoint.

1.2 Strategies for reducing CO_2

To minimize the impact of climate change, national policies have been implemented and international treaties signed aiming to reduce the amount of anthropogenic CO_2 emissions. No single solution to the issue of global warming has been presented. Instead, various different methods and technologies have been proposed both for reducing further emissions and for the removal of CO_2 from the atmosphere. Essentially, three strategies exist for the reduction of CO_2 buildup in the atmosphere: the reduction of the amount of CO_2 emitted, carbon capture and sequestration, and recycling of carbon dioxide by use as chemical feedstock [4].

The amount of CO_2 emitted can be reduced by improving energy efficiency and by changing primary energy sources. It has been estimated that up to 65% of the energy input of electric power plants and 60-80% of passenger cars is wasted in conversion losses [5]. The improvement of the technology for conversion and storage of energy would be one path to reducing energy consumption: the other would be the conservation of energy by societies as whole. The replacement of coal by the less carbon rich fossil fuels, oil or natural gas, as a primary energy source would reduce the amount of CO_2 emitted while still maintaining the convenience associated with fossil energy sources. In the long term, adopting renewable, non-fossil energy sources will be inevitable.

The second approach is known as carbon capture and sequestration (CCS). In this scheme, carbon dioxide is captured from emission sources and stored away from the atmosphere, for instance by injection into underground geological formations or oceans. Capture of CO_2 directly from the atmosphere has also been researched. This would allow capturing of the CO_2 emitted from small, dispersed sources such as transportation. CCS has been referred as the best currently available solution to CO_2 emissions [6]. However, capturing of CO_2 at sources such as power plants and industrial facilities brings additional costs and the subsequent storage of CO_2 creates no additional value. There are also safety and reliability concerns related to the underground storage of massive amounts of CO_2 [7].

Finally, the approach of carbon capture and recycle (CCR) aims to utilize captured CO_2 either in direct uses or as raw material for chemical processes. Direct application areas of CO_2 include the carbonation of beverages, uses as blowing agent or inert gas and as supercritical solvent [5]. The chemical conversion routes of CO_2 have been limited by the stabile nature of the carbon dioxide molecule and the requirement of sizable energy input, active catalysts and optimal reaction conditions to initiate reactions [8]. Currently, CO_2 is utilized as raw material in the production of urea, carbonates and salicylic acid [9].

1.3 Storage of energy

By advances in technology, renewable energy sources such as wind and solar are becoming more feasible and competitive with fossil energy. The cost of renewable electricity is already approaching the level of fossil based electricity [10]. However, renewable energy such as solar and wind are inherently limited by their periodic, fluctuating nature. Economical and effective methods of storing electricity to even out the fluctuating supply are required to allow significant reliance on solar and wind energy.

Various technologies have been developed for the storage of electricity, including batteries, compressed air, pumped hydro, flywheels and fuel cells [11]. The storage of energy as bond energy in chemical compounds is an effective alternative, allowing the storage of energy in a readily transportable form. A prime example of these chemical energy carriers is hydrogen, the potential of which has been underlined in the proposed “Hydrogen Economy” [12]. Hydrogen would be an ideal, clean burning fuel causing no CO_2 or other harmful emissions. However, the handling of hydrogen is difficult. Compression to high pressures or liquefaction at very low temperatures is required because of low energy density. Hydrogen is also not compatible with

the existing energy infrastructure, requiring the creation of an expensive new storage and distribution infrastructure.

1.4 Methanol: energy carrier and chemical feedstock

Currently, liquid fuels derived from petroleum are the established energy carrier, especially in transportation. Liquid fuels are generally much simpler to handle, transport and store compared to gaseous alternatives, such as hydrogen. Alternative, renewable liquid fuels would be readily integrated to the existing distribution infrastructure, with minor modifications. Olah has suggested methanol as a promising option and proposed the concept of “Methanol Economy” [13]. Methanol is a suitable fuel for internal combustion engines: it can be mixed with gasoline or even used alone after minor modifications to existing engines [14]. Additionally, methanol can be converted by dehydration to dimethyl ether (DME), which can be used as a fuel for diesel engines [15].

Other than use as fuel, methanol finds plenty of application as a feedstock chemical. Methanol is used as raw material for important commodity chemicals such as formaldehyde and acetic acid. By catalytic processes, methanol can be converted into important fuel and feedstock hydrocarbon compounds, including gasoline [16]. Through the various conversion routes, essentially any hydrocarbon product currently derived from petroleum oil can be produced from methanol.

1.5 Methanol from CO_2

The current industrial production of methanol is based on fossil raw materials. However, methanol can also be produced solely from CO_2 and H_2. The catalysts and processes employed for the synthesis of methanol via hydrogenation of CO_2 are highly similar to those used in conventional synthesis. As of now, methanol produced from CO_2 is as of yet not cost competitive with syngas derived methanol [17]. Various process options have been presented for methanol synthesis from CO_2 [18, 16].

The synthesis of methanol using captured CO_2 and hydrogen generated using renewable energy has been suggested as a renewable and sustainable route to fuels and chemicals products [7]. CO_2 capture from point sources or the atmosphere could provide a practically limitless carbon source, simultaneously reducing the harmful buildup of CO_2 in the atmosphere.

Through conversion to methanol, the captured CO_2 could be converted to practically any chemical product currently derived from fossil raw materials.

2 STORAGE OF ENERGY IN CHEMICALS

The storage of electricity produced from primary energy sources is an important component of an effective energy infrastructure. This is especially true for the emerging renewable energy sources, wind and solar. Wind and solar energy is by nature fluctuating and the amount of energy available varies both seasonally and on a daily and hourly basis. The excess electricity produced during peak periods needs to be stored for utilization during periods of lower production. The supply of electricity also needs to be balanced with the varying demand. The solutions proposed for storage of energy include batteries, pumped hydro, compressed air storage and flywheels [19]. Technologies such as pumped hydro and compressed air are only suited for large-scale, static energy storage [20], while batteries are applicable at smaller installations, including mobile uses such as consumer electronics and transportation.

An alternative is the conversion of electric energy into chemical energy by the production of chemical compounds using the electrical energy generated from primary energy sources. The advantages of chemical energy carriers compared to the alternatives are the higher energy density [21] and easier handling and distribution. Chemical energy carriers, or fuels, can be stored, transported and distributed to be used later and at another location. The chemical energy contained in the compounds can be released for the production of electricity or heat or used for transportation purposes. Currently, the established fuels are those derived from fossil sources, particularly from petroleum oil. Crude oil is refined into hydrocarbon fractions such as gasoline and diesel oil, which form the basis of the current energy infrastructure. These fuels contain the solar energy originally converted by plants millions of years ago in a liquid, simple to handle form and at high energy density.

The continuous increase in the use of fossil fuels has become questioned over the CO_2 emissions and the long-term availability of resources. Alternative fuels produced by utilizing renewable resources would be preferable as energy carriers. The proposed alternative energy carriers include hydrogen, alcohols, methane and synthetic hydrocarbons. While currently mostly produced from fossil sources, all of these can also be produced from renewable materials. Hydrogen can be produced by electrolysis of water, preferably by using electricity generated from renewable sources. Hydrogen can be utilized in the conversion of various

carbon sources into fuels and chemicals via hydrogenation reactions. The use of captured CO_2 as carbon source is particularly interesting. Through hydrogenation, CO_2 can be converted into a variety of fuels or chemical products, as illustrated in Figure 1.

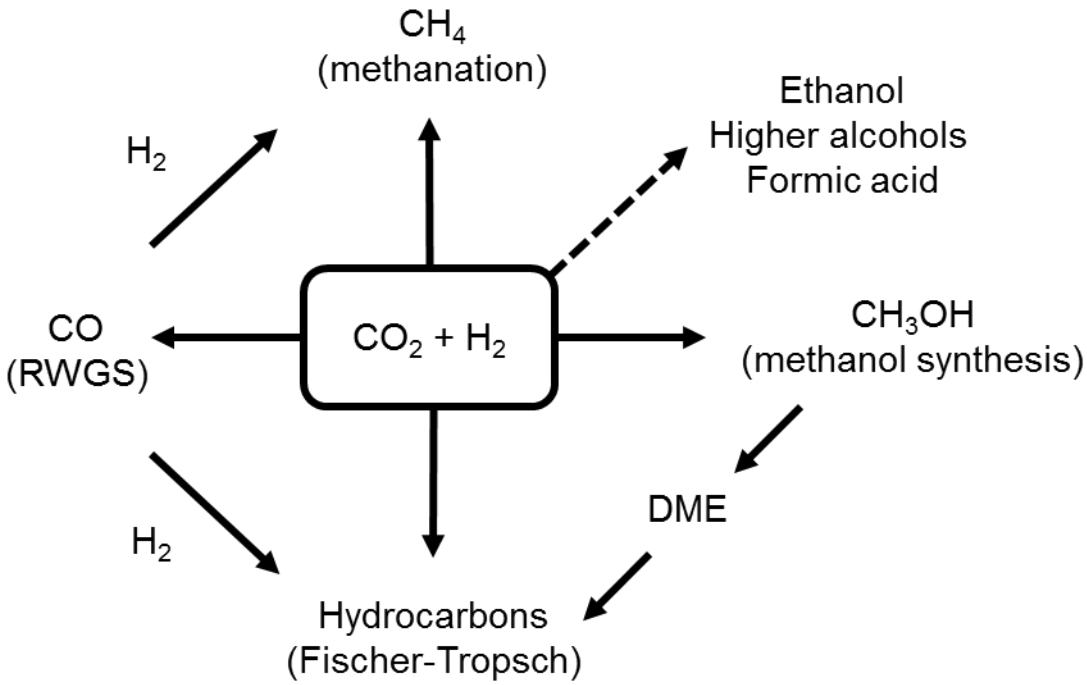

Figure 1. The products of CO_2 hydrogenation **[17, 22, 23]**.

This chapter provides a summary of the most important potential energy storage compounds. The production routes via the hydrogenation of CO_2 is the main focus. Initially, an overview of the production and use of hydrogen will be presented, as hydrogen is interesting both as an energy carrier and a reactant for the hydrogenation of CO_2. Sources and capture technologies for CO_2 will also be presented. Then, after introduction of the potential energy carriers, the advantages and limitations of the alternative compounds will be discussed.

2.1 Carbon dioxide capture

CO_2 capture has been considered an effective route to reducing the amount of CO_2 emitted into the atmosphere, while allowing the continuing use of fossil fuels. Carbon capture and

storage (CCS) refers to the capturing CO_2 from emission sources such as industrial or power generation facilities and sequestering the captured CO_2 away from the atmosphere, for example into oceans or underground geological formations [6]. Carbon sequestration has been demonstrated with multiple operations currently in action [24]. Capture of CO_2 directly from the air has also been researched, as it could potentially provide a limitless carbon source while also mitigating the carbon build-up in the atmosphere [25, 26].

Alternatively, captured carbon dioxide could be utilized as raw material for various chemical products, adding economic value [27]. The separation of CO_2 from concentrated gas streams is already performed in industrial operations, for example in the production of hydrogen and ammonia [28]. Capture of CO_2 from power plant flue gases is more challenging due to the lower concentration and partial pressure of CO_2 in the gas stream [29]. The presence of combustion products such as oxides of sulfur and nitrogen further complicate the separation processes. Further, a high purity of CO_2 is required as the end product of the capturing process, especially if the CO_2 is to be used as feedstock for chemical processes [28].

2.1.1 CO_2 separation methods

Multiple separation methods can be used for the separation of CO_2 from gas streams [30, 29, 31, 32]. These include chemical or physical absorption, adsorption on solid materials, cryogenic distillation and membrane separation. The suitability of any method depends on the conditions, the concentration of CO_2 and the pressure of the gaseous stream being the main parameters, along with the required purity and the degree of separation of CO_2 from the gas stream. CO_2 capture processes require energy for the separation, purification and compression of carbon dioxide. The purity of CO_2 after separation is decisive to the required energy input of the separation process [32].

2.1.1.1 Chemical absorption

In a chemical absorption process, CO_2 is removed from a gaseous stream by reaction with liquid absorbents. Amine-based solvents, especially 25-30 w-% of MEA (monoethanolamine) in aqueous solution, are commonly used [29]. The CO_2 containing gas is fed from the bottom of the absorption column, while the solvent is introduced from the top. Absorption is performed at approximately 40^{o}C. By reaction of the amine with CO_2, a soluble carbamate species is formed [33]. The CO_2 rich solvent is then fed to the stripping column, where the CO_2 is released

and the solvent regenerated at temperatures of 100°C to 140°C. The regenerated solvent is recycled to the absorption stage. Due to the high heat of absorption of CO_2 into the amine solution, significant amount of energy is required for regeneration. Other challenges of amine absorption include corrosion [34] and degradation of the solvent by the effect of oxygen and contaminants such as SO_x and NO_x [35].

While MEA is the standard solvent used for CO_2 separation, other types of amines and also inorganic solvents have been researched [29]. Mixtures of different amines have also been formulated [30]. Alternative amine solvents include secondary amines such as diethanolamine (DEA), tertiary amines (N-methyldiethanolamine, MDEA), and sterically hindered amines which contain bulky substituent groups. An example of the last type, 2-amino-2-methyl-1-propanol (AMP), has been found to form significantly less stable carbamates with CO_2, leading to lower regeneration energy input [33]. Basic inorganic solvents including aqueous potassium and sodium carbonate have also been proposed. In the chilled ammonia process, aqueous ammonia is used for absorption of CO_2 at low temperatures (0-20°C) and regeneration is carried out preferably at 100-150°C [36]. The reported advantages of this process include low heat of absorption in addition to low solvent degradation and corrosion.

2.1.1.2 Physical absorption

Alternatively to chemical absorbents, physical absorbents that capture CO_2 at high partial pressures and low temperatures may be used for the separation of CO_2 [29]. Solvents such as Selexol (dimethyl ethers of polyethylene glycol) and Rectisol (methanol chilled to -40°C) have been used for decades in the removal of acid gases (H_2S, CO_2) in natural gas and syngas processing [26]. These systems provide less energy intensive solvent regeneration compared to chemical solvents due to the weaker association of CO_2 with the sorbent material. However, physical absorption processes are only capable of capturing CO_2 from high-pressure, high concentration streams.

Ionic liquids, salt-like materials consisting of large organic cations and smaller inorganic anions, have also been researched in the context of CO_2 separation [29]. These compounds are liquid at ambient temperature and possess very low vapor pressures combined with substantial thermal stability and non-flammability. Like the physical solvents, ionic liquids interact with CO_2 by physical effects, leading to a low heat of adsorption and low energy requirement for

regeneration. Similarly, the CO_2 absorption capacity is improved with increasing pressure, limiting the applicability of ionic liquids to high-pressure streams. The high cost of preparation and purification of ionic liquids is also a major drawback considering the practical use [26].

2.1.1.3 Adsorption on solids

CO_2 can be separated by adsorption onto solid adsorbents by physisorption or chemisorption mechanisms [29]. In physisorption, gas molecules interact with the solid material by dispersive van der Waals forces, while in chemisorption, chemical bonding occurs in the adsorption process. Numerous adsorbent materials have been proposed, including carbon-based materials (activated carbon, carbon nanotubes), zeolites, metal oxides and amine-based adsorbents (amines supported on organic or inorganic solid, porous materials) [37]. A recent development in solid adsorbent materials are metal-organic frameworks [29]. Key selection factors for potential adsorbent materials are CO_2 adsorption capacity and selectivity, and the energy required for regeneration of the adsorbent [29].

In industrial operation, adsorption processes are carried out through adsorption-desorption cycles. Desorption can be performed either by change in temperature or pressure [31]. In pressure swing adsorption (PSA), adsorption at increased pressure is followed by desorption at ambient pressure. In vacuum swing adsorption (VSA), desorption is performed at lower than ambient pressure. The drawback of the pressure change based adsorption methods is that the CO_2 product is obtained at low pressure, requiring compression for storage and utilization. In temperature swing adsorption (TSA), desorption occurs following increase in temperature. In electric swing adsorption (ESA), the change of temperature is facilitated by electric current.

Zeolites are commonly used in gas separation processes, especially in the purification of hydrogen by pressure swing adsorption [29]. The difficulty of using zeolites for CO_2 capture arises from their high sensitivity to moisture. The adsorption capacity of zeolites is greatly reduced by water. For zeolites to be applied, the CO_2 containing gas would have to be thoroughly dried, creating extra costs. Carbon-based adsorbents are affordable compared to zeolites and are not sensitive to moisture. Generally, the adsorption capacity of activated carbon is lower compared to zeolites at low pressures, but higher at high pressures [37]. The adsorption capacity of both types of materials quickly lowers at increasing temperatures. [26].

Metal-organic frameworks (MOFs) are microporous materials consisting of metal ions connected by organic ligands, forming a network structure with uniform pore diameter [29]. The attributes of these materials include high thermal and chemical stability, very high specific surface area and low density. In CO_2 separation, MOFs have shown promising results, demonstrating high adsorption capacity compared to zeolites and carbon materials. However, these materials are still early in the research stage.

Chemisorption by amine-modified solid materials is similar in mechanism to the chemical absorption of CO_2 by amine solvents, such as MEA. The chemical interaction leads to stronger CO_2 affinity when compared to physisorption, especially at lower pressure conditions. The spectrum of materials researched is quite wide, as various types of amines can be supported on different support materials [37]. Reportedly the most commonly used amine is poly(ethyleneimine) (PEI), a polymeric amine with varying structures. Silica, particularly the highly porous MCM-41 type, is commonly used as the support. Other support materials include organic polymers and carbon materials. High CO_2 adsorption capacities have been reported, in combination with lower regeneration temperatures compared to liquid amine solvents [29]. The stability of amine impregnated materials during repeated adsorption-desorption cycles is problematic.

Metal oxides, especially CaO and MgO can be used for CO_2 capture in the carbonate looping process. Carbonate looping is usually based on the reversible carbonation of calcium oxide [38, 30]. In the carbonation step, calcium oxide reacts exothermally with CO_2 at a temperature of approximately 650^{o}C. The resulting calcium carbonate is then transferred to calcination, where CO_2 is released and the calcium oxide regenerated in an endothermic reaction above 750^{o}C, preferably at 900-950^{o}C. By utilizing the heat from the carbonation reaction, the energy requirement of CO_2 capture is potentially lower compared to solvent absorption processes. In addition, calcium carbonate is a relatively cheap sorbent material. Due to deactivation of the sorbent, fresh $CaCO_3$ needs to be continuously added. The spent calcium carbonate could be utilized in cement manufacturing, leading to integration potential [39].

2.1.1.4 Other methods

In cryogenic distillation, gases are separated by condensation at low temperatures [31]. Cryogenic processes are commonly operated for the separation of oxygen and nitrogen from

air. For CO_2 separation, the technology has been applied to high-concentration sources [40]. Highly pure, liquid CO_2 is obtained and compression is not needed for transportation or use of the CO_2. The process is, however, not considered applicable for large scale capture of CO_2 from diluted sources due to high energy intensity [26].

Gas separation by membranes has been industrially operated in processes such as air separation, hydrogen purification and CO_2 separation from natural gas [31]. Membranes have been found effective in the separation of CO_2 from pressurized, high concentration sources such as those present in natural gas processing. For low-pressure and low-concentration separation, such as CO_2 capture from flue gases, adequate membrane performance has not been reached [31]

Both polymeric and inorganic membranes have been studied for gas separation. Polymeric membranes show particular promise for CO_2 capture [31]. Various types of polymeric membranes capable of separating CO_2 from nitrogen have been developed [41]. Generally, the compromise between selectivity and permeability has been found challenging in membrane development [42]. High CO_2 selectivity is required for producing a highly pure CO_2 stream, while low permeability leads to increasing membrane surface area and pressure drop, leading to higher capital and compression costs. CO_2 capture by membranes has been estimated energy effective compared to solvent absorption at high (>20%) CO_2 concentrations, but not at lower concentrations [43, 44]

2.1.2 CO_2 capture from fossil-fired power plants

For the separation of CO_2 from power plant flue gases, separation technologies can be classified based on the positioning of CO_2 capture in the overall power plant process. These technologies include post-combustion capture, oxyfuel combustion and pre-combustion capture (Figure 2). In each of these processes, the composition of the CO_2 containing stream varies and consequently, different CO_2 separation methods are applicable.

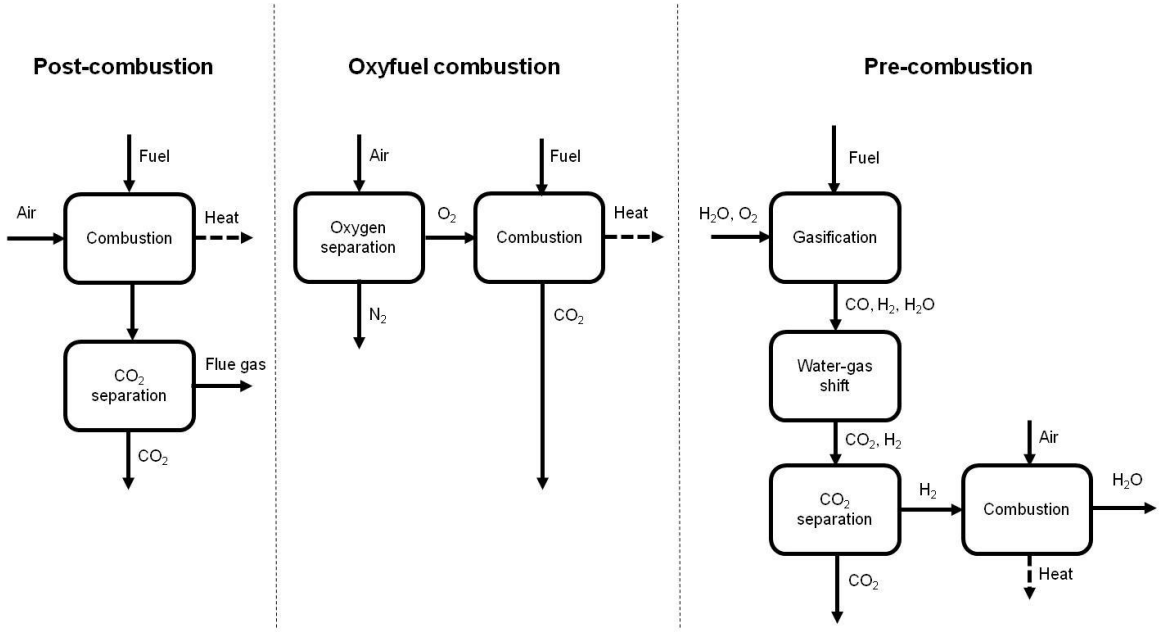

Figure 2. The technologies for capture of CO_2 from power generation processes.

2.1.2.1 Post-combustion capture

In post-combustion capture, CO_2 is captured from the flue gas after conventional combustion of the fuel in the presence of air [45]. The advantage of post-combustion capture is that no changes are required to the power plant process, allowing the retrofitting of existing plants with the CO_2 separation unit. However, separation is complicated by the low concentration of CO_2 (12-15 vol-%) and the vast volumes of flue gas to be processed [32]. The low pressure of the flue gas further limits the available separation technologies.

Chemical absorption by amine solvents is currently considered the best available option for post-combustion CO_2 capture [45, 32]. While high degree of separation and purity of CO_2 is achieved by the absorption processes, the high energy requirement and solvent degradation are an issue. The efficiency losses in power generation caused by the implementation of CO_2 capture by amine absorption are estimated to be 10-14 %-points (compared to base efficiency), including the compression of CO_2 [32].

While chemical absorption processes have been implemented in chemical industry and at pilot scale in power generation, the full scale implementation at power plants is a challenge [32]. In the current pilot scale operations, CO_2 is captured at maximum quantities of approximately 500 t per day, corresponding to electric power generation of less than 1 MW. In contrast, conventional power plants operate at capacities of 500 to 1000 MW of electricity generated. The potential developments in post-combustion capture include the development of more energy efficient solvents and alternative technologies such as carbonate looping.

2.1.2.2 Oxyfuel combustion

In the oxyfuel combustion process, fuel is combusted in the presence of pure oxygen instead of air. As a result, the flue gas consists of mostly CO_2 and steam, with the concentration of CO_2 approximately 89% by volume [32]. After condensation of water, a highly pure CO_2 stream is obtained, with only residual drying and purification required. In addition, the volume of flue gas is greatly reduced as dilution by nitrogen is avoided. The oxygen is separated from air in cryogenic air separation units, by condensation below -182^{o}C. In pure oxygen combustion, temperatures are higher than in air combustion. To reduce the combustion temperature, a significant fraction (approximately 2/3 by volume) of the flue gas is recycled to the combustion chamber.

While the energy-intensive CO_2 separation can be largely avoided by oxyfuel combustion, the separation of oxygen from air still requires a sizable energy input. With cryogenic separation, efficiency losses are approximately 10 %-points, including compression of CO_2, while optimized separation processes could reach an estimated efficiency loss of 8 %-points [32]. Oxygen separation by membranes has been discussed as a potential method of improving the overall efficiency of oxyfuel combustion, but further improvements in membrane materials are required before full implementation [46, 47]. Difficulties in oxyfuel CO_2 capture may arise from residual oxygen present in the flue gas, which complicates the purification of CO_2 [32]; excess oxygen is commonly fed to combustion processes to ensure complete combustion. Finally, oxyfuel combustion requires significant alterations to various power plant components and is only applicable at new installations. Oxyfuel combustion has been demonstrated in the pilot scale at power ratings up to 30 MW [48].

2.1.2.3 Pre-combustion capture

In the pre-combustion process, the fuel is first converted into hydrogen-rich syngas, followed by capture of CO_2 and combustion of the hydrogen. Coal or heavy oil fuels are gasified by partial oxidation into carbon monoxide and hydrogen. Next, the water gas shift reaction is carried out in presence of steam to convert CO into CO_2 (Section 2.1.1). The result is a stream consisting of hydrogen and CO_2 at a high pressure, allowing the separation of CO_2 by physical solvents [32].

Use of physical solvents such as methanol (the Rectisol process) is less energy-intensive compared to chemical absorption processes, leading to lower efficiency losses. The solvent simultaneously removes sulfur compounds such as H_2S, leading to cleaner combustion of the fuel gas (hydrogen). Alternatively, pressure swing adsorption can be used for the separation of CO_2 and hydrogen. While the capture of CO_2 can be performed with high energy efficiency in the post-combustion process, energy input is required for air separation to provide oxygen for gasification. The estimated efficiency losses are in the range of 10-12%-points for coal fired IGCC power plants [49, 50].

Fuel gasification followed by combustion is operated at integrated gasification combined cycle (IGCC) power plants, which mainly utilize coal as feedstock [32]. Plants without CO_2 capture have been in operation since the 1980's, but the establishment of IGCC technology has been limited by reliability issues and high investment costs. Integration of CO_2 capture is currently only at the planning and demonstration stage. Demonstration plants with capacities of up to 900 MW of electricity are in consideration [51]. Combustion of hydrogen rich fuel (as opposed to CO containing syngas at conventional IGCC plants) in large gas turbines is also under development. Integration of CO_2 capture is limited to new IGCC plants due to the required changes to the combustion processes.

2.1.3 CO_2 capture from the atmosphere

The capture of carbon dioxide directly from the atmosphere would provide several benefits. It would enable the capturing of CO_2 emitted from small, distributed sources such as building heating and transportation. The capture and subsequent collection of CO_2 directly from these sources would be impractical and uneconomical [26]. By direct air capture, the CO_2 emitted from any source could be removed from the atmosphere, with the capture facilities potentially

located anywhere in the world. Performed at large scale, this would allow reduction of the overall CO_2 concentration in the atmosphere, instead of being limited to the reduction of further emissions. Simultaneously, the captured CO_2 could provide an essentially limitless carbon source for the synthesis of fuels and chemicals [7].

The main obstacle to energy efficient and economical capture of CO_2 from the atmosphere is the low concentration of CO_2 in air. Additional difficulties arise from the presence of moisture and the need to perform the separation of CO_2 at close to ambient temperature and pressure; heating, cooling and compression of the massive volumes of air to be treated would very likely be uneconomical. These limitations eliminate many of the established and researched CO_2 separation technologies from the consideration for direct air capture. Physical adsorbents such as zeolites and activated carbon are ruled out due to the low adsorption capacity at ambient pressure and in the presence of moisture, physical solvents are similarly not applicable at the low pressure and the amine based solvents suffer from degradation in the presence of air [26].

The theoretical energy requirement for the separation of CO_2 from atmospheric concentration (approx. 20 kJ/mol of CO_2, based on enthalpy of mixing) is only 1.8 to 3 times the energy required for the separation from concentrated sources [25]. To minimize energy consumption, the capture processes could be optimized for efficiency rather than for complete separation of CO_2. While high (>90%) degree of CO_2 separation is desired in capture from point sources, separation of only 25% of the CO_2 might be satisfactory for an air capture unit [25]. Clearly, the energy consumption of actual processes would not be comparable to the theoretical minimum. Indeed, energy intensity is the main issue with many of the proposed processes for direct air capture. In addition to energy, significant land area would be required for large scale operation. The plants for direct air capture would be much larger compared to capture units for point sources due to the much larger volumes of gas to be treated [26].

The proposed technology options for direct air capture include chemisorption by inorganic, mainly basic, materials and the use of hybrid adsorbents consisting of organic amines supported on inorganic solids [26]. The use of basic materials such as sodium hydroxide can be considered the conventional route [52], while the development of solid hybrid sorbents has seen rise in more recent years [53].

2.1.3.1 Chemisorption by aqueous bases

Strong bases such as calcium, potassium and sodium hydroxides absorb CO_2 by chemical reaction, forming the respective carbonates [54]. Especially the absorption of CO_2 by aqueous sodium hydroxide has been considered [26]. Various methods for contacting the basic solution with air have been developed. In packed absorption columns, efficient separation of CO_2 can be reached but the pressure drop associated with blowing large volumes of air through the packed bed is problematic. As a result, a column geometry with a large cross-section combined with a low height has been proposed [55]. Another issue caused by the large volume of air through the column is the significant evaporation of water. A water loss of 90 g per gram of CO_2 captured has been noted [56]. Avoiding significant pressure drops by employing open absorption towers with no packing has also been considered [57].

The most energy intensive phase in the sodium hydroxide based scrubbing process is the regeneration of NaOH from the sodium carbonate formed in the reaction with CO_2. In the causticization process, sodium carbonate is reacted with calcium hydroxide, forming NaOH and precipitating $CaCO_3$. The calcium carbonate is then calcined at temperatures above >700^oC, releasing CO_2 and resulting in calcium oxide. By hydration with water, calcium hydroxide is again obtained, closing the cycle. The causticization process is widely employed at Kraft pulp mills for the recovery of sodium hydroxide.

Usually the significant amount of heat required for the calcination reaction is provided by firing fossil fuels in air, meaning that a secondary CO_2 capture unit would be required to remove CO_2 from the outlet gas [26]. By oxygen firing, a stream of concentrated CO_2 would be obtained instead, simplifying the separation of CO_2 [54]. The overall energy requirement of the sodium hydroxide capture process has been estimated at 12 to 17 GJ per ton of CO_2 captured [25, 55]. For comparison, the combustion of coal provides 9 GJ of energy per ton of CO_2 emitted [55]. It can be concluded, that the economic and environmental feasibility of this energy intensive process is questionable [26].

Alternative causticization cycles have been developed with the goal of reducing the energy intensity. Cycles utilizing borates [58] and titanates [59] have been proposed. However, high temperatures are still required in both processes for the release of CO_2. Alternatively, the use of calcium hydroxide as the absorbent material instead of sodium hydroxide has been researched. In this simplified process, calcium carbonate is precipitated by reaction of calcium

hydroxide with CO_2. Calcium carbonate is then calcined as previously described, again leading to high energy consumption. Additional problems are caused by the low solubility of calcium hydroxide in water and mass transfer limitations [26]. As a summary, the high energy requirement, water losses by evaporation and also corrosion issues associated with the aqueous base scrubbing of CO_2 make these types of processes seem impractical [60].

2.1.3.2 Supported amine adsorbents

Solid, amine based adsorbents were already introduced in the context of CO_2 capture from point sources (Section 2.7.1). However, these types of materials are particularly interesting when capture from air is considered, as they seem to offer properties particularly well suited for this purpose. Through the chemical interaction of the amine functional groups with CO_2, the binding of CO_2 is weaker compared to strong bases, leading to more energy effective regeneration. The interaction is however stronger compared to physical adsorbents such as zeolites, generally leading to improved adsorption capacities at ambient conditions [61]. Opposed to aqueous amine solutions, evaporation is not an issue with the solid amine based adsorbents.

The amine based adsorbents can be classified based on the mechanism used to embed the active amine component onto the inorganic support [62]. In the first group, the support material is physically impregnated with monomeric or polymeric amines. These materials generally suffer from degradation due to the weak interaction between the amine and the support [26]. Alternatively, amines can be covalently bonded with the support, leading to increased stability. This can be performed by binding amines to silica through silane bonds or by creating polymeric supports with amine side chains. The final option is the in situ polymerization of polyamines with an inorganic support material.

Silica and mesoporous silica (such as MCM-41 and SBA-15) are commonly used as support materials, alternatives including alumina and carbon fibers [26]. A wide range of amines have been studied. Polyethylenimines (PEIs) physically loaded onto supports have been found promising, combining simple and inexpensive preparation with good CO_2 adsorption capacity and regenerability [26]. As an example of in situ polymerized adsorbents, hyperbranched aminosilicas (HAS) have been found promising [63]. Varied desorption methods have been used for the regeneration of amine based solid adsorbents [26]. Pressure, vacuum and

temperature swing adsorption processes have all been studied. Moisture swing adsorption based on desorption in contact with moisture or water has also been demonstrated with an anionic ion exchange resin used as the adsorbent [64]. In addition to regeneration ability, the adsorbents should have good stability under process conditions to allow practical use. Adsorption capacity can be irreversibly reduced by degradation of either the amine or the support [26], with degradation by acidic gases (NO_x, SO_x) and oxygen the main concern.

Despite the low concentration of CO_2 in air, direct air capture has been considered technically feasible [26]. However, the concept is often considered uneconomical due to excessive costs [65]. Cost estimations of CO_2 capture from the air range from under 20€ all the way to over 800€ per ton of CO_2, with the low estimates considered overly optimistic by some [26]. In comparison, the estimated cost of capture from concentrated sources is reported from under 30€ to 90€ per ton of CO_2. Pilot and demonstration projects of direct air capture have already been launched by multiple companies [66, 67, 68]. These operations should provide more information about the technological and economic feasibility of capturing CO_2 from the atmosphere.

2.2 Hydrogen

Hydrogen has been widely considered a potential energy carrier, leading to the proposed “hydrogen economy”, a future energy system where fossil fuels are widely replaced by hydrogen and electricity [69, 70]. While hydrogen is abundant and compounds of hydrogen are available throughout the planet, it does not occur in pure form.

Hydrocarbon sources of hydrogen include fossil fuels and biomass. Fossil sources add up to approximately 96% of total hydrogen production [71]. Reforming of natural gas is the preferred route, while partial oxidation of liquid hydrocarbons and gasification of coal are also practiced. Large scale production and use of hydrogen is associated with ammonia production, petroleum refining and methanol synthesis [72]. Fossil based production of hydrogen is associated with sizable CO_2 emissions and in the long term, transition to renewable sources would be preferable. Renewable, biomass sources of hydrogen include energy crops in addition to domestic, agricultural and forest wastes. Processes based on gasification and pyrolysis of biomass have been developed for the production of hydrogen from these sources.

Other than biomass, water would be the preferred source of hydrogen on the basis of renewability. As water is widely available and essentially limitless, the production of hydrogen from water is usually considered the basis for a future hydrogen economy [69]. Various methods have been studied and developed for the splitting of water into oxygen and hydrogen. The most important is electrolysis, which presently contributes an estimated 4% of commercial hydrogen production [71]. Other means of splitting water include thermochemical cycles, photoelectrolysis and biological processes [73, 74]. Only electrolysis, along with biomass based processes are considered mature enough to compete with fossil based production in the short to medium term [75]. The possible hydrogen production routes with estimated near-term commercial importance are summarized in Figure 3.

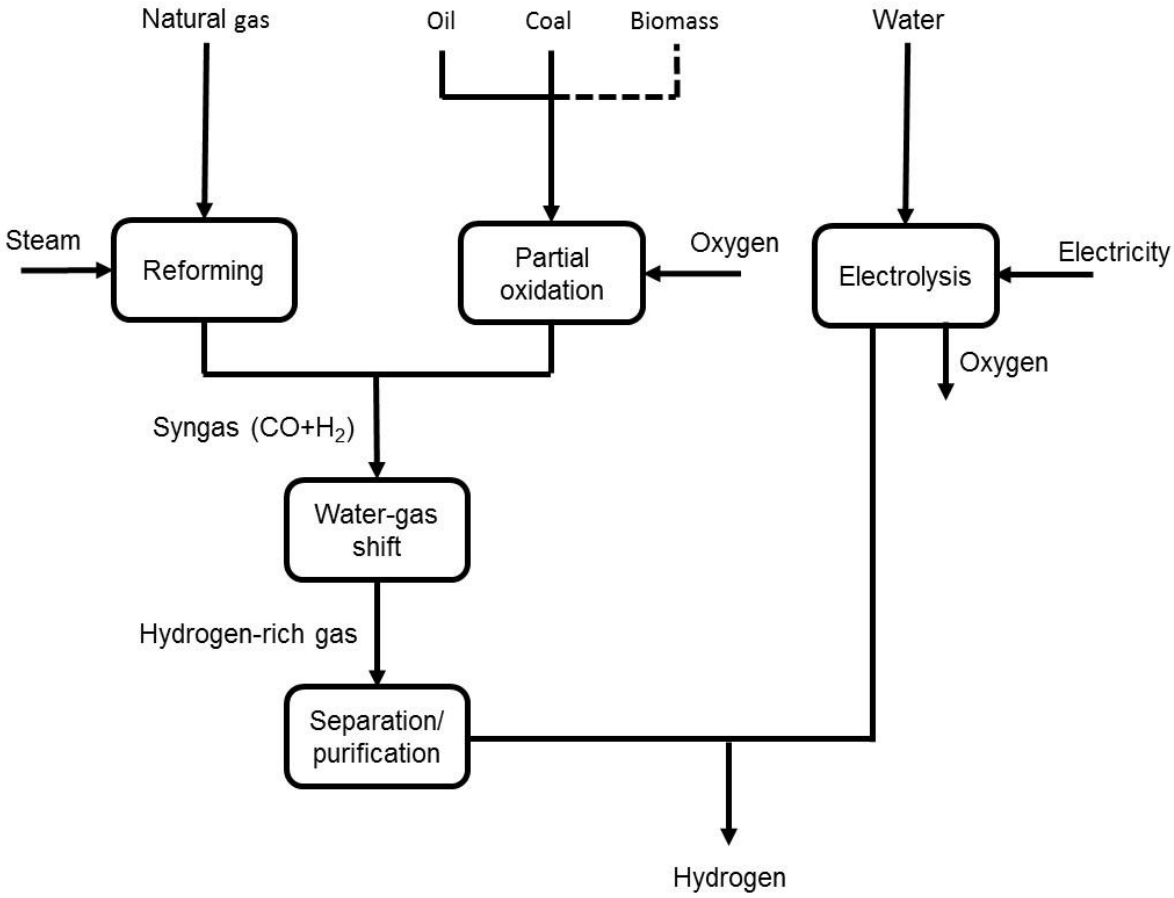

Figure 3. Hydrogen production routes with current or near-term commercial significance **[73, 75, 74].**

2.2.1 Production of synthesis gas

Hydrogen production from hydrocarbon sources is based on the production of synthesis gas (syngas) by endothermic reforming reactions and exothermic partial oxidation reactions and their combinations. The products of these processes are synthesis gases containing varying proportions of hydrogen and carbon monoxide, usually accompanied by carbon dioxide and/or methane. The resulting gas can be used in various conversion processes, with the composition of the gas depending on the gas generation method and the intended use. Examples of important syngas based processes include the synthesis of ammonia and methanol. If hydrogen is the desired product, the composition of the gas is adjusted towards higher hydrogen content and the hydrogen is then separated and purified. Commercially, the largest share of hydrogen produced is originated from the steam reforming of methane (natural gas):

$$\mathrm{CH_4 + H_2O \rightleftarrows CO + 3H_2} \quad \Delta H = 206\ \mathrm{kJ/mol} \tag{1}$$

The strongly endothermic reaction is carried out over nickel-based catalysts at temperature range of 800-1000°C, requiring an external heat source. Thermodynamically, the reaction is favored by low pressures. However, pressures exceeding 20 bar are often employed as further processing of product gases is thus simplified [76]. Steam reforming of methane (SMR) produces gas mixtures containing 70-75% hydrogen, 7-10% CO, 6-14% CO_2 and 2-6% methane [71]. Methane is an ideal feedstock for reforming due to the ease of handling of the gaseous material and the low level of sulfur contaminants [77]. Sulfur compounds such as hydrogen sulfide poison the catalysts used in reforming, even at very low concentrations [78]. In addition to natural gas, other hydrocarbons such as light liquid fractions can also be fed to reforming processes.

Formation of carbon deposits on catalyst surfaces is a common difficulty associated with reforming operations [76, 79]. Carbon is formed by the Boudoard reaction (Eq. 2) and by methane decomposition (Eq. 3). Carbon formation can be limited by the optimization of catalysts and reaction conditions and by adjusting the ratio of steam to carbon in the reformer feed [78].

$$\mathrm{2\ CO \rightleftarrows CO_2 + C} \tag{2}$$

$$\mathrm{CH_4 \rightleftarrows C + 2H_2} \tag{3}$$

The water-gas-shift (WGS) reaction is utilized in syngas processing to adjust the gas composition. The reaction is useful for changing the ratio of CO/H_2 in the product gas by the conversion of carbon monoxide and water into carbon dioxide and hydrogen, as shown in Eq. 4:

$$\mathrm{CO} + \mathrm{H_2O} \rightleftarrows \mathrm{CO_2} + \mathrm{H_2} \qquad \Delta H = -41\ \mathrm{kJ/mol} \tag{4}$$

Thermodynamically, the WGS reaction is driven to the forward direction by lower temperatures, but higher temperatures are desired for increased rate of reaction. For this reason, a system consisting of a high-temperature reactor (>350°C) followed by a low-temperature reactor (210-330°C) is often employed [75]. Iron oxide catalysts are used for the high-temperature WGS and catalysts based on copper and zinc oxide are used for the low-temperature WGS.

The partial oxidation route can be utilized for syngas production from any hydrocarbon resource. This process is used for gasification of coal at locations with vast coal reserves but limited natural gas, such as China and South Africa [77]. It is also ideal for heavy petrochemical residues unsuitable for further processing or fuel use due to high sulfur and heavy metal content. Gaseous feedstocks are only used if high amount of sulfur impurities are present, preventing reforming [78]. Equations 5 and 6 correspond to the partial oxidation of coal and methane, respectively:

$$\mathrm{C} + \tfrac{1}{2}\mathrm{O_2} \rightarrow \mathrm{CO} \quad \Delta H = -123\ \mathrm{kJ/mol} \tag{5}$$

$$\mathrm{CH_4} + \tfrac{1}{2}\mathrm{O_2} \rightarrow \mathrm{CO} + 2\mathrm{H_2} \quad \Delta H = -36\ \mathrm{kJ/mol} \tag{6}$$

The exothermic partial oxidation can be performed with or without catalysts. Without catalysts, temperatures may reach 1500°C – lower operating temperatures are applicable when catalysts are used [75]. Pure oxygen is preferably fed to the reactor to avoid dilution of the product by nitrogen. Partial oxidation of coal is combined with steam treatment (Eq. 7) and the water-gas-shift reaction (equation 4) to adjust the ratio of CO/H_2 in the product gas. Partial oxidation leads to syngas with low H_2/CO ratio, which is a disadvantage for many applications, including the production of hydrogen.

$$\mathrm{C} + \mathrm{H_2O} \rightleftarrows \mathrm{CO} + \mathrm{H_2} \quad \Delta H = 131\ \mathrm{kJ/mol} \tag{7}$$

Autothermal reforming is the combined process of steam reforming and partial oxidation. In this type of process, the heat for the steam reforming reaction (Eq. 1) is provided by the exothermic partial oxidation of the hydrocarbon feedstock. The process is carried out in a single reformer unit. The partial oxidation occurs in the thermal zone followed by reforming and possibly WGS in the catalytic zone [80]. The composition of the product gas can be controlled by the steam to carbon and oxygen to carbon ratios of the feed, and by the operating pressure. In addition to not needing external heating, the advantages of autothermal reforming over steam reforming include quick start-up and shutdown [75], compact construction and low capital costs [81]. Compared to partial oxidation processes, a more hydrogen rich syngas is produced in autothermal reforming.

2.2.2 Separation and purification of hydrogen

Various processes exist for the separation and purification of hydrogen from gas streams. The low-temperature processes utilize the low boiling point (-252.9^{o}C) of hydrogen by condensation or sublimation of impurities [82]. Methane, carbon monoxide and nitrogen are all separable by lowering the temperature of the gas mixture to the respective boiling points. Refrigeration can be provided by decompression of process streams or by external refrigeration. Scrubbing or adsorption processes performed at low-temperatures can also be performed, utilizing liquid nitrogen or methane for the removal of carbon monoxide.

Adsorption processes are effective in separating and purifying hydrogen due to the low interaction of hydrogen with commonly used adsorbents [82]. Different adsorbents used to remove particular impurities include aluminum oxides, silica, activated carbon and zeolites. Temperature-swing adsorbers are regenerated at higher temperature after capacity is reached at the adsorption temperature. Pressure-swing adsorption (PSA) is widely utilized in hydrogen purification. After adsorption at higher pressure, desorption is carried out by lowering the pressure. Hydrogen in purities of >99.9 % is commonly produced by PSA systems consisting of multiple individual adsorbers.

Catalytic processes can be employed to convert contaminants in the syngas stream either into hydrogen or into easily removable and less harmful compounds [82]. Carbon monoxide can be converted into methane by the methanation reaction (Eq. 8) or into carbon dioxide by preferential oxidation (Eq. 9) [79]. Methanation is carried out on nickel oxide catalysts and

noble metal catalysts are used for preferential oxidation. For preferential oxidation, air is fed to the gas mixture as an oxygen source.

$$\mathrm{CO} + 4\,\mathrm{H_2} \rightleftarrows \mathrm{CH_4} + 2\,\mathrm{H_2O} \quad \Delta H = -252\ \mathrm{kJ/mol} \tag{8}$$

$$\mathrm{CO} + \frac{1}{2}\mathrm{O_2} \rightarrow \mathrm{CO_2} \quad \Delta H = -283\ \mathrm{kJ/mol} \tag{9}$$

Sulfur compounds can be removed by hydrogenation to hydrogen sulfide and subsequent removal. Cobalt-molybdenum or nickel-molybdenum catalysts are commonly used for hydrogenation of organic sulfur compounds [83]. Hydrogen sulfide is then removed by scrubbing or in lower concentrations adsorbed on zinc oxide [82]. Oxygen can be removed by catalytic combination with hydrogen into water on platinum or palladium based catalysts. Nitrogen oxides can be removed by reduction to ammonia or by oxidation into nitrogen dioxide followed by alkaline scrubbing.

In physical scrubbing processes, hydrogen is purified by dissolving impurities into the scrubbing agent. In chemical scrubbing, a reaction occurs between the removed compound and the scrubbing agent. Chemical scrubbing is applied for removal of acid gases such as CO_2, H_2S and HCN. Various amine-based or caustic agents are used for scrubbing. An example of physical scrubbing is the Rectisol process, which uses methanol as a solvent for removal of sulfur compounds and carbon dioxide [84].

Membrane processes are also applicable for hydrogen purification. Efficient separation can be achieved due to the high permeability of hydrogen compared to other gases [82]. Of inorganic membranes, palladium and its alloys are effective and capable of producing hydrogen at purities of >99.99% [85]. Alloys of palladium with copper, silver and various other metals have been used. Ceramic and carbon-based membranes have also been studied. Organic, polymeric membranes are used industrially for the separation of hydrogen from mixtures with nitrogen, CO and hydrocarbons [86]. Membrane materials include polysulfone, polystyrene and poly(methyl methacrylate).

2.2.3 Thermochemical conversion of biomass

Sources of biomass include wood, crops and various wastes and residual materials including agricultural, wood, municipal, food and animal waste and residues from pulp and paper industry [87]. Biomass is an attractive energy source due to renewability and wide availability

at low cost. Use of biomass as fuel is also CO_2 neutral as the carbon dioxide emitted was originally adsorbed from the atmosphere through photosynthesis. After hydrothermal energy, biomass is the second largest renewable energy source in the world [1]. Combustion of biomass is a major source of energy especially in developing countries. Instead of direct combustion for the generation of heat, biomass can be converted into liquid and gaseous compounds for easier transport and for further conversion into various chemical products. The main thermochemical processes for the conversion of biomass are gasification and pyrolysis [88, 89].

2.2.3.1 Gasification

In gasification, biomass is decomposed at high temperatures in presence of steam to generate a gaseous mixture similar to fossil derived syngas. The product gas may be called producer gas or bio-syngas, and typically contains 28-36% CO, 22-32% H_2, 21-30 CO_2 and 8-11% CH_4 [88]. Temperatures above 800^{o}C are required to generate gaseous products from the biomass decomposition. The addition of steam leads to reforming reactions and the formation of CO and H_2. Air or oxygen may be added to enable partial oxidation, which provides heat and reduces or eliminates the need of external heating. Gasification is energy intensive because of the evaporation of the moisture present in biomass [87].

Catalytic gasification allows lower operation temperatures. Catalysts also reduce the formation of condensable organic compounds (tar), reducing operating difficulties, and convert methane to the desired CO and H_2 [90]. As fluidized bed reactors are commonly used in gasification, the catalysts have to be strong to not suffer excessive attrition. Mineral catalysts such as dolomite (mixture of magnesium and calcium carbonate) and olivine (mixture of magnesium and iron silicates) and supported metal catalysts based on nickel have been found effective [89]. Catalysts may either be used directly in the gasification step or in a separate gas purification/reforming step [90]. If hydrogen is the desired product, a WGS reactor can be employed to convert most of the CO into hydrogen [91].

2.2.3.2 Pyrolysis

Conversion of biomass into syngas-like mixtures can be performed indirectly via pyrolysis [73]. Pyrolysis is performed in the absence of oxygen at approximately 500^{o}C. In a fast pyrolysis

process, with residence time of less than 2 seconds, mostly liquid products are obtained, forming a mixture called pyrolysis oil or bio-oil [89]. The major constituents of pyrolysis oil include carboxylic acids, aldehydes, alcohols and phenolic compounds derived from lignin. The liquid can be transported and processed at a separate location. By steam reforming of pyrolysis oil, producer gas containing CO and H_2 can be produced, similarly to direct gasification of biomass. Nickel and noble metal based catalysts have been researched for this process [89]. Difficulties include tar formation and carbon deposition due to the high reactivity of the oxygen-containing components and thermal instability of the lignin derived compounds [73].

2.2.4 Electrolysis

Electrolysis is based on the dissociation of water into hydrogen and oxygen by electricity [92]. Two electrodes, a cathode and an anode, are immersed in an electrolyte solution with high ionic conductivity. A direct current flows between the electrodes, which are connected through an external circuit. Hydrogen and oxygen are generated according to the following overall reaction:

$$\mathrm{H_2O} \rightarrow \mathrm{H_2(g)} + \frac{1}{2}\mathrm{O_2(g)} \tag{10}$$

The specific cathode and anode reactions depend on the type of electrolyzer. The reduction half-reaction reaction takes place at the cathode and the oxidation half-reaction at the anode. Thus, hydrogen is generated at the cathode and oxygen at the anode. The electrodes are separated by a diaphragm, which prevents the recombination of the product gases into water. The diaphragm resists electricity but is ion conducting, allowing the passage of ions between the electrodes. Based on thermodynamics, the voltage required to operate the water splitting reaction (Eq. 10) isothermally is 1.482 V [93]. However, due to various electric and thermal losses, larger potentials are required in practice [94, 95]. The efficiency of electrolyzer systems is commonly represented by the ratio of the higher heating value of hydrogen (3.53 kWh/m^3) to the energy consumption in kWh/m^3 [92]:

$$\eta_E = \frac{\mathrm{HHV(H_2)}}{c_E} \cdot 100\% \tag{11}$$

Electrolyzer modules are built up of cells, each consisting of two electrodes and the diaphragm, connected in parallel or in series [92]. In the monopolar configuration, each cell is connected to the power supply, corresponding to a parallel installation. The same voltage is

supplied to all the cells, while the current input of the module is the sum of the individual cell currents. In the bipolar configuration, the cells are connected in series, with only the first and last cells connected to the power supply. Each electrode forms cells with the two adjacent electrodes, with the other side of the electrode acting as a cathode and the other as an anode [94]. In this case, the module voltage is the sum of the individual cell voltages while the same current goes through all the cells.

The advantage of monopolar construction is the simple and robust construction, which however, requires more space [92]. In contrast, the more compact bipolar modules require less space. Maintenance of monopolar modules is simpler, as individual cells can be disconnected while the rest of the module can remain in action. In bipolar construction, production has to be stopped and usually the whole module replaced. However, bipolar modules are generally preferred due to the large currents and resulting sizable electric losses of the monopolar design [94]. Most commercial electrolyzers are built from bipolar modules [92]. In addition to the electrolyzer module(s), the electrolysis plant needs auxiliary equipment. These include the equipment for the purification, compression and storage of hydrogen and oxygen, the power supply and the water purification equipment. Highly pure water is required for electrolysis to avoid unwanted side reactions and corrosion or fouling [94].

2.2.4.1 Alkaline electrolyzers

Alkaline electrolysis is the most mature technology for the electrolysis of water, having been widely in operation already in the early 20th century [96]. In an alkaline electrolysis cell, the electrodes are immersed in a liquid, alkaline electrolyte. A 25-30% by weight solution of potassium hydroxide is commonly used as an electrolyte. The electrodes are often based on nickel due to the combination of good electrochemical activity, resistance to alkali corrosion and affordable price [94]. Catalytic coatings with noble metals or metal oxides are often added [75]. Separating the electrodes is the diaphragm, traditionally made from asbestos. Presently, inorganic membranes have been developed for use as diaphragms [92]. The cathode and anode reactions in an alkaline electrolyzer are presented in Eq. 12 and 13, respectively:

$$2\,H_2O + 2\,e^- \rightarrow H_2(g) + 2\,OH^-(aq) \quad (12)$$

$$2\,OH^-(aq) \rightarrow \frac{1}{2}O_2(g) + 2\,e^- \quad (13)$$

The efficiency of modern alkaline electrolyzers is reportedly in the range of 62-82% [97]. Cell voltages vary from 1.8 to 2.4 volts, with maximum current densities at 0.4 A/cm^2. Current density is an important parameter of electrolyzer operation, determining the rate of electrochemical reactions in the cell [94]. Operation temperatures are commonly 60 to 80°C, and pressures can be up to 30 bar. High pressures are preferred due to the reduced need of compression of the hydrogen product. Higher temperatures generally lead to increased efficiency due to thermodynamic effects and the increased conductivity of the electrolyte [93]. Hydrogen production capacities for individual units can reach 760 Nm^3/h [97]. The purity of the hydrogen produced is up to 99.9% even without additional purification equipment [98].

2.2.4.2 PEM electrolyzers

Proton exchange membrane (PEM) electrolysis, also known as polymer electrolyte membrane or solid polymer electrolyte electrolysis, was first developed in the 1960s [99]. However, commercial use of PEM electrolyzers has been limited to niche uses in laboratories or for special purposes, e.g. on spacecraft and submarines [100, 101]. The present limitations of PEM electrolyzers are the limited capacity, short lifetime and high investment cost compared to alkaline electrolyzers [102, 103]. The advantages of PEM electrolyzers include the high current densities and the ability to operate under a wide capacity range, in contrast to alkaline electrolyzers which must generally operate at a range of 25-100% of the full capacity [92].

In PEM electrolyzers, a thin polymeric membrane with a cross-linked structure and acidic functionality acts as the electrolyte. The membrane is gas-proof, but conducts protons due to the presence of sulfonic acid functional groups. A commonly used membrane is known by the trade name Nafion, marketed by DuPont [104]. The membrane is installed between noble metal electrodes commonly made of platinum or iridium [100]. The expensive membrane and electrode materials are mainly responsible for the high capital cost of PEM electrolyzers [92]. Water is oxidized at the anode, forming oxygen, electrons and protons (Eq. 14). The protons pass through the membrane to the cathode, where hydrogen is produced (Eq. 15).

$$H_2O \rightarrow \frac{1}{2}O_2(g) + 2\,H^+(aq) + 2\,e^- \quad (14)$$

$$2\,H^+(aq) + 2\,e^- \rightarrow H_2(g) \quad (15)$$

High purity of hydrogen is obtained due to the very low gas permeability of the membrane. Purities up to 99,999% have been achieved [105]. Operating temperature is limited to 80°C for the preservation of the membrane, but pressures up to 85 bar have been used [92]. In addition, large pressure differentials can be applied between the electrodes, leading to the possibility of producing pressurized hydrogen in combination with atmospheric oxygen, if desired. Voltages in the region of 2 volts are used while current densities may reach 2 A/cm^2, increasing the efficiency of PEM units [103].

2.2.4.3 Solid oxide electrolyzers

Solid oxide electrolyzers (SOE) operate at high temperatures of 600-900°C. Electrolysis occurs in the gas and vapor phase. The high temperatures lead to high efficiencies due to favorable thermodynamic and kinetic effects [106]. Part of the electrical energy required for electrolysis is replaced by thermal energy [75]. Consequently, cell voltages as low as 1.0 V have been reported [107]. The operation of a SOE cell is based on the passage of oxygen anions through the solid electrolyte. The oxygen anions are formed, along with hydrogen, on the cathode by reduction of water (Eq. 16). On the anode, the oxygen anions form oxygen and release electrons that then circulate to the cathode (Eq. 17).

$$H_2O(g) + 2\,e^- \rightarrow H_2(g) + O^{2-} \quad (16)$$

$$O^{2-} \rightarrow \frac{1}{2}O_2(g) + 2\,e^- \quad (17)$$

The electrolyte commonly consists of a film made of yttria stabilized zirconia (YSZ: Y_2O_3-ZrO_2), which combines high oxygen ion conductivity with sufficient mechanical strength and chemical stability [108]. The electrolyte is gas-proof and avoids mixing of the hydrogen and the oxygen. Cathodes often consist of a composite of nickel with YSZ, while anodes combine YSZ with perovskites such as lanthanum manganite ($LaMnO_3$) or ferrite ($LaFeO_3$), further doped with strontium [108]. The electrodes are highly porous to maximize the contact area of the gaseous components with the solid electrodes [92]. While the high operation temperatures of SOE cells minimize the consumption of electricity, it also leads to problems with material stability. The fast degradation of SOE cells has been considered the main issue preventing commercial use [92]. In addition, the hydrogen produced is mixed with steam, requiring further separation.

2.2.5 Storage of hydrogen

While the energy density of hydrogen is very high on a mass basis (140.4 MJ/kg), compared to 47.3 MJ/kg for gasoline [109], the very low density of hydrogen leads to a small volumetric energy density. The density of hydrogen at 0°C and atmospheric pressure is 0.09 kg/m^3. This means that while 1 kg of hydrogen contains roughly the energy content of 3 kg of gasoline, a volume of 11 m^3 would be required to store this hydrogen at ambient conditions [110]. For practical purposes, hydrogen has to be compressed into much smaller volumes to increase the volumetric energy density while utilizing light enough storage methods to maintain the high gravimetric energy density. Additional difficulties in the storage of hydrogen are brought upon by the flammability of hydrogen-air mixtures at a wide composition range [111] and the reactivity and diffusivity of hydrogen in contact with various materials [112].

2.2.5.1 Compressed and liquified hydrogen

Conventionally, hydrogen is stored either as compressed gas or as liquid at low temperatures. Gaseous hydrogen is stored in high pressure cylinders often at pressures between 200 to 350 bar, with systems up to 700 bar having been developed [113]. The ideal materials for fabrication of the cylinders should possess high tensile strength combined with low density to save weight. The materials should also not react with or allow the diffusion of hydrogen [110]. Conventionally, stainless steel and alloys of copper and aluminum have been used, leading to quite heavy systems. With these types of containers, only approximately 1% of the total system weight is hydrogen [113].

Newer composite materials consist of an inner polymer or metal liner surrounded by a strong carbon fiber composite structure. Higher storage pressures at lower cylinder weight have been achieved with these types of cylinders, with the mass-based hydrogen content up to 5 times that of metal cylinders [113]. For automotive applications, compressed gaseous storage of hydrogen is currently the established option [114].

Hydrogen can be stored as liquid at temperatures of -252°C and below at ambient pressure [115]. The density of liquid hydrogen is 70.8 kg/m^3. The energy-intensive liquefaction of hydrogen is carried out by the Joule-Thomson cycle consisting of compression followed by isenthalpic expansion in a throttle valve. The energy required for liquefaction is approximately one third of the chemical energy stored in hydrogen, based on the higher heating value of

hydrogen [116]. Heat leaking into the storage vessel causes evaporation of hydrogen, leading to boil-off losses. The losses are inversely proportional to the size of the vessel, due to the decreasing surface-to-volume ratio. The losses are in the order of 0.4%/day for well insulated tanks of 50 m^3 in volume, and 0.06%/day for tanks of 20,000 m^3 [110]. Because of these losses, liquid hydrogen storage is only applicable for relatively short storage periods.

2.2.5.2 Physisorption

Hydrogen molecules can be adsorbed onto solid surfaces by the effect of dispersive Van der Waals forces. Due to the weak interaction between the gas molecules and the atoms on the solid surface, significant adsorption only occurs at low temperatures and high temperatures [114]. Either temperatures only reachable by liquid nitrogen cooling (-196^{o}C) or pressures exceeding 50 bar have been employed in the experimental work. Highly porous materials with large specific surface areas and pore sizes below 2 nm are ideal for use as adsorbents. Carbon materials such as activated carbon, carbon nanotubes and graphene have been widely studied, along with zeolites. More recently, microporous polymers [117] and metal-organic frameworks [118] have been proposed, reaching hydrogen storage capacities of up to 7% by weight. Even if low temperatures and/or high pressures are required, physisorption has been considered a promising method - particularly compared to liquefied hydrogen [114].

2.2.5.3 Metal and complex hydrides

At elevated temperatures, hydrogen reacts with transition metals and their alloys, forming hydrides in which hydrogen atoms occupy vacancies in the metal lattice structure [110]. By alloying two or more metals, the properties of the resulting hydrides can be modified. Often a rare earth or an alkaline earth metal (forming stable hydrides) is combined with a transition metal (forming unstable hydrides). The reaction of hydrogen with the metal is exothermic, and heat is required for the endothermic desorption. Desorption temperature is related to the stability of the hydride. For a stable MgH_2, 300^{o}C is required, while some hydrides can be absorbed and desorbed at ambient temperature. Metal hydrides can reach high volumetric hydrogen densities: for example, 115 kg/m^3 for $LaNi_5$-hydride. However, the gravimetric hydrogen densities are limited to a maximum of 3 %.

In complex hydrides, hydrogen forms a complex anion by binding covalently to the central atom, which is one of the light metals Li, Mg, B or Al [110]. The complex anion is then ionically bonded to a cation, forming a salt-like material. Many of the complex hydrides have excellent gravimetric and volumetric hydrogen densities [119]. For example, lithium borohydride ($LiBH_4$) contains 18% of hydrogen by weight. However, borohydrides have been found too stable, requiring high desorption temperatures [114]. Complex aluminum hydrides such as $NaAlH_4$ have the advantage of lower stability. Another class of complex hydrides consists of the amides such as $LiNH_2$ [120].

2.2.5.4 Liquid hydrogen carriers

Liquid hydrogen containing compounds would be simple to use and transport compared to gaseous hydrogen [121]. Organic molecules such as hydrocarbons, alcohols and formic acid have been suggested as potential hydrogen carriers. Further, specialized compounds with high hydrogen content have been researched, an example being N-ethylperhydrocarbazole (H_{12}-NEC) [119]. This compound contains 5.8% of hydrogen by weight and can be quantitatively dehydrogenated, forming N-ethylcarbazole (NEC) and releasing 6 mol of hydrogen in the process. The hydrogenation/dehydrogenation cycle can be repeated by applying suitable catalysts [122].

Hydrogen can be released from hydrocarbon and alcohols by reforming [114]. The reforming reactions are similar to the steam reforming and partial oxidation of methane, as shown in Eq. 1 and 2. The concept is based on integrating the functionality of a large-scale reforming plant into a small fuel processing unit, capable of providing hydrogen for use in fuel cells. The fuel processing unit should ideally be compact enough to be installed onboard vehicles. As in large-scale hydrogen production, the reforming or oxidation process is followed by water-gas shift reaction and preferential oxidation Eq. (9), leading to a complex system requiring multiple catalysts. The residual concentration of CO must be low to allow operation of the fuel cell. High temperatures (<600^{o}C) are required for reforming of hydrocarbons, creating further difficulty in mobile operation.

Reforming of alcohols, such as methanol and ethanol, for the generation of hydrogen has also been researched [123, 124]. The advantage of alcohol, especially methanol, reforming would be the lower temperatures (250-300^{o}C) required. Also, CO concentration of <1% has been

observed in the reforming products, making fuel cell operation possible without the water-gas shift reaction and only the preferential oxidation step [123]. The catalysts for methanol reforming are similar to methanol synthesis catalysts; the reforming reaction is essentially a reverse methanol synthesis reaction [114]. Due to the lower operating temperatures, methanol reforming has been considered a more promising option compared to hydrocarbon reforming. However, instead of fuel processing of methanol followed by use in a hydrogen fuel cell, methanol can also be used in direct methanol fuel cells (DMFC) [125], allowing more straightforward and possibly more effective operation.

Formic acid contains 4.4% by weight and 52 grams per liter of hydrogen and can be decomposed into hydrogen and carbon dioxide under relatively mild conditions [119]. Formic acid can be synthesized from carbon dioxide electrochemically and by catalytic hydrogenation [126]. For the decomposition reaction, both homogeneous and heterogeneous catalysts have been developed, both often based on noble metals. In addition to formic acid, hydrogenation/dehydrogenation cycles based on various other compounds have been proposed. Examples include decalin (7.2 w-% hydrogen), cyclohexane (7.1 w-% hydrogen), and methylcyclohexane (6.1 w-% hydrogen) [114]. For these compounds, dehydrogenation temperatures over 300^{o}C would be required and the hydrogenation could only be carried out at a centralized, industrial facility. However, the technology is available and promising for non-transport, stationary applications.

2.2.6 Distribution of hydrogen

Most of the hydrogen consumed by industry is produced on-site, avoiding the need of transportation [112]. For applications and users requiring lower quantities of hydrogen, the hydrogen is transported either as compressed gas or as liquid. Gaseous hydrogen is transported via pipelines or by road or rail. For example, a hydrogen pipeline with a total length of 208 km, operating at a pressure of 22 bar, was built in Germany already in 1938. In cylinders or larger transportation vessels, gaseous hydrogen can be delivered at pressures of 200 bar, carried either by trucks or on railroad. Alternatively, liquid hydrogen can be transported in dewars for smaller uses and in transportation tanks in larger quantities. The liquid hydrogen is evaporated at the delivery site. Transportation of liquid hydrogen over oceans by tankers has been proposed and smaller scale transport by barges has already been performed [70].

Transportation of gaseous hydrogen is limited by the low energy density. Due to the heavy construction of the pressure cylinders or vessels, only a fraction of the total transported weight is hydrogen. It has been estimated, that a 40-ton truck can carry 350 kg of hydrogen compressed to 200 bar – this means that it would take 22 loads to deliver the amount of energy contained in a single truckload of gasoline [127]. In addition, only approximately 80% of the hydrogen can be transferred from the transportation vessel at the delivery site, with the remaining 20% returning to the supplier.

In case of liquid hydrogen, the higher density allows more hydrogen to be transported, leading to higher transportation efficiency. The boil-off losses of liquid hydrogen would, however, limit the transportation times and distances. Pipelines are considered the most cost effective means of transportation, with the road or rail transport of liquid hydrogen estimated 5 times and gaseous hydrogen 50 times as expensive [112]. Compared to natural gas, 3.5 to 4 times the amount of compression energy would be required to deliver the same energy content through the pipeline due to the lower volumetric energy density of hydrogen. The energy of compression is commonly provided by gas removed from the pipeline [127]. Thus, for hydrogen, up to 4 times the material loss per distance of pipeline would be encountered compared to natural gas.

2.3 Methane

Methane, being the main component of natural gas, is an important part of the current energy and chemical infrastructure. Thus, increasing the role of methane as an energy carrier could be performed rather smoothly by utilizing the existing natural gas pipeline and storage facilities. In addition to the infrastructure advantages, the main advantage of methane over hydrogen is the higher volumetric energy density, which is three times that of hydrogen [21]. Methane can be converted into electricity either by combustion in gas turbines or possibly by using solid electrolyte fuel cells [21].

Other than from natural gas, methane can be produced by the hydrogenation of CO or CO_2 and by anaerobic digestion. Syngas generated from fossil feedstocks or by gasification of biomass and also captured CO_2 can constitute carbon sources for hydrogenation. By anaerobic digestion, organic waste can be converted into a methane containing biogas. The production of methane from biomass and organic waste would be preferable from the environmental standpoint, as the methane produced would be essentially carbon neutral. However, the energy

required for the production, and convertion of the biomass has to be considered when the overall environmental effects are considered.

The methanation of CO_2 proceeds by the Sabatier reaction, as shown in Eq. 18:

$$\mathrm{CO_2} + 4\,\mathrm{H_2} \rightarrow \mathrm{CH_4} + 2\,\mathrm{H_2O} \quad \Delta H = -165{,}0\ \mathrm{kJ/mol} \tag{18}$$

The catalytic reaction is utilized in the purification of syngas from CO and CO_2 in the production of hydrogen and ammonia and is commonly performed on nickel based catalysts [128]. The reaction is also used in the synthesis of methane for the production of substitute natural gas (SNG). In comparison to the methanation of CO, the utilization of the Sabatier is hindered by kinetic limitations, fueling the research for more active catalysts for the methanation of CO_2 [129]. In addition to more advanced nickel catalysts, noble metal catalysts have been researched. The reaction mechanism of both CO and CO_2 methanation is much discussed and not entirely clear [129]. Currently, the overall energy efficiency of direct hydrogenation of CO_2 to methane is estimated at 75% [21].

2.4 Liquid hydrocarbons

The Fischer-Tropsch (FT) synthesis of hydrocarbons from syngas is a mature technology. In Germany, industrial scale FT plants started operation in the 1930s and the technology was utilized at a substantial scale during the Second World War for the production of liquid fuels from coal [130]. Commercial operation has been limited since the second half of the 20th century. The plants operated by SASOL in South Africa, with the first of three facilities commissioned in 1955, are the best known example of the commercial use of this technology [130]. More recently, much effort has been put into the development of FT facilities in China. In both of these countries, the motivation has been to utilize the vast available coal resources for the production of fuels, with the aim of limiting the dependence on foreign oil. Recently, large-scale plants have also been commissioned in Qatar and Nigeria [131]

In conventional Fischer-Tropsch synthesis, syngas generated is catalytically converted into a range of products mostly consisting of liquid hydrocarbons [130]. A mixture of hydrocarbons is always obtained as a product, with the components ranging from methane to long-chain waxes. Only methane can be selectively obtained, with the other fractions following a statistical distribution as dictated by the chain-growth reaction mechanism [132, 130]. Fractionation and refining of the reaction products is required to obtain usable final products, such as gasoline

and diesel. Oxygenated products such as alcohols, aldehydes and ketones may also be generated. Equations 19 and 20 show the respective formation of alkanes and alkenes in the FT process:

$$2\mathrm{n}\ \mathrm{H_2} + \mathrm{n}\ \mathrm{CO} \rightarrow \mathrm{C}_n\mathrm{H}_{2\mathrm{n}} + \mathrm{n}\ \mathrm{H_2O} \quad (19)$$

$$(2\mathrm{n}+1)\ \mathrm{H_2} + \mathrm{n}\ \mathrm{CO} \rightarrow \mathrm{C}_n\mathrm{H}_{2\mathrm{n}+2} + \mathrm{n}\ \mathrm{H_2O} \quad (20)$$

The product distribution is affected by the catalyst, temperature, pressure and ratio of H_2/CO [133]. Higher temperatures (330-350 °C) are used for the production of gasoline and light alkenes, while lower temperatures (220-250 °C) lead to the formation of waxes and diesel fuel as the main products [130]. Various types of reactors have been used, including fixed-bed, fluidized bed and slurry reactors, with different types of reactors suitable for different operating temperatures [133, 130]. The catalysts for Fischer-Tropsch synthesis are mostly based on iron or cobalt. Cobalt catalysts are generally more suited for low-temperature FT, yielding longer chain products, while iron catalyst are used at higher temperatures for the production of gasoline and alkenes [134].

The hydrogenation of CO_2 into hydrocarbons can be considered a modification of the Fischer-Tropsch process [17]. CO_2 can be converted into hydrocarbon products either by direct hydrogenation or via RWGS followed by conventional, syngas based, FT synthesis. When CO_2 instead of CO is used as feedstock, a significant change in catalyst activity has been observed, with the cobalt based catalysts found to produce mainly methane [17, 135, 136]. However, on iron catalysts, the product distribution has been found to be similar for the hydrogenation of both CO and CO_2. With iron-based catalysts, CO_2 can be effectively hydrogenated into short-chain alkenes at around 80% selectivity with conversion up to 68% reported [135].

Alternative routes to synthetic hydrocarbons include the gasification of biomass followed by FT synthesis or the conversion of methanol, which is presented in Section 2.4.2. Related, biodiesel type products can be obtained by transesterification or hydrogenation of plant oils. However the production of energy crops in competition with food production is not necessarily sustainable at a large scale [21]. Regardless of the raw material, the hydrocarbon products are very advantageous because of high energy density and the compatibility with the existing infrastructure.

2.5 Methanol and derived products

Methanol is both a capable fuel and an important feedstock chemical. The main chemical products derived from methanol are formaldehyde and acetic acid, corresponding to 25% and 8% of the estimated demand of methanol in 2016 [137]. Other important uses include the conversion to alkenes (the MTO process) with 22%, fuel uses (conversion to or blending with gasoline) with 16%, the production of dimethyl ether (DME) with 8% and the production of fuel additives methyl tert-butyl ether (MTBE) and tert-amyl methyl ether (TAME) with 7% of the 2016 demand, respectively. Methanol is also used as solvent and converted into chemical products such as dimethyl terephthalate (DMT), methylamines and methyl methacrylate (MMA), among many others [138]. The total demand of methanol in 2016 has been estimated at close to 100 million tons [137].

Methanol can be blended with gasoline and even pure methanol fuel can be used to power internal combustion engines. The favorable fuel properties of methanol include high octane number [14], high efficiency and low NOx, hydrocarbon and CO emissions [139]. Disadvantages include low energy density compared to gasoline (see Section 2.6), increased formaldehyde emissions and high vapor pressure [140]. Engine and fuel system modifications are also required because of corrosion and wear issues associated with methanol fuel [141]. For conversion into electricity, methanol can be combusted in gas turbines [139] or used in fuel cells, either by reforming to hydrogen for hydrogen fuel cells [79], or used in direct methanol fuel cells [125, 142].

2.5.1 Dimethyl ether

Methanol can be converted into dimethyl ether (DME), which is a promising diesel fuel substitute [15]. The production of DME is related to methanol synthesis, as methanol is an intermediate in the synthesis DME. DME is produced by the dehydration of methanol on acidic catalysts, as shown in Eq. 21:

$$2\ \mathrm{CH_3O}H \ \rightleftarrows \mathrm{CH_3OCH_3} + \mathrm{H_2O} \quad \Delta H = -23{,}5\ \mathrm{kJ/mol} \tag{21}$$

Commonly, adiabatic reactors with γ-Al_2O_3 as catalyst are used [143]. The reaction equilibrium is affected by the reaction conditions, with typical conversions of 70-85% achieved at 250-400 °C [143]. In separate DME synthesis, pure methanol is fed to the dehydration reactor.

Alternatively, the process can be integrated with the synthesis of methanol and subsequent hydration to DME occurring in single reactor, using a combination of methanol synthesis and dehydration catalysts [17, 144]. Further, the direct synthesis of DME from syngas is also possible, based on the alternative reactions shown in Eq. 22 and 23 [17]:

$$2\,CO + 4\,H_2 \rightleftarrows\ CH_3OCH_3 + H_2O \tag{22}$$

$$3\,CO + 3\,H_2 \rightleftarrows\ CH_3OCH_3 + CO_2 \tag{23}$$

With a boiling point of -24,8 °C, DME is a colorless, non-toxic gas at ambient conditions [145]. DME is soluble in most organic solvents and partly soluble in water (76 g/dm^3 at 18 °C) [145]. The industrial uses of DME include the reaction with sulfur trioxide to form dimethyl sulfate, the production of acetic acid by reaction with carbon monoxide and the use as a propellant and solvent in aerosol products. DME is also a potential alternative fuel as a substitute for diesel oil for compression ignition engines. According to Arcoumanis, et al., DME possesses the following advantages as a fuel [15]:

1. The high oxygen content (34,8% by mass) and the absence of C-C bonds leads to smokeless, particulate free combustion.
2. The low boiling point leads to instant evaporation in the cylinder, allowing low injection pressure.
3. High cetane number (above 55, compared to 40-50 for diesel fuel) resulting from the low auto-ignition temperature and instant evaporation.

The cetane number is a relative rating of the auto-ignition capability of fuels, measuring the time delay of combustion following fuel injection [146]. The reported disadvantages of DME fuel include the low combustion enthalpy compared to diesel fuel and low viscosity. [15]. The low combustion enthalpy corresponds to low energy density (see Section 2.6), while the low viscosity leads to leakage from the fuel system. DME can be condensed and stored as a liquid at pressures above 5 bar. Careful handling is required due to the gaseous state at ambient conditions and the wide flammability range (3.4-18.6% by volume) [15]. In comparison to diesel fuel, fuel consumption has been found only slightly higher with DME. The emissions of particulates and NOx are lower, while the hydrocarbon and CO emissions have been reported lower than or equal to diesel fuel [15].

The practical use of DME as a diesel fuel replacement has been demonstrated by Volvo [147] by a test run of slightly modified diesel trucks on DME. Interestingly, the DME was produced from gasified black liquor, showcasing the possibility of producing DME from renewable, biomass derived materials.

2.5.2 Conversion of methanol to hydrocarbons

Furthermore, methanol can be converted into hydrocarbon fuels or base chemicals [148]. The methanol-to-gasoline (MTG) process enables the conversion of methanol into hydrocarbons in the gasoline range [149], while in the methanol-to-olefins (MTO) process alkenes are obtained as the main product [150]. The short-chain alkenes ethene and propene are important feedstock chemicals for the polymer industry. These processes allow the production of important hydrocarbon compounds from raw materials other than the conventional petroleum oil.

In the MTG process, methanol is reacted on H-ZSM-5 type of zeolite catalyst, forming a mixture consisting of saturated, unsaturated and aromatic hydrocarbons, mostly in the gasoline range. The synthetic gasoline produced is of high quality and contains no sulfur or nitrogen [149]. A significant amount of water is formed as byproduct, as the reaction proceeds through the dehydration of methanol into DME, followed by further dehydration of DME [148]. The distribution of products is affected by the reaction conditions. Reaction temperatures are commonly in the range of 300 to 450 °C [149].

The process was commercially operated in Motunui, New Zealand from 1986 until 1996 [151, 149]. The capacity of the plant was 570,000 t/a of gasoline, satisfying one third of the gasoline demand of New Zealand. Natural gas was used as raw material, with the first stage of the process being the synthesis of methanol. Following dehydration to DME, hydrocarbons were formed on the ZSM-5 catalyst at 19-23 bar of pressure. At complete methanol conversion, a yield of 56% of water and 44% of hydrocarbons by weight was obtained, with up to 90% of the hydrocarbon products in the gasoline range. The process was highly energy efficient, with the overall efficiency reported at 92-93%. 95% of the energy content of the methanol feed was preserved in the final product. In China, a MTG plant based on coal started operation in 2009 [149]. The planned capacity of the plant is 100,000 t/a, with the process yielding 387 t of gasoline, 46 t of LPG (liquefied petroleum gas) and 560 t of water from 1000 t of methanol.

The MTO process is a variation of the MTG process, with the product selectivity adjusted towards short-chain alkenes [150]. The main conventional route to these compounds is steam-cracking of naphta, a process in which the oil derived feedstock is mixed with steam and heated above 800 °C for pyrolysis. The MTO process allows a wider range of feedstocks combined with lower energy consumption and CO_2 emissions. Additionally, the alkene products are of higher, polymer-grade purity.

As the mechanism of conversion of methanol to alkenes is similar to the MTG process, zeolite catalysts have also been used in the MTO process [148, 150]. Particularly the silicoaluminophosphate SAPO-34 has been found effective, however the ZSM-5 catalyst used in MTG is also used. The ZSM-5 catalyst shows a particularly high selectivity to propene [152]. A two-step process with the initial methanol dehydration stage followed by the hydrocarbon conversion stage is usually employed. Higher temperatures in the conversion stage compared to the MTG process lead to increased alkene selectivity.

Commercial MTO technology is provided by UOP, ExxonMobil and Lurgi [152]. The processes by UOP and ExxonMobil are based on the SAPO-34 or similar catalysts, operating at temperature range of approximately 350 to 500 °C. The ExxonMobil process yields 14% ethene and 18% propene, while the UOP process employs a further upgrading step, yielding 26% ethene and 33% propylene. The ExxonMobil process additionally yields 29% of gasoline. The Lurgi process uses the ZSM catalyst at 400-450 °C, yielding 46% propylene and no ethylene with a gasoline yield of 20%. The MTO technology has recently seen rise in China, with 16 separate facilities due for start-up in 2012 to 2015, with total capacity of 10 million tones/year [150].

2.6 Ethanol

Similarly to methanol, ethanol is a versatile compound with uses as both a feedstock chemical and a fuel [153]. The chemical intermediates derived from ethanol include acetaldehyde, butadiene, ethyl acetate and ethylamines. Some of the intermediate chemicals produced from ethanol can replace petroleum based raw materials, with examples being acetaldehyde and ethylene. Ethanol is the most important solvent after water, with major use in the manufacture of household and food products and pharmaceuticals [153]. Ethanol is also an important fuel component, being currently mixed with gasoline in various ratios in many countries. The most traditional use of ethanol is as the functional component in alcoholic beverages.

Ethanol has been produced by the fermentation of carbohydrates for thousands of years; the concentration of ethanol by distillation dates back to the 14th century or earlier [153]. Currently, in most countries, the ethanol produced by fermentation is mostly consumed in alcoholic beverages. In Brazil and India, fermentation ethanol is also used for chemical purposes. The largest producers of fermentation ethanol are the US, where production is based on corn, and Brazil, where sugar is used as raw material. The use of food crops for the production of ethanol is problematic due to competition with food production. The utilization of alternative, more sustainable raw materials including lignocellulosic biomass and municipal waste have been researched [154, 155] In addition to fermentation, ethanol can be produced by chemical processes. The major commercial route is the catalytic hydration of ethane on acidic catalysts:

$$\mathrm{C_2H_4 + H_2O \rightleftarrows C_2H_5OH} \quad \Delta H = -43.4\ \mathrm{kJ/mol} \tag{24}$$

Ethanol can also be derived from methanol by homologation (Eq. 25). In the homologation reaction, an alcohol is reacted with syngas leading to an increase in chain length of the alcohol [153]. The reaction is not selective to ethanol as higher alcohols and other side-products are also formed.

$$\mathrm{CH_3OH + CO + 2\ H_2 \rightarrow C_2H_5OH + H_2O} \tag{25}$$

The direct conversion of syngas into ethanol is closely related to the methanol synthesis and Fischer-Tropsch processes. Both modified methanol synthesis catalysts (based on Cu) and modified Fischer-Tropsch catalysts (based on Fe, Ni, Co) have been studied for the synthesis of ethanol [156, 157, 153, 158]. Catalysts based on noble metals and Mo have also been examined [156, 158]. However, the conversion of syngas to ethanol at high selectivity and yield has not been achieved, with the formation of ethanol accompanied by side-products such as methane, methanol and higher alcohols [156, 158]. Similar catalysts have been researched for the hydrogenation of CO_2 to ethanol, but similarly, the selectivity and yield of ethanol has been limited [17].

Ethanol can be blended with both gasoline and diesel to fuel internal combustion engines [159]. Blended with gasoline, ethanol increases the octane number of the fuel blend, replacing octane boosting additives such as MTBE and TAME [157]. Ethanol is also an effective fuel by itself. Ethanol-gasoline mixtures are commonly distributed as transportation fuel in many countries, both in low-ethanol mixtures such as E10 (10% ethanol) which can be readily used in

conventional gasoline powered engines, and in high-ethanol mixtures such as E85 (85% ethanol) which can be used in specialized engines [160, 161, 162]. Some modifications to the fuel supply system are required for high-ethanol blends due to corrosion issues [157]. The blending of gasoline with ethanol generally improves the engine performance and lowers emissions [159, 155]. While the blending of ethanol with diesel fuel is not as widely practiced, beneficial effects such as lower emissions have been observed [159, 163].

2.7 Comparison of energy carriers

When comparing the potential energy carriers, the following general requirements should be considered [21]:

1. The gravimetric and volumetric energy density should be as high as possible.
2. The compound should be simple and economical to handle, transport and store.
3. The toxicity and flammability should be low.
4. High cycle efficiency, the ratio of electricity generated from the compound compared to the electricity consumed in the production of the compound

The last point is applicable when the energy carrier is to be used for storage of electricity. For fuel compounds, the energy efficiency of production should be as high as possible. In addition to these requirements, economic and infrastructure factors also need to be considered. It is clear that no single compound can completely fulfill all the requirements. Table I presents the gravimetric and volumetric energy densities and the estimated cycle efficiency of the potential energy carriers, compared to gasoline and diesel [159, 21].

Table I. The gravimetric and volumetric energy density and the cycle efficiency (the conversion of electricity to the compound followed by reconversion to electricity) of potential energy carriers compared to gasoline and diesel fuel. Data from 1) Schüth, 2011 **[21]** and 2) Agarwal, 2007 **[159]**.

Compound	Gravimetric energy density, MJ/kg	Volumetric energy density, MJ/dm^3	Cycle efficiency, %
Hydrogen[1]	120	0.0107 (gas), 8.52 (liquid at 20,4 K)	~30%
Methane[1]	50	0.0357(gas), 21 (liquid at 111 K)	~25%
Synthetic hydrocarbons[1]	43	35	~20%
Ethanol[1]	27	21	-
Methanol[1]	20	16	~20%
DME[2]	29	19	-
Gasoline[2]	43	32	-
Diesel[2]	42	36	-

While the gravimetric energy density of gaseous hydrogen and methane is high, the volumetric energy density is very low compared to the liquid alternatives. From the energy density comparison, methane is superior to hydrogen with the volumetric energy density approximately three times that of hydrogen. For the liquid energy carriers, the gravimetric storage density is more important. Especially in mobile applications, the amount of fuel carried is generally limited by weight, and not by volume. The advantage of liquid hydrocarbons over alcohols is clear, as the gravimetric energy density of hydrocarbons is over double that of methanol. Even the difference between methanol and ethanol is quite significant, the gravimetric energy density of ethanol being 35% higher.

From the cycle efficiency, it is noted that hydrogen is the most efficient alternative, leading to the lowest energy losses in the conversion and reconversion cycle of electrical energy. This is logical considering that hydrogen can be directly produced from primary energy sources while the alternatives require a second conversion step. In this step, hydrogen is used as a reactant when the compounds are produced via the hydrogenation route. From this standpoint, the use of hydrogen for the production of hydrocarbon or alcohol energy carriers seems counter-intuitive, since the hydrogen could be directly used at higher efficiency.

However, considering the difficulties in hydrogen storage and transportation, the conversion of hydrogen to liquid compounds could be justified. Even if both exist as gases in ambient conditions, the handling of methane and DME is simpler compared to hydrogen due to higher volumetric density in the gaseous state and lower pressure required for liquefaction, both points making high pressure storage unnecessary. The requirement of a presently nonexistent hydrogen infrastructure also complicates the large-scale application of hydrogen.

The infrastructure already exists for methane (pipelines, underground storage facilities) and especially for liquid hydrocarbons. For alcohols, the existing distribution networks could probably be utilized to some degree, with the amount of modifications and redevelopments required not quite clear. The proponents of the methanol economy consider the existing infrastructure essentially compatible with methanol [164], while others maintain that a whole new system would be required [21]. In terms of infrastructure demands, significant differences would not be expected between different alcohols.

For the liquid energy carriers, the choice exists between hydrocarbons and alcohols. Due to the higher energy density of hydrocarbon fuels, their use will probably remain necessary in some transportation uses, especially in aviation. For large scale energy storage including the storage of electricity, the high energy density is also advantageous. The alcohols methanol and ethanol would seem suitable fuels primarily for road traffic. Both have been found capable fuels for internal combustion engines, providing good engine performance and low emissions. The fuel characteristics of ethanol are better than those of methanol: the energy content is higher, volatility lower and solubility in hydrocarbons better [157]. Further, ethanol is less corrosive to engine parts [157] and much less toxic than methanol. The present use of fuel ethanol is dependent on the fermentation of food crops, which is not sustainable at a massive scale. Alternative raw materials would be preferred for increasing production: lignocellulosic materials

would be abundantly available, and the processes for the utilization of this type of feedstock are developing.

The advantage of methanol over synthetic hydrocarbons and ethanol is the highly selective and comparably energy efficient synthesis route, presently from synthesis gas and potentially from CO_2 in the near-medium term. Methanol is also highly versatile, as it can be readily converted into various useful chemicals. Through the methanol-to-gasoline process, hydrocarbon fuels and chemicals are attainable from methanol. Methanol can also be converted into DME, which shows potential as a diesel fuel replacement.

Considering the safety of production, handling and use, the gaseous hydrogen, methane and DME seem most hazardous from the flammability and explosiveness standpoint, while methanol is generally viewed as the most toxic of these compounds. However, all the potential fuels are flammable and liquid hydrocarbons are not much less toxic than methanol. It is clear that careful handling of all the compounds is required. The greatest environmental risks might be associated with the liquid hydrocarbons (evidenced by the witnessed major releases to environment) and also methane in case of major leaks, due to the strong greenhouse gas effect [165].

Essentially, not a single compound should be chosen to act as a universal energy carrier for all uses. Rather, different compounds should be used for different purposes and at different locations, taking the local economic and political factors into account. Gaseous and liquid energy carriers with compatibility to the existing energy infrastructure could be used to gradually replace petroleum fuels. Methane, synthetic hydrocarbons and alcohols would probably suit this purpose. While the use of fossil fuels is continued, the technologies for the capture and utilization of CO_2 and the use of renewable raw materials should be advanced. As the technology for renewable hydrogen generation advances, hydrogen will be economically and sustainably available for conversion processes. In the long run, hydrogen would probably be the ideal energy carrier, providing the development of more efficient storage and distribution systems.

Finally, the versatility of the compound and its potential uses should be considered when comparing the alternatives. Some of the compounds discussed have various, existing uses both as a fuel and as a chemical feedstock or intermediate. A summary of these uses is given in Table II.

Table II. Various fuel and chemical uses of the discussed energy storage compounds.

Compound	Fuel uses	Chemical uses	Other uses
Hydrogen	Heat and power generation by combustion Production of electricity in fuel cells	Synthesis of ammonia and methanol Petroleum processing (hydrocracking and other reactions) Fischer-Tropsch synthesis Hydroformulation reactions (alkenes to alcohols and aldehydes) Steel production (reduction of iron ore)	
Methane	Heat and power generation by combustion	Production of synthesis gas	
Liquid hydrocarbons	Powering internal combustion engines (gasoline and diesel ranges)		Synthetic lubrication oils
Methanol	Heat and power generation by combustion Blending with gasoline Electricity from direct methanol fuel cells (in development) Production of fuel additives (MTBE, TAME)	Synthesis of formaldehyde, acetic acid and dimethyl ether Production of various other chemicals including dimethyl terephtalate (DMT), methylamines and methyl methacrylate (MMA) Conversion to gasoline range hydrocarbons and alkenes by MTG and MTO processes	Solvent
Dimethyl ether	Diesel fuel substitute for compression ignition engines		Aerosol propellant
Ethanol	Fueling internal combustion engines (mixed with gasoline)	Derivatives include acetaldehyde, butadiene, diethyl ether, ethyl acetate and ethylene	Alcoholic beverages Solvent

3 METHANOL SYNTHESIS

Methanol, both an important feedstock chemical and a fuel component, is currently produced at an annual rate nearing 100 million tons [137]. The industrial production of methanol is based on the conversion of syngas generated from fossil raw materials. The technology of methanol synthesis is quite mature, with commercial synthesis beginning in the 1920s and the modern catalysts and processes based on the developments made in the 1960s [139]. The production of methanol by the hydrogenation of CO_2 is an interesting route due to the possibility of converting carbon dioxide into a useful and large scale chemical and energy product. Certain challenges do, however, exist with the synthesis of methanol from CO_2 and resultantly the process has so far not seen commercial importance. Ongoing research on catalysts and process technologies seeks to overcome these difficulties, aiming to commercialize hydrogenation of CO_2 into methanol at large scale. This chapter presents an overview of methanol synthesis, starting from the conventional production and then progressing to the synthesis from CO_2. In the later part of this chapter, particular focus is given to the liquid-phase, alcohol promoted methanol synthesis method, which is one of the technologies with potential to allow more efficient production of methanol from CO_2.

3.1 Conventional methanol synthesis

Commercial methanol production is based on the processing of syngas generated from fossil raw materials, mainly natural gas and coal. Different syngas generation processes, such as steam reforming, partial oxidation and autothermal reforming are used depending on the available feedstock and the plant capacity. These processes are presented in more detail in Section 2.1.1. While steam reforming of methane is commercially the most important process, the gasification (partial oxidation) of coal is gaining significance especially in countries with vast coal resources, such as China. In fact, China has become the largest producer of methanol, with most of the production based on coal [166].

Synthesis gas consists of mixtures of CO, CO_2, H_2, H_2O and CH_4 at varying compositions. The composition is dependent on both the feedstock and the gas generation process. Steam reforming produces syngas rich in hydrogen, while coal gasification produces more CO-rich syngas. The stoichiometric number (SN), defined by the ratio $(H_2\text{-}CO_2)/(CO+CO_2)$ is an important parameter concerning the intended use of the gas [139]. For methanol production, a SN of slightly above 2 is optimal, following the reaction stoichiometry of methanol synthesis

with a slight excess of hydrogen. The hydrogen content can be adjusted by the water-gas shift reaction. Purification of syngas from trace impurities such as sulfur and arsenic is also required, as these contaminants cause poisoning of the catalysts used in methanol synthesis.

3.1.1 Reaction system

The major reactions occurring in methanol synthesis are the hydrogenation reactions of CO and CO_2 to methanol and the reverse water-gas shift reaction (RWGS) [139, 158]:

$$\mathrm{CO} + 2\,\mathrm{H_2} \rightleftarrows \mathrm{CH_3OH} \quad \Delta H = -90{,}77\ \mathrm{kJ/mol} \tag{26}$$

$$\mathrm{CO_2} + 3\,\mathrm{H_2} \rightleftarrows \mathrm{CH_3OH} + \mathrm{H_2O} \quad \Delta H = -49{,}16\ \mathrm{kJ/mol} \tag{27}$$

$$\mathrm{CO_2} + \mathrm{H_2} \rightleftarrows \mathrm{CO} + \mathrm{H_2O} \quad \Delta H = -90{,}77\ \mathrm{kJ/mol} \tag{28}$$

As both of the hydrogenation equilibrium reactions are exothermic and result in a decrease in the number of molecules, the formation of methanol is favored by low temperatures and high pressures. However, increased temperatures lead to higher rate of reaction, which means that operating temperatures are a compromise between kinetic and thermodynamic effects. The equilibrium is also dependent on the feed gas composition, with higher CO_2 content leading to lower equilibrium conversion. Figure 4 shows the equilibrium conversion of CO and CO_2 with hydrogen at temperatures 180-260 °C and pressures of 40 and 60 bar [167]. However, the presence of some CO_2 has been found essential both for methanol productivity and catalyst stability [140]. In practice, syngas containing 2-8% of CO_2 is typically used [140].

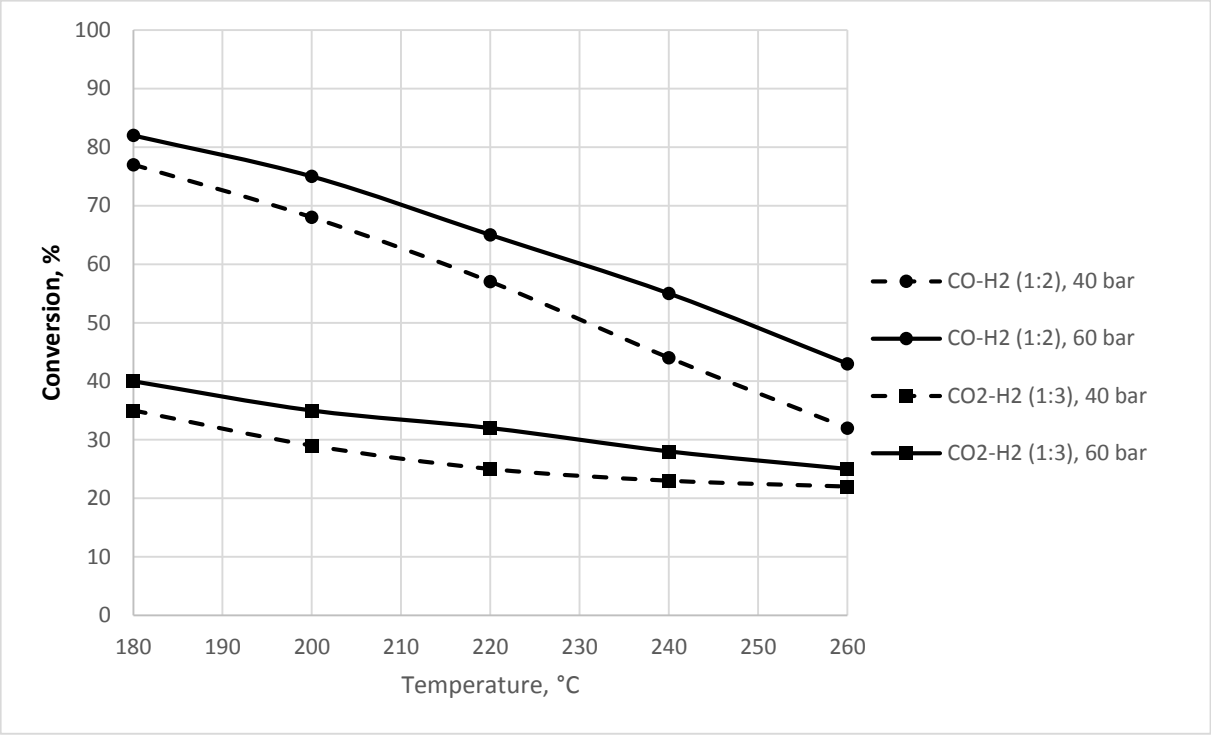

Figure 4. The equilibrium conversion of stoichiometric CO-H_2 (1:2) and CO_2-H_2 (1:3) mixtures at 180-260 °C and pressures of 40 and 60 bar. Data from Arena, et al. (2014) **[167].**

In addition to the thermodynamic effects, the maximum allowable operating temperature is dictated by catalyst stability. Temperatures above 300 °C lead to significant sintering and deactivation of the catalyst [168]. Typically reaction temperatures between 220 °C and 270 °C and pressures of 50 to 100 bar are used [140]. These conditions correspond to the low-pressure methanol synthesis processes, first developed in the 1960s, which replaced the previous high-pressure processes operated at 320- 450 °C and 250-350 bar. The milder operating conditions were made possible by the replacement of the original ZnO-Cr_2O_3 catalyst by the more active copper based catalysts.

Even if the catalytic activity of copper was known earlier, only improved feedstock purification allowed the use of the highly sulfur and chlorine sensitive copper-based catalysts [158]. Presently, methanol production is based on catalysts consisting of the Cu-ZnO-Al_2O_3 structure [139], where copper is the main active component, ZnO a promoter/stabilizer and Al_2O_3 a stabilizing support. The catalysts are very selective to methanol, with methanol selectivity commonly over 99% [168]. The main side-products are higher alcohols, ethers, esters,

hydrocarbons and ketones [139]. Even with the improved purification of feed gas, irreversible catalyst deactivation caused by trace contaminants and thermal degradation does occur. The presence of sulfur leads to blocking of surface sites on the catalyst, while local temperature peaks may lead to sintering of the catalyst. The sintering can be accelerated by halide components present in the feed. In practice, the catalyst lifetimes range from 2 to 5 years [139].

The mechanism of methanol synthesis on Cu-based catalysts has been much debated, with some disagreement on whether methanol is formed primarily from CO or CO_2. At present, it seems to be concluded that methanol is mostly formed from the hydrogenation of CO_2 [169, 170, 171, 172, 173]. Reaction mechanisms and corresponding kinetic models have been developed by Askgaard, et al. [174] and Vanden Bussche & Froment [175]. Both of the models are reportedly widely accepted and verified by process data [158]. The reaction mechanism proposed by Vanden Bussche & Froment is shown in Table III**.**

Table III. Proposed reaction mechanism for methanol synthesis and the reverse water-gas shift reaction. The rate-determining steps are bolded. * Represents adsorption site on the catalyst. Adapted from Vanden Bussche & Froment **[175]**. Symbol * corresponds to an adsorption site on the catalyst surface.

	Methanol synthesis
Step	Surface reaction
1	$H_2(g) + 2^* \rightleftharpoons 2\ H^*$
2	$CO_2(g) + O^* + * \rightleftharpoons CO_3^{**}$
3	$CO_3^{**} + H^* \rightleftharpoons HCO_3^{**} + *$
4	$HCO_3^{**} + H^* \rightleftharpoons H_2COO^{**} + *$
5	$\mathbf{H_2COO^{**} \rightleftharpoons H_2CO^* + O^*}$
6	$H_2CO^* + H^* \rightleftharpoons H_3CO^* + *$
7	$H_3CO^* + H^* \rightleftharpoons CH_3OH(g) + 2^*$
	Reverse water-gas shift
1	$H_2(g) + 2^* \rightleftharpoons 2\ H^*$
2	$\mathbf{CO_2(g) + * \rightleftharpoons O^* + CO(g)}$
3	$O^* + H^* \rightleftharpoons OH^* + *$
4	$OH^* + H^* \rightleftharpoons H_2O^* + *$
5	$H_2O^* \rightleftharpoons H_2O(g) + *$

According to this mechanism, the reaction is assumed to be initiated by formation of the carbonate species (CO_3**) in the reaction of CO_2 with oxygen (from the catalyst) on the catalyst surface (step 2). The hydrogenation of the formate intermediate (H_2COO**, step 5) is considered the rate-determining step. The water gas-shift reaction (WGS) has a significant contribution to the overall reaction system, with the direction of the reaction depending on the composition of the reaction mixture. The WGS is catalyzed by the methanol synthesis catalysts [140]. The reaction rate is much higher compared to the methanol synthesis reactions and the water-gas shift reaction is always in equilibrium in the system [158].

3.1.2 Process design

The main process stages in the production of methanol are the following [139, 167]:

1. Production of syngas
2. Methanol synthesis
3. Methanol purification

The preparation and compression of syngas typically contributes to approximately 60% of the capital cost and close to 100% of the energy consumption of the methanol synthesis plant [167]. The adopted syngas generation process and the composition of the syngas depends on the carbon source. The most common process, steam reforming of natural gas, produces syngas with the stoichiometric number close to 3 and high ratio of CO/CO_2. CO_2 can be added to the syngas either before or after reforming to adjust the hydrogen to carbon ratio [168, 139]. As mentioned, the addition of CO_2 also improves methanol productivity and catalyst life [140]. Partial oxidation of carbon sources with lower H/C ratio, such as coal, results in syngas with lower stoichiometric numbers. In this case, the hydrogen content may be increased by a separate WGS step [139]. The syngas is also purified from sulfur compounds and other catalyst-poisoning contaminants.

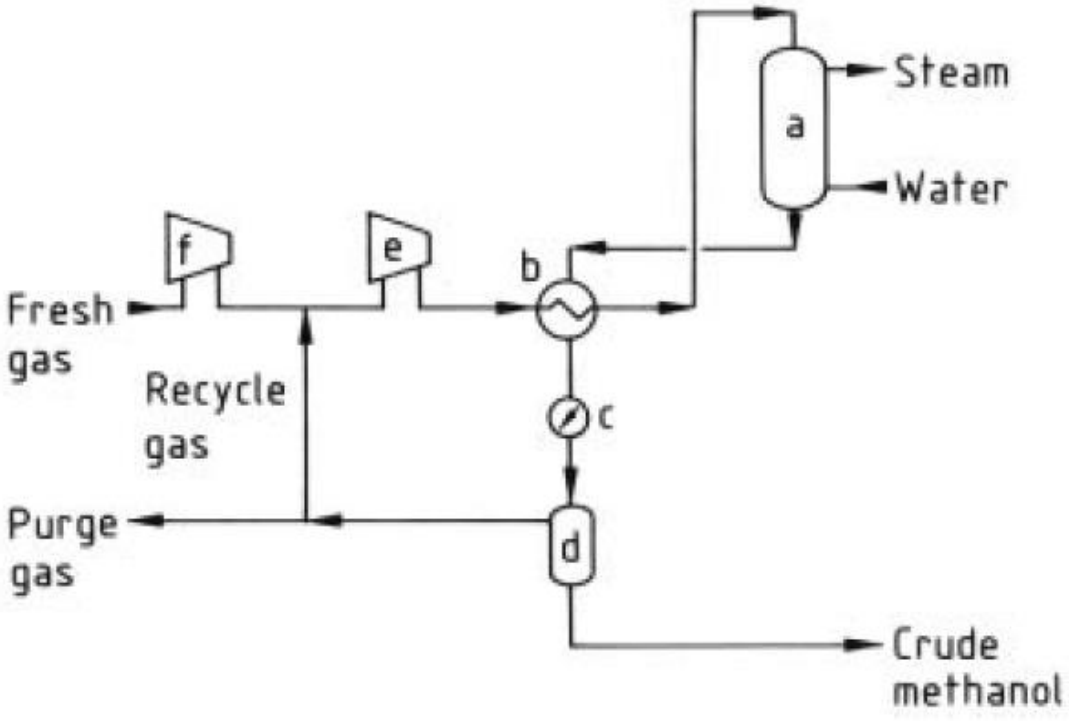

Figure 5. Simplified flowsheet of the methanol synthesis process: (a) reactor, (b) heat exchanger, (c) cooler, (d) separator, (e) recycle compressor, (f) fresh gas compressor. From Ott, et al. (2012) **[139]**.

Figure 5 shows the simplified flowsheet of methanol synthesis [139]. Due to the thermodynamic equilibrium, carbon conversion can only reach 50 to 80% in one pass through the reactor. Conversion is often further limited to avoid excessive reaction temperatures [176]. Consequently, after the separation of methanol and water formed in reaction by condensation (d), the unreacted gas mixture is recycled and mixed with fresh syngas (make-up gas, MUG) for further reaction. The ratio of the recycled to fresh gas depends on the technology applied, typically being in the range of 7-9 [177]. A fraction of the recycle gas is purged to control the concentration of inert components and adjust the stoichiometric number [139].

Temperature control is the key parameter in reactor design. The heat generated by the exothermic reaction has to be effectively removed both to improve the conversion and to protect the catalyst. The reactors generally consist of a heat-exchanger type structure with the catalyst installed either in the tubes or on the shell side. The reactor systems used can be based on

adiabatic or quasi-isothermal reactors [139]. Adiabatic reactor systems may include quench reactors or multiple adiabatic reactors in series [167, 177]. In quench reactors, cold feed gas is introduced at several intermediate points to a single reactor containing multiple catalyst beds, leading to a sawtooth-shaped temperature profile in the reactor. Alternatively, multiple reactors can be installed in series with intermediate cooling between the reactors.

In quasi-isothermal reactors, a more uniform temperature distribution is achieved either by cooling by water, resulting in steam generation (boiling water reactor, BWR), or by cooling with cold feed gas (gas-cooled reactor, CGR). Different types of reactors might be combined to optimize the overall process. For example, in the MegaMethanol process designed by Lurgi, a boiling water reactor is first employed for conversion of the very reactive feed gas, providing effective heat removal [139]. The preconverted gas is then fed to a gas-cooled reactor which is cooled by the inlet gas of the first reactor. Simultaneously, the feed gas is preheated. In the second reactor, the temperature is continuously reduced, leading to continuous generation of methanol driven by the shifting reaction equilibrium. A simplified flowsheet of the MegaMethanol process is shown in Figure 6:

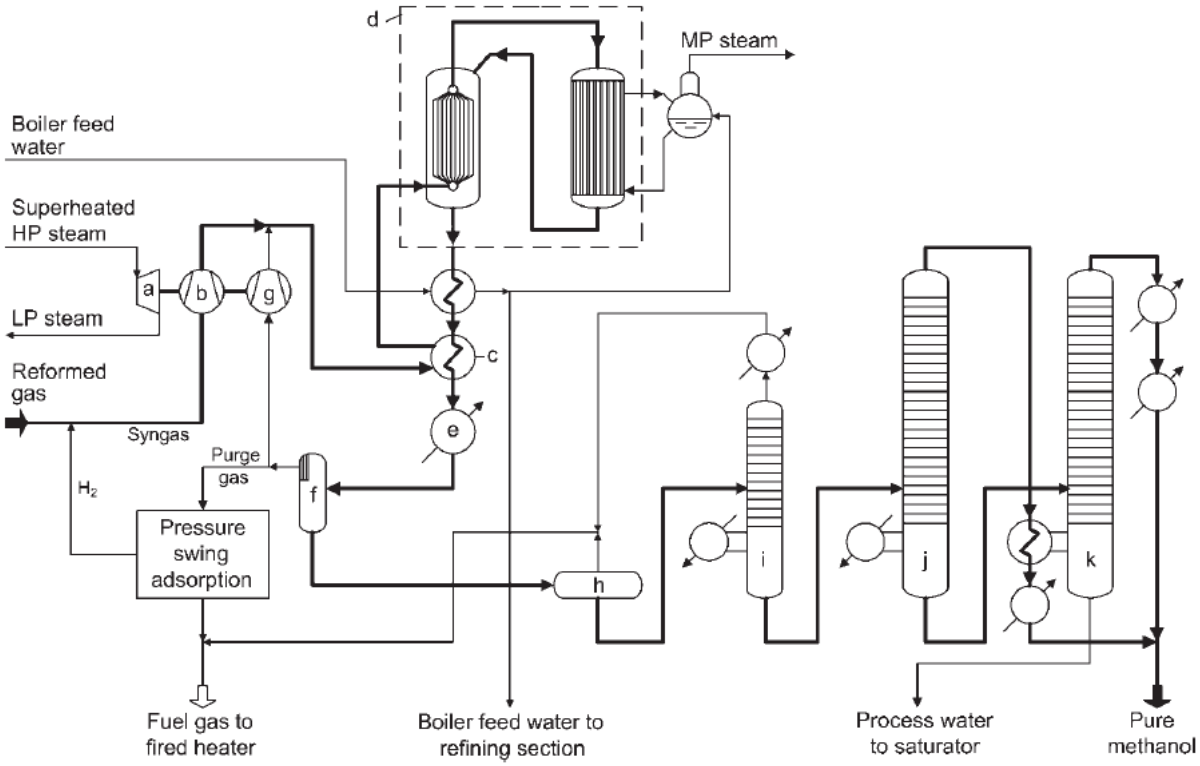

Figure 6. Simplified flowsheet of the Lurgi MegaMethanol process: (a) compressor turbine, (b) syngas compressor, (c) heat-exchanger, (d) reactor system, (e) cooler, (f) separator, (g) recycle gas compressor, (h) separation vessel, (i) light ends column, (j) pressure distillation column, (k) atmospheric distillation column. From Ott, et al. (2012) **[139]**.

The combined reactor system is shown on the flowsheet (d), with the boiling water reactor on the right followed by the gas-cooled reactor on the left. The reactor outlet is cooled by heat exchange with the cold inlet gas (c), simultaneously preheating the feed. The feed is further heated by passing through the tubes in the gas-cooled reactor, concurrently cooling the reactant gas flowing counter-current on the shell side. The reactor outlet is further cooled (e) and the condensed methanol and water separated (f). In this installation, the hydrogen content of the recycle gas is increased by pressure swing adsorption before mixing with the make-up gas.

The crude methanol separated from the unreacted gases contains water and a small amount of other by-products [139]. The methanol purification sequence is also shown in Figure 6. The low-boiling components, including dissolved gases, dimethyl ether and methyl formate are

removed in the light ends column (i), following flashing in a separation vessel (h). Methanol is then separated at one or more distillation columns operated at successively lowering pressures. In the MegaMethanol process, a pressure column (j) is followed by an atmospheric column (k), both from which methanol is obtained as the head product. Water and other high-boiling components, such as higher alcohols and hydrocarbons, ketones and esters are removed as bottoms.

The MegaMethanol process showcased here is just one of the process options developed by technology providers. Various alternative processes have been developed [178, 139, 177]. The processes are somewhat similar and operate at the low-pressure conditions with similar catalysts, with the main differentiating features being in syngas generation and reactor design. In 2011, 27% of the plants in operation were licensed by Lurgi, 25% by JM/Davy and 16% by Haldor-Topsøe, with the rest of the share divided between smaller companies.

Until 1997, plants with a maximum capacity of 3000 t/d were in operation. [139]. Since then, plant capacities have increased, with capacities up to 10 000 t/d reached by some processes [177]. The increase in single-plant capacities is driven by economies of scale. The overall methanol production capacity is increasing, following the increasing demand [137]. Cheap natural gas in the Americas and especially the Middle East allows cost-effective production, with 2011 average production costs as low as 70 €/t in the Middle East [137]. The production from coal is significantly more cost-intensive, with the average production cost of over 260 €/t reported in China [137]. For comparison, the current market price of methanol is approximately 300 €/t [179].

3.2 Methanol from CO_2

The synthesis of methanol from CO_2 and hydrogen does not greatly differ from the conventional synthesis based on CO containing syngas. After all, the hydrogenation of CO_2 is considered the main contributor to methanol formation even if CO_2 is only present in small amounts. However, the use of pure CO_2 with hydrogen does bring about some difficulties. The formation of water as a by-product of CO_2 hydrogenation (Eq. 27) leads to lowered productivity both through thermodynamic limitation [140] and by inhibition or degradation of catalysts [167]. The crude methanol product contains approximately 30-40% of water (compared to 10-12% from syngas) [180] leading to increased separation costs. The amount of other byproducts is, however, much smaller at approximately 400 ppm, compared with up to 2000 ppm from syngas

[180]. This is attributed both to lower reaction temperatures on the catalyst surface and to better inherent selectivity of CO_2 conversion.

The water formed in the hydrogenation reaction and also in the RWGS reaction (Eq. 28) affects the equilibrium of methanol synthesis, limiting conversion. Water also inhibits catalytic activity by occupying adsorption sites on the catalyst surface [181]. This effect has been found particularly strong on the established alumina supported Cu/ZnO catalysts [182], which in part drives the development of alternative catalyst compositions for the synthesis of methanol from CO_2.

3.2.1 Catalyst developments

The research on heterogeneous catalysts for the hydrogenation of CO_2 to methanol has been recently reviewed by many authors [22, 8, 16, 183, 23]. Catalysts based on multiple different metals and their combinations have been prepared. Noble metal catalysts based on Rh and Ru have been found to produce CO and/or CH_4 with no activity for methanol; the same applies to Ni [184]. However, a Ni-Ga catalyst was recently found capable of reducing CO_2 to methanol at ambient pressure [185]. Au and Ag have been found very selective for methanol, but their activity has not matched that of Cu [186, 187]. Palladium has been quite widely studied [188, 189, 190, 191], with the activity found to be significantly influenced by the support material. Pd promoted by G_2O_3 has also been studied [192]. While some Pd-based formulations have shown promising activity, there would not seem to be significant enough improvement over Cu-based catalysts to justify the high catalyst cost.

Generally, copper has remained the most effective active catalytic component, with the majority of the research focused on modification of the Cu/ZnO structure with various additional components. Zr and Ga have been found particularly effective. Cu/ZnO supported on Ga_2O_3, ZrO_2 and Cr_2O_3 was found to possess improved activity and stability compared to a commercial methanol synthesis catalyst, with Ga_2O_3 showing the highest activity [193]. The combination of Cu/Zn with Ga_2O_3 was found effective in another study, with the highest activity obtained upon addition of silica support [194]. In comparison of Cu/ZnO catalysts supported on Al_2O_3, ZrO_2 and CeO_2, ZrO_2 was found the most effiective [195]. Promising results have also been shown with Cu/ZnO/Cr_2O_3 [196]. Catalysts consisting of Cu/ZnO/TiO_2 have been reported, too [197].

The conventional $Cu/ZnO/Al_2O_3$ structure has also been modified with various components. Multicomponent catalyst such as $Cu/ZnO/ZrO_2/Al_2O_3$ [198, 199, 200] and $Cu/ZnO/ZrO_2/Al_2O_3/Ga_2O_3$ [198] have been found active. The addition of Y to $Cu/ZnO/Al_2O_3$ was found similarly effective to Zr [201]. Catalysts consisting of Cu/ZrO_2 have also been studied. This type of catalyst was found the most active when metal/zirconia catalysts were compared [184]. Recently, active copper-ceria and copper-ceria-titania catalysts, altering the reaction route of CO_2 conversion to methanol, were reported [202].

ZrO_2 modified catalyst structures have gathered particular interest among the Cu/ZnO catalysts.. The reported benefits of added ZrO_2 include the increased dispersion of copper [203], high specific surface of both the catalyst and the active copper phase [182] and advantageous surface effects [204]. Compared to $Cu/ZnO/Al_2O_3$, the lower affinity to water is also beneficial [182]. Yang, et al. found Cu/ZnO doped with ZrO_2 particularly effective for conversion of CO_2 rich syngas, with an increase in both CO_2 conversion and methanol selectivity compared to unmodified Cu/ZnO [203]. Sloczynski, et al. studied the effect of various metal oxide additives on $Cu/ZnO/ZrO_2$ [205]. The additives were found to influence both the catalytic activity and the stability of the catalyst. The addition of G_2O_3 was found particularly beneficial. The promoting effect of Ga was also reported by other groups [206, 207]. The addition of La, Cr and Ce was also found effective, especially at lower reaction temperatures (220 °C) [207]. Finally, the addition of Mg and Mn oxides was found useful, leading to increased copper dispersion and improved adsorptive properties of the catalyst [208]. Improvement on methanol productivity by a promoting effect of Mn on $Cu/ZnO/ZrO_2$ has been noted [209].

As a summary, various catalyst compositions have been found to show improved activity and/or stability in methanol synthesis from CO_2 over the conventional $Cu/ZnO/Al_2O_3$ structure. Some of the available experimental results are compiled in Table IV [22, 23]. Based on this data, the modified Cu and Cu/ZnO based catalysts seem promising. With these types of catalysts, CO_2 conversions of 20% and above have been reported at moderate (50-70%) methanol selectivity. The $Cu/ZnO/ZrO_2$ and its modifications (especially with Ga) show some of the best results. Some alternate structures show excellent selectivity but lower conversion. Examples include $Au/ZnO-ZrO_2$ [186], Fe-Cu/MCM-41 [210] and $LaCr_{0.5}Cu_{0.5}O_3$ [211]. Some of the recent developments, such as Cu-Ce [202] and Ni-Ga [185] are interesting but there is not much available information about the performance and potential of these catalysts at this time.

Table IV. Experimental performance of catalysts for the hydrogenation of CO_2 to methanol **[22, 23]**.

Catalyst	Temperature, °C	Pressure, bar	Conversion, %	Methanol selectivity, %	Space-time yield, g/kgh(1	Reference
Cu/ZnO	240	30	16,5	78,2	550	[212]
Cu/ZnO/CNT(2	270	50	19,6	35,5	343	[213]
Cu/ZnO/ZrO_2	220	80	21	68	179,4	[186]
Cu/ZnO/ZrO_2	240	30	17	41,5	48,8	[214]
Cu/ZnO/ZrO_2	240	30	18	51,2	305	[215]
Cu/ZnO/ZrO_2	240	50	9,7	62	1200	[195]
Cu/ZnO/Ga	270	20	6	88	378,0	[216]
Cu/ZnO/Ga	270	30	15,9	29,7	135,9	[217]
Cu/ZnO/Ga/SiO_2	270	20	5,6	99,5	349,2	[194]
Cu/ZnO/ZrO_2/Ga	250	70	22	72	704	[206]
Cu/ZnO/γ-Al_2O_3	250	30	10,1	78,2	76,8	[218]
Cu/ZnO/Al_2O_3/Y	250	50	26,9	52,4	520	[201]
Cu/ZnO/TiO_2-ZrO_2	240	30	17,4	43,8	52,7	[214]
Cu/ZnO/TiO_2	220	30	14,8	50,5	51,5	[197]

Table IV. (cont.)

CuO/ZnO/PdO	**240**	**60**	**9,2**	**66,2**	**322**	**[219]**
Cu/ZrO_2/CNT(2	260	30	16,3	43,5	84	[220]
Cu/ZrO_2/Ga	250	20	13,7	75,5	60,9	[221]
Ag/Zn/ZrO_2	220	80	2	97	14,7	[186]
Au/Zn/ZrO_3	220	80	1,5	100	12,8	[186]
Pd/G_2O_3	250	50	17,3	51,6	175,6	[222]
Pd/Ga/CNT(2	250	50	16,5	52,5	512	[223]
Pd/Zn/CNT(2	260	30	6,3	99,6	35,2	[191]
La-Mn-Zn-Cu-O	270	50	13,1	54,5	100	[224]
$LaCr_{0.5}Cu_{0.5}O_3$	250	20	10,4	90,8	278	[211]

1) g of methanol formed/kg of catalyst·h; 2) Carbon nanotubes

3.2.2 Feasibility of methanol production from CO_2

The technical feasibility of CO_2 conversion to methanol has essentially been proven [167] and several pilot scale operations have already been started. Utilizing conventional methanol synthesis catalyst and technology, a pilot plant developed by Lurgi has demonstrated good productivity combined with promising catalyst stability [143]. Per-pass CO_2 conversions of 35-45% with high methanol selectivity are reported, however productivity (space-time yield) was low compared to syngas feed. A pilot plant developed by Mitsui Chemicals has been in operation since 2009, with a capacity of 100 t per year of methanol [225, 180].

The CAMERE process developed in South Korea is based on a separate RWGS reactor and methanol synthesis reactor [226, 180]. In the RWGS step, part of the CO_2 is converted to CO and H_2O. After removal of water, the resulting gas mixture is fed to the methanol synthesis reactor. This configuration reportedly results in twice the yield of methanol compared to direct CO_2 hydrogenation. A pilot plant based on this concept and producing 100 kg/day of methanol is in operation.

So far the only commercial plant converting CO_2 to methanol is operated by Carbon Recycling International in Iceland [77, 227]. The plant became operational in 2011 with an initial capacity of 10 tons of methanol per day. The process is based on the availability of CO_2 from a geothermal power station and the production of hydrogen by electrolysis using cheap geothermally produced electricity. The methanol product is used as fuel by blending with gasoline.

The technology of methanol synthesis from CO_2 is quite similar to conventional methanol synthesis and already demonstrated at pilot to small commercial scale operations. With the development of more active catalysts, productivity values of up to 1200 g/(kg·h) have been obtained (Table IV) for the synthesis of methanol from CO_2. For conventional methanol synthesis, productivity values in the range of 400-1000 g/(l·h) have been reported [228]. In a comparison study, the productivity has been found higher with feeds containing CO on a conventional methanol synthesis catalyst [143]. However, it would seem that with the more advanced catalysts, the productivity from CO_2 might be comparable to conventional synthesis.

Considering small scale production, the lower productivity values with CO_2 might not prove problematic. The practical implication of lower productivity (per catalyst volume or mass) is that larger units are required to reach identical production rates. In small operations, the increased unit size may not lead to intolerable cost increases.

The main obstacles of large-scale operation are the economical production of hydrogen from CO_2-free, renewable sources and the cost-effective capture of CO_2. Other than fossil feedstocks, water electrolysis is currently the only available large-scale source of hydrogen. However, the electricity consumption is high with current technology, and electricity cost is high particularly when renewable sources of electricity are used. Currently, the production cost of methanol from CO_2 is estimated at 510-900 €/t [77], which is considerably higher compared to the production from fossil raw materials (natural gas: 90€-175 €/t, coal: 260-350 €/t) [137].

Currently, the advantage of CO_2 based production is the significant drop in capital costs due to the elimination of the syngas generation stage [77].

3.3 Liquid-phase methanol synthesis

As an alternative to the established gas-phase, heterogeneously catalyzed synthesis, methanol synthesis in the liquid phase has been proposed. Potential advantages of liquid-phase methanol synthesis include the operation at lower, thermodynamically favored temperatures, and the efficient heat transfer provided by the liquid medium, allowing effective temperature control of the exothermic synthesis reaction. The efficiency of gas-phase methanol synthesis with the commercial copper based catalysts is limited by the low equilibrium conversion, which requires significant recycling of unreacted gases. In liquid systems utilizing various types of catalysts, methanol synthesis can be operated at lower temperatures, leading to higher achievable conversions.

3.3.1 The BNL method

Much of the research on liquid-phase methanol synthesis has focused on systems based on basic catalysts. In the Brookhaven National Laboratory method, a catalyst system consisting of nickel acetate, tert-amyl alcohol and sodium hydride is used at temperature range of 80 ^{o}C to 120 ^{o}C, preferably at pressure of approximately 20 bar [228]. The liquid medium is formed by the alcohol and an additional solvent such as tetrahydrofuran. In a variation of this process, a homogeneous catalyst based on nickel tetracarbonyl and an alkali methoxide is used [229]. High yield and selectivity of methanol has been reported for both of these processes, with yields in excess of 70%. However, possibly because of the rather complex catalyst system, this process does not seem to have seen development since the original patents.

3.3.2 Methanol synthesis via methyl formate

Low-temperature methanol synthesis through the formation of methyl formate has been pursued by some researchers. In this type of process, methanol is produced from syngas via carbonylation of methanol to methyl formate, followed by hydrogenation of the methyl formate into methanol [230]:

$$CH_3OH + CO \rightarrow HCOOCH_3 \quad (29)$$

$$HCOOCH_3 + 2\,H_2 \rightarrow 2\,CH_3OH \quad (30)$$

The catalyst system for this process consists of an alkali alkoxide, such as potassium or sodium methoxide combined with a heterogeneous copper [231, 232, 233] or nickel-based [234, 235, 236] catalyst. The solid catalyst is slurried with the liquid medium consisting of solvents such as xylene [237]. The alkali alkoxide acts as catalyst for the carbonylation reaction (Eq. 29), while the metal catalyst is active in the hydrogenation step (Eq. 30). Synthesis has been performed at temperatures as low as 100 °C at pressures of 30 to 65 bar [238]. Methanol productivity of up to 172 g/(l·h) has been reported [234].

The two-step reaction can be carried out either in one reactor or in separate reactors. While a single reactor leads to simple and cost-effective operation, a two-reactor process could be better optimized for each of the reaction stages [239]. While most of the experimental work has been carried out in single autoclave type reactors, alternative reactor types have also been proposed. An integrated two-stage reactor separates the liquid carbonylation catalyst and the solid hydrogenation catalyst, allowing the optimization of reaction temperature for both reaction steps and the efficient separation of reaction products [239]. Additionally, a slurry bubble reactor was developed with the aim of scale-up of the process from the laboratory scale [240]. However, this concept suffered from poor catalyst stability.

The catalyst stability is a shared disadvantage of the methanol synthesis processes utilizing basic catalysts. Carbon dioxide and water deactivate the catalyst even at trace concentrations, requiring the purification of the feed gas from these components [236]. The high cost of feed gas purification and re-activation of the catalyst make the industrial implementation of this technology difficult. The requirement of CO_2-free syngas is not practical, especially when considering methanol synthesis in the context of CO_2 utilization.

3.3.3 The LPMEOH project

A liquid-phase methanol synthesis process was developed in co-operation of Air Products and Eastman companies and the U.S. Department of Energy [241, 242, 243]. The goal was to develop a process capable of utilizing syngas generated by the gasification of coal. The process would allow the integration of methanol production into an IGCC power plant, leading to increased product flexibility and the possibility of utilizing excess syngas at periods of off-low electricity demand.

The liquid-phase methanol synthesis process is based on a slurry bubble column reactor, in which powdered catalyst particles are suspended in an inert mineral oil. The mineral oil acts as a heat transfer medium, transferring the reaction heat to an internal heat exchanger. The efficient temperature control provided by this system results in a highly uniform temperature profile in the reactor leading to improved syngas conversion compared to gas-phase synthesis. The process is capable of operating on varied syngas compositions, with both CO-rich gas and any content of CO_2 allowed. The process is also capable of flexible operation with quick and reliable startup and shutdown, allowing periodic operation based on the availability of excess syngas from the power plant.

A demonstration plant with a design capacity of 235 t/d of methanol began operation in 1997 and was run for 69 months. Production rates exceeding the design capacity were reached and the overall plant availability was 97.5%. Catalyst stability was monitored at varied operating temperatures. At the initial 250 °C, catalyst deactivation (1.3% per day) was higher than the design basis. At 235 °C, which was experimented for over three years, a catalyst deactivation rate of 0.6% per day was observed, while at 215 °C the rate was 0.17%. In-situ catalyst activation procedures were developed and temperature programming (slow increase of temperature to maintain methanol production rate) was implemented to improve the catalyst stability. Trace contaminants such as arsenic and sulfur in the syngas feed were identified as the main cause of catalyst deactivation.

The methanol product was used as chemical feedstock and also tested for use in transportation and electricity generation. The water content of the methanol product was small (<1%) when CO-rich syngas was used, allowing non-chemical use without the separation of water. Overall, the project was reported successful and the integration of methanol production to IGCC power generation promising. The main challenges were considered the cost of syngas from coal gasification, the improved purification of syngas for protection of catalyst and the scale-up of the slurry bubble column reactor.

3.3.4 Cascade catalytic systems

Cascade catalytic systems have been proposed for the hydrogenation of CO_2 to methanol. In these processes, the overall methanol synthesis reaction is divided into separate steps, which are performed using different catalysts. Huff & Sanford studied the homogeneous hydrogenation of CO_2 into methanol via the following steps [244]:

1. Hydrogenation of CO_2 into formic acid
2. Esterification of formic acid to form a formate ester
3. Hydrogenation of the ester to form methanol

The reaction series was performed in a single vessel with multiple catalysts, using a strategy of separating thermodynamically unfavorable and unstable intermediates to improve the overall reaction. Using a combination of complex catalysts in liquid solvents at low temperature (135 °C), the initial feasibility of this type of process was established. However, some incompatibility both among the catalysts and between CO_2 and the catalysts was noticed. Further optimization of the catalyst system is required. Wesselbaum, et al. developed the concept by utilizing a single homogeneous transition metal catalyst based on a ruthenium phosphine complex with ethanol and organic acid additives [245]. At 140 ^oC and relatively high pressures (H_2 partial pressure 60 bar, CO_2 20 bar), promising results were obtained.

A cascade catalytic system using heterogeneous catalysts was also recently developed [246]. The advantage of heterogeneous catalysts would be the easier separation of the catalyst from the product mixture. Copper and Mo_2C based catalysts were investigated for the cascade reaction, with the combination of Cu-Cr and Cu/Mo_2C catalysts found the most effective. 1,4-dioxane was used as solvent. The addition of ethanol was found to improve the rate of reaction, leading to the reaction proceeding through the formate intermediate and not via formic acid. At 135 °C and partial pressures of 10 bar for CO_2 and 30 bar for H_2, a turnover frequency of $4.7 \cdot 10^{-4}$ s^{-1} was reported, which is in the range of results obtained by homogeneous cascade catalysts [244]. However, the value is low compared to the reported activity of gas-phase heterogeneous catalysts (0.003-0.018 s^{-1}) [246].

3.4 Alcohol promoted methanol synthesis

A methanol synthesis process based on the combination of a solid, copper-based catalyst and a liquid alcohol promoter has been developed [247]. This process does not rely on basic catalysts and is therefore not sensitive to carbon dioxide and water. Syngas containing carbon dioxide and even pure CO_2 can be fed to the process, leading to increased flexibility and potential, especially when the utilization of CO_2 is considered. At reaction temperatures of approximately 170^oC and pressures of 30 to 50 bar, thermodynamically more favorable conditions can be provided when compared to conventional methanol synthesis.

The solid catalysts used in this process are similar to the commercial methanol synthesis catalysts. Various alcohols have been used as the promoter. The alcohol acts as a catalytically active solvent and is not consumed in the reaction. The promoting effect of the alcohol is based on the alteration of the reaction route, i.e. methanol is formed through an ester intermediate.

3.4.1 Reaction route and the effect of process variables

Alcohol promoted, low temperature methanol synthesis starting from CO_2 and H_2 was studied by Fan, et al. [248]. A commercial Cu/ZnO catalyst was compared with Cu-Cr-O and Pd-Cu-Cr-O (5% Pd) catalysts, with ethanol as the liquid medium. At 30 bar and a relatively high temperature of 473 K (200 °C), the commercial catalyst showed the highest activity with CO_2 conversion of 7.5% and methanol selectivity of 73.3%. Moderate activity was shown by the Cr-containing catalyst (CO_2 conversion 5.2%; methanol selectivity 59.6%), while the addition of Pd was not found beneficial. CO was formed by all catalysts through the activity of the reverse water-gas shift reaction. In all experiments, ethyl formate was present in the reaction products.

The effect of reaction temperature and time was also studied. At 390-430 K, the selectivity to ethyl formate increased, while at 430-470 K, a decrease in ethyl formate was accompanied by increasing selectivity to methanol. With the reaction time running from 2 h to 20 h, a decrease in the concentration of ethyl formate was accompanied by methanol formation. These results pointed to ethyl formate being the intermediate to the formation of methanol. This was confirmed by a blank experiment with no ethanol added, which resulted in very slow formation of methanol. Further, methanol was formed at very high rate when ethyl formate was added to the reaction mixture.

The authors proposed a reaction scheme with the following steps (equilibrium notation added):

3. Hydrogenation of carbon dioxide into formic acid

$$\mathrm{CO_2 + H_2 \rightleftarrows HCOOH} \tag{31}$$

4. Reaction of formic acid with ethanol, forming ethyl formate

$$\mathrm{HCOOH + C_2H_5OH \rightleftarrows HCOOC_2H_5 + H_2O} \tag{32}$$

5. Hydrogenation of ethyl formate, forming methanol and ethanol

$$HCOOC_2H_5 + 2\,H_2 \rightleftarrows CH_3OH + C_2H_5OH \quad (33)$$

The hydrogenation of ethyl formate (Eq. 33) was proposed to be the rate-determining step, indicated by the accelerated methanol formation upon addition of ethyl formate. The large amount of ethanol present was not favorable for this reaction step. Finally, it is noted that the net reaction was not dependent on the type of alcohol used.

Similar results pointing to the promoting effect of alcohols were found when CO_2 (5%) containing syngas was reacted on a Cu/ZnO (molar ratio of Cu:Zn = 1) catalyst in ethanol by Tsubaki et al. [249]. A batch reactor with a volume of 70 ml was used for the experiments, with 0.2 g of catalyst and 10 ml of ethanol per batch. At the initial pressure of 30 bar, the direct reaction did not occur below 483 K in the absence of ethanol. Upon addition of ethanol, the formation of methanol and ethyl formate was observed at 423 K. At 443 K, the yield of methanol increased at increasing reaction time (from 2 h to 20 h) while the yield of ethyl formate was nearly constant. The selectivity to methanol increased with decreasing selectivity to ethyl formate. Carbon conversion was quite low, with the conversion of 2.1% at 2 hours increasing to 19.0% after 20 hours. Again, the addition of ethyl formate led to very fast formation of methanol.

A more detailed reaction route was proposed by these authors (equilibrium notation added):

$$CO + H_2O \rightleftarrows CO_2 + H_2 \quad (34)$$

$$CO_2 + \frac{1}{2}H_2 + Cu \rightleftarrows HCOOCu \quad (35)$$

$$HCOOCu + ROH \rightleftarrows HCOOR + CuOH \quad (36)$$

$$HCOOR + 2\,H_2 \rightleftarrows ROH + CH_3OH \quad (37)$$

$$CuOH + \frac{1}{2}H_2 \rightleftarrows H_2O + Cu \quad (38)$$

Net reaction:

$$CO_2 + 2\,H_2 \rightleftarrows CH_3OH \quad (39)$$

Here, Cu represents catalytic sites on the copper catalyst and ROH is the alcohol used as the promoter. Figure 7 illustrates the difference between the alcohol promoted reaction route (B) and the conventional gas-phase methanol synthesis (A):

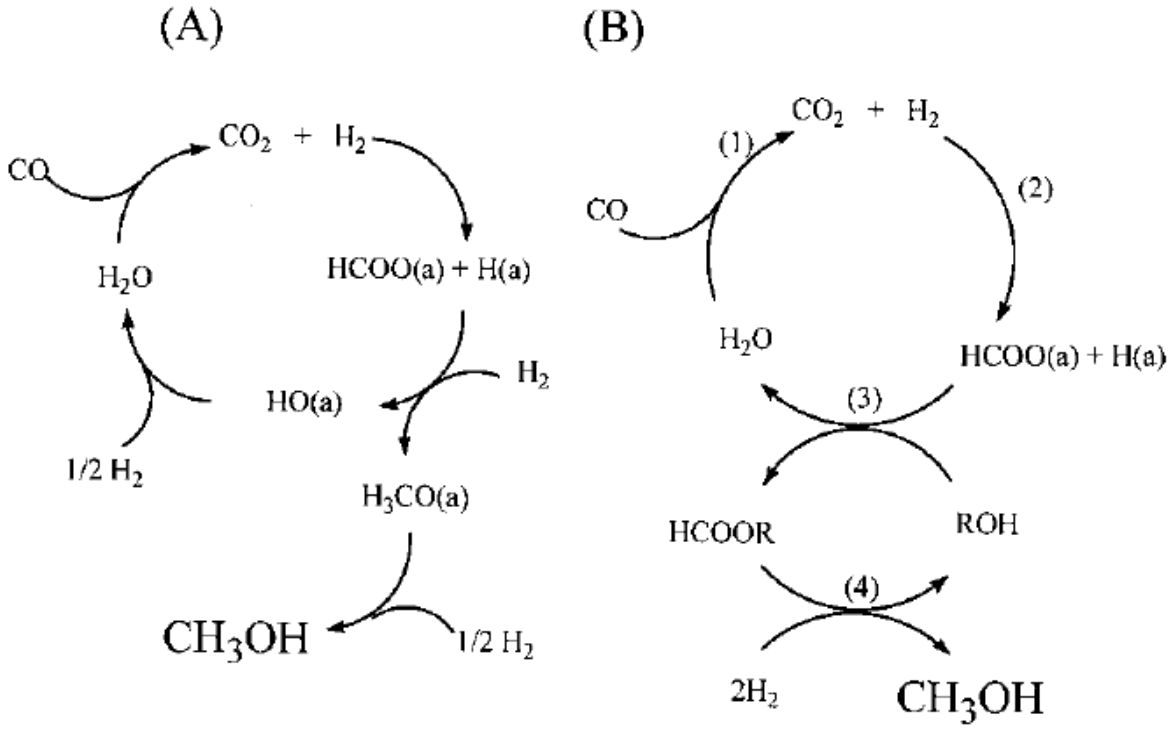

Figure 7. Comparison of the conventional methanol synthesis reaction route (A) with the alcohol promoted reaction route (B) proceeding via ester formation. From Tsubaki, et al. (2001) **[249]**.

A commercial Cu/ZnO catalyst was compared with the self-prepared Cu/ZnO catalyst described above. Lower activity was observed with the commercial catalyst. Additionally, a Cu/Al_2O_3 catalyst was used, both alone and in combination with the commercial Cu/ZnO catalyst. With only the Cu/Al_2O_3 catalyst, only ethyl formate and no methanol was formed, while the combination catalyst showed the highest conversion of all the catalyst compositions tested. However, higher selectivity of methanol was observed with the self-prepared Cu/ZnO catalyst. It was proposed that the Cu/Al_2O_3 catalyst is active for the reactions 34-36, while Cu/ZnO catalyzes the hydrogenation of the ester (37).

In addition to ethanol, the influence of other alcohols was tested. N-butanol was found to result in the highest activity. Straight chain alcohols were found more effective compared to branched alcohols. On the basis of these observations, reaction (36) was considered the rate-determining step: the higher electron density of oxygen atoms on the higher alcohols leads to more efficient nucleophilic attack of the alcohol on the carbon atom of the HCOOCu intermediate. With branched alcohols, the steric obstacle hinders the rate of the nucleophilic reaction. With 10 ml of n-butanol and 0.2 g of catalyst, a space time yield of 0.17 kg MeOH/l h was reached at 443 K and 30-50 bar of initial and final pressure. In comparison, a value of 0.4 to 1.0 kg MeOH/l h was reported for a commercial methanol synthesis plant.

The effect of different alcohols was also investigated by Zeng, et al. [250], as was the influence of the feed gas composition. Both a self-prepared Cu/ZnO catalyst similar to the one used in the work described above [249] and a commercial Cu/ZnO catalyst were used. For testing of alcohols, the reactions were performed on the self-prepared catalyst at 30 bar of initial pressure and at a temperature of 443 K (170 °C). 20 ml of solvent and 2 g of catalyst were used per batch and the feed gas consisted of $CO/CO_2/H_2$ at a ratio of approximately 32/5/60 (with argon as internal standard). For the experiments with different feed gas compositions, the commercial catalyst was used at 423 K and 30 bar of initial pressure, with 0.2 g of catalyst and 5 ml of solvent (ethanol). The reaction time was 2 hours in both experiments. A similar reaction route was proposed as described by Tsubaki et al [249].

For the 1-alcohols from ethanol to 1-hexanol, the total conversion (CO and CO_2) and the yield of methanol and the corresponding ester decreased with the increasing carbon number. With ethanol, the conversion was 11.35%, the yield of methanol 10.22% and the yield of ethyl formate 1.13%. For the alcohols with the same carbon number but different structure, the second alcohols were found to have the higher activity. 2-propanol showed the highest activity with a conversion of 23.46%, yield of methanol of 13.19% and yield of ethyl formate of 10.27%. Low activity was reported for alcohols with bulkier structures: iso-butanol, tert-butyl alcohol and cyclopentanol showed low activity, while ethylene glycol and benzyl alcohol showed no activity.

The structural differences of alcohols with the same carbon number were proposed to have both a spatial and an electronic effect on the rate of reaction [250]. The electron density of the oxygen atom is higher on the bulkier and more branched alcohols, leading to the increasing rate of nucleophilic attack on the formate intermediate. However, the same nucleophilic

reaction is simultaneously hindered by the spatial obstacle caused by the bulkier molecular structure. It was postulated, that from the 4 different butanols tested, 2-butanol shows the optimal balance between these two factors, leading to highest activity.

As for the different feed gas compositions, the reaction rate was found to increase with increasing CO_2 content. Highest reaction rate was observed for pure CO_2 and H_2. At a H_2 partial pressure of 22.5 bar and CO_2 partial pressure of 7.5 bar, the yield of methanol was 0.4% and yield of ethyl formate 0.55%, indicating quite low activity of the commercial catalyst. With only CO and H_2, only ethyl formate and no methanol was formed. Also, if only CO with no hydrogen was contacted with the ethanol solvent, no reaction occurred. This shows that the alcohol cannot be directly carbonylated to ester. It is speculated that when CO was fed with H_2, CO_2 was first formed in the water gas-shift reaction with water contained in the ethanol, and ethyl formate was then formed from the reaction of CO_2 with H_2 (Eq. 35-36).

Continuous alcohol-promoted methanol synthesis has also been investigated. A semibatch autoclave reactor was used for methanol synthesis from CO_2 containing syngas on Cu/ZnO catalysts [251]. A self-prepared catalyst as previously described [249] and a commercial Cu/ZnO catalyst were used. The volume of the reactor was 85 ml. The reactor was filled with a batch of 3 g of catalyst and 20 ml of alcohol and a continuous feed of reactant gases and removal of effluent gases were implemented. The reaction temperature was 443 K (170 °C) and pressure 50 bar. The feed gas consisted of $CO/CO_2/H_2/Ar$ (internal standard) at a ratio of approximately 33/5/59/5.

The activity of different self-prepared catalysts was studied in a 85 ml batch reactor. The best activity was found with a catalyst consisting of Cu/ZnO at a molar ratio of 1. Higher or lower Cu/ZnO ratios led to decreasing activity. In characterization of the catalysts, the catalyst with the molar ratio of 1 was found to have the highest BET and Cu surface area, at 60 m^2/g and 30.1 m^2/g, respectively. The activity of the catalysts was found to be almost proportional to the metallic copper surface area. The catalyst with the Cu:Zn molar ratio of 1 was then used for the continuous experiments. Similar results have been found in another study, where $Cu/ZnO/Al_2O_3$ catalysts were compared and the best results were obtained with the Cu/Zn molar ratio of 1 [252].

The effect of different alcohols was also tested in the batch reactor, with a reaction time of 20 h and the conditions as described above. Methanol was found most effective of the 1-alcohols,

showing a total carbon conversion of 40.3% with a methanol selectivity of 98.7%. Again, from the alcohols with the same number of carbon atoms but different structure, the 2-alcohol was found most effective. 2-butanol showed the highest activity of the alcohols tested, with a carbon conversion of 47.0% and a methanol selectivity of 98.9%. Thus, 2-butanol was used for the continuous reaction experiments.

In continuous operation, steady state was observed after 12 hours of operation. With 2-butanol as the solvent, the CO conversion was reported at 60% and CO_2 conversion at -8%, implying that carbon dioxide was formed in the reactor. The total carbon conversion was 47%, with a high methanol selectivity of 98.9%. For comparison, a total conversion of 29.1% at a methanol selectivity of 98% was obtained with the commercial catalyst. The reaction scheme described earlier (Eq. 34-39, Figure 7) was again proposed in this work. The reaction did not occur without the alcohol, as was demonstrated by using n-hexane as the solvent.

Finally, the effect of increasing the amount of catalyst and solvent in the continuous reaction was tested. With the increase of catalyst mass from 3 g to 6 g, the total carbon conversion increased from 29.1% to 44.6% was observed, with methanol selectivity increasing from 98.0% to 99.1%. It should be noted, that these experiments were carried out with the commercial catalyst with lower activity. With 6 g of catalyst and an increase in the volume of 2-butanol from 20 ml to 40 ml, no significant changes were observed. From the effect of the catalyst weight, it is reported that the reaction was rate and not equilibrium limited at the catalyst mass used. As the increase in volume of solvent showed no effect, the original amount of solvent was considered plentiful.

3.4.2 Catalyst developments

A mesoporous Cu/ZnO catalyst was prepared by the sol-gel method instead of the conventional technique of co-precipitation of copper and zinc nitrates [253]. The goal was to develop a catalyst with a large specific surface area and a homogeneous distribution of elements. The catalyst was compared with a commercial methanol synthesis catalyst. The catalyst performance was tested in a batch reactor with 2-butanol as the solvent. A mixture of $CO/CO_2/H_2/Ar$ at ratios of approximately 33/5/59/3 was fed to the reactor at an initial pressure of 30 bar.

The BET surface area of the prepared catalyst was 66.2 m^2/g, compared to 52.8 m^2/g of the commercial catalyst. The reaction temperature was found to have a significant effect on the catalyst activity. At all the temperatures tested (443, 453, 463 K), the prepared catalyst reached higher total carbon conversion compared to the commercial catalyst. The highest conversions were observed at 453 K, at 30.43% for the prepared catalyst and 22.57% for the commercial catalyst. However, at 443 K, the selectivity of methanol was only 62.2% with the prepared catalyst, compared to 98.77% with the commercial catalyst. At the other temperatures, high methanol selectivity was reached with both catalysts. However, the prepared catalyst generally showed higher performance than the commercial catalyst.

The addition of alkali metal salts to the copper-alcohol catalytic system has also been proposed [254]. Cu/MnO and Cu/MgO catalysts were used with ethanol as the solvent. The addition of alkali salts was considered to increase the rate of formation of the alkyl formate (Eq. 35-36) [247]. The effect of various alkali salts on the formation of ethyl formate from syngas in the presence of ethanol was tested. Potassium carbonate was found more effective than potassium bicarbonate or potassium formate. Particularly high activity was found with cesium carbonate.

Methanol synthesis was then experimented with both potassium carbonate and potassium formate. With 4 g of the Cu/MnO catalyst and 0.2 g of K_2CO_3, a total carbon conversion of 90.2% was reached with a methanol selectivity of 99,1%. With only the Cu/MnO catalyst and no alkali added, the conversion was only 37.5% (methanol selectivity 100%), demonstrating the catalytic effect of the alkali salt. Similar results were obtained with potassium formate.

The combination of alkali components with alcohol solvents seems promising. In a variation of this scheme, a Cu/MgO catalyst impregnated with sodium carbonate was used in an ethanol solution containing alkali formates [255]. Sodium formate was found the most effective of the tested formates. The addition of the formate led to much higher activity of the catalytic system: with only the Cu/MgO-Na catalyst in ethanol, the CO conversion was 20.5%, while the addition of HCOONa resulted in a conversion of 82.4%. In addition, the methanol selectivity increased from 54.7% to 88.3%. A space time yield of 12.2 mmol MeOH/g h was noted. The reaction temperature was 433 K (160 °C) and pressure 50 bar. Similar experiments were carried out by using a combination of a Cu/MgO catalyst and potassium formate, in ethanol solvent [256].

In addition to the alkali catalyst, the alkali doping of the solid catalyst is also important for the performance of the system [257]. The alkali impregnation is reported to improve the interaction

between the solid catalyst and the soluble formate, leading to more efficient formation of the alkyl ester intermediate (Eq. 35-36) [258]. While this type of processes have shown promise, it should be noted that the good results have been obtained with a syngas feed containing no CO_2 and the stability of the basic catalysts in the presence of water and CO_2 has been reported problematic.

3.4.3 Reaction mechanism

To investigate the reaction mechanism of the alcohol promoted methanol synthesis process, in-situ DRIFTS (Diffuse reflectance infrared Fourier transform spectroscopy) studies were performed with the ethanol [259] and 2-propanol [260] promoted reaction on Cu/ZnO catalyst. The ethanol promoted reaction was reported to consist of the following steps:

1. Formation of formate adsorption species by syngas adsorbed on the Cu/ZnO catalyst surface.
2. Reaction of the adsorbed formate species with gas-phase ethanol, forming gas-phase and physisorbed ethyl formate.
3. Reduction of ethyl formate by hydrogen atoms on the catalyst surface, forming gas-phase methanol.

The formation of ethyl formate was found to be a significant step in the low-temperature methanol synthesis, as ethyl formate is both effectively formed and quickly reduced by hydrogen at temperatures below those required in conventional methanol synthesis. The ethanol promoter facilitates the low-temperature route but is not consumed in the overall reaction, thus acting as a catalytic solvent. A reaction mechanism, illustrated in Figure 8, was proposed for the ethanol promoted methanol synthesis. For 2-propanol and other alcohols, the reaction steps and the underlying mechanism are similar, with the corresponding formate being the key intermediate.

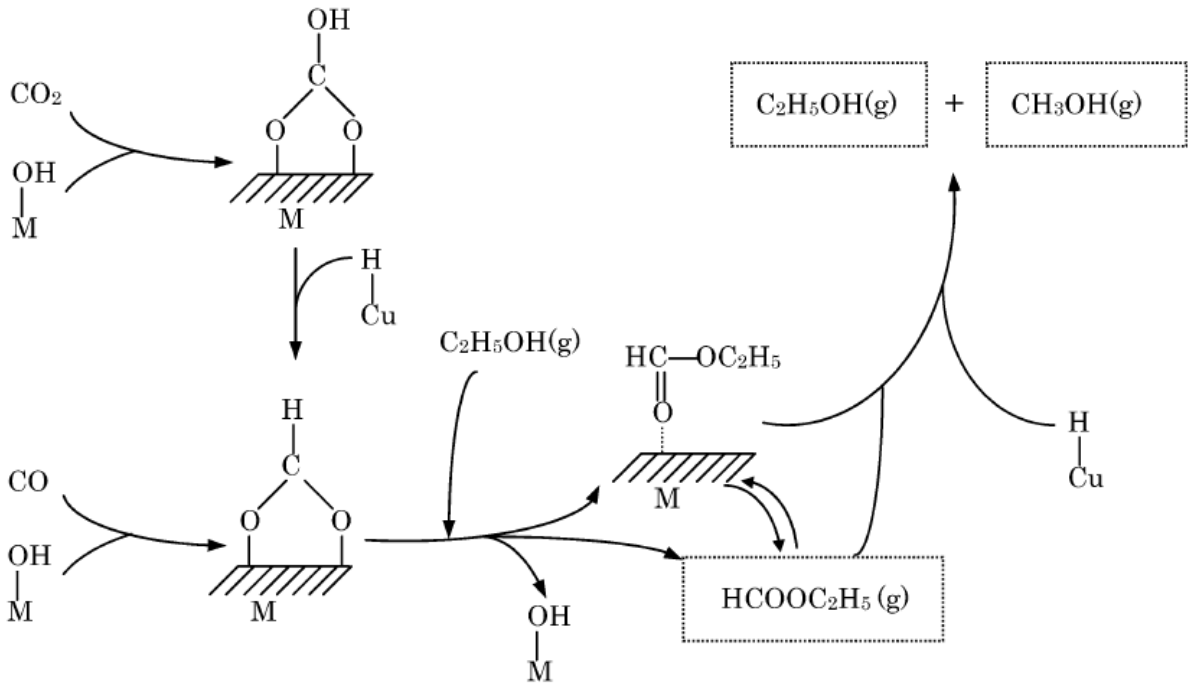

Figure 8. Proposed reaction mechanism for ethanol promoted methanol synthesis from syngas on Cu/ZnO (M). From Yang, et al. (2004).

The formation of ethyl formate, which was considered the rate determining step in the low-temperature methanol synthesis reaction, was further investigated [261]. A Rideal type mechanism was identified for this reaction step. Further, kinetic studies were performed to compare the rate of reaction with ethanol and 2-propanol as the promoter [262]. It was found that both the reaction of alcohol with the formate intermediate (step 2) and the hydrogenation of the resulting ester were faster with 2-propanol than ethanol. Thus, the promoting effect of 2-propanol is more significant than that of ethanol. This result is in line with the experimental studies comparing different alcohols [250].

3.4.4 Summary of process information

To summarize the experimental information available, it seems that temperatures in the range of 170 to 200 ^{o}C would be applicable in this process. When comparing reaction temperatures, Fan, et al. achieved the best results at 200 ^{o}C [248], but the other experiments have been conducted at 170 or 180 ^{o}C, with improved results. Methanol formation seems to be favored by

increased pressures, which is in line with the assumption based on thermodynamics. Reaction pressures of 50 bar and higher would seem favorable. Interestingly, Zeng, et al. found the increasing CO_2 content in feed gas beneficial, with the best results obtained with pure CO_2 and hydrogen [250].

Of the different alcohols, 2-butanol and 2-propanol were found the most effective, with ethanol also showing good promoting effect. The volumes of alcohol used in the experiments were plentiful as noted by Reubroycharoen, et al. [251]. In that study, the amount of catalyst initially used (3 g) in relation to the alcohol (20 ml) was high compared to other studies. Even in that case, the increase of catalyst loading showed improved results. It seems that the amount of catalyst should be maximized to the practical limits in order to increase the reaction rate. Cu/ZnO catalysts similar to the conventional methanol synthesis catalysts seem to be active, among with other Cu-based catalysts such as Cu/MgO. However, not a very wide range of catalysts have been tested for the alcohol promoted synthesis, compared to the range of catalysts studied for the gas-phase reaction. Table VI provides a summary of the types of catalysts studied, including experiments with alkali co-catalysts. Alkali doping of solid catalysts and the addition of homegeneous alkali compounds has shown to accelerate methanol formation, but at the result of incompatibility with water and CO_2.

Table VI. Activity of selected catalyst and solvent combinations for alcohol promoted, liquid phase methanol synthesis. Conversion refers to total carbon conversion, unless only CO or only CO_2 is present in the feed.

Catalyst/solvent	Temperature, °C	Pressure, bar	Reaction time, h	Conversion, %	Methanol selectivity, %	Reference
Cu-Cr-O[1] ethanol	200	30	2	5.2 (CO_2)	59.6	[248]
Pd-Cu-Cr-O[1] ethanol	200	30	2	4.1 (CO_2)	51.2	[248]
Cu/ZnO[2] 2-butanol	180	30	4	30.4 (total)	97.8	[253]
Cu/ZnO methanol	170	50	20	40.3 (total)	98.7	[251]
Cu/ZnO 1-propanol	170	50	20	35.2 (total)	98.1	[251]
Cu/ZnO 2-butanol	170	50	20	47.0 (total)	98.9	[251]
Cu/ZnO/Al_2O_3[3] 2-butanol	220	50	20	12.2 (total)	96.4	[252]
Cu/MgO + HCOOK ethanol	150	50	12	61.9 (total)	98.9	[256]
Cu/MgO-Na_2CO_3 + HCOONa[4] ethanol	160	50	24	82.4 (CO)	88.3	[255]

1) $CO_2 + H_2$ feed
2) Catalyst prepared by sol-gel method
3) Space-time yield 6,3 g / kg h
4) No CO_2 in feed

EXPERIMENTAL SECTION

The experimental part of the thesis consisted of laboratory scale experiments on the alcohol promoted methanol synthesis process. A description of the synthesis process was given in Section 3.4 of the literature review. The following experimental section presents the methods, procedures and results of the experiments. Based on the results from the laboratory experiments, the process was scaled to an electrolyser unit with a hydrogen production capacity of 1 Nm^3. A preliminary design for the process is presented.

4 AIM OF THE EXPERIMENTS

The following aims were assigned to the experimental work. The feasibility of the synthesis method was to be confirmed: whether methanol could be produced at rates comparable to those presented in the previous, related studies. The proposed, ester-intermediated reaction route was to be validated by finding supporting evidence. Importantly, the influence of the main process parameters on the productivity of methanol would be studied.

4.1 Process parameters

Based on the literature review, the reaction temperature and pressure and the type and amount of catalyst used were considered the main process parameters. The reaction temperature would have a significant effect on both the kinetics and the thermodynamic equilibrium of the methanol synthesis reaction. Initially, the temperature range of 150 to 200 °C was considered interesting. At this range, the process could be viewed as a low-temperature process in comparison to the conventional gas-phase methanol synthesis, which is operated in the temperature range of 200-300 °C [139].

The effect of pressure was expected to be more straightforward, with the methanol productivity favored by increasing pressures. However, lower operating pressures would be preferred for practical purposes. Due to equipment limitations, the maximum total pressure was 60 bar in the experiments. Instead of the total operating pressure, the partial pressure of the reactant gases most significantly affects the rate of reaction. In the alcohol-promoted process, the vapor pressure of the alcohol solvent may constitute a significant fraction of the total pressure, depending on the temperature and the alcohol used.

A conventional methanol synthesis catalyst with a Cu/ZnO –based structure was chosen to be used in the experiments. Ideally, multiple catalysts with different types of composition and structure would be compared. However, due to time and availability constraints, only the single catalyst was decided to be used. This decision was supported by the seemingly competitive performance of the conventional methanol synthesis catalysts according to available information. A relatively large amount of catalyst was used per batch in order to promote the rate of reaction. Characterization of the catalyst was considered outside the scope of this work, as was testing of long-term catalyst stability.

For the alcohol solvent, 2-butanol and ethanol were chosen based on their good performance according to previous studies. Using methanol as the solvent would have been interesting but was ruled out due to expected difficulties in the analysis of reaction products, i.e. quantifying the amount of methanol formed in reaction from the methanol matrix.

4.2 Experimental plan

The experimental work consisted of batch reaction experiments performed in an autoclave reactor. Two types of experiments were performed with slightly different objectives and procedures. These are categorized as batch and semibatch experiments. In the batch experiments, the reactor was pressurized with the feed gas at the start of reaction, after which the feed of gas was stopped. In the semibatch experiments, the feed gas was continuously fed to the reactor at the set pressure. In both cases, a fresh batch of the solid catalyst and the alcohol solvent were added at the start of each experiment.

The first purpose of the batch experiments was to confirm the feasibility of the process and to test the performance of the experimental setup, i.e. to see if any methanol would be detected in the reaction mixture. Second, the effect of the main process parameters was roughly screened by running the experiments at different temperatures and pressures, using both alcohols, and varying the amount of catalyst used. Third, the operation of a batch reaction system allowed the monitoring of pressure changes in the reactor. The pressure data would provide useful information about the behavior of the reaction system.

In the batch experiments, two data points were used for each of the main process parameters. The temperature was set at 160 °C and 180 °C, total pressure at 30 and 60 bar, and the mass of catalyst at 10 and 20 g. Both ethanol and 2-butanol were used as solvents. Additionally, a

blank experiment with a non-alcoholic solvent was performed in order to confirm the promoting effect of the alcohols. Table VII lists all the batch experiments that wereperformed.

The effect of water in the reaction system was studied by two special experiments. First, 5 g (approximately 30 000 ppm by mass) of water was added to 2-butanol prior to reaction. In another run, 20 g of molecular sieve with a pore size of 3 Å was added to 2-butanol in an attempt to reduce the concentration of water in the reaction mixture. The removal of water would be based on the molecular size based, selective adsorption of water by the adsorbent material.

Table VII. List of the batch experiments. Total pressure corresponds to the initial pressure at the start of reaction and initially following sampling.

Experiment	Solvent	Mass of catalyst, g	Temperature, °C	Total pressure, bar
1	2-butanol	10	180	30
2	Ethanol	10	180	30
3	Ethanol	10	180	60
4	2-butanol	10	180	60
5	2-butanol	20	180	60
6	2-butanol	20	160	60
7	Ethanol	20	160	60
8	Ethanol	20	180	60
Non-alcohol	Hexane	20	180	60
Added water	2-butanol	10	180	60
Removal of water	2-butanol	10	180	60

The aim of the semibatch experiments was to provide more accurate information about the influence of the process conditions, particularly the partial pressure of the feed gas. Also, the productivity of methanol could presumably be maximized at constant pressures. The sequence of these experiments and the process conditions employed were planned based on the information provided by the batch experiments.

First, the effect of the partial pressure of the feed gas was studied. Partial pressures of 30, 40 and 50 bar were used in the experiments with 2-butanol. With ethanol, lower partial pressures of 20, 30 and 40 bar were used due to the higher vapor pressure of the solvent. The next set

of experiments tested the effect of reaction temperature. In these experiments, only 2-butanol was used, allowing the use of higher temperatures. The experiments were performed at the temperature range of 160 °C to 200 °C. Finally, the effect of reducing the amount of catalyst used was studied by an experiment with 5 g of catalyst in 2-butanol. Table VIII provides a listing of all the semibatch experiments.

Table VIII. List of the semibatch experiments. Partial pressure of feed gas is calculated by subtraction of total pressure by the calculated vapor pressure of the solvent.

Partial pressure experiments

Experiment	Solvent	Mass of catalyst, g	Temperature, °C	Partial pressure of feed gas
1	2-butanol	10	180	30
2	2-butanol	10	180	40
3	2-butanol	10	180	50
4	Ethanol	10	180	20
5	Ethanol	10	180	30
6	Ethanol	10	180	40

Temperature experiments

Experiment	Solvent	Mass of catalyst, g	Temperature, °C	Partial pressure of feed gas
7	2-butanol	10	160	40
8	2-butanol	10	170	40
2	2-butanol	10	180	40
9	2-butanol	10	190	40
10	2-butanol	10	200	40

Catalyst mass experiments

Experiment	Solvent	Mass of catalyst, g	Temperature, °C	Partial pressure of feed gas
11	2-butanol	5	180	40

5 MATERIALS AND METHODS

The experimental setup is pictured in Figure 9. A Parr 4520 autoclave reactor with an inner volume of 450 ml was used in the reaction experiments. The reactor was connected to a Parr 4848 control unit. SpecView –software was used to record of temperature and pressure data during reaction. The reaction temperature was automatically controlled by a combination of

external electric heating and a cooling water coil inside the reactor. Mixing was provided by a magnetic-driven stirrer with controlled frequency of rotation. The frequency was set at 600 rpm in all of the experiments.

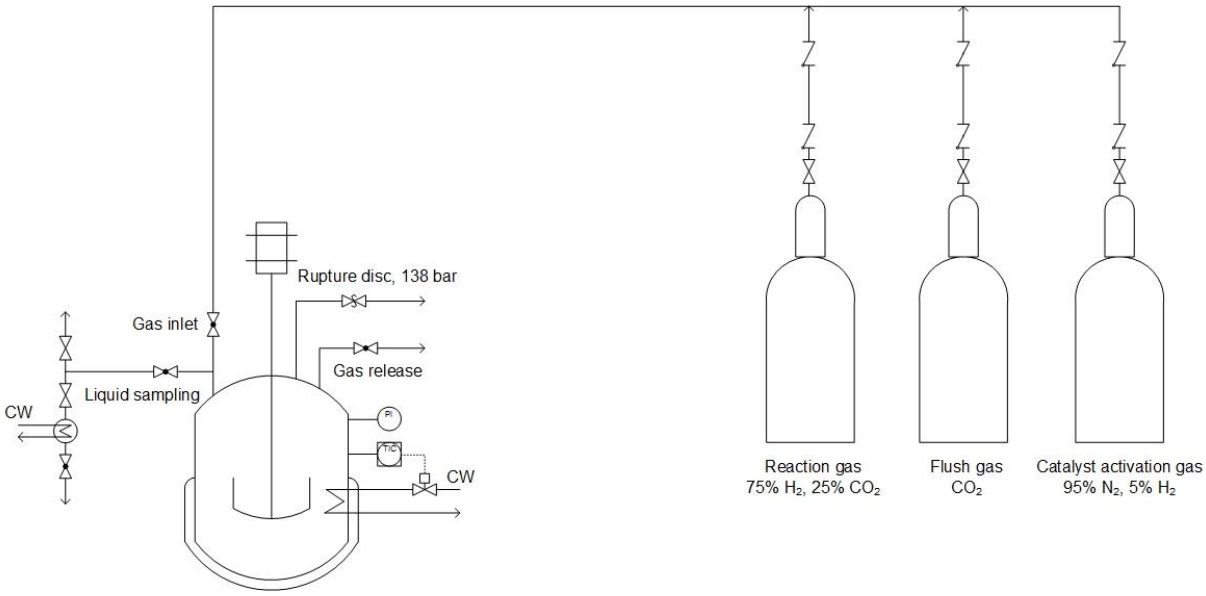

Figure 9. The experimental setup for the reaction experiments.

A commercially supplied catalyst with the reported composition of 63,5% CuO, 24,7% ZnO, 10,1% Al_2O_3 and 1,3% MgO was used. Ethanol and 2-butanol (both analysis grade) were used as the alcoholic solvents, and an isomeric mix of hexane (99% C-6 hydrocarbons) as the non-alcoholic solvent. Purified water (ELGA PURELAB flex) was used in the experiment with added water.

A mixed gas containing 75% hydrogen and 25% carbon dioxide was used as the reactant gas. For activation of the catalyst, a mixed gas containing 5% hydrogen in nitrogen was used. The purpose and method of catalyst activation will be described below. Pure carbon dioxide was used for purging the reactor and gas lines. The gases were fed from gas cylinders through the reactor gas inlet valve. The pressure inside the reactor could be lowered through the gas release valve. The outlet gas was not collected or analyzed.

Liquid samples from the reaction mixture could be collected using a water-cooled sample collection vessel. By cooling the collected sample, any vapors present in the sample would be

condensed. The liquid sampling valve was connected to the dip tube that was also used as gas inlet, allowing the flushing of the tube by gas prior to collecting the sample. This ensured that the collected samples are a good representation of the reaction mixture at the time of sampling.

5.1 Experimental procedure

The preparation of the catalyst consisted of grinding followed by activation. The catalyst was ground and sieved to a particle size of 150-500 μm and placed inside the reactor, where the activation was performed *in-situ*. The purpose of activation is to reduce the passivated metal catalyst, forming the active catalytic sites for the reaction.

Following purging with carbon dioxide, the reactor was pressurized with 5 bar of the activation gas. The mixer was set at 600 rpm, and the heating of the reactor started. During heating, the pressure was maintained at approximately 5 bar. According to the instructions provided by the catalyst supplier, the activation was continued for two hours at 150 °C. The gas was not continuously fed to the reactor during activation. However, some of the gas inside the reactor was periodically replaced with fresh gas in order to maintain the reducing environment. After the temperature of 150 °C had been maintained for two hours, the reactor was cooled. Following cooling, the catalyst was left overnight in 2 bar of the activation gas.

The following day, the activation gas was removed and the reactor was purged with CO_2 and opened. 200 ml of the alcohol (or hexane) solvent was poured on top of the activated catalyst, leaving 250 ml of gas and vapor space inside the reactor. The solvent was added quickly in order to avoid passivation of the catalyst by oxygen. After closing, the reactor was carefully purged with CO_2 to remove oxygen. From this point on, the procedure slightly differed between the batch and semibatch experiments.

5.1.1 Batch experiments

After purging, an approximate CO_2 pressure of 2 bar was left inside the reactor. Mixing was started at 600 rpm, and heating of the reactor to the reaction temperature was initiated. Upon reaching the reaction temperature, an initial liquid sample was collected by the following sampling sequence. First, the dip tube was flushed by feeding a small amount of CO_2, and the mixing was stopped. A few minutes of settling time was allowed in order to minimize the amount of catalyst contained in the liquid sample. The sample was then collected by opening and

closing the sampling valve. Mixing was then restarted. The sample was allowed to cool for at least 30 seconds and then removed from the sampling device.

The reaction was started by introducing the reaction gas mixture. The total pressure in the reactor was adjusted by using the pressure control valve of the gas cylinder. After setting the pressure, the gas inlet was closed. The reaction was allowed to run for 2 hours, at which point the next liquid sample was collected. The sample was collected as described above, except the dip tube was flushed using the reaction gas instead of CO_2. Two more samples were collected at 2 hour intervals, with the total reaction time being 6 hours. After collecting the final sample the reactor was cooled and emptied.

5.1.2 Semibatch experiments

In the semibatch experiments, the reactor was pressurized to 10 bar of the reactant gas prior to heating to the reaction temperature. This was done in an attempt to minimize the effect of side reactions during heating (see Section 6.1 Batch experiments). After reaching the reaction temperature, the initial sample was collected as described above, only using the reactant gas to flush the sampling tube instead of CO_2.

Following the initial sampling, a brief purging of the reactor with the reactant gas was performed with the aim of removing any other components other than H_2, CO_2 and the solvent vapor from the gas phase. The purging was however limited by the associated drop in temperature. After this step, the total pressure was adjusted and the feed of gas was left open for the duration of the experiment. Liquid samples were collected every 2 hours, with the sampling procedure identical to the batch experiments. The total reaction time was again 6 hours.

5.2 Analysis

The liquid samples were analyzed by gas chromatography. Agilent Technologies 6890N gas chromatograph with a thermal conductivity detector and a polar capillary column (Zebron ZB-WAXplus) was used. An isothermal method with a column temperature of 70 °C and detector temperature of 250 °C was employed. The sample injection volume was 0,2 µl and helium (1,1 ml/min) was used as the carrier gas.

Identification and calibration standards were prepared using methanol, ethanol and 2-butanol (all analysis grade), ethyl formate (technical grade) and purified water (PURELAB flex). Acetaldehyde (analysis grade) was used for identification but quantification was not possible due to difficulties with preparing accurate standard solutions. More information about the analysis can be found in Appendix II.

6 RESULTS AND DISCUSSION

6.1 Batch experiments

The information collected from the batch experiments consists of the recorded pressure data and the composition of the analyzed liquid samples. This information was used to make general observations about the behavior of the reaction system and to measure the productivity of methanol. Specific productivity parameters were used to characterize and compare the effectiveness with which methanol was produced in each experiment.

6.1.1 Alcohol dehydrogenation

When heating the alcohol solvent in presence of the activated catalyst, the pressure inside the reactor was found to increase to levels above the vapor pressure of the solvent. This was observed with both of the alcohols, with 2-butanol showing the more significant amount of excess pressure. The deviation was increased at higher reaction temperatures. This phenomenon could be explained by catalytic dehydrogenation of the alcohols. In fact, copper based catalysts have been explicitly studied for these reactions in the context of reforming alcohols into hydrogen [263, 264, 265, 266, 267]. On $Cu/ZnO/Al_2O_3$, ethanol is mainly decomposed into acetaldehyde at temperatures below 350 °C [267], according to the following equation:

$$C_2H_5OH \rightarrow C_2H_4O + H_2 \tag{40}$$

2-butanol is decomposed into 2-butanone [268]:

$$C_4H_8OH \rightarrow C_4H_8O + H_2 \tag{41}$$

The hydrogen formed in these reactions is considered to cause of the observed increase in pressure. The reactions were confirmed by the detection of acetaldehyde and 2-butanone in

the reaction mixtures. The concentration of these species was at the highest in the initial samples taken after heating of the reaction mixture, prior to feeding the reactant gas. Figures Figure 10 and Figure 11 illustrate the excess pressure observed over the calculated vapor pressure. The Figures also show the concentration of acetaldehyde and 2-butanol in the initial liquid samples.

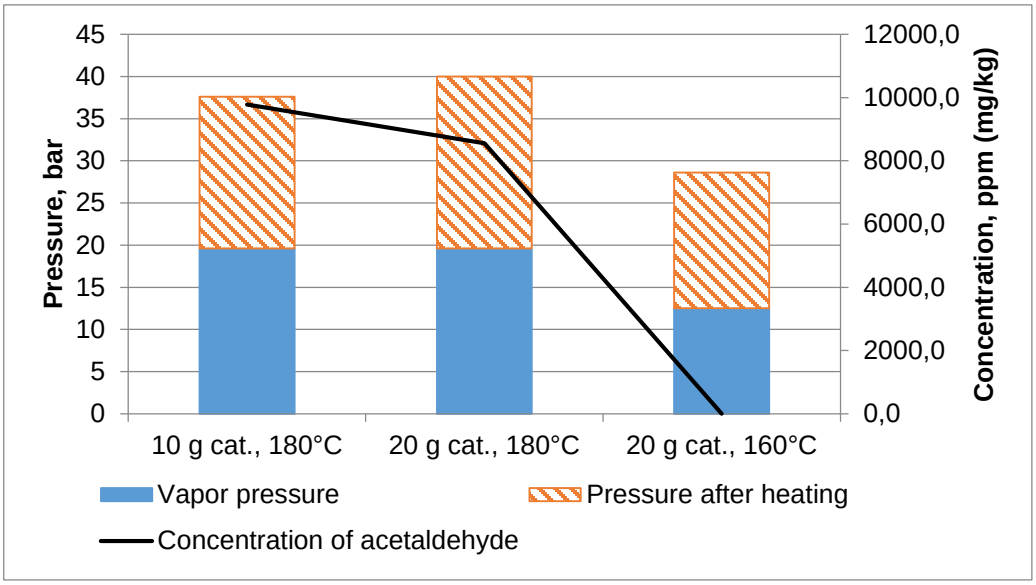

Figure 10. The calculated vapor pressure, the measured total pressure and the concentration of acetaldehyde in ethanol after heating of the reaction mixture. The concentrations of acetaldehyde are only illustrative and of unknown accuracy.

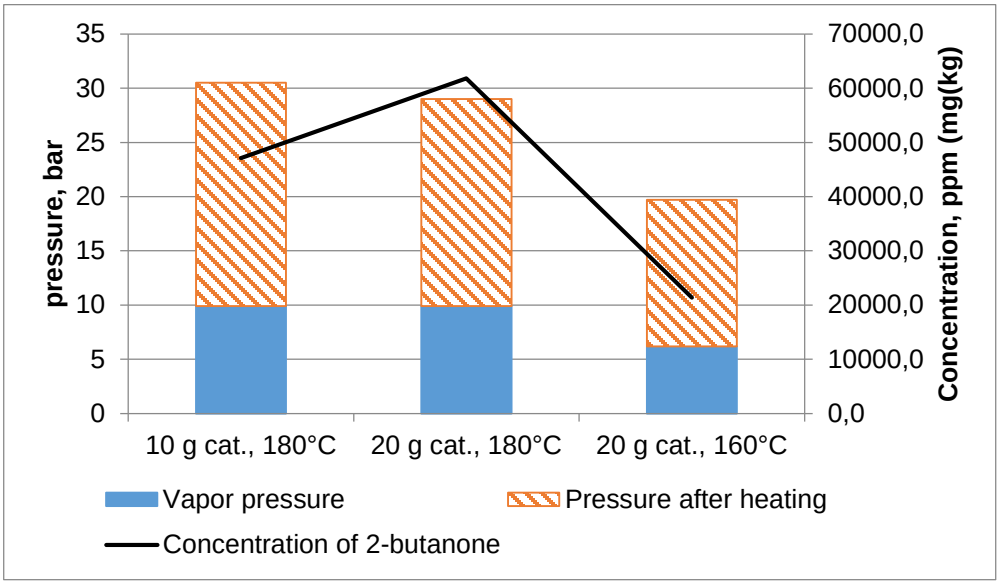

Figure 11. The calculated vapor pressure, the measured total pressure and the concentration of 2-butanone in 2-butanol after heating of the reaction mixture.

It can be noted that the excess pressure generated by the dehydrogenation reactions is quite significant, especially in the case of 2-butanol. In 2-butanol, the total pressure is approximately triple the vapor pressure while in ethanol, the total pressure is approximately double the vapor pressure. The concentration of 2-butanone is increased with increasing the amount of catalyst from 10 g to 20 g and lowered with decreasing the reaction temperature from 180 °C to 160 °C.

Contrastingly, in the case of ethanol, a lower concentration of acetaldehyde was detected with increased mass of catalyst. At 160 °C, no acetaldehyde was detected at all. Presumably, the concentration of acetaldehyde was below the detection limit. Though, as previously noted, the concentration data for acetaldehyde should be viewed with caution due to inaccuracy of analysis.

6.1.2 Pressure and composition data from the batch experiments

The combination of pressure data and the results from analysis of the liquid samples provides important information about the behavior of the reaction system. By looking at the changes in total pressure and the concentration of various components in the reaction mixture over time, observations about the relative effects of the main and side reactions can be made.

Examples of the combined data from single experiments in 2-butanol and ethanol are shown in FiguresFigure 12 and Figure 13, respectively. These experiments were performed at identical reaction conditions, allowing direct comparisons between the two alcohols. The data from these two experiments is also a good representation of the general behavior observed in all of the experiments. Similar figures for the rest of the experiments can be found in Appendix III.

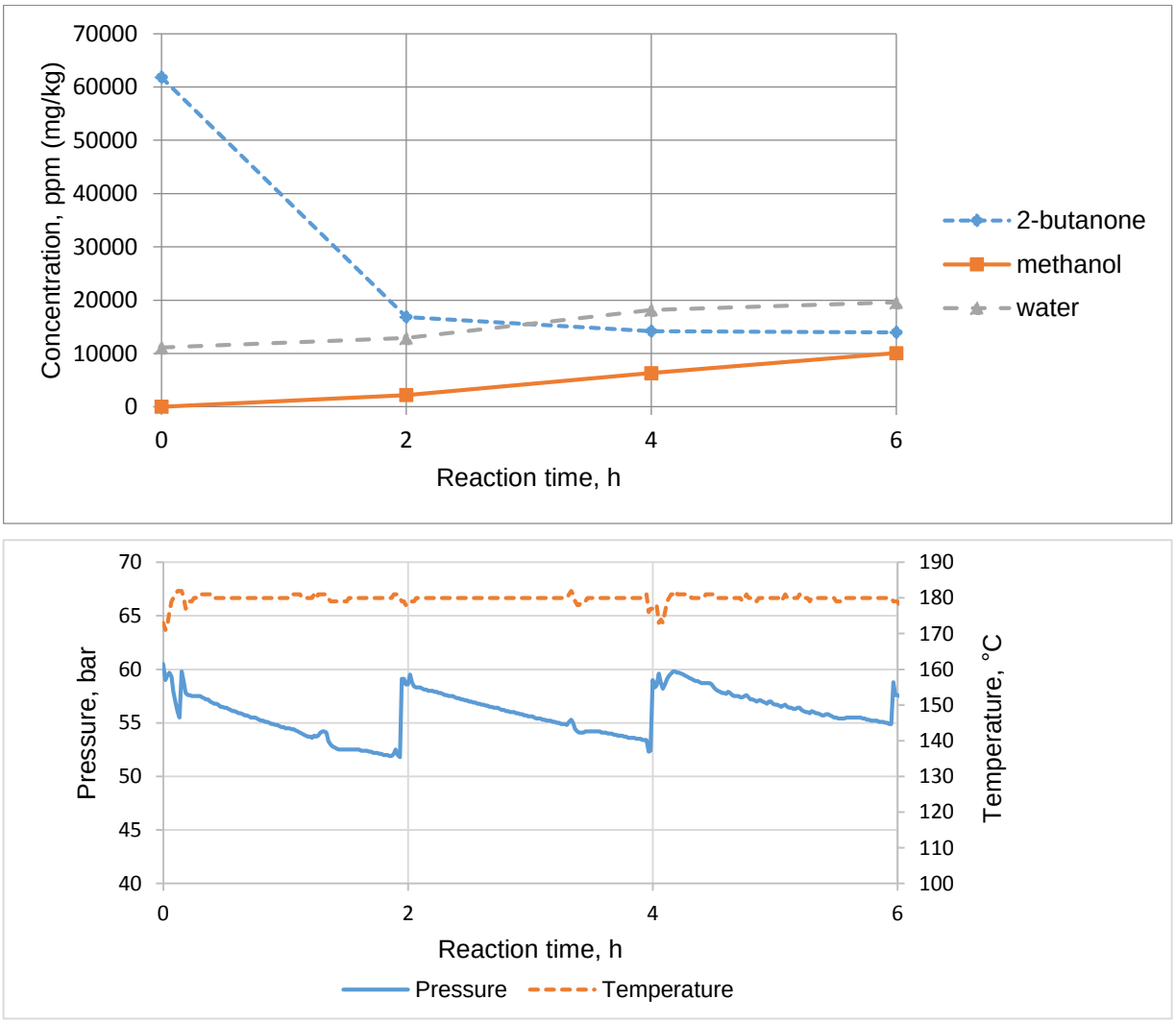

Figure 12. The concentration of reaction products and the pressure and temperature over reaction time in the experiment with 2-butanol and 20 g of catalyst, at 180 °C and 60 bar of total pressure.

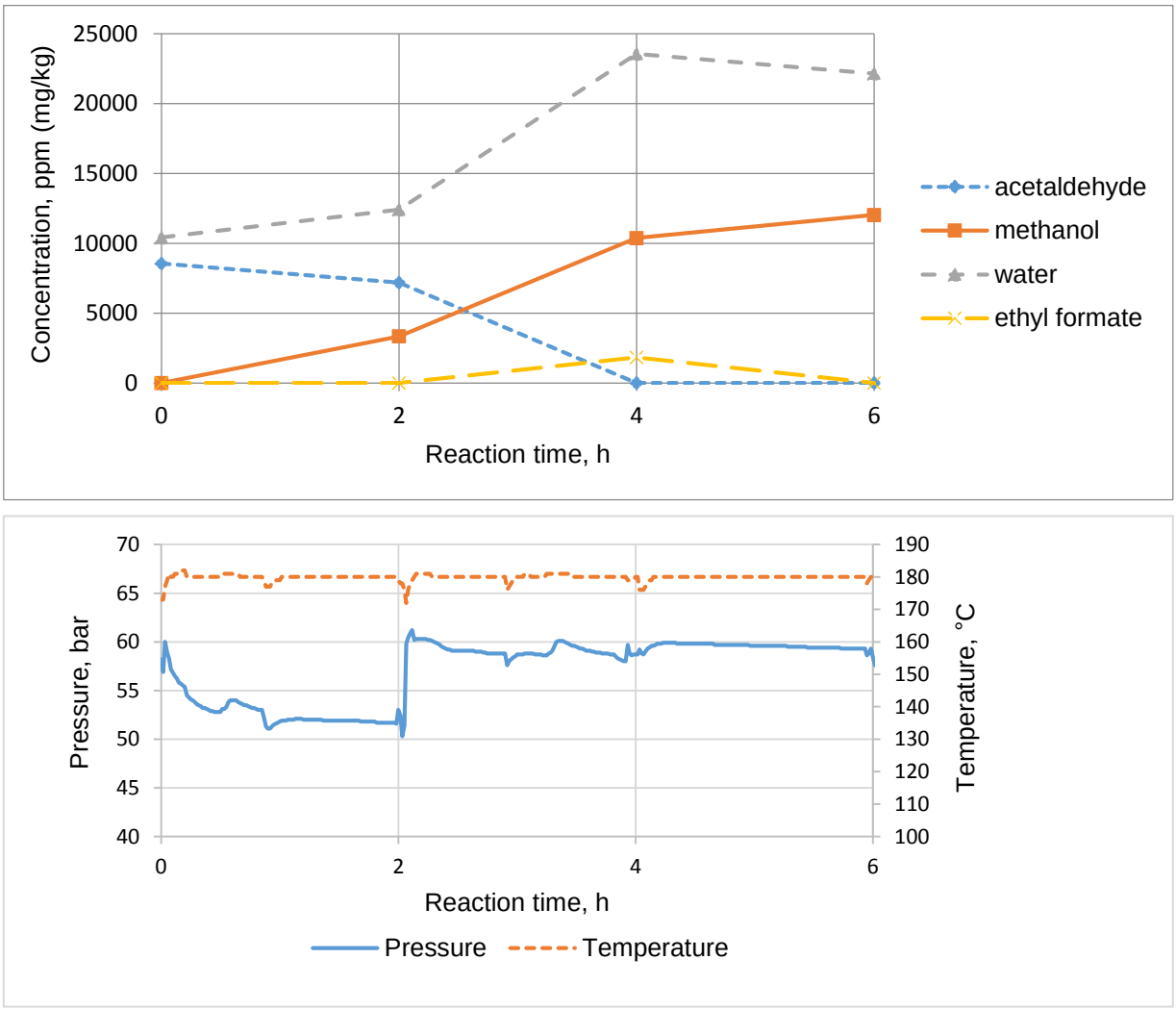

Figure 13. The concentration of reaction products and the pressure and temperature over reaction time in the experiment with ethanol and 20 g of catalyst, at 180 °C and 60 bar of total pressure. The concentrations of acetaldehyde are only illustrative and of unknown accuracy.

6.1.2.1 Effects of alcohol dehydrogenation

After heating, the dehydrogenation products of the alcohols and water are found in the reaction mixture. The samples taken at this stage correspond to the point zero on the reaction time axis in the figures above. In 2-butanol, 2-butanone is formed according to reaction (41), hydrogen being released in the process. Similarly, ethanol is dehydrogenated into acetaldehyde

according to reaction (40). 2-butanone is generally found in more significant quantities than acetaldehyde. In the examples, the concentration of 2-butanone is six times the concentration of acetaldehyde at identical reaction conditions.

After introducing the feed gas, the concentration of 2-butanone and acetaldehyde significantly decrease with reaction time. Presumably, the increased hydrogen pressure leads to the dehydrogenation reactions proceeding to the reverse direction. 2-butanone and acetaldehyde combine with hydrogen, forming again the corresponding alcohols. Due to the consumed hydrogen, a drop in pressure is observed, as can be seen from the pressure curves in Figures Figure 12 and Figure 13.

Generally, the drop in pressure is the most significant between zero and two hours of reaction time. The reduction in the concentration of the dehydrogenation products is also the most rapid at this time interval, creating a link between the dehydrogenation reactions and the pressure changes in the system. The disappearance of 2-butanone and acetaldehyde is slower after 2 hours of reaction. In many experiments, the concentration appears to find an equilibrium between 4 to 6 hours of reaction time. This is especially the case with 2-butanone, with Figure 12 giving a good example.

6.1.2.2 Methanol synthesis and the role of water

The concentration of methanol seems to generally increase rather linearly with reaction time. In some experiments, a decrease in the rate of methanol formation can be noted after 4 hours of reaction. The slowing reaction rate is probably explained by the increasing concentration of water and by the methanol synthesis reaction (27) slowly approaching equilibrium. However, the concentration of methanol does not stagnate in any experiment, so it can be concluded that 6 hours of reaction time is not enough to reach the equilibrium composition at the present reaction conditions.

The presence of water prior to introducing the feed gas could be explained by the reverse water-gas shift (RWGS) reaction (28), in which water and carbon monoxide is formed from CO_2 and hydrogen.

Carbon dioxide would be present in the reactor during the heating stage due to the use of CO_2 in purging of the reactor. Hydrogen would in turn be formed by dehydrogenation of the alcohols. The RWGS reaction could be confirmed by identifying CO in the reaction outlet gas. However,

the significance of the RWGS reaction with this type of catalyst and reaction system has been well documented (Section 3.1.1). As such, it provides a very convincing explanation for the presence of water.

The water gas-shift reaction would be expected to run to the reverse direction after introduction of CO_2 and hydrogen, forming water. In addition to the water-gas shift reaction, the concentration of water is influenced by the methanol synthesis reaction in which water is formed as by-product. The water content would increase by the methanol synthesis reaction running in the forward direction.

The concentration of water generally shows an increasing trend with reaction time. However, the formation of water seems to slow down or even stop after 4 hours of reaction time in some experiments. In some of the experiments with ethanol, the concentration of water even decreases at this stage of reaction. An example can be seen in Figure 12. These observations would imply that the water concentration is approaching equilibrium. Simultaneously, the methanol synthesis reaction still proceeds to the forward direction. Thus, only the water-gas shift reaction could reasonably explain the stagnating or decreasing concentration of water. It appears that the water-gas shift reaction approaches equilibrium and changes direction, consuming water produced in the methanol synthesis reaction.

The relationship between the concentrations of methanol and water is illustrated in Figure 14, which shows the ratio of the molar concentrations of these species in all of the experiments performed with 2-butanol, including the semibatch experiments. It can be seen that the concentration of methanol is increased faster than that of water, leading to increasing relative concentration of methanol over the reaction time. In the methanol synthesis reaction, equimolar amounts of methanol and water are formed, and it is apparent that water is produced and consumed in side reactions. A similar trend can be found in the experiments with ethanol.

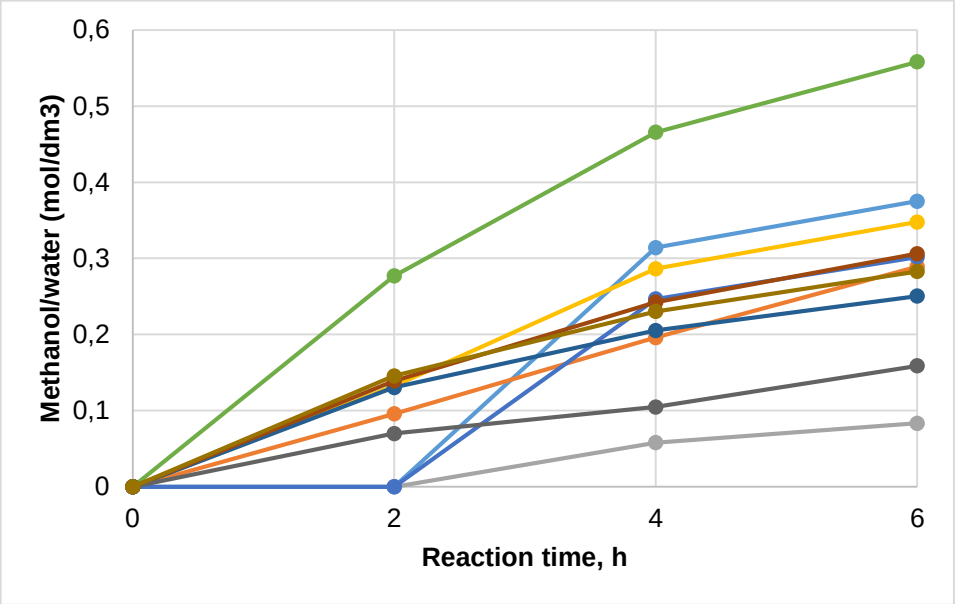

Figure 14. The ratio of the molar concentrations of methanol and water over reaction time in the experiments with 2-butanol, including both batch and semibatch experiments. The individual experiments are not identified as the purpose of the graph is to demonstrate the general pattern.

The methanol synthesis reaction also leads to decreased total pressure, both due to reduction in the number of molecules and the condensation of the products methanol and water to the liquid phase. The relative effects of this reaction and the alcohol dehydrogenation reactions to the total pressure are difficult to quantify. However, the decrease in pressure is the most significant between 0 to 2 hours of reaction time, a time period also corresponding to a marked decrease in the concentration of acetaldehyde and 2-butanone. It would seem that at least during the initial stages of reaction, the dehydrogenation reactions have a more pronounced effect on the total pressure compared to the methanol synthesis reaction.

At the later time periods, the concentration of acetaldehyde and 2-butanone more or less stabilizes, and the pressure changes are mainly influenced by the methanol synthesis reaction. As the concentration of methanol is increased almost linearly, the effect of this reaction on the total pressure is close to constant throughout the time of reaction. Finally, the RWGS reaction would also lead to pressure changes due to the condensation of water to the liquid phase. This adds to the quite complex connection of the main and side reactions to the total pressure of the system.

More information about the role of water in the system was given by the special experiments in which water was added or removed by adsorption on a molecular sieve. The concentration graph for the experiment with added water is presented in Figure 16, and a similar graph for the molecular sieve experiment is shown in Figure 17. For comparison, Figure 15 shows the concentration data from the base experiment in 2-butanol at identical reaction conditions.

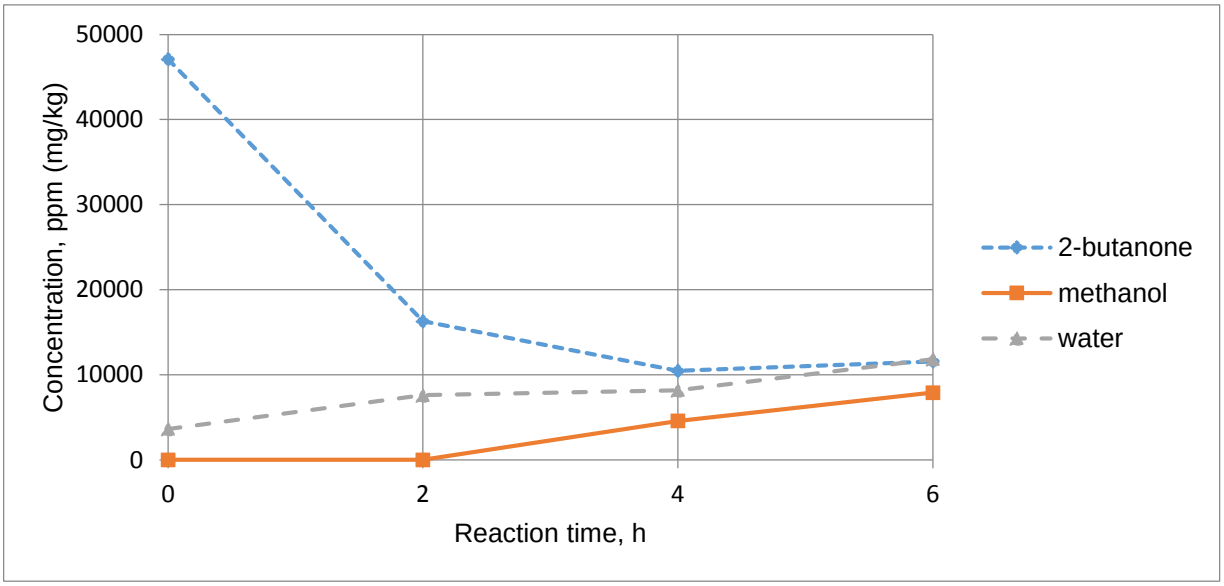

Figure 15. The concentration of reaction products over time in the experiment with 2-butanol and 10 g of catalyst, at 180 °C and 60 bar of total pressure.

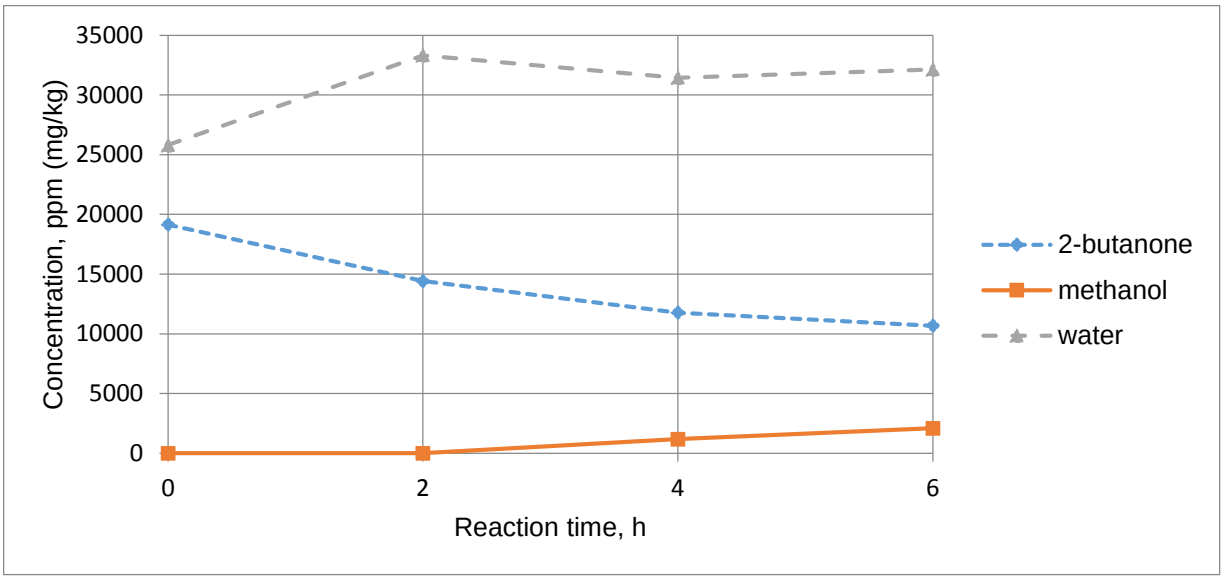

Figure 16. The concentration of reaction products over time in the experiment with 2-butanol, 5 g of water and 10 g of catalyst, at 180 °C and 60 bar of total pressure.

The detrimental effect of water on the synthesis of methanol is apparent when comparing Figures Figure 15 and Figure 16. With approximately 30000 ppm (mass) of water added, the concentration of methanol after 6 hours of reaction is approximately 75% lower compared to the base experiment. The concentration of water is close to constant over the reaction time, with the water content just above the 30 000 ppm mark. It would seem that the equilibrium concentration of water in the system is located around this level at these reaction conditions.

In addition to the lower concentration of methanol, the concentration of 2-butanone is also lowered by the addition of water. The 2-butanone content after heating is lower by over 50% in the experiment with added water compared to the base experiment. This would suggest that the limiting effect of water on the production of methanol is more significantly related to the inhibiting effects on the catalyst compared to thermodynamic effects. The expected thermodynamic effect would be the shift in the reaction equilibrium of the methanol synthesis reaction (27) caused by the accumulation of water. However, such an effect would not be relevant for the alcohol dehydrogenation reaction, yet this reaction also seems to be limited by the increased concentration of water.

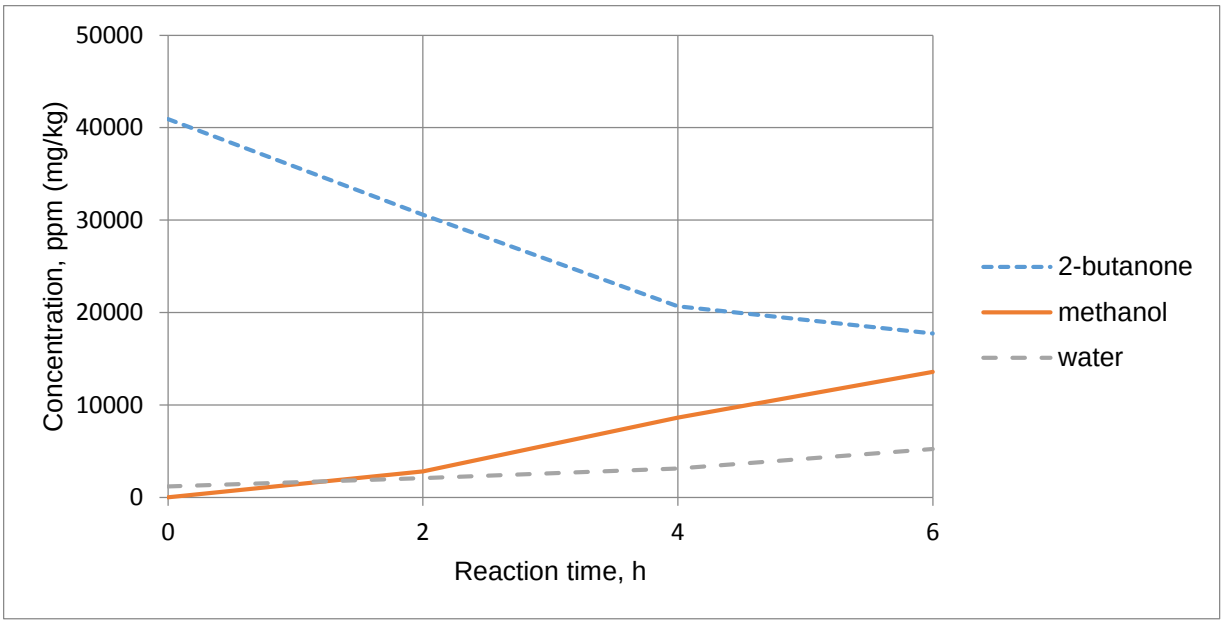

Figure 17. The concentration of reaction products over time in the experiment with 2-butanol, 10 g of catalyst and 20 g of 3Å molecular sieve, at 180 °C and 60 bar of total pressure.

The removal of water from the reaction mixture by a molecular sieve is based on the selective adsorption of water based on molecular size. On the type of molecular sieve used, the pore size is such (3 Å, or $3 \cdot 10^{-10}$ m) that water can enter the pores but the rest of the components in the reaction mixture cannot fit. As a result, the amount of surface area available for adsorption is miniscule for the other components compared to that for water. The addition of the molecular sieve proved quite effective: the concentration of water was lowered by approximately 50% in comparison to the base experiment. The concentration of methanol was in turn increased by over 50%, providing more evidence of the important effect of water on the production of methanol.

6.1.2.3 Intermediates and reaction mechanism

According to the proposed reaction route (see Section 3.4.1), the synthesis of methanol proceeds through the formate esters of the corresponding alcohol solvent. In case of ethanol, the intermediate species is ethyl formate, while in 2-butanol it is butyl formate.

Ethyl formate was detected in many of the experiments performed in ethanol. A good example in seen in Figure 18, showing the composition data from the experiment with 20 g of catalyst, at 160 °C and 60 bar. In this experiment, ethyl formate was found at concentrations below 5000 ppm (mass) at 2 to 6 hours of reaction time, while in some of the experiments, ethyl formate was only detected in some of the samples. In some experiments, ethyl formate was not detected at all, presumably due to the concentration falling below the detection limit.

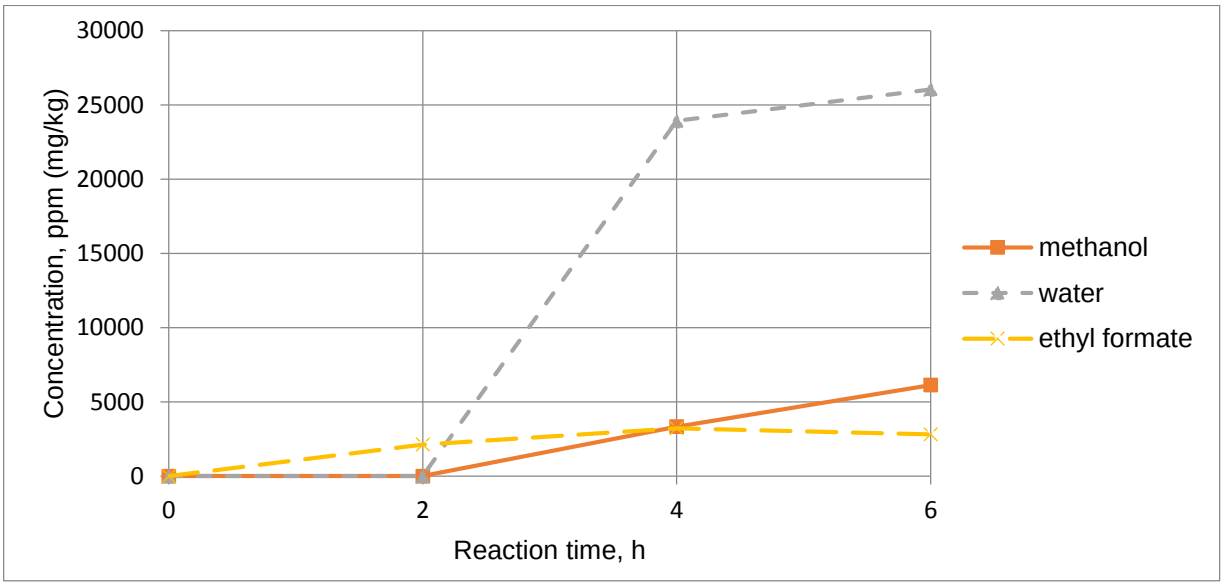

Figure 18. The concentration of reaction products and the pressure and temperature over time in the experiment with ethanol and 20 g of catalyst, at 160 °C and 60 bar of total pressure. The concentrations of acetaldehyde are illustrative and of unknown accuracy.

Generally, the behavior of ethyl formate seems to follow a pattern that is compatible with the proposed reaction route. The stagnant concentration at a low level indicates that ethyl formate is consumed in a further reaction. The concentration reaches an equilibrium level dictated by the relative rates of the reactions in which ethyl formate is formed and consumed. Under the proposed reaction scheme, ethyl formate is formed in the reaction of formic acid with ethanol (32) and then consumed by hydrogenation, forming methanol and ethanol (33).

The formic acid is first formed by the hydrogenation of CO_2. Fan et al. [248] have proposed that the hydrogenation of ethyl formate (33) is the rate-determining step of the overall reaction. This view is supported by the presence of ethyl formate in the reaction mixture. At the observed peak concentration of ethyl formate, the rate of the hydrogenation reaction (33) is increased to equal the rate of the formation reaction (32), and, an equilibrium concentration is reached. If the formation of the ester (32) was the rate determining step, the ethyl formate would be instantly consumed by hydrogenation and would not be detected.

Further, in the experiment depicted in Figure 18, the concentration of ethyl formate is higher than that of methanol after 2 hours of reaction time. After that point, the methanol content begins to increase, reaching the concentration of ethyl formate after 4 hours and surpassing it during the last 2 hours. These observations also support the role of ethyl formate as an intermediate in the synthesis of methanol as the formation of methanol seems to increase after ethyl formate is present in the reaction mixture.

The experiments with 2-butanol gave no information about reaction intermediates. Butyl formate could not be analyzed even qualitatively due to unavailability of the compound for use as analytical standard. Further, no unidentified peaks potentially indicating this compound were detected in the analysis of 2-butanol reaction mixtures.

However, butyl formate could reasonably be expected to be present based on the information given by the ethanol experiments, which suggest that an analogous role of butyl formate in 2-butanol would be likely. As for not showing up in analysis, the concentration of butyl formate might have been too low for detection or the compound might have been masked by other components.

Finally, the experiment with hexane showed no methanol formation, providing further evidence for the ester intermediated reaction scheme and the importance of the alcoholic solvents.

6.1.2.4 Conversion and selectivity

Conversion is defined as the ratio of the amount of reactant consumed in reaction to the amount of reactant in the system at the start of reaction (Eq. 42). With the stoichiometric ratio of CO_2 and H_2 in the feed gas, the calculated conversion values apply for both of the gases individually.

$$X = \frac{n_0 - n_1}{n_0} \cdot 100\% \quad (42)$$

n_0 Amount of reactant at the start of reaction, mol

n_1 Amount of reactant at the end of reaction, mol

As composition data from the reactor outlet gas was not available, the consumption of feed gas was used for the calculation of conversions. The consumption was estimated based on the decrease in total pressure during the reaction time:

$$X = \frac{p_1 - p_2}{p_1} \cdot 100\% \quad (43)$$

X Conversion, %

p_1 Total pressure at the start of reaction time, bar

p_2 Total pressure at the end of reaction time, bar

In the experiments, p_1 corresponds to the initial pressure set at the start of reaction and after the collection of the liquid samples. Thus, separate conversion values were calculated for each of the 2 hour reaction time intervals between sampling. Due to the effect of the side reactions (see below), the conversion values at 2 to 4 and 4 to 6 hours of reaction time are considered to more accurately relate to the methanol synthesis reaction. The conversion values at these time intervals are presented in Table IX.

Table IX. The conversion of feed gas (CO_2 + H_2) during 2-4 and 4-6 hours of reaction time, based on the decrease in pressure during reaction time.

Solvent	Mass of catalyst, g	Temperature, °C	Total pressure, bar	Conversion (2-4 h), %	Conversion (4-6 h), %
2-butanol	10	180	60	9 %	9 %
2-butanol	20	180	60	11 %	10 %
2-butanol	20	160	60	4 %	3 %
Ethanol	20	160	60	5 %	8 %
Ethanol	20	180	60	4 %	1 %

It is not only the methanol synthesis reaction that leads to changes in the total pressure. The side reactions, especially the alcohol dehydrogenation reactions, have a significant effect on the pressure in the system. For this reason, this calculation method is not very accurate for the estimation of conversion in the methanol synthesis reaction. Analysis of the reactor outlet gas would be required in order to calculate the amount of feed gas consumed more accurately.

The effect of the alcohol dehydrogenation reaction is most clearly seen during the first 2 hours of reaction time. As previously discussed (Section 6.1.2 Pressure and composition data), the significant decrease in pressure at this stage is associated with a decreasing concentration of the dehydrogenation products acetaldehyde and 2-butanol. These compounds react with hydrogen after the feed gas is introduced, forming the corresponding alcohols.

This consumption of hydrogen is probably the main factor in the decreasing pressure at the first 2 hours of reaction time. The consumption of feed gas by the methanol synthesis reaction would be small in comparison. Resultantly, the conversion values calculated at this stage of reaction are not very informative as to the progress of the methanol synthesis reaction.

At the later reaction time intervals, the degrees of conversion range from 1% to 11% per 2 hours of reaction. At this stage, the effect of the alcohol dehydrogenation reactions is not as significant and the conversion values are probably more relevant to the methanol synthesis reaction. However, the effect of the side reactions is still not completely eliminated. For this reason, these conversion values should be viewed as rough estimates, essentially providing a maximum value to the actual conversion by the main reaction.

Conversion values presented in the previous studies were given in Table VI. The values obtained here are in the range of the previous results obtained with a feed of CO_2, as opposed to CO-containing mixtures. Conversion values of 4.1% and 5.2% have been presented, however on differing types of catalysts. The values reported for gas-phase synthesis from CO_2 with various types of catalysts (Table IV in the literature review) are somewhat higher, generally ranging from 10 to 20%, with up to 27% reported.

Selectivity of methanol is defined as the fraction of methanol in the total amount of products produced by reaction:

$$S_{\mathrm{MeOH}} = \frac{n_{\mathrm{MeOH}}}{n_{\mathrm{MeOH}} + \sum_1^i n_{\mathrm{i}}} \cdot 100\% \qquad (44)$$

S_{MeOH} Selectivity of methanol, %

n_{MeOH} Amount of methanol produced in reaction, mol

n_{i} Amount of product *i* produced in reaction, mol

Selectivity is commonly defined in respect of a certain component in the reaction feed. Choosing CO_2 as the basis, only the products originated from the conversion of CO_2 would be counted when calculating the selectivity. This definition excludes the products of alcohol dehydrogenation, leaving ethyl formate as the only side product detected.

In this case, selectivity of methanol would be 100% in all of the experiments in 2-butanol and also in the experiments in ethanol where no ethyl formate was detected. However, a selectivity of 100% would not be realistic based on the literature. In the least, the formation of gaseous byproducts CO and possibly CH_4 would be expected [248]. The presence of these components could not be confirmed as the reactor outlet gas was not analyzed. For this reason, selectivity estimations based on the available results were not considered beneficial.

6.1.3 Methanol productivity

Specific methanol productivity was calculated in order to effectively compare literature information and the results of the experiments and to quantify the effect of the process variables. The calculated productivity also facilitates direct comparisons to the results of previous studies. The specific productivity per catalyst mass measures the mass of methanol produced per mass of catalyst per hour:

$$\text{Catalyst specific productivity} = \frac{\text{g of methanol produced}}{\text{kg of catalyst} \cdot \text{h}} \tag{45}$$

The productivity per volume measures the mass of methanol produced per volume of solvent per hour:

$$\text{Volumetric productivity} = \frac{\text{g of methanol produced}}{\text{l of solvent} \cdot \text{h}} \tag{46}$$

The catalyst specific productivity is commonly used to measure the activity of heterogeneous catalysts. As such, this parameter allows direct comparisons between the results of the present experiments and the results available from previous liquid and gas-phase methanol synthesis studies. When used to compare the individual experiments, the productivity measures the efficiency with which the mass of catalyst is utilized and allows the optimization of the catalyst

mass. It could also point out any non-kinetic limitations in the system if non-linearity between the mass of catalyst used and the amount of methanol produced is observed.

The volumetric productivity is a more suitable quantity for comparing the results of the individual experiments. It provides a more absolute measure of the effectiveness with which methanol is produced. It allows the overall optimization of the process conditions, including the mass of catalyst, with the aim of maximizing the rate of methanol production in the reactor volume. The productivity results are thus primarily presented and discussed using the volumetric productivity.

6.1.3.1 Effect of temperature in the batch experiments

Figure 19 presents the volumetric productivity of methanol in both ethanol and 2-butanol at the temperatures of 160 °C and 180 °C, with 20 g of catalyst and 60 bar of total pressure. The productivity was found to be higher at higher temperature, while ethanol showed better results of the two solvents. In case of ethanol, the volumetric productivity increased from 0.8 to 1.6 g/(l·h) when going from 160 °C to 180 °C. In 2-butanol, the increase was even more significant, going from 0.3 to almost 1.4 g/(l·h), an increase of nearly 80%.

At the higher temperature, methanol is formed faster due to the increased reaction rate. However, the equilibrium of the methanol synthesis reaction is more favorable at the lower temperature. If the reaction time was adequate to reach the equilibrium, the productivity would be expected to be higher at the lower temperature due to the larger equilibrium concentration of methanol. At 6 hours of reaction time, the equilibrium is clearly not reached, and the overall production of methanol is increased by the increased temperature.

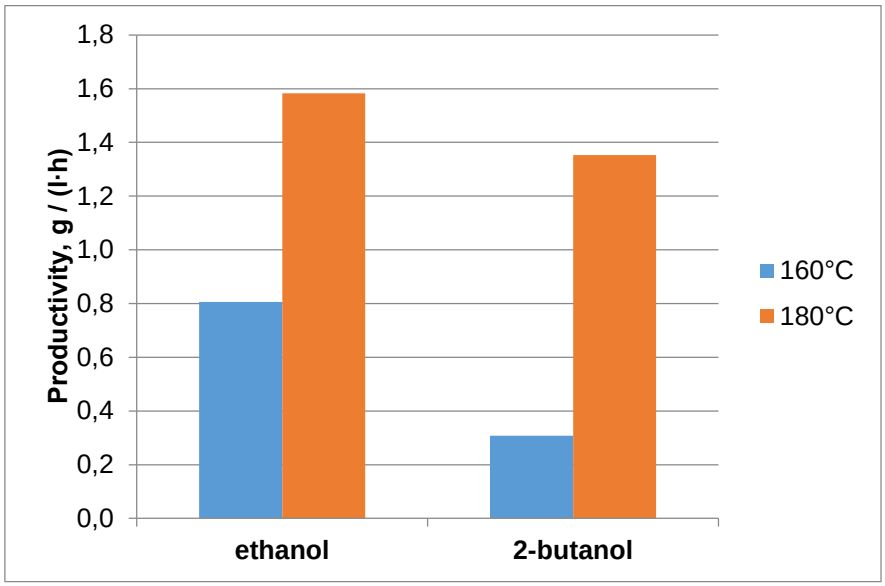

Figure 19. Volumetric productivity of methanol at 160 °C and 180 °C. 20 g of Cu/ZnO catalyst, 60 bar total pressure, 2-butanol and ethanol solvents.

6.1.3.2 Effect of total pressure in the batch experiments

Figure 20 presents the volumetric productivity of methanol in ethanol and 2-butanol at 30 and 60 bar of total pressure, with 20 g of catalyst at 180 °C. As the reaction temperature and vapor pressure of the solvent remains constant, the increased total pressure corresponds to an increase in the concentration of the feed gas components. The productivity of methanol is expected to increase with the increasing concentration of reactants.

The two alcohols show very different results. In 2-butanol, no methanol was found in the experiment carried at 30 bar of total pressure. At 60 bar, methanol was produced with a productivity of over 1.0 g/(l·h). In ethanol, the productivity at the higher pressure was identical to that measured in 2-butanol. However, the amount of methanol formed was even higher at the lower pressure, leading to a productivity value of 1.6 g/(l·h).

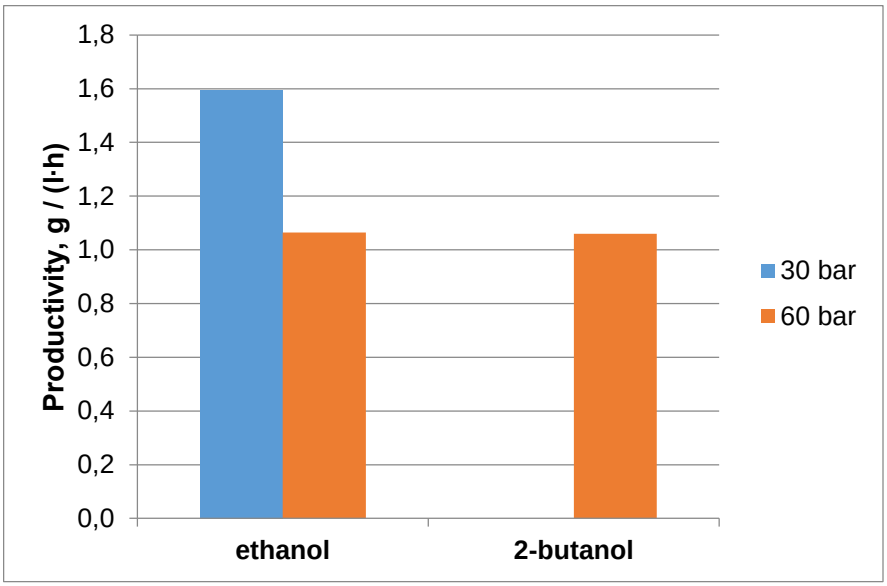

Figure 20. Volumetric productivity of methanol at 30 and 60 bar of total pressure. 20 g of Cu/ZnO catalyst, 180 °C, ethanol and 2-butanol solvents.

The effect of increased total pressure and the higher partial pressure of feed gas should be straightforward. With the increased pressure, the concentration of the reacting species is higher, leading to increased rate of reaction. At 180 °C, the vapor pressure of 2-butanol is 9.9 bar and the vapor pressure of ethanol 19.6 bar. Resultantly, at 30 bar of total pressure, the partial pressure of the feed gas (CO_2+H_2) is approximately 20 bar in 2-butanol and only 10 bar in ethanol. Additionally, the solubility of CO_2 and hydrogen in the alcohols is higher at increased pressure [269, 270], and a larger amount of the gases should be available for reaction in the liquid phase.

The partial pressures are quite low in these experiments, as pressures in the range of 100 bar are commonly applied in industrial practice. Thus it is not unexpected that no methanol was detected at all in the low pressure experiment with 2-butanol. Given the even lower partial pressure of the feed gas in ethanol, no methanol formation would be expected in this case, either. In this context, the results of the 30 bar experiment with ethanol are quite suspect and should probably be discounted.

6.1.3.3 Effect of catalyst mass in the batch experiments

Figure 21 shows the volumetric productivity of methanol with 10 and 20 g of catalyst in ethanol and 2-butanol, at 180 °C and 60 bar of total pressure. The productivity was found to be identical with both solvents when 10 g of catalyst was used with over 1.0 g of methanol produced per liter per hour. In both solvents, the amount of methanol produced was increased after doubling the mass of catalyst to 20 g with productivity values of almost 1.6 g/(l·h) found in ethanol and almost 1.4 g/(l·h) in 2-butanol.

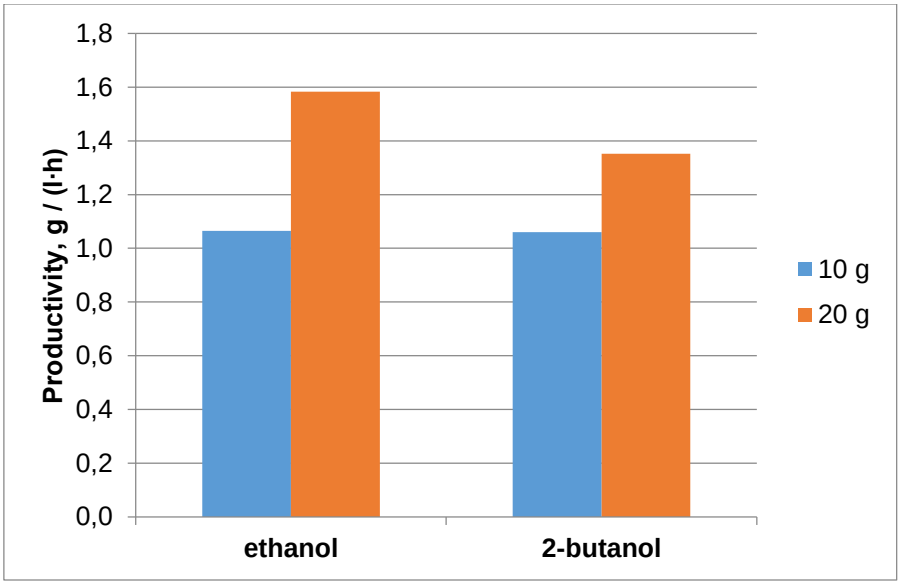

Figure 21. Volumetric productivity of methanol with 10 and 20 g of Cu/ZnO catalyst in ethanol and 2-butanol. 180 °C, 60 bar total pressure.

The relative increase in volumetric productivity is approximately 60% in ethanol and 40% in 2-butanol. By doubling the amount of catalyst, an increase of 100% would be predicted in the absence of non-kinetic limitations to the overall reaction rate. In this case, there clearly are some limitations. With 20 g of catalyst, the amount of methanol produced per catalyst mass is lower, and the catalyst is essentially utilized less efficiently. This is illustrated by Figure 22, presenting the catalyst specific productivity in these experiments.

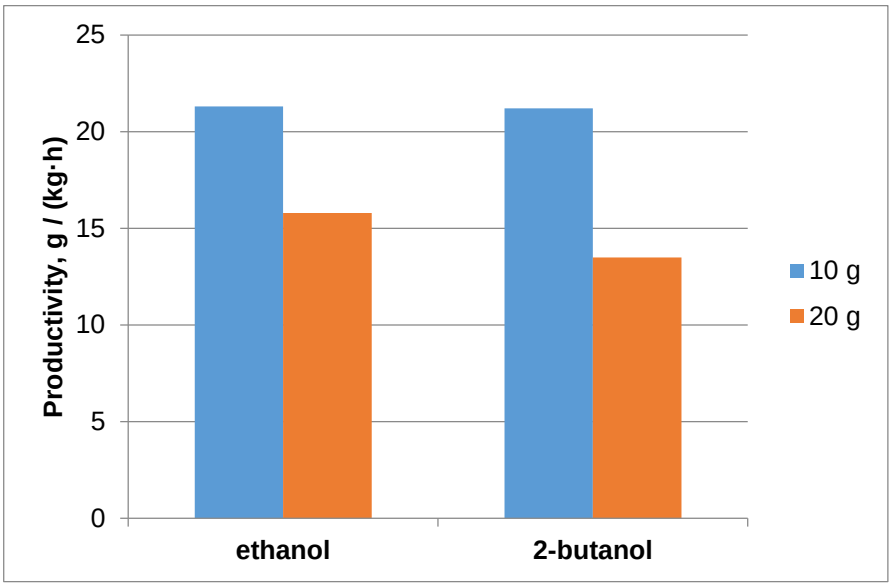

Figure 22. Catalyst specific productivity of methanol with 10 and 20 g of Cu/ZnO catalyst in ethanol and 2-butanol. 180 °C, 60 bar total pressure.

In both ethanol and 2-butanol, approximately 21 g of methanol is produced per kilogram of catalyst per hour with 10 g of catalyst. With 20 g of catalyst, the specific productivity falls to just over 15 g/(kg·h) in ethanol and to approximately 14 g/(kg·h) in 2-butanol. The relative decrease is approximately 30% in both cases.

The decrease in specific productivity could be caused by heat or mass transfer limitations or by the effects of side reactions or byproducts. Heat transfer could limit the average reaction rate if the initially increased reaction rate brought upon by the increased amount of catalyst would lead to non-uniform temperature distribution or hot spots in the reaction mixture. However, heat transfer limitations can be ruled out due to the observed uniformity of reaction temperature in all of the experiments. The heat transfer capacity of the alcoholic solvents combined with the automatic temperature control allowed near isothermal operation of the system.

In case of limitations caused by mass transfer, the diffusion of reactants and reaction products to and from the catalyst surface would be slow enough to limit the rate of the overall reaction. Limitations could be caused by inadequate mixing: the solid catalyst might not be adequately dispersed or the gaseous components effectively diffused in the liquid phase. In a three-phase system, these types of limitations would not be unexpected. However, only the distribution of

the catalyst should be affected by the increase in the amount of catalyst used. The increase should have no effect on the distribution and diffusion of the feed gases.

More likely, the decreased productivity is explained by side reactions and formation of byproducts. While the concentrations of acetaldehyde and 2-butanone are not significantly changed with the increased amount of catalyst, there is a clear increase in the amount of water formed (Appendix III: Figures A-16, A-17, A-20, A-22). Figure 23 shows the concentration of water in the experiments with 10 and 20 g of catalyst in ethanol and 2-butanol. In both solvents, the concentration of water is higher throughout the reaction time (except for ethanol at 0 hours) when 20 g of catalyst was used. The final water concentration after 6 hours of reaction is increased by approximately 30% in ethanol and by 40% in 2-butanol.

The effect of the catalyst preparation on the catalyst specific productivity should also be considered. As the catalyst was ground, sieved and activated separately for each experiment, the particle size distribution and activity of the catalyst could not be standardized. The method of catalyst activation may have caused heterogeneousness in the catalyst surface activity. The catalyst, placed on the bottom of the reaction vessel, was not mixed during the activation stage and the contact of the some of the particles may with the activation gas may have been limited. This is especially likely when larger amounts of catalyst was used. Repeat experiments with identical amount of catalyst used at identical conditions were not performed and some uncertainty in the results caused by catalyst preparation should be expected.

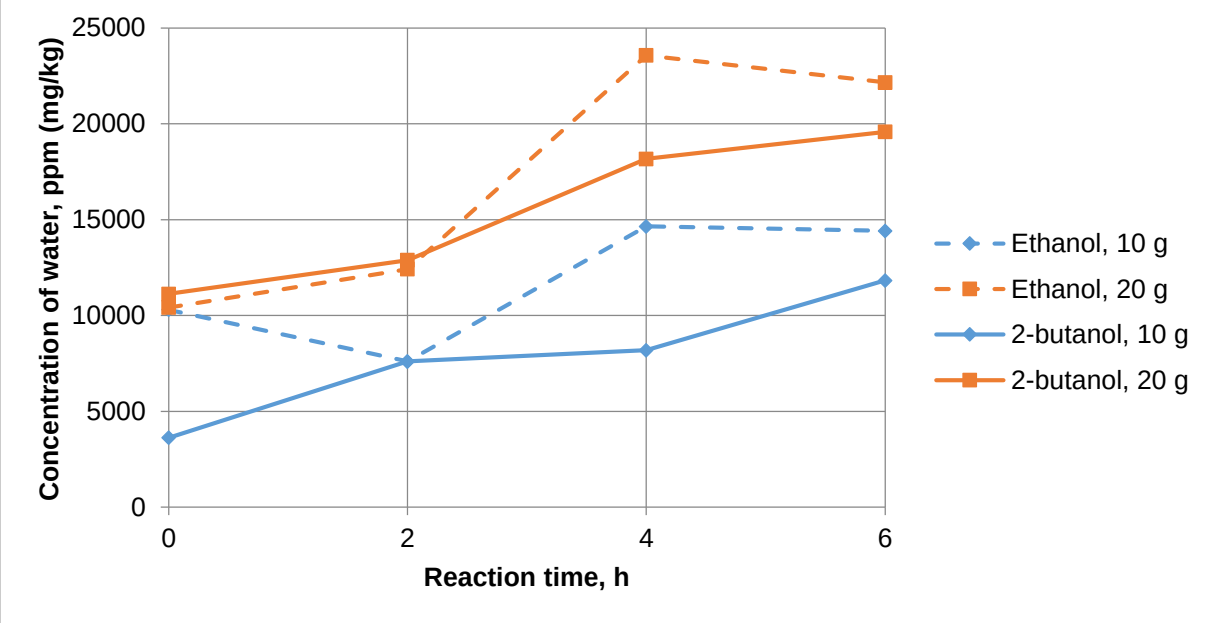

Figure 23. The concentration of water in the experiments with 10 and 20 g of catalyst in ethanol and 2-butanol. Reaction temperature 180 °C and total pressure 60 bar.

For comparison, the concentration of methanol was increased by approximately 60% in ethanol and 40% in 2-butanol when 20 g of catalyst was used instead of 10 g (Figure 21). The increased concentration of water could be partly explained by the methanol synthesis reaction (27), in which water is also formed. However, in 2-butanol, the amount of water is already increased before the feed gas is introduced and methanol synthesis begins. This increase can only be explained by the RWGS reaction (28). The increased rate of the RWGS reaction with increased amount of catalyst would be logical, since the catalyst used is also active for this reaction.

In the experiments with 20 g of catalyst, the concentration of water is higher in ethanol (approaching 25 000 ppm) compared to 2-butanol (under 20 000 ppm), and actually decreases during the last 2 hours of reaction time. This might suggest that the concentration in ethanol is high enough to reach an equilibrium level, leading to the consumption of water by the water-gas shift reaction. In the experiment with added water, the apparent equilibrium water concentration was found to lie above 30 000 ppm (Figure 16). However, the equilibrium could have been shifted due to the initial addition of water.

6.2 Semibatch experiments

In the semibatch experiments, the effects of the process parameters on the productivity of methanol were more accurately studied at standardized reaction conditions. The partial pressure of the feed gas was standardized by subtraction of the calculated vapor pressure of the solvents from the total pressure. The feed gas was continuously fed to the reactor at the set pressure. The sequence of the semibatch experiments is presented in Table VIII.

The components present in the reaction mixture and their concentration changes do not significantly differ from those found in the batch experiments. The concentration data can be found in Appendix IV. The effects of the alcohol dehydrogenation reactions are similar to those observed in the batch experiments, except for the associated pressure drop. Other than that, the previous discussion about these reactions applies to the semibatch experiments, and will not be repeated. The behavior of water and the water-gas shift reaction were also discussed in detail in context of the batch experiments. Any additional observations will be only briefly commented in this section.

The effect of the partial pressure of the feed gas was studied in both ethanol and 2-butanol, with three pressure data points set for each solvent. Due to the higher vapor pressure of ethanol, the partial pressures studied were lower than those with 2-butanol. In ethanol, the partial pressure range was 20-40 bar, while in 2-butanol, the range was 30-50 bar.

The temperature experiments were only carried out in 2-butanol. The lower vapor pressure allowed experimentation at a wider temperature range, while maintaining a sufficiently high partial pressure of the feed gas at all temperatures. The temperature range of 160-200 °C was covered by five experiments. Through adjustment of the total reaction pressure according to the temperature and the corresponding vapor pressure of the solvent, the partial pressure of the feed gas could be held constant throughout the temperature range.

The results of the partial pressure and temperature experiments were used to prepare a simplistic kinetic model for the methanol synthesis reaction in 2-butanol. The effect of catalyst mass was briefly explored by a single experiment in 2-butanol. In this experiment, the mass of catalyst was halved from the 10 g used in the rest of the semibatch experiments.

6.2.1 Effect of partial pressure in the semibatch experiments

Figure 24 shows the volumetric productivity of methanol at the partial pressure ranges of 20 to 40 bar for ethanol and 30 to 50 bar for 2-butanol. In 2-butanol, the productivity increases from above 0.6 g/(l·h) at 30 bar to 1.7 g/(l·h) at 50 bar, showing a logical pattern.

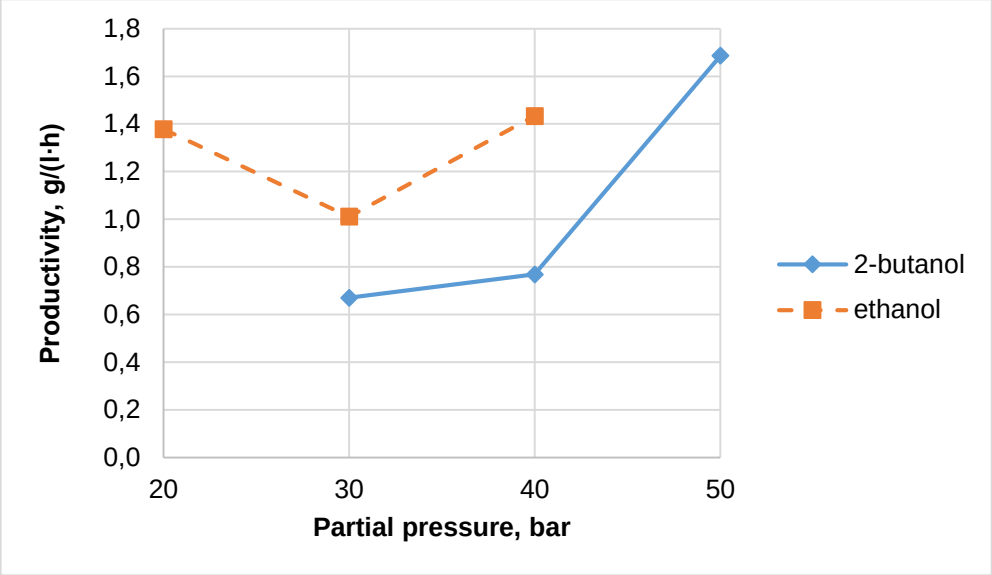

Figure 24. The volumetric productivity of methanol at varied partial pressures of feed gas (CO_2+H_2) in ethanol and 2-butanol. 10 g of catalyst was used, and the reaction temperature was 180 °C.

The results in ethanol are not similarly logical. The apparent productivity at 20 bar of partial pressure was found roughly equal to that at 40 bar, approximately 1.4 g/(l·h), while the productivity at 30 bar was only approximately 1.0 g/(l·h). As was the case in the batch experiments (Figure 20), a curious result showing high productivity at low pressure is observed. Again, there would be no reasonable explanation for this behavior, so the result at 20 bar should probably be discounted due to experimental or analytical error.

At the more reliable data points, it can be seen that the productivity is higher in ethanol than in 2-butanol at identical partial pressures. The results of the batch experiments generally showed the same pattern.

The concentrations of methanol and water over the 6 hours of reaction time in 2-butanol are displayed in Figure 25. The final concentration of both methanol and water is increased with increasing partial pressure. The amount of methanol formed shows a significant increase going from 40 bar to 50 bar, while the difference between 30 and 40 bar is not very large. These observations of course directly correlate with the exponential increase in volumetric productivity at these partial pressures.

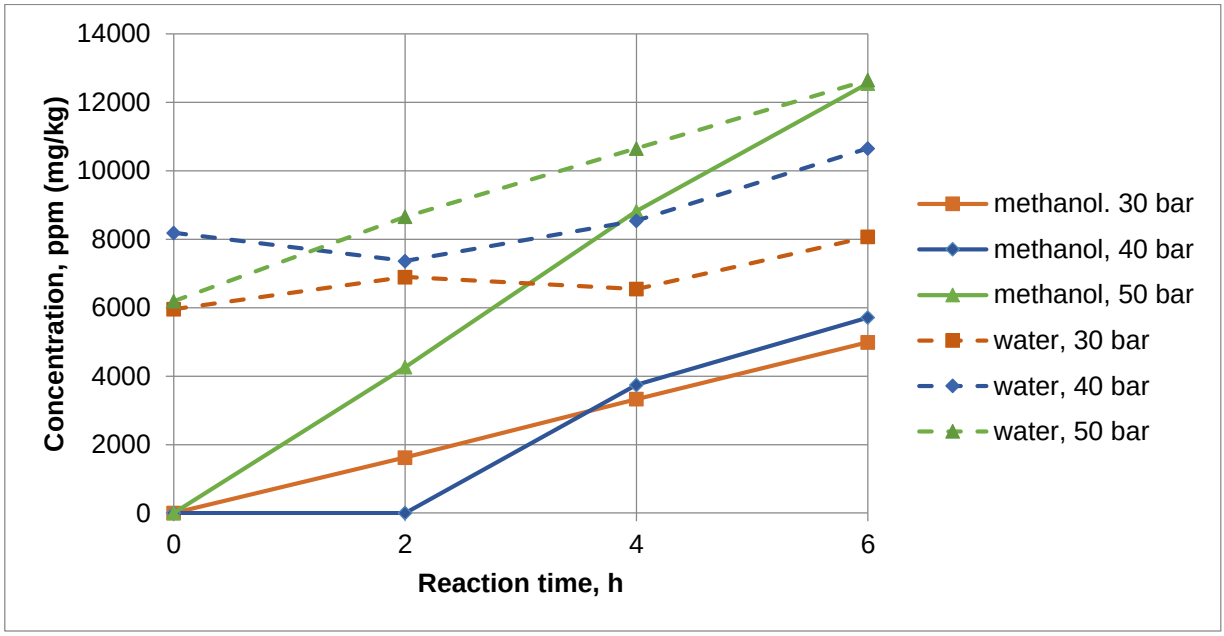

Figure 25. The concentrations of methanol and water over reaction time in 2-butanol with varied partial pressure of feed gas. 10 g of catalyst, reaction temperature 180 °C.

As for water, the final concentrations range from 8000 ppm at 30 bar to over 12000 ppm at 50 bar. At 50 bar, the concentration shows a continuous, near linear increase over reaction time, while at the lower partial pressures, the concentration slightly fluctuates between 0 and 4 hours of reaction time. At 50 bar of partial pressure, the methanol concentration reaches that of water after 6 hours of reaction. At the lower partial pressures, the water content remains above methanol at all times, with the concentrations of water and methanol maintaining a somewhat linear relationship.

It would seem that at 50 bar, the rate of the methanol synthesis reaction is high enough so that the amount of water formed as byproduct is sufficient to maintain an increasing water

concentration throughout the reaction time. However, water seems to be consumed by side reactions, presumably the water-gas shift reaction, and thus the overall rate of water formation is slower than the rate at which methanol is formed. At the lower partial pressures, the relative rates of the methanol synthesis reaction and the water-gas shift reaction are closer to each other, leading to the fluctuation and overall slow increase in water concentration over the reaction time.

The concentration curves of the ethanol experiments are quite similar, however the results are somewhat distorted by the unexpected results of the 20 bar experiment. The concentration data of the ethanol experiments can be seen in Figures A-28 to A-30 in Appendix IV.

6.2.2 Effect of temperature in the semibatch experiments

Figure 26 presents the volumetric productivity of methanol in 2-butanol at five temperatures in the range of 160 to 200 °C. The partial pressure of feed gas was 40 bar at all temperatures. The productivity ranges from under 0.5 g/(l·h) at 160 °C to approximately 1.9 g/(l·h) at 200 °C, continuously increasing with the increasing temperature. An exponential curve with a reasonable fit ($R^2 = 0.95$) can be fitted to the data. The temperature dependence of the reaction rate (and productivity) is expected to show an exponential behavior as dictated by the Arrhenius equation (see Section 6.2.4 Kinetic model of reaction).

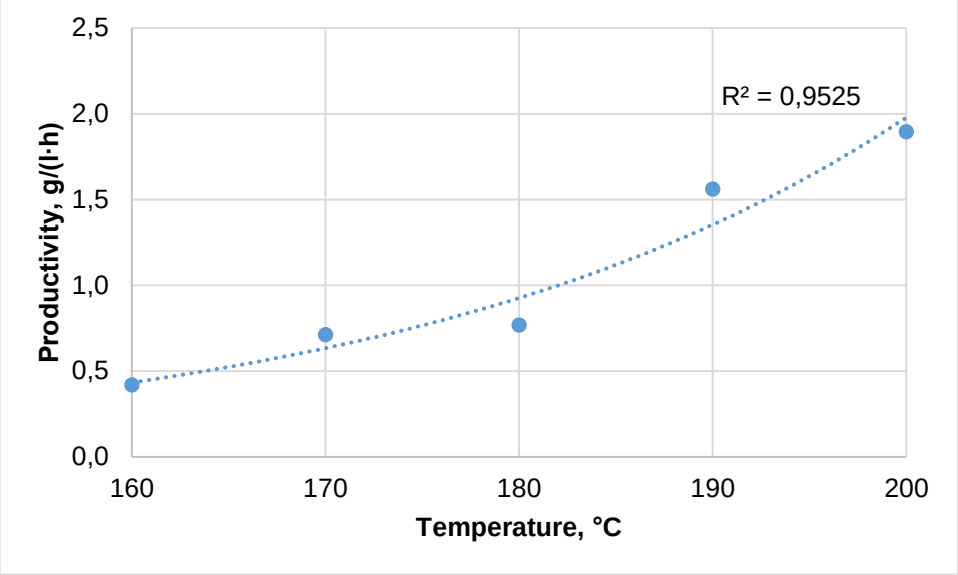

Figure 26. The volumetric productivity of methanol at the temperature range 160-200 °C in 2-butanol, with 10 g of catalyst. Partial pressure of feed gas (CO_2+H_2) was maintained at 40 bar, total pressure varying from 46.2 bar to 54.8 bar.

The continuous improvement of productivity with increasing temperature suggests that the methanol synthesis reaction does not reach the chemical equilibrium at this temperature range within the 6 hours of reaction time. The equilibrium is shifted away from the product side with increasing temperature. The steady-state concentration is also reached faster at increased temperature due to the increased reaction rate. This would suggest that at a sufficiently high temperature, the equilibrium could be reached in the 6 hour timeframe, and the maximum productivity would be reached at this temperature. However, with significantly increased temperatures, the vapor pressure of the solvent, the behavior of side reactions and even the stability of catalyst would become issues to consider.

Figure 27 shows the concentration of methanol over reaction time in the temperature experiments. The increase in methanol content is markedly linear at all temperatures, except for the 180 °C experiment, which shows no methanol at 2 hours of reaction time. However, this could be attributed to analysis error. If the actual concentration would lie around the 2000 ppm mark, the experiment would show a similarly linear concentration curve.

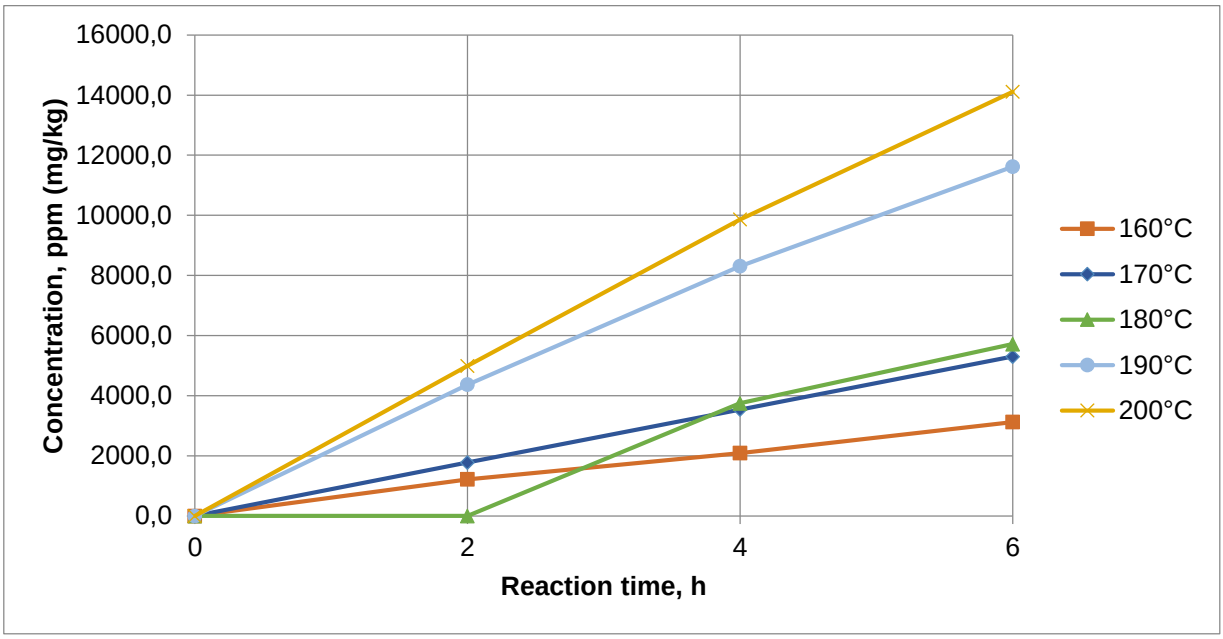

Figure 27. Concentration of methanol over the reaction time with reaction temperatures varied from 160 to 200 °C. 10 g of catalyst, partial pressure of feed gas 40 bar, total pressure 46.2-54.8 bar.

The concentration profile of the 180 °C experiment also deviates from the pattern created by the rest of the experiments in that the methanol concentration at 4 to 6 hours is very close to the concentrations found in the 170 °C experiment. The final concentrations in the rest of the experiments appear to be fairly evenly dispersed going from 160 °C to 200 °C. This deviation can also be observed in Figure 26, where the productivity of the 180 °C experiment lies below the exponential curve fitted to the results. In general, the linearity of methanol formation is the main observation to be made from the evolution of concentrations in Figure 27. This linearity further reinforces the view that at this temperature range, the rate of methanol formation is not limited by the reaction equilibrium during the 6 hours of reaction time.

Figure 28 shows the concentration of water over time in the temperature experiments. Before the start of reaction (at 0 hours), there seems to be no correlation at all between the reaction temperature and the observed concentration of water. As previously discussed, it is presumably the RWGS reaction that leads to the presence of water at this stage. However, the seemingly random scattering of the water concentrations in respect to the reaction temperatures does not allow any general conclusions to be made about this reaction.

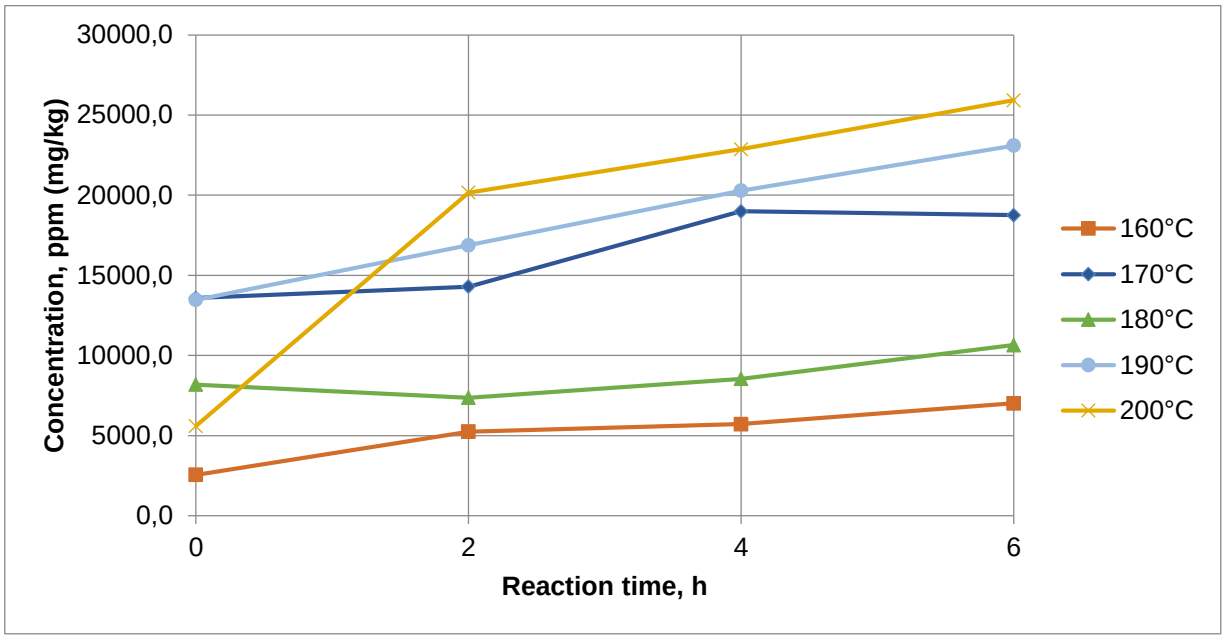

Figure 28. Concentration of water over the reaction time with the reaction temperature varied from 160 to 200 °C. 10 g of catalyst, partial pressure of feed gas 40 bar, total pressure 46.2-54.8 bar.

At 2 to 6 hours of reaction time, the concentration of water is increased at increased temperatures. An exception is the location of the 170 °C curve above the 180 °C curve. At higher temperatures (190 °C and 200 °C), the concentration of water shows a linear increase, while at the lower temperatures, the increase is both slower and more fluctuating. At 170 °C, the amount of water is slightly reduced between 4 and 6 hours of reaction time.

A similar explanation for the varying behavior of water could be given as which was speculated with the partial pressure experiments. At the higher temperatures, the rate of the methanol synthesis reaction is increased and more water is formed as byproduct. The relative rate of water formation is high compared to the rate with which water is consumed in side reactions (water-gas shift reaction), leading to the continuous increase in water concentration over the entire reaction time. At lower temperatures, the relative rates of water formation and disappearance are closer to each other, leading to a more fluctuating concentration profile.

6.2.3 Effect of catalyst mass in the semibatch experiments

Figure 29 presents the volumetric productivity of methanol in 2-butanol with 5 and 10 g of catalyst. The reaction temperature was 180 °C and the partial pressure of feed gas 40 bar in both cases. Paradoxically, the productivity and thus the amount of methanol produced is higher with the smaller amount of catalyst used. The productivity is 1.0 g/(l·h) with 5 g of catalyst, while it is only approximately 0.8 g/(l·h) with 10 g of catalyst. Figure 30 compares the catalyst specific productivity with 5 and 10 g of catalyst. At 40 g/(kg·h), the specific productivity is almost 170% higher with the smaller amount of catalyst.

Potential explanations for the lowered catalyst specific productivity with increased amount of catalyst were discussed earlier (Section 6.1.3 Methanol productivity). Mass transfer limitations related to the inefficient distribution of the catalyst or the diffusion of the gaseous reactants, and the effect of side reactions and byproducts were identified as potential causes. The increased amount of water formed, both as a byproduct in the methanol synthesis reaction, and in the RWGS reaction, was suggested to limit the rate of methanol formation.

Variations in the preparation and activation of the catalyst may also have contributed to the unexpected results. With 5 g of catalyst of used, the contact of the catalyst particles with the activation gas would likely be more complete compared to the case of 10 g of catalyst. Also, the grinding of a smaller amount of catalyst may have altered the particle size distribution of the catalyst batch.

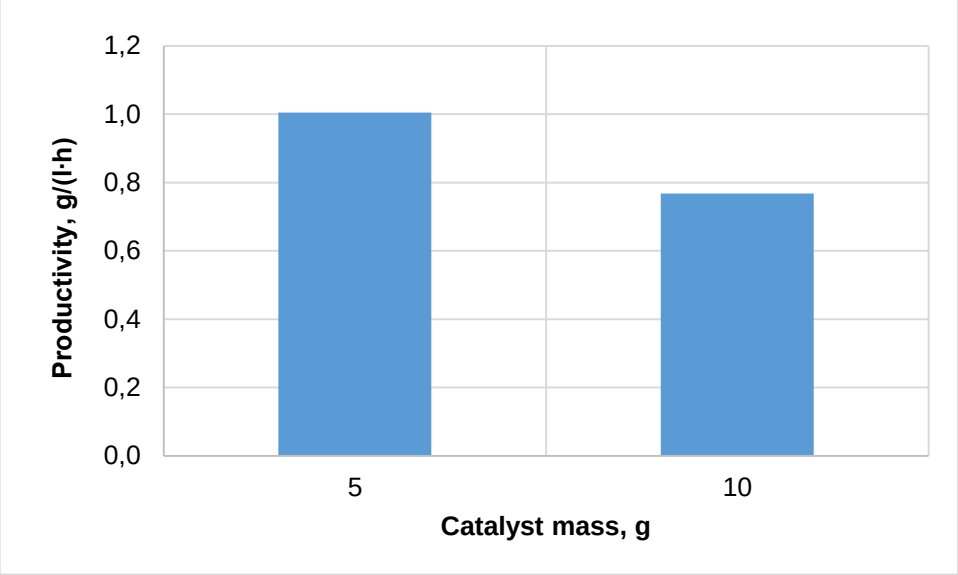

Figure 29. Volumetric productivity of methanol with 5 and 10 grams of catalyst in 2-butanol. Partial pressure of feed gas (CO_2+H_2) was 40 bar and the total pressure 46.9 bar. Reaction temperature was 180 °C.

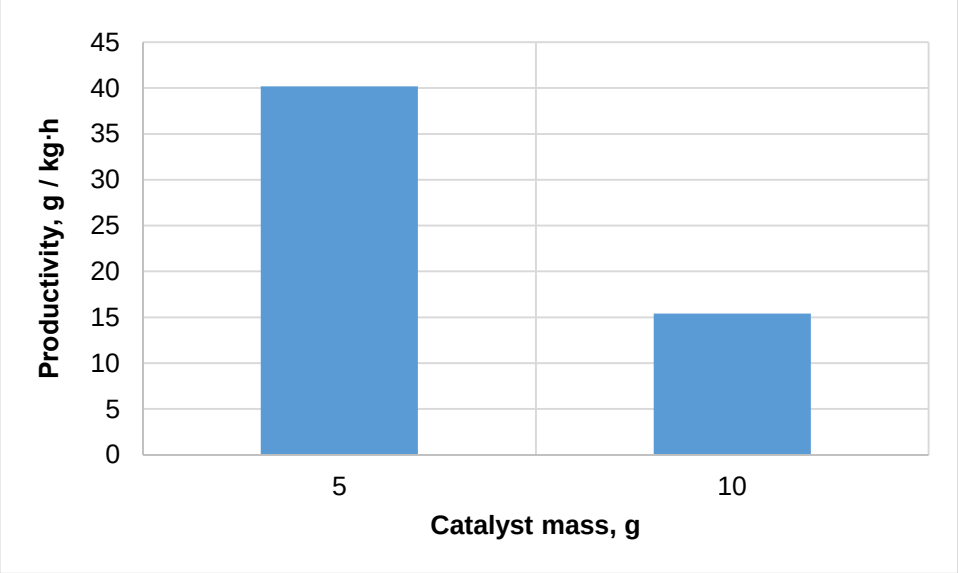

Figure 30. Catalyst specific productivity of methanol with 5 and 10 grams of catalyst in 2-butanol. Partial pressure of feed gas (CO_2+H_2) was 40 bar and the total pressure 46.9 bar. Reaction temperature was 180 °C.

Figure 31 depicts the concentrations of methanol and water during the 6 hours of reaction time in the 5 and 10 g experiments. The concentration of water is higher at all times when the larger amount of catalyst was used. The situation is comparable to that seen in Figure 23, relating to the batch experiments with 10 and 20 g of catalyst. However, in the batch experiments, only the specific productivity of the catalyst was lowered when the amount of catalyst was increased. The volumetric productivity, or the total amount of methanol formed, was still higher with the higher amount of catalyst.

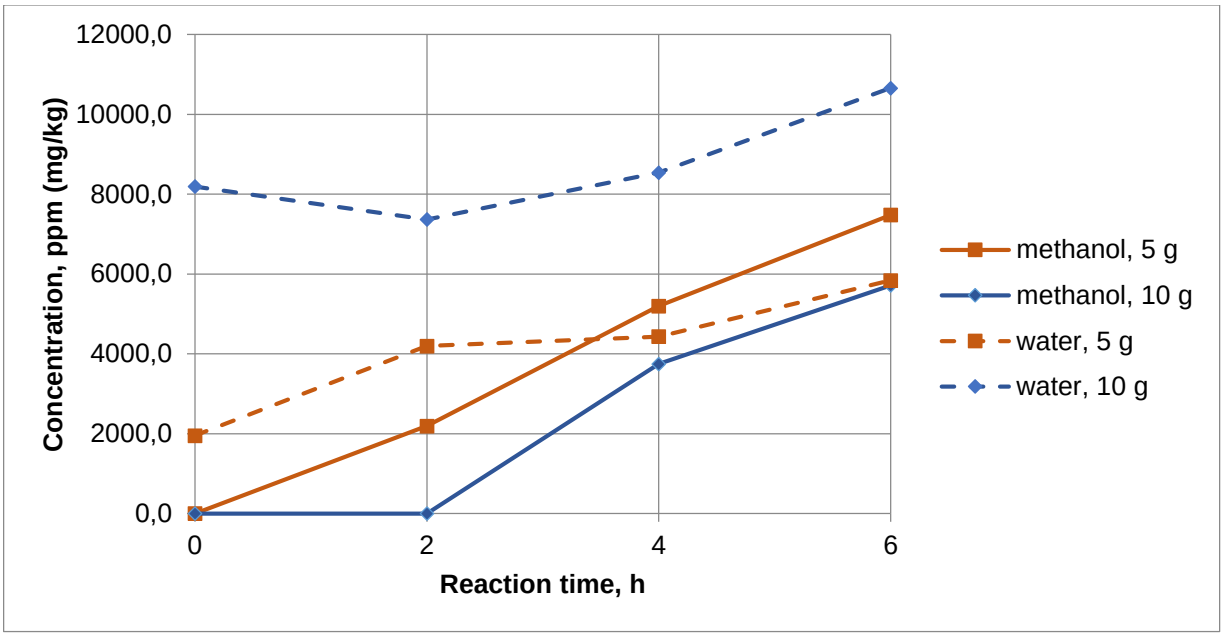

Figure 31. Concentration of methanol and water over the reaction time with 5 and 10 g of catalyst used. The reaction temperature was 180 °C, the partial pressure of feed gas 40 bar, and the total pressure 46.9 bar.

As such, there is no obvious explanation for the lowered volumetric productivity. Perhaps the results have been skewed by variations in the experimental process or by inaccuracies in analysis. The 10 g experiment here is the same 180 °C experiment that is shown in Figures Figure 26 andFigure 27 and was discussed in Section 6.2.2 Effect of temperature. It would seem that the amount of methanol formed in that experiment is not as high as would be expected based on the comparative experiments. However, even if the “optimal” amount of

methanol could have been produced in that experiment, the catalyst specific productivity would still be significantly lower compared to the 5 g experiment.

Alternatively, the smaller amount of catalyst used creates such an optimized reaction environment that methanol is indeed produced at significantly increased efficiency. The balance between the methanol synthesis reaction and the various side reactions would in that case be optimized for the formation of methanol. From Figure 31, it can be noted that the concentration of methanol surpasses that of water already after 4 hours of reaction in the 5 g experiment, which is quite exceptional compared to the results from the other experiments. This might suggest that the balance between methanol and water and the relevant reactions really could be optimized by lowering the amount of catalyst used. Further experiments with varied amounts of catalyst used should be performed to obtain more information.

6.2.4 Kinetic model of reaction

A simple kinetic model for the methanol synthesis reaction was developed based on the results of the semibatch experiments in 2-butanol. See Appendix I for the detailed calculations performed in developing the model. The partial pressure and temperature experiments allowed the creation of a reaction rate law of the following form:

$$r = \frac{-dc_{\mathrm{MeOH}}}{dt} = \frac{-dp_{\mathrm{CO_2+H_2}}}{dt} = k \cdot p^{m}_{\mathrm{CO_2+H_2}} \quad (47)$$

r Reaction rate, mol/s

c_{MeOH} Concentration of methanol, mol/dm^3

$p_{\mathrm{CO_2+H_2}}$ Combined partial pressure of carbon dioxide and hydrogen

k Rate constant, bar$^{-1.89}$ · mol/s

m Order of reaction in respect to the partial pressure of CO_2 and H_2

The temperature dependence of the rate constant is determined by the Arrhenius equation:

$$k = A \cdot e^{-E_a/RT} \quad (48)$$

A Pre-exponential factor, bar $^{-1.89}$ · mol/s

E_a	Activation energy, kJ/mol
R	Gas constant, J/mol·K
T	Absolute temperature, K

The order of the reaction was calculated with the following equation [271]:

$$m = \frac{\log\left(\frac{r_1}{r_2}\right)}{\log\left(\frac{p_1}{p_2}\right)} \tag{49}$$

where r_1 and r_2 are the measured reaction rates in mol/s at the partial pressures p_1 and p_2. The data from the experiments at 30 and 50 bar of partial pressure was used for the calculations. In order to roughly approximate the initial reaction rates, average reaction rates were calculated from the amount of methanol formed during 0 to 2 hours of reaction time. As a result, the reaction order m was calculated as 1.89.

The rate constant k was then calculated by substituting the values of r, $p_{\mathrm{CO_2+H_2}}$ and m into equation (47). For verification, the calculation was repeated with both of the combined (CO_2+H_2) partial pressures and the corresponding values of r, yielding the same result. A value of approximately $1.82 \cdot 10^{-9}$ $\mathrm{bar}^{-1.89} \cdot$ mol/s was obtained for k at 180 °C.

The temperature dependence of the rate constant k was examined using the following equation, derived from the Arrhenius equation (48) [271]:

$$\frac{d \ln k}{d\left(\frac{1}{T}\right)} = -\frac{E_a}{R} \tag{50}$$

By plotting the values of $\ln k$ against $1/T$ based on data from experiments at varied temperatures, the slope of the fitted curve gives $-E_a/R$. The average reaction rates at 0 to 2 hours of reaction from the experiments at 160, 170, 190 and 200 °C were used in deriving the graph, utilizing the value of the reaction order calculated before. The data from the 180 °C experiment was not utilized as no methanol was detected after 2 hours of reaction. As a result, activation energy E_a of approximately 63.5 kJ/mol was obtained.

To calculate a value for the pre-exponential factor A, the activation energy and the respective values of k at the temperature points T were substituted into equation (9), and an average

value was taken of the slightly differing values calculated at different temperatures. A result of A = 0.036 bar $^{-1.89}$ · mol/s was obtained. To summarize, the reaction rate law is of the form

$$r = 1.82 \cdot 10^{-9} \cdot p_{\mathrm{CO_2+H_2}}^{1.89} \mathrm{mol/s} \quad (51)$$

with the temperature dependence determined by the activation energy of 63.5 kJ/mol and the pre-exponential factor of 0.036 bar$^{1.89}$ · s/mol. To assess the accuracy of these values, comparisons are made to the model of gas-phase methanol synthesis created by Askgaard et al. [174]. In that work, an activation energy of 68.3 kJ/mol has been proposed for a feed with H_2:CO_2 = 1:1, at 270 °C and 2 bar of total pressure. For the same feed composition at identical conditions, the model suggests reaction orders of 1.44 for H_2 and 1.00 for CO_2, corresponding to a total reaction order of 2.44. It can be concluded that the calculated activation energy seems very realistic and the reaction order also appears to be in a realistic range.

The kinetic model is quite simplified and not at all related to the actual mechanism of the methanol synthesis reaction. The potential use of the model would be to model the reaction in 2-butanol at the temperature and pressure range employed (160-200 °C, 30-50 bar partial pressure). The ratio of the amount of catalyst to the amount of solvent should be maintained at the same level unless the fit of the model at differing ratios is verified.

6.3 Design of a demonstration process

The present thesis is connected to the REFLEX research platform at Lappeenranta University of Technology (LUT). The platform is focused on the development of sustainable energy systems, based on the recycle of carbon dioxide into energy carriers and chemical raw materials [272]. As part of the ongoing research, an electrolyser unit with a design hydrogen production capacity of 1 Nm^3/h has been constructed [273]. In this chapter, the alcohol promoted liquid-phase methanol synthesis process is scaled to the hydrogen input, and a preliminary design of a demonstration scale process is presented.

The feedstock of the methanol synthesis process consists of CO_2 and hydrogen. The CO_2 is preferably captured from point sources or directly from the atmosphere. Research into CO_2 capture is currently performed at LUT. The sourcing of CO_2 and the design of the capture unit is omitted in this work and CO_2 is considered readily available. Hydrogen is produced by the PEM electrolyser unit at a capacity of 1 Nm^3/h with a nominal power input of 5.5 kW [273].

The overall process consists of a synthesis step followed by the separation stage. The synthesis step employs a slurry reactor containing a solid methanol synthesis catalyst suspended in 2-butanol. According to the experiments, the expected main reaction products are methanol and water (byproducts and intermediates are not considered), with the reactor outlet majorly consisting of 2-butanol. In the separation stage, methanol is separated and removed as the main product. Water is also removed from 2-butanol, facilitating the recycle of 2-butanol to the synthesis stage. A block diagram depicting the main process stages is presented in Figure 32:

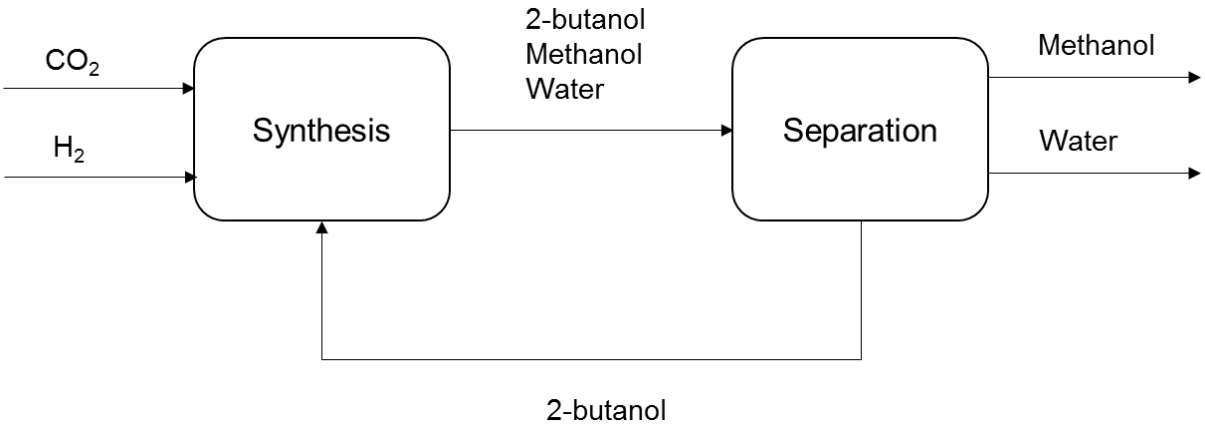

Figure 32. Block diagram showing the main process stages of the methanol synthesis process.

6.3.1 Synthesis

The synthesis stage utilizes a slurry reactor containing a solid catalyst and the alcoholic solvent. Presumably, a catalyst with the conventional Cu/ZnO structure will be used, with 2-butanol as the solvent. The synthesis could be operated in batch, semibatch or continuous modes, with the choice of the operating mode potentially having a drastic influence on the overall performance of the system. Based on the laboratory scale experiments, the choice of the operating mode should be based on the following, partially overlapping considerations:

- Maintaining the driving force for the methanol synthesis reaction
- Optimizing the residence time of the reaction mixture

In order to maintain a high reaction rate, the reactant gas mixture should be continuously fed to the reactor at the maximum allowable pressure. However, the gas should not be continuously removed because the reaction is quite slow and conversion would remain low at reasonable residence times. Recycling of the unreacted gases would be required, adding to the complexity and cost of the overall system. With this mode of operation, the gases remain in the reaction vessel until condensing liquid products are formed in reaction. At the same time, fresh gas is continuously fed to the reactor and the maximum concentration of reactants maintained.

Based on the experiments, the reaction rate and productivity of methanol are significantly affected by the residence time of the liquid phase in the reactor. The formation of methanol is rather slow, and the concentration of methanol generally increased over the entire 6 hours of reaction time in the experiments. The residence time should be long enough to allow the formation of methanol at reasonable quantities.

However, at long residence times, the formation of water and the accompanying decrease in the rate of methanol formation can become issues. The inhibiting effect of water on the synthesis of methanol was clearly shown by the experiments. In order to maintain an adequate production rate, the concentration of water in the reaction mixture should be minimized. A continuous removal of liquids is thus used to avoid significant buildup of water. Methanol and water are separated from the removed liquid and the 2-butanol is recycled. The recycled 2-butanol is fed continuously to the reactor in order to maintain the liquid level.

In order to maximize productivity, the reactor would initially be operated at 200 °C, unless lower temperatures are desired for practical purposes. As was observed in the experiments, the reaction heat is expected to be efficiently controlled by the liquid-phase system, and significant cooling of the reactor should not be necessary. The maximum allowable pressure should be used.

The hydrogen input to the reactor is 1 Nm^3/h, corresponding to 90 mol/h or 0.09 kg/h. Following the stoichiometric ratio of the methanol synthesis reaction (27) (H_2:CO_2 = 3:1), 30 mol/h or 1.3 kg/h of CO_2 is required. If a 100% selectivity to methanol is assumed, approximately 29.7 mol/h or 0.95 kg/h of methanol is formed in reaction. The volume of the reactor is 0.236 m^3, and the diameter and height of the cylindrical reactor are 0.67 m. See Appendix I for the calculations performed for sizing of the reactor.

The volume of 2-butanol in the reactor is 118 l. If half of the liquid volume is removed from the reactor per hour, the average residence time is 2 hours. 2-butanol is removed at a rate of 59 l/h, or 47.6 kg/h. We assume that the amount of methanol removed from the reactor is identical to the amount of methanol formed in reaction, at 0.95 kg/h. For simplicity, we assume that water is removed at the identical rate of 0.95 kg/h. The total mass flow at the reactor outlet is then 49.5 kg/h. The mass fraction of 2-butanol is 96% and that of both methanol and water 2%.

6.3.2 Separation

The objectives of the separation stage are to produce a methanol product with a high purity and to remove water from the 2-butanol to be recycled to the synthesis stage. The separation is performed by distillation. The distillation sequence was modelled in Aspen Plus 8.6. The simulation was based on the activity coefficient based UNIFAC method. The results were verified by using the WILSON, NRTL and UNIQUAC methods, which yielded similar outcomes. The RadFrac distillation unit model was used to model the columns and the number of equilibrium stages was estimated by an iterative process.

The flowsheet of the separation stage is shown in Figure 33. The flowsheet streams are defined inTable X. Three columns are required to obtain a methanol product with a purity of 97.0% (w/w). The production rate is 0.87 kg/h, thus 91.9% of the methanol incoming to the separation stage is recovered. Pure 2-butanol at a rate of 45.0 kg/h is obtained as a bottoms product from the first column, which means that 94.5% of the 2-butanol in the reactor outlet can be readily recycled. The bottom streams of the columns 1 and 2 should not be recycled due to the high water content. A makeup stream of 2.6 kg/h of 2-butanol is required to maintain the liquid level in the reactor.

Specification of the distillation columns is presented in Table XI. Each column contains 15 equilibrium stages. The first column is operated with a reflux ratio of 4, and the columns 2 and 3 with a reflux ratio of 3. The three columns require a combined hot utility duty of 12.7 kW for reboilers and a combined cold utility duty of 10.5 kW for condensers.

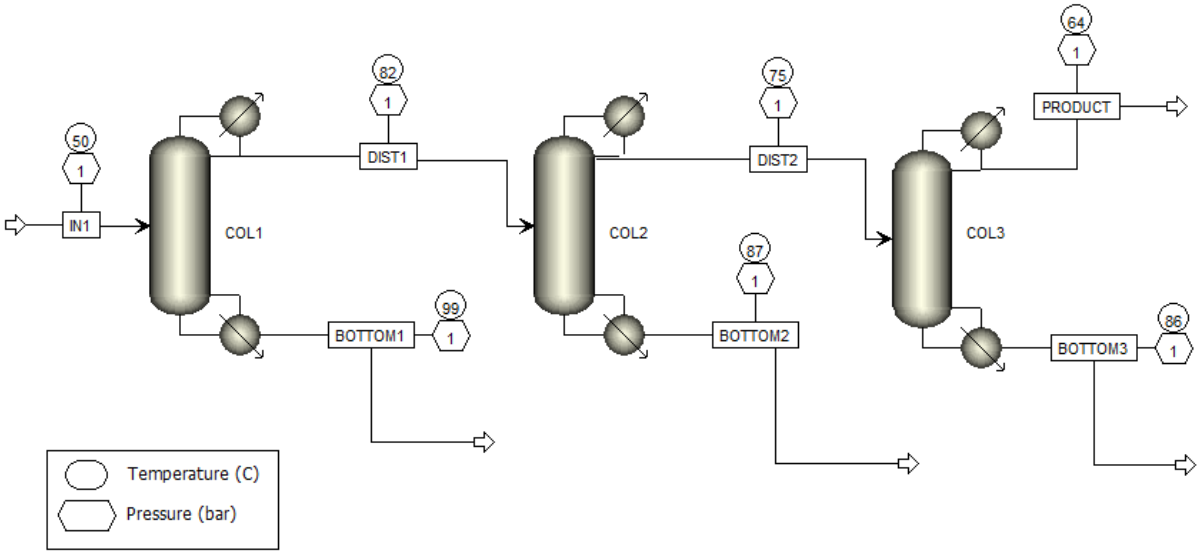

Figure 33. Aspen Plus 8.6 simulation flowsheet of the separation stage.

Table X. Stream data from the simulation of the separation stage.

Stream	IN1	BOTTOM1	DIST1	BOTTOM2	DIST2	BOTTOM3	PRODUCT
Temperature, °C	50	99,4	82	86,7	75,1	86,4	64,8
Pressure, bar	1	1	1	1	1	1	1
Mass flow, kg/h							
2-butanol	47,6	44,997	2,603	1,901	0,702	0,691	0,011
Methanol	0,95	0,001	0,949	0,037	0,912	0,039	0,873
Water	0,95	0,002	0,948	0,562	0,386	0,371	0,016
Total	49,5	45	4,5	2,5	2	1,1	0,9
Mass fraction							
2-butanol	0,962	1	0,578	0,76	0,351	0,628	0,012
Methanol	0,019	0	0,211	0,015	0,456	0,035	0,97
Water	0,019	0	0,211	0,225	0,193	0,337	0,018

Table XI. Specification of the distillation columns.

Column	Stages	Reflux ratio	Reboiler duty, kW	Condenser duty, kW
1	15	4	9	-6,7
2	15	3	2,6	-2,6
3	15	3	1,1	-1,1

6.3.3 Mass balance

An overall mass balance for the methanol synthesis process is presented in Figure 34. 0.87 kg/h of methanol is produced from a feed of 0.09 kg/h H_2 and 1.3 kg/h CO_2. A makeup stream of 2.6 kg/h of 2-butanol is required.

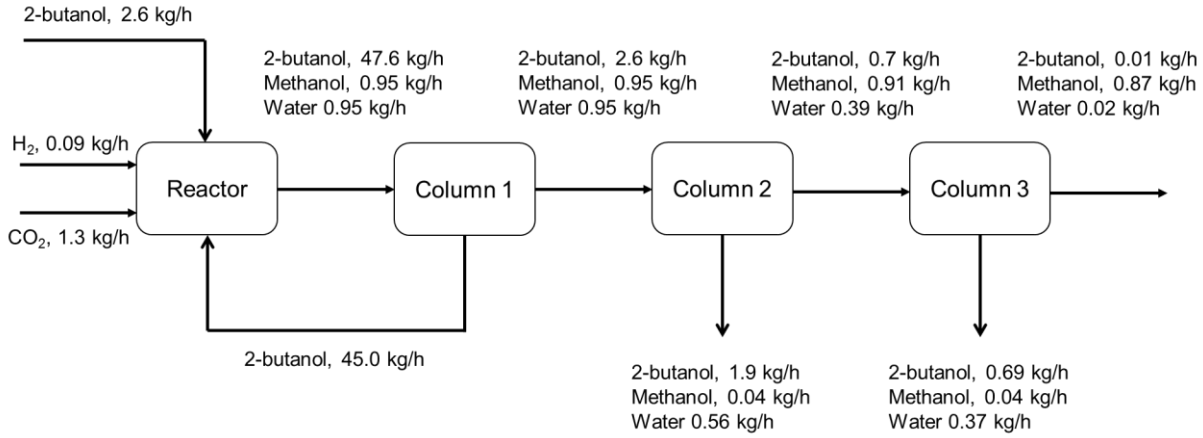

Figure 34. Mass balance of the methanol synthesis process.

6.4 Summary of results

The main results of the batch experiments are summarized in Table XII, and the results of the semibatch experiments in Table XIII. Figures Figure 35 and Figure 36 provide a comparison of the volumetric productivity of methanol in the batch and semibatch experiments, respectively.

Table XII. Summary of the results of the batch experiments. $Cu/ZnO/Al_2O_3$ catalyst was used, and the reaction time was 6 hours, during which the feed of CO_2+H_2 was closed. Pressures correspond to the initial pressures at the start of reaction and following sampling. 200 ml of solvent was used, and the total volume of the reactor was 450 ml. Mixing speed was 600 rpm.

Experiment	Solvent	Mass of catalyst, g	Temperature, °C	CO_2+H_2 pressure, bar	Total pressure, bar	Conversion/2 h[1]	Productivity, g/(l·h)[2]	Productivity, g/(kg·h)[3]
1	2-butanol	10	180	20.1	30	N.A.	-	-
2	ethanol	10	180	10.4	30	N.A.	1.6	31.9
3	ethanol	10	180	40.4	60	N.A.	1.1	21.3
4	2-butanol	10	180	50.1	60	10.4 %	1.1	21.2
5	2-butanol	20	180	50.1	60	11.4 %	1.4	13.5
6	2-butanol	20	160	53.8	60	10.9 %	0.3	3.1
7	ethanol	20	160	47.5	60	11.9 %	0.8	8.1
8	ethanol	20	180	40.4	60	7.8 %	1.6	15.8
Non-alcohol	hexane	20	180	46.9	60	N.A.	-	-
Added water	2-butanol	10	180	50.1	60	N.A.	0.3	5.6
Removal of water	2-butanol	10	180	40.4	60	N.A.	1.2	24.0

1) Conversion was estimated based on the decrease in total pressure during 2 hour reaction time intervals. The values are the average of the three intervals during the experiment.
2) Grams of methanol produced per liter of solvent per hour.
3) Grams of methanol produced per kg of catalyst per hour.

Table XIII. Summary of the results of the semibatch experiments. $Cu/ZnO/Al_2O_3$ catalyst was used, and the reaction time was 6 hours, during which the feed of CO_2+H_2 remained open. 200 ml of solvent was used, and the total volume of the reactor was 450 ml. Mixing speed was 600 rpm.

Partial pressure experiments

Experiment	Solvent	Mass of catalyst, g	Temperature, °C	CO_2+H_2 pressure, bar	Total pressure, bar	Productivity, g/(l·h)[1]	Productivity, g/(kg·h)[2]
1	2-butanol	10	180	30	39.9	0.7	13.4
2	2-butanol	10	180	40	49.9	0.8	15.4
3	2-butanol	10	180	50	59.9	1.7	33.7
4	ethanol	10	180	20	39.6	1.4	27.6
5	ethanol	10	180	30	49.6	1.0	20.2
6	ethanol	10	180	40	59.6	1.4	28.7

Temperature experiments

Experiment	Solvent	Mass of catalyst, g	Temperature, °C	Partial pressure of feed gas	Total pressure		
7	2-butanol	10	160	40	46.2	0.4	8.4
8	2-butanol	10	170	40	47.9	0.7	14.2
2	2-butanol	10	180	40	49.9	0.8	15.4
9	2-butanol	10	190	40	52.2	1.6	31.2
10	2-butanol	10	200	40	54.8	1.9	37.9

Catalyst mass experiments

Experiment	Solvent	Mass of catalyst, g	Temperature, °C	Partial pressure of feed gas	Total pressure		
11	2-butanol	5	180	40	49.9	1.0	40.2

1) Grams of methanol produced per liter of solvent per hour.

2) Grams of methanol produced per kg of catalyst per hour.

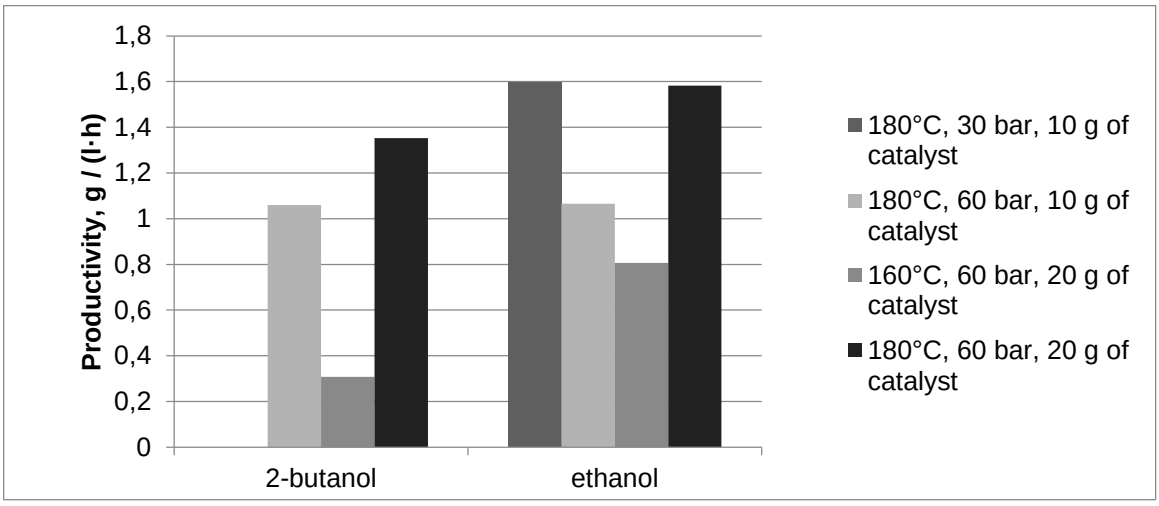

Figure 35. The volumetric productivity of methanol in the batch experiments. $Cu/ZnO/Al_2O_3$ catalyst was used, and the reaction time was 6 hours, during which the feed of CO_2+H_2 was closed. Pressures correspond to the initial pressures at the start of reaction and following sampling. 200 ml of solvent was used, and the total volume of the reactor was 450 ml. Mixing speed was 600 rpm.

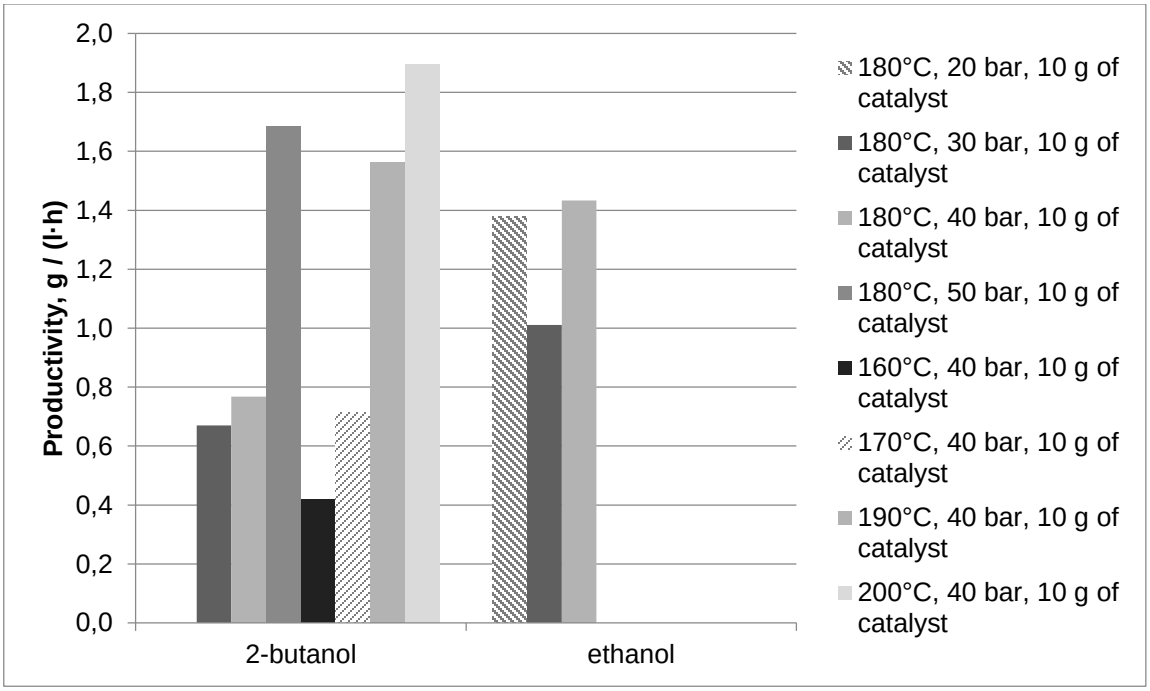

Figure 36. The volumetric productivity of methanol in the semibatch experiments. $Cu/ZnO/Al_2O_3$ catalyst was used, and the reaction time was 6 hours, during which the feed of CO_2+H_2 remained open. 200 ml of solvent was used, and the total volume of the reactor was 450 ml. Mixing speed was 600 rpm.

6.4.1 Process feasibility

The potential advantages of the alcohol-promoted synthesis process are the lowered reaction temperature and pressure enabled by the altered reaction route, and the efficient temperature control provided by the liquid medium. Experiments were carried out in the temperature range of 160 to 200 °C and pressures up to 60 bar. The temperature range can be considered low compared to the temperatures of 200-300 °C [139] used in industrial methanol production. The pressure is also low compared to industrial standards, where pressures in the region of 100 bar are often employed.

Based on the results of the experiments, the productivity of the process could be improved by further increases in temperature and pressure. To maximize the productivity, pressure should likely be increased to the maximum level dictated by cost and safety considerations. For temperature, there seems to be an optimum point where the productivity is maximized. The temperature cannot exceed the level of approximately 300 °C in order avoid rapid degradation of the catalyst. Unexpected effects from the side reactions could also arise at significantly increased temperatures.

The maximum volumetric productivity of 1.9 g/(l·h) was found in 2-butanol at 200 °C and 40 bar of total pressure. In a previous work on the alcohol promoted synthesis method, a productivity of 170 g/(l·h) has been reported [249]. In this case, the feed gas contained 30% CO and 5% CO_2. The much higher productivity may in part illustrate the difficulty of synthesis from pure CO_2. At the present reaction conditions, the productivity of the alcohol-promoted liquid-phase process is low compared to industrial methanol synthesis. For industrial synthesis, a productivity (space-time yield) range of 400-1000 g/(l·h) has been reported at pressures of 50 to 100 bar [249].

The maximum catalyst specific productivity obtained was 40.2 g/(kg·h). The result compares favorably to a value previously reported for the alcohol-promoted synthesis, at 6.3 g/(kg·h) [252]. In that case, the feed also contained CO. However, productivity values of up to 1200 g/(kg·h) have been reported for the gas-phase synthesis from CO_2, with Cu/ZnO/ZrO_2 catalysts at at 240 °C and 50 bar [195]. On a Cu/ZnO catalyst, productivity of up to 550 g/(kg·h) has been reported at 240 °C and 30 bar [212]. The significantly larger productivity values cannot be explained by different reaction conditions, as the temperatures are not drastically elevated and the pressures are even low compared to the present experiments.

The lower operating temperatures and pressures may not be justified if the productivity falls well below the gas-phase processes. The liquid-phase process should probably be tested at temperatures and pressures matching those in the gas-phase processes to see if there is any difference in the intrinsic productivity, or if the different results can be explained by the reaction conditions. Considering large-scale production, the benefits of the somewhat lower temperatures of the liquid-phase process probably cannot outweigh the loss in productivity.

However, in small-scale operations, the cost and safety benefits of the milder reaction conditions might prove useful. Smaller productivity means that larger equipment size is required for matching production rate. In small-scale units, the increased equipment size may not lead to unacceptable cost increases. The batch or semibatch operation of the slurry reactor also leads to simple operation and requires less space compared to tubular gas-phase systems. If operated in a similar fashion to the semibatch experiments reported in the present study, gas is continuously fed to the reactor but not removed. Thus, an optimal reaction pressure can be maintained but no recycle of outlet gases is required. In gas-phase synthesis, a significant fraction of the outlet gas needs to be recycled in order to maintain adequate conversion.

A preliminary design for a demonstration scale unit was proposed (Section 6.3 Design of a demonstration process). 0.87 kg/h of methanol is produced from a feed of 0.09 kg/h H_2 and 1.3 kg/h CO_2. A relatively intensive separation stage is required for the separation of the small amount of methanol present in the reaction products. If methanol was used as the solvent, the separation costs could be significantly reduced.

The productivity of the alcohol promoted liquid-phase process needs to be increased. More active catalysts should be tested. Currently, a limited range of catalyst have been experimented, mostly limited to conventional methanol catalysts and combinations with basic co-catalysts (Table V). Very promising catalysts have been developed for the gas-phase synthesis from CO_2 (Table IV). Modified Cu/ZnO catalyst with additives such as ZrO_2 should be also explored for liquid-phase synthesis.

Alternative reactor options should also be considered. The batch autoclave reactor, while simple in structure and operation, is likely limited to small-scale operation. For continuous, scaled-up production, alternatives such as bubble columns should be considered. Reactive distillation or membrane separation might be employed for in-situ removal of reaction product, helping to maintain the thermodynamic driving force of reaction.

Dual-catalyst systems with the reaction stages (CO_2 -> formate -> methanol) separated on different types of catalyst might prove advantageous. Homogeneous catalysts are also continuously being developed for methanol synthesis. Considering the difficulties faced with a pure CO_2 feed, perhaps a two-step process with partial conversion of CO_2 into CO (water-gas shift) followed by methanol synthesis, might prove beneficial. The CAMERE process has already demonstrated this approach in the gas-phase [226].

7 CONCLUSIONS

The alcohol-promoted liquid-phase methanol synthesis process was studied at a laboratory scale. The process combines a conventional solid methanol synthesis catalyst with a catalytic alcoholic solvent. In the alcohol, the synthesis of methanol proceeds through an alternate reaction route, through the formate ester of the alcohol. A conventional methanol synthesis catalyst with a $Cu/ZnO/Al_2O_3$ structure was used in the experiments. Ethanol and 2-butanol were used as the alcoholic solvents. The feed gas consisted of CO_2 and H_2 (3:1). The experiments were conducted in the temperature range of 160-200 °C and at pressures of up to 60 bar.

Significant dehydrogenation of the alcohols was noticed. In these reactions, 2-butanone and acetaldehyde are formed from 2-butanol and ethanol, respectively, with hydrogen released in the process. Dehydrogenation was found more significant at increased temperatures and in 2-butanol compared to ethanol.

The water-gas shift reaction found an important component in the overall reaction system. The reaction initially proceeds in the reverse direction, forming water and CO from CO_2 and H_2. At the later stages of reaction, the reaction seems to shift to the forward direction, consuming water. The limiting effect of water on the synthesis of methanol was apparent. The limitation appears to be more related to the inhibition of catalyst instead of thermodynamic effects. The proposed reaction mechanism was supported by the detection of ethyl formate in some of the ethanol experiments. Additionally, the blank experiment with hexane showed no methanol formation.

The volumetric productivity of methanol generally increased at increased temperature and pressure. Compared to 2-butanol, the productivity was found equal or higher in ethanol at

identical reaction conditions, however more reliable results were obtained with 2-butanol. The highest volumetric productivity obtained was 1.9 g/(l·h) at 200 °C and 40 bar of partial pressure.

When the amount of catalyst was increased, the catalyst specific productivity was lowered. This suggests that the rate of methanol formation is limited by effects other than the intrinsic rate of reaction. The likely cause is the increased water formation caused by the increased rate of the methanol synthesis and water-gas shift reactions. Variations in catalytic activity caused by the catalyst pretreatment procedure could also have affected the results. The highest catalyst specific productivity was 40.2 g/(kg·h), with 5 g of catalyst in 2-butanol at 180°C and 40 bar of partial pressure.

The productivity values are low compared to industrial methanol synthesis and the gas-phase synthesis from CO_2. However, the experiments were carried out at lower temperatures. Considering large-scale production, the benefits of the somewhat lower temperatures of the liquid-phase process may not outweigh the loss in productivity. However, in small-scale operations, the benefits of the milder reaction conditions and simple operation with no recycle of unreacted gases might prove useful.

A preliminary design for a demonstration scale unit was proposed (Section 6.3 Design of a demonstration process). 0.87 kg/h of methanol is produced from a feed of 0.09 kg/h H_2 and 1.3 kg/h CO_2. A relatively intensive separation stage is required for the separation of the small amount of methanol present in the reaction products. If methanol was used as the solvent, the separation costs could be significantly reduced.

REFERENCES

[1] International Energy Agency, "Key World Energy Statistics," 2014.

[2] IPCC, "Climate Change 2014: Synthesis Report. Contribution of Working Groups I, II and III to the Fifth Assessment Report of the Intergovernmental Panel on Climate Change [Core Writing Team, R.K. Pachauri and L.A. Meyer (eds.)]," IPCC, Geneva, Switzerland, 2014.

[3] World Energy Council, World Energy Resources - 2013 Survey, London: World Energy Council, 2013.

[4] M. Mikkelsen, M. Jorgensen and F. Krebs, "The teraton challenge. A review of fixation and transformation of carbon," *Energy Environ. Sci.,* vol. 3, pp. 43-81, 2010.

[5] C. Song, "Global challenges and strategies for control, conversion and utilization of CO2 for sustainable development involving energy, catalysis, adsorption and chemical processing," *Catal. Today,* vol. 115, pp. 2-32, 2006.

[6] International Energy Agency, "CO2 capture and storage - A key carbon abatement option," International Energy Agency, 2008.

[7] G. Olah, G. Surya Prakash and A. Goeppert, "Anthropogenic Chemical Carbon Cycle for a Sustainable Future," *J. Am. Chem. Soc.,* vol. 133, pp. 12881-12898, 2011.

[8] N. A. M. Razali, K. T. Lee, S. Bhatia and A. R. Mohamed, "Heterogeneous catalysts for production of chemicals using carbon dioxide as raw material: A review," *Renewable Sustainable Energy Rev.,* vol. 16, pp. 4951-4964, 2012.

[9] I. Omae, "Recent developments in carbon dioxide utilization for the production of organic chemicals," *Coord. Chem. Rev.,* vol. 256, pp. 1384-1405, 2012.

[10] International Energy Agency, "Projected Costs of Generating Electricity, 2015 Edition (Executive Summary)," International Energy Agency, 2015.

[11] N. Muradov and T. Veziroglu, "‘"Green’’ path from fossil-based to hydrogen economy: An overview of carbon-neutral technologies," *Int. J. Hydrogen Energy,* vol. 33, pp. 6804-6839, 2008.

[12] National Research Council, The Hydrogen Economy - Opportunities, Costs, Barriers, and R&D Needs, Washington, D.C.: The National Academies Press, 2004.

[13] G. Olah, "Beyond Oil and Gas: The Methanol Economy," *Angew. Chem. Int.,* no. 44, pp. 2636-2639, 2005.

[14] G. Olah, A. Goeppert and G. Surya Prakash, "Chemical Recycling of Carbon Dioxide to Methanol and Dimethyl Ether: From Greenhouse Gas to Renewable, Environmentally Carbon Neutral Fuels and Synthetic Hydrocarbons," *J. Org. Chem.,* no. 74, pp. 487-498, 2009.

[15] C. Arcoumanis, C. Bae, R. Crookes and E. Kinoshita, "The potential of di-methyl ether (DME) as an alternative fuel for compression-ignition engines: A review," *Fuel,* no. 87, pp. 1014-1030, 2008.

[16] A. Goeppert, M. Czaun, J. Jones, G. K. Surya Prakash and G. A. Olah, "Recycling of carbon dioxide to methanol and derived products – closing the loop," *Chem. Soc. Rev.,* no. 43, pp. 7995-8048, 2014.

[17] G. Centi and S. Perathoner, "Opportunities and prospects in the chemical recycling of carbon dioxide to fuels," *Catal. Today,* vol. 148, pp. 191-205, 2009.

[18] I. Ganesh, "Conversion of carbon dioxide into methanol – a potential liquid fuel: Fundamental challenges and opportunities (a review)," *Renewable Sustainable Energy Rev.,* vol. 31, pp. 221-257, 2014.

[19] H. Ibrahim, A. Ilinca and J. Perron, "Energy storage systems—Characteristics and comparisons," *Renewable and Sustainable Energy Reviews,* vol. 12, pp. 1221-1250, 2008.

[20] I. Hadjipaschalis, A. Poullikkas and V. Efthimiou, "Overview of current and future energy storage technologies for electric power applications," *Renewable and Sustainable Energy Reviews,* vol. 13, pp. 1513-1522, 2009.

[21] F. Schüth, "Chemical Compounds for Energy Storage," *Chem. Ing. Tech.,* vol. 83, no. 11, pp. 1984-1993, 2011.

[22] W. Wang, S. Wang, X. Ma and J. Gong, "Recent advances in catalytic hydrogenation of carbon dioxide," *Chem. Soc. Rev.,* vol. 40, pp. 3703-3727, 2011.

[23] M. D. Porosoff, B. Yan and J. G. Chen, "Catalytic reduction of CO2 by H2 for synthesis of CO, methanol and hydrocarbons: challenges and opportunities," *Energy Environ. Sci.,* vol. 9, pp. 62-73, 2016.

[24] R. Steeneveldt, R. Berger and T. A. Torp, "CO2 CAPTURE AND STORAGE: Closing the Knowing–Doing Gap," *Chem. Eng. Res. Des.,* vol. 84, no. 9, p. 739–763, 2006.

[25] D. W. Keith, M. Ha-Duong and J. K. Stolaroff, "Climate Strategy with CO2 Capture from the Air," *Clim. Change,* vol. 74, pp. 17-45, 2006.

[26] A. Goeppert, M. Czaun, G. K. Surya Prakash and G. A. Olah, "Air as the renewable carbon source of the future: an overview of CO2 capture from the atmosphere," *Energy Environ. Sci,* vol. 5, pp. 7833-7853, 2012.

[27] M. Mikkelsen, M. Jorgensen and F. Krebs, "The teraton challenge. A review of fixation and transformation of carbon," *Energy & Environmental Science,* vol. 3, pp. 43-81, 2010.

[28] M. Peters, B. Köhler, W. Kuckshinrichs, W. Leitner, P. Markewitz and T. E. Müller, "Chemical Technologies for Exploiting and Recycling Carbon Dioxide into the Value Chain," *ChemSusChem,* vol. 4, p. 1216 – 1240, 2011.

[29] D. M. D'Alessandro, B. Smit and J. Long, "Carbon Dioxide Capture: Prospects for New Materials," *Angew. Chem. Int. Ed.,* vol. 49, pp. 6058-6082, 2010.

[30] N. MacDowell, N. Florin, A. Buchard, J. Hallett, A. Galindo, G. Jackson, C. S. Adjiman, C. K. Williams, N. Shah and P. Fennell, "An overview of CO2 capture technologies," *Energy Environ. Sci,* vol. 3, pp. 1645-1669, 2010.

[31] J. C. M. Pires, F. G. Martins, M. C. M. Alvim-Ferraz and M. Simões, "Recent developments on carbon capture and storage: An overview," *Chem. Eng. Res. Des.,* vol. 89, pp. 1446-1460, 2011.

[32] P. Markewitz, W. Kuckshinrichs, W. Leitner, J. Linssen, P. Zapp, R. Bongartz, A. Schreiber and T. E. Müller, "Worldwide innovations in the development of carbon capture technologies and the utilization of CO2," *Energy Environ. Sci.,* vol. 5, pp. 7281-7305, 2012.

[33] P. D. Vaidya and E. Y. Kenig, "CO2-Alkanolamine Reaction Kinetics: A Review of Recent Studies," *Chem. Eng. Technol.,* vol. 30, pp. 1467-1474, 2007.

[34] J. Kittel, R. Idem, D. Gelowitz, P. Tontiwachwuthikul, G. Parrain and A. Bonneau, "Corrosion in MEA units for CO2 capture: pilot plant studies," *Energy Procedia,* vol. 1, pp. 791-797, 2009.

[35] B. R. Strazisar, R. R. Anderson and C. M. White, "Degradation Pathways for Monoethanolamine in a CO2 Capture Facility," *Energy Fuels,* vol. 17, pp. 1034-1039, 2003.

[36] V. Darde, K. Thomsen, W. J. M. van Well and E. H. Stenby, "Chilled ammonia process for CO2 capture," *Int. J. Greenhouse Gas Control,* vol. 4, pp. 131-136, 2010.

[37] S. Choi, J. H. Drese and C. W. Jones, "Adsorbent Materials for Carbon Dioxide Capture from Large Anthropogenic Point Sources," *ChemSusChem,* vol. 2, pp. 796-854, 2009.

[38] Y. Li, C. Zhao, H. Chen, C. Liang, L. Duan and W. Zhou, "Modified CaO-based sorbent looping cycle for CO2 mitigation," *Fuel,* vol. 88, pp. 697-704, 2009.

[39] A. Bosoaga, O. Masek and J. E. Oakey, "CO2 Capture Technologies for Cement Industry," *Energy Procedia,* vol. 1, pp. 133-140, 2009.

[40] A. A. Olajire, "CO2 capture and separation technologies for end-of-pipe applications - A review," *Energy,* vol. 35, pp. 2610-2628, 2010.

[41] C. E. Powell and G. G. Qiao, "Polymeric CO2/N2 gas separation membranes for the capture of carbon dioxide from power plant flue gases," *J. Membr. Sci.,* vol. 279, pp. 1-49, 2006.

[42] L. M. Robeson, "Correlation of separation factor versus permeability for polymeric membranes," *J. Membr. Sci.,* vol. 2, pp. 165-185, 1991.

[43] R. Bounaceur, N. Lape, D. Roizard, C. Vallieres and E. Favre, "Membrane processes for post-combustion carbon dioxide capture: A parametric study," *Energy,* vol. 31, pp. 2556-2570, 2006.

[44] E. Favre, "Carbon dioxide recovery from post-combustion processes: Can gas permeation membranes compete with absorption?," *J. Membr. Sci.,* vol. 294, pp. 50-59, 2007.

[45] M. Wang, A. Lawal, P. Stephenson, J. Sidders and C. Ramshaw, "Post-combustion CO2 capture with chemical absorption: A state-of-the-art review," *Chem. Eng. Res. Des.,* vol. 89, pp. 1609-1624, 2011.

[46] R. Castillo, "Thermodynamic analysis of a hard coal oxyfuel power plant with high temperature three-end membrane for air separation," *Appl. Energy,* vol. 88, pp. 1480-1493, 2011.

[47] H. Stadler, F. Beggel, M. Habermehl, B. Persigehl, R. Kneer, M. Modigell and P. Jeschke, "Oxyfuel coal combustion by efficient integration of oxygen transport membranes," *Int. J. Greenhouse Gas Control,* vol. 5, pp. 7-15, 2011.

[48] M. Anheden, U. Burchhardt, H. Ecke, R. Faber, O. Jidinger, R. Giering, H. Kass, S. Lysk, E. Ramström and J. Yan, "Overview of operational experience and results from test activities in Vattenfall's 30 MWth oxyfuel pilot plant in Schwarze Pumpe," *Energy Procedia,* vol. 4, pp. 941-950, 2011.

[49] C. Kunze and H. Spliethoff, "Modelling of an IGCC plant with carbon capture for 2020," *Fuel Process. Technol.,* vol. 91, pp. 934-941, 2010.

[50] M. Gräbner, O. von Morstein, D. Rappold, W. Günster, G. Beysel and B. Meyer, "Constructability study on a German reference IGCC power plant with and without CO2-capture for hard coal and lignite," *Energy Convers. Manage.,* vol. 51, pp. 2179-2187, 2010.

[51] ZEP, "EU Demonstration Programme for CO2 Capture and Storage (CCS) - ZEP's Proposal," Brussels, 2008.

[52] H. A. Blum, L. F. Stutzman and W. S. Dodds, "Gas Absorption - Absorption of Carbon Dioxide from Air by Sodium and Potassium Hydroxides.," *Ind. Eng. Chem.,* vol. 44, no. 12, pp. 1969-2974, 1952.

[53] Q. Wang, J. Luo, Z. Zhong and A. Borgna, "CO2 capture by solid adsorbents and their applications: current status and new trends," *Energy Environ. Sci.,* vol. 4, pp. 42-55, 2011.

[54] F. Zeman, "Energy and Material Balance of CO2 Capture from Ambient Air," *Environ. Sci. Technol.,* vol. 41, pp. 7558-7563, 2007.

[55] R. Baciocchi, G. Storti and M. Mazzotti, "Process design and energy requirements for the capture of carbon dioxide from air," *Chem. Eng. Process.,* no. 45, pp. 1047-1058, 2006.

[56] F. Zeman, "Experimental results for capturing CO2 from the atmosphere," *AIChE J.,* vol. 54, no. 5, pp. 1396-1399, 2008.

[57] J. K. Stolaroff, D. W. Keith and G. V. Lowry, "Carbon Dioxide Capture from Atmospheric Air Using Sodium Hydroxide Spray," *Environ. Sci. Technol.,* vol. 42, no. 8, pp. 2728-2735, 2008.

[58] D. K. Lindberg and R. V. Backman, "Effect of Temperature and Boron Contents on the Autocausticizing Reactions in Sodium Carbonate/Borate Mixtures," *Ind. Eng. Chem. Res.,* vol. 43, no. 20, pp. 6285-6291, 2004.

[59] M. Mahmoudkhani and D. W. Keith, "Low-energy sodium hydroxide recovery for CO2 capture from atmospheric air—Thermodynamic analysis," *Int. J. Greenhouse Gas Control,* vol. 3, no. 4, pp. 376-384, 2009.

[60] K. S. Lackner, "Capture of carbon dioxide from ambient air," *Eur. Phys. J. Special Topics,* vol. 176, pp. 83-106, 2009.

[61] S. Choi, J. H. Drese, P. M. Eisenberger and C. W. Jones, "Application of Amine-Tethered Solid Sorbents for Direct CO2 Capture from the Ambient Air," *Environ. Sci. Technol.,* vol. 45, pp. 2420-2427, 2011.

[62] W. Li, S. Choi, J. H. Drese, M. Hornbostel, G. Krishnan, P. M. Eisenberger and C. W. Jones, "Steam-Stripping for Regeneration of Supported Amine-Based CO2 Adsorbents," *ChemSusChem,* vol. 3, pp. 899-903, 2010.

[63] S. Choi, J. H. Drese, P. M. Eisenberger and C. W. Jones, "Application of Amine-Tethered Solid Sorbents for Direct CO2 Capture from the Ambient Air," *Environ. Sci. Technol.,* vol. 45, no. 6, pp. 2420-2427, 2011.

[64] T. Wang, K. S. Lackner and A. Wright, "Moisture Swing Sorbent for Carbon Dioxide Capture from Ambient Air," *Environ. Sci. Technol.,* vol. 45, no. 15, pp. 6670-6675, 2011.

[65] M. Ranjan and H. J. Herzog, "Feasibility of air capture," *Energy Procedia,* vol. 4, pp. 2869-2876, 2011.

[66] A. Eisenberg, "The New York Times: Pulling Carbon Dioxide Out of Thin Air," 2013. [Online]. Available: http://www.nytimes.com/2013/01/06/business/pilot-plant-in-the-works-for-carbon-dioxide-cleansing.html?_r=2&. [Accessed 15 February 2016].

[67] E. Kintisch, "MIT Technology Review: Can Sucking CO2 Out of the Atmosphere Really Work?," 2014. [Online]. Available: https://www.technologyreview.com/s/531346/can-sucking-co2-out-of-the-atmosphere-really-work/. [Accessed 15 February 2016].

[68] M. Gunther, "The Guardian: Startups have figured out how to remove carbon from the air. Will anyone pay them to do it?," 2015. [Online]. Available:

http://www.theguardian.com/sustainable-business/2015/jul/14/carbon-direct-air-capture-startups-tech-climate. [Accessed 15 February 2016].

[69] G. Crabtree, M. Dresselhaus and M. Buchanan, "The Hydrogen Economy," *Phys. Today,* no. December 2004, 2004.

[70] C. Winter, "Hydrogen energy - Abundant, efficient, clean: A debate over the energy-system-of-change," *International Journal of Hydrogen Energy,* vol. 34, pp. 1-52, 2009.

[71] T. Lipman, "What Will Power the Hydrogen Economy? Present and Future Sources of Hydrogen Energy," Institute of Transportation Studies - University of California, Davis, Davis, CA, 2004.

[72] G. Stiegel and M. Ramezan, "Hydrogen from coal gasification: An economical pathway to a sustainable energy future," *International Journal of Coal Geology,* no. 65, pp. 173-190, 2006.

[73] J. Turner, G. Sverdrup, M. Mann, P. Maness, B. Kroposki, M. Ghirardi, R. Evans and D. Blake, "Renewable hydrogen production," *International Journal of Energy Research,* no. 32, pp. 379-407, 2008.

[74] O. Bicáková and P. Straka, "Production of hydrogen from renewable resources and its effectiveness," *Int. J. Hydrogen Energy,* vol. 37, pp. 11563-11578, 2012.

[75] J. Holladay, J. Hu, D. King and Y. Wang, "An overview of hydrogen production technologies," *Catal. Today,* vol. 139, pp. 244-260, 2009.

[76] J. Armor, "The multiple roles for catalysis in the production of H2," *Appl. Catal., A,* vol. 176, pp. 159-176, 1999.

[77] A. Goeppert, M. Czaun, J. Jones, G. K. Surya Prakash and G. A. Olah, "Recycling of carbon dioxide to methanol and derived products – closing the loop," *Chem. Soc. Rev.,* vol. 43, pp. 7995-8048, 2014b.

[78] P. Häussinger, R. Lohmüller and A. Watson, "Hydrogen, 2. Production," in *Ullmann's Encyclopedia of Industrial Chemistry*, Weinheim, Wiley-VCH, 2012, pp. 249-307.

[79] C. Song, "Fuel processing for low-temperature and high-temperature fuel cells - Challenges, and opportunities for sustainable development in the 21st century," *Catalysis Today,* no. 77, pp. 17-49, 2002.

[80] F. Joensen and J. Rostrup-Nielsen, "Conversion of hydrocarbons and alcohols for fuel cells," *J. Power Sources,* vol. 105, pp. 195-201, 2002.

[81] D. Wilhelm, D. Simbeck, A. Karp and R. Dickenson, "Syngas production for gas-to-liquids applications: technologies, issues and outlooks," *Fuel Process. Technol.,* vol. 71, pp. 139-148, 2001.

[82] P. Häussinger, R. Lohmüller and A. Watson, "Hydrogen, 3. Purification," in *Ullmann's Encyclopedia of Industrial Chemistry* , Weinheim, Wiley-VCH, 2012, pp. 309-333.

[83] I. Babich and J. Moulijn, "Science and technology of novel processes for deep desulfurization of oil refinery streams: a review," *Fuel,* vol. 82, pp. 607-631, 2003.

[84] G. Ranke and F. Siegert, "Energy efficient scrubbing of sulfur compounds from moist gaseous mixtures". United States of America Patent 4,332,596, 1982.

[85] S. Adhikari and S. Fernando, "Hydrogen Membrane Separation Techniques," *Ind. Eng. Chem. Res.,* vol. 45, pp. 875-881, 2006.

[86] B. Freeman and I. Pinnau, "Gas and Liquid Separations Using Membranes: An Overview," in *Advanced Materials for Membrane Separations*, I. Pinnau and B. Freeman, Eds., Washington D.C., American Chemical Society, 2004, pp. 1-23.

[87] A. Demirbas, "Combustion characteristics of different biomass fuels," *Prog. Energy Combust. Sci.,* vol. 30, pp. 219-230, 2004.

[88] A. Demirbas, "Progress and recent trends in biofuels," *Prog. Energy Combust. Sci.,* vol. 33, pp. 1-18, 2007.

[89] D. Bulushev and J. Ross, "Catalysis for conversion of biomass to fuels via pyrolysis and gasification: A review," *Catal. Today,* vol. 171, pp. 1-13, 2011.

[90] D. Sutton, B. Kelleher and J. Ross, "Review of literature on catalysts for biomass gasification," *Fuel Process. Technol.,* vol. 73, pp. 155-173, 2001.

[91] G. Weber, Q. Fu and H. Wu, "Energy Efficiency of an Integrated Process Based on Gasification for Hydrogen Production from Biomass," *Dev. Chem. Eng. Mineral Process.,* vol. 14, pp. 33-49, 2006.

[92] A. Ursua, "Hydrogen Production From Water Electrolysis: Current Status and Future Trends," *Proc. IEEE,* vol. 100, no. 2, 2012.

[93] C. Grimes, O. Varghese and S. Ranjan, "Hydrogen Generation by Water Splitting," in *Light, Water, Hydrogen - The Solar Generation of Hydrogen by Water Photoelectrolysis*, C. Grimes, O. Varghese and S. Ranjan, Eds., Springer US, 2008, pp. 35-113.

[94] K. Zeng and D. Zhang, "Recent progress in alkaline water electrolysis for hydrogen production and applications," *Prog. Energy Combust. Sci.,* vol. 36, pp. 307-326, 2010.

[95] M. Wang, Z. Wang, X. Gong and Z. Guo, "The intensification technologies to water electrolysis for hydrogen production – A review," *Renewable Sustainable Energy Rev.,* vol. 29, pp. 573-588, 2014.

[96] W. Kreuter and H. Hofmann, "Electrolysis: The Important Enegry Transformer in a World of Sustainable Energy," *Int. J. Hydrogen Energy,* vol. 23, no. 8, pp. 1661-666, 1998.

[97] T. Smolinka, M. Günther and J. Garche, "Stand und Entwicklungspotenzial der Wasserelektrolyse zur Herstellung von Wasserstoff aus regenerativen Energien," Fraunhofer ISE, 2011.

[98] J. Ivy, "Summary of Electrolytic Hydrogen Production," National Renewable Energy Laboratory, 2004.

[99] J. Russell, L. Nuttall and A. Fickett, "Hydrogen generation by solid polymer electrolyte water electrolysis," *Prepr. Pap. - Am. Chem. Soc., Div. Fuel Chem.,* vol. 18, no. 3, pp. 24-40, 1973.

[100] S. Grigoriev, V. Porembsky and V. Fateev, "Pure hydrogen production by PEM electrolysis for hydrogen energy," *Int. J. Hydrogen Energy,* vol. 31, pp. 171-175, 2006.

[101] P. Millet, D. Dragoe, S. Grigoriev, V. Fateev and C. Etievant, "GenHyPEM: A research program on PEM water electrolysis supported by the European Commission," *Int. J. Hydrogen Energy,* vol. 34, pp. 3974-4982, 2009.

[102] S. Marini, P. Salvi, P. Nelli, R. Pesenti, M. Villa, M. Berrettoni, G. Zangari and Y. Kiros, "Advanced alkaline water electrolysis," *Electrochim. Acta,* vol. 82, pp. 384-391, 2012.

[103] M. Carmo, D. Fritz, J. Mergel and D. Stolten, "A comprehensive review on PEM water electrolysis," *Int. J. Hydrogen Energy,* vol. 38, pp. 4901-4934, 2013.

[104] DuPont, "Nafion PFSA Membranes," 2016. [Online]. Available: http://www.dupont.com/products-and-services/membranes-films/fluoropolymer-films/brands/nafion-pfsa-membranes.html. [Accessed 1 February 2016].

[105] F. Barbir, "PEM electrolysis for production of hydrogen from renewable energy sources," *Sol. Energy,* vol. 78, pp. 661-669, 2005.

[106] J. Udagawa, P. Aguiar and N. Brandon, "Hydrogen production through steam electrolysis: Control strategies for a cathode-supported intermediate temperature solid oxide electrolysis cell," *J. Power Sources,* vol. 180, pp. 354-364, 2008.

[107] A. Brisse, J. Schefold and M. Zahid, "High temperature water electrolysis in solid oxide cells," *Int. J. Hydrogen Energy,* vol. 33, pp. 5375-5382, 2008.

[108] M. Ni, M. Leung and D. Leung, "Technological development of hydrogen production by solid oxide electrolyzer cell (SOEC)," *Int. J. Hydrogen Energy,* vol. 33, pp. 2337-2354, 2008.

[109] T. Abbasi and S. Abbasi, "'Renewable' hydrogen: Prospects and challenges," *Renewable and Sustainable Energy Reviews,* no. 15, pp. 3034-3040, 2011.

[110] A. Züttel, "Materials for hydrogen storage," *Materials Today,* no. September 2003, pp. 24-33, 2003.

[111] Air Products, "Material Safety Data Sheet: Hydrogen, compressed," 1994. [Online]. Available: http://avogadro.chem.iastate.edu/msds/hydrogen.pdf. [Accessed 2 February 2016].

[112] P. Häussinger, R. Lohmüller and A. Watson, "Hydrogen, 5. Handling," in *Ullmann's Encyclopedia of Industrial Chemistry*, Weinheim, Wiley-VCH, 2012, pp. 341-352.

[113] M. Klell, "Storage of Hydrogen in the Pure Form," in *Handbook of Hydrogen Storage*, M. Hirscher, Ed., Weinheim, Wiley-VCH, 2010, pp. 1-37.

[114] U. Eberle, M. Felderhoff and F. Schüth, "Chemical and Physical Solutions for Hydrogen Storage," *Angew. Chem.,* vol. 48, pp. 6609-6630, 2009.

[115] A. Züttel, "Hydrogen storage methods," *Naturwissenschaften,* vol. 91, pp. 157-172, 2004.

[116] U. Bossel and B. Eliasson, "Energy and the Hydrogen Economy," 2003. [Online]. Available: http://www.afdc.energy.gov/pdfs/hyd_economy_bossel_eliasson.pdf. [Accessed 3 February 2016].

[117] P. Budd, A. Butler, J. Selbie, K. Mahmood, N. McKeown, B. Ghanem, K. Msayib, D. Book and A. Walton, "The potential of organic polymer-based hydrogen storage materials," *Phys. Chem. Chem. Phys.,* vol. 9, pp. 1802-1808, 2007.

[118] U. Mueller, M. Schubert, F. Teich, H. Puetter, K. Schierle-Arndt and J. Pastré, "Metal–organic frameworks—prospective industrial applications{," *J. Mater. Chem.,* vol. 16, pp. 626-636, 2006.

[119] A. Dalebrook, W. Gan, M. Grasemann, S. Moret and G. Laurenczy, "Hydrogen storage: beyond conventional methods," *Chem. Commun.,* vol. 49, pp. 8735-8751, 2013.

[120] J. Graetz, "New approaches to hydrogen storage," *Chem. Soc. Rev.,* vol. 38, pp. 73-82, 2009.

[121] D. Teichmann, W. Arlt and P. Wasserscheid, "Liquid Organic Hydrogen Carriers as an efficient vector for the transport and storage of renewable energy," *Int. J. Hydrogen Energy,* vol. 37, pp. 18118-18132, 2012.

[122] F. Sotoodeh, L. Zhao and K. Smith, "Kinetics of H2 recovery from dodecahydro-N-ethylcarbazole over a supported Pd catalyst," *Appl. Catal., A,* vol. 362, pp. 155-162, 2009.

[123] D. Palo, "Methanol Steam Reforming for Hydrogen Production," *Chem. Rev.,* vol. 107, pp. 3992-4021, 2007.

[124] A. Haryanto, S. Fernando, N. Murali and S. Adhikari, "Current Status of Hydrogen Production Techniques by Steam Reforming of Ethanol: A Review," *Energy Fuels,* vol. 19, pp. 2098-2106, 2005.

[125] M. Hogarth and G. Hards, "Direct Methanol Fuel Cells," *Platinum Met. Rev.,* vol. 40, no. 4, pp. 150-159, 1996.

[126] W. Leitner, "Carbon Dioxide as a Raw Material: The Synthesis of Formic Acid and Its Derivatives from CO2," *Angew. Chem. Int. Ed. Engl.,* vol. 34, pp. 2207-2221, 1995.

[127] U. Bossel, "Does a Hydrogen Economy Make Sense?," *Proc. IEEE,* vol. 94, no. 10, pp. 1826-1837, 2006.

[128] W. Boll, G. Hochgesand, C. Higman, E. Supp, P. Kalteier, W. Müller, M. Kriebel, H. Schlichting and H. Tanz, "Gas Production, 3. Gas Treating," in *Ullmann's Encyclopedia of Industrial Chemistry*, Weinheim, Wiley-VCH, 2012, pp. 483-539.

[129] W. Wang and J. Gong, "Methanation of carbon dioxide: an overview," *Front. Chem. Sci. Eng.,* vol. 5, pp. 2-10, 2011.

[130] T. Kaneko, F. Derbyshire, E. Makino, D. Gray, M. Tamura and K. Li, "Coal Liquefaction," in *Ullmann's Encyclopedia of Industrial Chemistry*, Weinheim, Wiley-VCH, 2012, pp. 1-83.

[131] C. Paun, J. Sá and K. Jalama, "Fischer–Tropsch - Fuel Production with Cobalt Catalysts," in *Fuel Production with Heterogeneous Catalysis*, J. Sá, Ed., Boca Raton, CRC Press, 2015, pp. 147-168.

[132] M. E. Dry, "Practical and theoretical aspects of the catalytic Fischer-Tropsch process," *Appl. Catal., A,* vol. 138, pp. 319-344, 1996.

[133] J. A. Moulijn, M. Makkee and A. van Diepen, "Fischer-Tropsch process," in *Chemical Process Technology*, J. A. Moulijn, M. Makkee and A. van Diepen, Eds., Chichester, John Wiley & Sons, 2001, pp. 193-203.

[134] H. Schulz, "Short history and present trends of Fischer–Tropsch synthesis," *Appl. Catal., A,* vol. 186, pp. 3-12, 1999.

[135] R. W. Dorner, D. R. Hardy, F. W. Williams and H. D. Willauer, "Heterogeneous catalytic CO2 conversion to value-added hydrocarbons," *Energy Environ. Sci.,* vol. 3, pp. 884-890, 2010.

[136] S. Saeidi, N. A. S. Amin and M. R. Rahimpour, "Hydrogenation of CO2 to value-added products - A review and potential future developments," *J. CO2 Util.,* vol. 5, pp. 66-81, 2014.

[137] IHS, "Global Methanol Market Review," IHS, 2012.

[138] M. Bertau, K. Räuchle, N. Ballarini and M. S. Wiehn, "Methanol-Derived Chemicals: Methanol as a C1-Base," in *Methanol: The Basic Chemical and Energy Feedstock of the Future,*, M. Bertau, H. Offermanns, L. Plass, F. Schmidt and H. Wernicke, Eds., Springer Verlag Berlin Heidelberg, 2014, pp. 332-410.

[139] J. Ott, V. Gronemann, F. Pontzen, E. Fiedler, G. Grossmann, D. Kersebohm, G. Weiss and C. Witte, "Methanol," in *Ullmann's Encyclopedia of Industrial Chemistry*, Weinheim, Wiley-VCH , 2012.

[140] S. Lee, "Methanol Synthesis from Syngas," in *Handbook of Alternative Fuel Technologies*, S. Lee, J. G. Speight and S. K. Loyalka, Eds., Boca Raton, CRC Press, 2007, pp. 297-321.

[141] U. Standt and F. Seyfried, "Methanol as Fuel," in *Methanol: The Basic Chemical and Energy Feedstock of the Future*, M. Bertau, H. Offermanns, L. Plass, F. Schmidt and H. Wernicke, Eds., Springer-Verlag Berlin Heidelberg, 2014, pp. 410-423.

[142] J. Mergel and H. Dohle, "Methanol for fuel cells without reformers (DMFC)," in *Methanol as an Energy Carrier*, P. Biedermann, T. Grube and B. Höhlein, Eds., Jülich, Forschungszentrum Jülich GmbH, 2006, pp. 25-34.

[143] F. Pontzen, W. Liebner, V. Gronemann, M. Rothaemel and B. Ahlers, "CO2-based methanol and DME – Efficient technologies for industrial scale production," *Catal. Today,* vol. 171, pp. 242-250, 2011.

[144] A. Urakawa and J. Sá, "CO2 to Fuels," in *Fuel Production with Heterogeneous Catalysis*, J. Sá, Ed., Boca Raton, CRC Press , 2015, pp. 93-122.

[145] M. Müller and U. Hübsch, "Dimethyl Ether," in *Ullmann's Encyclopedia of Industrial Chemistry*, Weinheim, Wiley-VCH, 2012, pp. 305-308.

[146] J. Yanowitz, M. A. Ratcliff, R. L. McCormick, J. D. Taylor and M. J. Murphy, "Compendium of Experimental Cetane Numbers, Technical Report NREL/TP-5400-61693," August 2014. [Online]. Available: http://www.nrel.gov/docs/fy14osti/61693.pdf. [Accessed 8 March 2016].

[147] Volvo, "Volvo Bio-DME: Unique field test in commercial operations, 2010-2012," 2012. [Online]. Available: http://www.volvotrucks.com/SiteCollectionDocuments/VTC/Corporate/News%20and%20Media/publications/Volvo%20BioDME.pdf. [Accessed 8 March 2016].

[148] M. Stöcker, "Methanol-to-hydrocarbons: catalytic materials and their behavior," *Microporous Mesoporous Mater.,* vol. 29, pp. 3-48, 1999.

[149] L. Reichelt and F. Schmidt, "Methanol-to-Gasoline Process," in *Methanol: The Basic Chemical and Energy Feedstock of the Future*, M. Bertau, H. Offermanns, L. Plass, F. Schmidt and H. Wernicke, Eds., Springer-Verlag Berlin Heidelberg, 2014, pp. 440-453.

[150] F. Schmidt and C. Pätzold, "Methanol-to-Olefins Processes," in *Methanol: The Basic Chemical and Energy Feedstock of the Future*, M. Bertau, H. Offermann, L. Plass, F. Schmidt and H. Wernicke, Eds., Springer-Verlag Berlin Heidelberg, 2014, pp. 454-472.

[151] J. Packer, "The Production of Methanol and Gasoline - New Zealand Institute of Chemistry," [Online]. Available: http://nzic.org.nz/ChemProcesses/energy/7D.pdf. [Accessed 9 March 2016].

[152] T. Ren, M. K. Patel and K. Blok, "Steam cracking and methane to olefins: Energy use, CO2 emissions and production costs," *Energy,* vol. 33, pp. 817-833, 2008.

[153] N. Kosaric, Z. Duvnjak, A. Farkas, H. Sahm, S. Bringer-Meyer, O. Goebel and D. Mayer, "Ethanol," in *Ullmann's Encyclopedia of Industrial Chemistry*, Weinheim, Wiley-VCH, 2012, pp. 333-403.

[154] A. Demirbas, "Progress and recent trends in biofuels," *Prog. Energy Combust. Sci.,* vol. 33, pp. 1-18, 2007.

[155] S. K. Thangevalu, A. S. Ahmed and F. N. Ani, "Review on bioethanol as alternative fuel for sparki gnition engines," *Renewable Sustainable Energy Rev.,* vol. 56, pp. 820-835, 2016.

[156] V. Subramani and S. K. Gangwal, "A Review of Recent Literature to Search for an Efficient Catalytic Process for the Conversion of Syngas to Ethanol," *Energy Fuels,* vol. 22, pp. 814-839, 2008.

[157] V. R. Surisetty, A. K. Dalai and J. Kozinski, "Alcohols as alternative fuels: An overview," *Appl. Catal., A,* vol. 404, pp. 1-11, 2011.

[158] M. Muhler and S. Kaluza, "Syngas to Methanol and Ethanol," in *Fuel Production with Heterogeneous Catalysis*, J. Sá, Ed., Boca Raton, CRC Press, 2014, pp. 169-192.

[159] A. K. Agarwal, "Biofuels (alcohols and biodiesel) applications as fuels for internal combustion engines," *Prog. Energy Combust. Sci.,* vol. 33, pp. 233-271, 2007.

[160] UN-Energy, "Ethanol fuel in Brazil," 2011. [Online]. Available: http://www.un-energy.org/stories/38-ethanol-fuel-in-brazil. [Accessed 8 March 2016].

[161] J. Lane, "Biofuels Digest - Biofuels Mandates Around the World: 2015," 31 December 2014. [Online]. Available: http://www.biofuelsdigest.com/bdigest/2014/12/31/biofuels-mandates-around-the-world-2015/. [Accessed 8 March 2016].

[162] Alternative Fuels Data Center, "Ethanol Fuel Basics," 2015. [Online]. Available: http://www.afdc.energy.gov/fuels/ethanol_fuel_basics.html. [Accessed 8 March 2016].

[163] S. Kumar, J. H. Cho, J. Park and I. Moon, "Advances in diesel–alcohol blends and their effects on the performance and emissions of diesel engines," *Renewable Sustainable Energy Rev.,* vol. 22, pp. 46-72, 2013.

[164] G. A. Olah, "Towards Oil Independence Through Renewable Methanol Chemistry," *Angew. Int. Ed.,* vol. 52, pp. 104-107, 2013.

[165] EPA, "Overview of Greenhouse Gases - Methane Emissions," 2016. [Online]. Available: http://www3.epa.gov/climatechange/ghgemissions/gases/ch4.html. [Accessed 5 March 2016].

[166] L. Su, X. Li and Z. Sun, "The consumption, production and transportation of methanol in China: A review," *Energy Policy,* vol. 63, pp. 130-138, 2013.

[167] F. Arena, G. Mezzatesta, L. Spadaro and G. Trunfio, "Latest Advances in the Catalytic Hydrogenation of Carbon Dioxide to Methanol/Dimethylether," in *Transformation and Utilization of Carbon Dioxide*, B. M. Banage and M. Arai, Eds., Springer-Verlag Berlin Heidelberg, 2014, pp. 103-130.

[168] J. A. Moulijn, M. Makkee and A. van Diepen, "Methanol," in *Chemical Process Technology*, J. A. Moulijn, M. Makkee and A. van Diepen, Eds., Chichester, John Wiley & Sons, 2001, pp. 180-193.

[169] J. Lee, K. H. Lee, S. Lee and Y. Kim, "A Comparative Study of Methanol Synthesis from CO2/H2 and CO/H2 over a Cu/ZnO/Al2O3 Catalyst," *J. Catal.,* vol. 144, no. 2, pp. 414-424, 1993.

[170] S. Fujita, M. Usui, H. Ito and N. Takezawa, "Mechanisms of Methanol Synthesis from Carbon Dioxide and from Carbon monoxide at Atmospheric Pressure over Cu/ZnO," *J. Catal.,* vol. 157, pp. 403-413, 1995.

[171] J. Skrzypek, M. Lachowska, M. Grzesik, J. Sloczynski and P. Nowak, "Thermodynamics and kinetics of low pressure methanol synthesis," *Chem. Eng. J. ,* vol. 58, pp. 101-108, 1995.

[172] L. C. Grabow and M. Mavrikakis, "Mechanism of Methanol Synthesis on Cu through CO2 and CO Hydrogenation," *ACS Catal.,* vol. 1, pp. 365-384, 2011.

[173] F. Studt, M. Behrens, E. L. Kunkes, N. Thomas, S. Zander, A. Tarasov, J. Schumann, E. Frei, J. B. Varley, F. Abild-Pedersen, J. K. Norskov and R. Schlögl, "The Mechanism of CO and CO2 Hydrogenation to Methanol over Cu-Based Catalysts," *ChemCatChem,* vol. 7, pp. 1105-1111, 2015.

[174] T. S. Askgaard, J. K. Norskov, C. V. Ovesen and P. Stoltze, "A Kinetic Model of Methanol Synthesis," *J. Catal.,* vol. 156, pp. 229-242, 1995.

[175] K. M. Vanden Bussche and G. F. Froment, "A Steady-State Kinetic Model for Methanol Synthesis and the Water Gas Shift Reaction on a Commercial Cu/ZnO/Al2O3 Catalyst," *J. Catal.,* vol. 161, pp. 1-10, 1996.

[176] X. Liu, G. Q. Lu, Z. Yan and J. Beltramini, "Recent Advances in Catalysts for Methanol Synthesis via Hydrogenation of CO and CO2," *Ind. Eng. Chem. Res.,* vol. 42, pp. 6518-6530, 2003.

[177] H.-J. Wernicke, "Methanol Generation," in *Methanol: The Basic Chemical and Energy Feedstock of the Future*, M. Bertau, H. Offermanns, L. Plass, F. Schmidt and W. H.-J., Eds., Springer-Verlag Berlin Heidelberg, 2014, pp. 51-301.

[178] C. Song, "Global challenges and strategies for control, conversion and utilization of CO2 for sustainable development involving energy, catalysis, adsorption and chemical processing," *Catalysis Today,* vol. 115, pp. 2-32, 2006.

[179] MMSA, "MMSA Methanol Market Weekly," MMSA, 2015.

[180] T. Lorenz, M. Bertau, F. Schmidt and L. Plass, "Methanol Production from CO2," in *Methanol: The Basic Chemical and Energy Feedstock of the Future*, M. Bertau, H.

Offermanns, L. Plass, F. Schmidt and H. Wernicke, Eds., Springer-Verlag Berlin Heidelberg, 2014, pp. 266-276.

[181] M. Saito, T. Fujitani, M. Takeuchi and T. Watanabe, "Development of copper/zinc oxide-based multicomponent catalysts for methanol synthesis from carbon dioxide and hydrogen," *Appl. Catal., A,* vol. 138, pp. 311-318, 1996.

[182] F. Arena, K. Barbera, G. Italiano, G. Bonura, L. Spadaro and F. Frusteri, "Synthesis, characterization and activity pattern of Cu–ZnO/ZrO2 catalysts in the hydrogenation of carbon dioxide to methanol," *J. Catal.,* vol. 249, pp. 185-194, 2007.

[183] K. A. Ali, A. Z. Abdullah and A. R. Mohamed, "Recent development in catalytic technologies for methanol synthesis from renewable sources: A critical review," *Renewable Sustainable Energy Rev.,* vol. 44, pp. 508-518, 2015.

[184] J. Wambach, A. Baiker and A. Wokaun, "CO2 hydrogenation over metal/zirconia catalysts," *Phys. Chem. Chem. Phys.,* vol. 1, pp. 5071-5080, 1999.

[185] F. Studt, A.-P. F. Sharafutdinov, C. F. Elkjaer, J. S. Hummelshoj, S. Dahl, I. Chorkendorff and J. K. Norskov, "Discovery of a Ni-Ga catalyst for carbon dioxide reduction to methanol," *Nat. Chem.,* vol. 6, pp. 320-324, 2014.

[186] J. Sloczynski, R. Grabowski, A. Kozlowska, P. Olszewsi, J. Stoch, J. Skrzypek and M. Lachowska, "Catalytic activity of the M/(3ZnO.ZrO2) system (M = Cu, Ag, Au) in the hydrogenation of CO2 to methanol," *Appl. Catal., A,* vol. 278, pp. 11-23, 2004.

[187] H. Sakurai and M. Haruta, "Synergism in methanol synthesis from carbon dioxide over gold catalysts supported on metal oxides," *Catal. Today,* vol. 29, pp. 361-365, 1996.

[188] T. Fujitani, M. Saito, Y. Kanai, T. Watanabe, J. Nakamura and T. Uchijima, "Development of an active Ga2O3 supported palladium catalyst for the synthesis of methanol from carbon dioxide and hydrogen," *Appl. Catal., A,* vol. 125, pp. L199-L202, 1995.

[189] C. Kim, J. S. Lee and D. L. Trimm, "The Preparation and Characterisation of Pd–ZnO Catalysts for Methanol Synthesis," *Top. Catal.,* vol. 22, no. 3, pp. 319-324, 2003.

[190] N. Iwasa, H. Suzuki, M. Terashita, M. Arai and N. Takezawa, "Methanol synthesis from CO2 under atmospheric pressure over supported Pd catalysts," *Catal. Lett.,* vol. 96, pp. 75-78, 2004.

[191] X. Liang, X. Dong, G. Lin and H. Zhang, "Carbon nanotube-supported Pd–ZnO catalyst for hydrogenation of CO2 to methanol," *Appl. Catal., B,* vol. 88, pp. 315-322, 2009.

[192] S. E. Collins, D. L. Chiavassa, A. L. Bonivardi and M. A. Baltanás, "Hydrogen Spillover in Ga2O3–Pd/SiO2 Catalysts for Methanol Synthesis from CO2/H2," *Catal. Lett.,* vol. 103, pp. 83-88, 2005.

[193] M. Saito, T. Fuhitani, M. Takeuchi and T. Watanabe, "Development of copper/zinc oxide-based multicomponent catalysts for methanol synthesis from carbon dioxide and hydrogen," *Applied Catalysis A: General,* vol. 138, pp. 311-318, 1996.

[194] J. Toyir, P. Ramirez de la Piscina, J. L. G. Fierro and N. Homs, "Highly effective conversion of CO2 to methanol over supported and promoted copper-based catalysts: influence of support and promoter," *Appl. Catal., B,* vol. 29, pp. 207-215, 2001.

[195] F. Arena, G. Mezzatesta, G. Zafarana, G. Trunfio, F. Frusteri and L. Spadaro, "Effects of oxide carriers on surface functionality and process performance of the Cu–ZnO system in the synthesis of methanol via CO2 hydrogenation," *J. Catal. ,* vol. 300, pp. 141-151, 2013.

[196] L. Ma, T. Tran and M. S. Wainwright, "Methanol Synthesis from CO2 Using Skeletal Copper Catalysts Containing Co-precipitated Cr2O3 and ZnO," *Top. Catal.,* vol. 22, no. 3, pp. 295-304, 2003.

[197] J. Xiao, D. Mao, X. Guo and J. Yu, "Methanol Synthesis from CO2 Hydrogenation over CuO–ZnO–TiO2 Catalysts: The Influence of TiO2 Content," *Energy Technol.,* vol. 3, pp. 32-39, 2015.

[198] M. Saito and K. Murata, "Development of high performance Cu/ZnO-based catalysts for methanol synthesis and the water-gas shift reaction," *Catal. Surv. Asia,* vol. 8, no. 4, pp. 285-294, 2004.

[199] X. An, J. Li, Y. Zuo, Q. Zhang, D. Wang and J. Wang, "A Cu/Zn/Al/Zr Fibrous Catalyst that is an Improved CO2 Hydrogenation to Methanol Catalyst," *Catal. Lett.,* vol. 118, no. 3, pp. 264-269, 2007.

[200] C. Li, X. Yuan and K. Fujimoto, "Development of highly stable catalyst for methanol synthesis from carbon dioxide," *Appl. Catal., A,* vol. 469, pp. 306-311, 2014.

[201] P. Gao, F. Li, N. Zhao, F. Xiao, W. Wei, L. Zhong and Y. Sun, "nfluence of modifier (Mn, La, Ce, Zr and Y) on the performance of Cu/Zn/Al catalysts via hydrotalcite-like precursors for CO2 hydrogenation to methanol," *Appl. Catal., A,* vol. 468, pp. 442-452, 2013.

[202] J. Graciani, K. Mudiyanselage, F. Xu, A. E. Baber, J. Evans, S. D. Senanayake, D. J. Stacchiola, P. Liu, J. Hrbek, J. Fernández Sanz and J. A. Rodriguez, "Highly active copper-ceria and copper-ceria-titania catalysts for methanol synthesis from CO2," *Science,* vol. 345, pp. 546-550, 2014.

[203] C. Yang, Z. Ma, N. Zhao, W. Wei, T. Hu and Y. Sun, "Methanol synthesis from CO2-rich syngas over a ZrO2 doped CuZnO catalyst," *Catal. Today,* vol. 115, pp. 222-227, 2006.

[204] I. A. Fisher and A. T. Bell, "In-Situ Infrared Study of Methanol Synthesis from H2/CO2 over Cu/SiO2 and Cu/ZrO2/SiO2," *J. Catal.,* vol. 172, pp. 222-237, 1997.

[205] J. Sloczynski, R. Grabowski, P. Olszewski, A. Kozlowska, J. Stoch, M. Lachowska and J. Skrzypek, "Effect of metal oxide additives on the activity and stability of Cu/ZnO/ZrO2 catalysts in the synthesis of methanol from CO2 and H2," *Appl. Catal., A,* vol. 310, pp. 127-137, 2006.

[206] R. Ladera, F. J. Pérez-Alonso, J. M. González-Carballo, M. Ojeda, S. Rojas and J. L. G. Fierro, "Catalytic valorization of CO2via methanol synthesis with Ga-promoted Cu–ZnO–ZrO2 catalysts," *Applied Catalysis B: Environmental,* Vols. 142-143, pp. 241-248, 2013.

[207] M. Madej-Lachowska, A. Kasprzyk-Mrzyk, H. Moroz, A. I. Lachowski and H. Wyzgol, "Methanol Synthesis from Carbon Dioxide and Hydrogen over CuO/ZnO/ZrO2 promoted catalysts," *Chemik,* vol. 68, pp. 61-18, 2014.

[208] J. Sloczynski, R. Grabowski, A. Kozlowska, P. Olszewski, M. Lachowska, J. Skrzypek and J. Stoch, "Effect of Mg and Mn oxide additions on structural and adsorptive properties of Cu/ZnO/ZrO2 catalysts for the methanol synthesis from CO2," *Appl. Catal., A,* vol. 249, pp. 129-138, 2003.

[209] M. Lachowska and J. Skrzypek, "Methanol synthesis from carbon dioxide and hydrogen over Mn-promoted copper/zinc/zirconia catalysts," *React. Kinet. Catal. Lett.,* vol. 83, pp. 269-273, 2004.

[210] S. Kiatphuengporna, M. Chareonpanicha and J. Limtrakulb, "Effect of unimodal and bimodal MCM-41 mesoporous silica supports on activity of Fe–Cu catalysts for CO2 hydrogenation," *Chem. Eng. J.,* vol. 240, pp. 527-533, 2014.

[211] L. Jia, J. Gao, W. Fang and Q. Li, "Carbon dioxide hydrogenation to methanol over the pre-reduced LaCr0.5Cu0.5O3 catalyst," *Catal. Commun.,* vol. 10, no. 15, pp. 2000-2003, 2009.

[212] H. Lei, R. Nie, G. Wu and Z. Hou, "Hydrogenation of CO2 to CH3OH over Cu/ZnO catalysts with different ZnO morphology," *Fuel,* vol. 154, pp. 161-166, 2015.

[213] X. Liang, J. Xie and Z. Liu, "A Novel Pd-decorated Carbon Nanotubes-promoted Pd-ZnO Catalyst for CO2 Hydrogenation to Methanol," *Catal. Lett.,* vol. 145, no. 5, pp. 1138-1147, 2015.

[214] J. Xiao, D. Mao, X. Guo and J. Yu, "Effect of TiO2, ZrO2, and TiO2–ZrO2 on the performance of CuO–ZnO catalyst for CO2 hydrogenation to methanol," *Appl. Surf. Sci.,* vol. 338, pp. 146-153, 2015.

[215] G. Bonura, M. Cordaro, C. Cannilla, F. Arena and F. Frusteri, "The changing nature of the active site of Cu-Zn-Zr catalysts for the CO2 hydrogenation reaction to methanol," *Appl. Catal., B,* Vols. 152-153, pp. 152-161, 2014.

[216] J. Toyir, P. Ramírez de la Piscina, J. L. G. Fierro and N. Homs, "Catalytic performance for CO2 conversion to methanol of gallium-promoted copper-based catalysts: influence of metallic precursors," *Appl. Catal., B,* vol. 34, no. 4, pp. 255-266, 2001.

[217] W. Cai, P. Ramirez de la Piscina, J. Toyir and N. Homs, "CO2 hydrogenation to methanol over CuZnGa catalysts prepared using microwave-assisted methods," *Catal. Today,* vol. 242, pp. 193-199, 2015.

[218] H. Ahouari, A. Soualah, A. Le Valant, L. Pinard, P. Magnoux and Y. Pouilloux, "Methanol synthesis from CO2 hydrogenation over copper based catalysts," *React. Kinet., Mech. Catal.,* vol. 110, no. 1, pp. 131-145, 2013.

[219] I. Melián-Cabrera, M. López Granados and J. L. G. Fierro, "Effect of Pd on Cu-Zn Catalysts for the Hydrogenation of CO2 to Methanol: Stabilization of Cu Metal Against CO2 Oxidation," *Catal. Lett.,* vol. 79, no. 1, pp. 165-170, 2002.

[220] G. Wang, L. Chen, Y. Sun, J. Wu, M. Fu and D. Ye, "Carbon dioxide hydrogenation to methanol over Cu/ZrO 2/CNTs: effect of carbon surface chemistry," *RSC Adv.,* vol. 5, pp. 45320-45330, 2015.

[221] X. Liu, G. Q. Lu and Y. Z, "Nanocrystalline zirconia as catalyst support in methanol synthesis," *Appl. Catal., A,* vol. 279, pp. 241-245, 2005.

[222] J. Qu, X. Zhou, F. Xu, X. Gong and S. C. E. Tsang, "Shape Effect of Pd-Promoted Ga2O3 Nanocatalysts for Methanol Synthesis by CO2 Hydrogenation," *J. Phys. Chem.* , vol. 118, pp. 24452-24466, 2014.

[223] H. Kong, H. Li, G. Lin and H. Zhang, "Pd-Decorated CNT-Promoted Pd-Ga2O3 Catalyst for Hydrogenation of CO2 to Methanol," *Catal. Lett.,* vol. 141, pp. 886-694, 2011.

[224] H. Zhan, F. Li, C. Xin, N. Zhao, F. Xiao, W. Wei and Y. Sun, "Performance of the La–Mn–Zn–Cu–O Based Perovskite Precursors for Methanol Synthesis from CO2 Hydrogenation," *Catal. Lett.,* vol. 145, no. 5, pp. 1177-1185, 2015.

[225] J. Tremblay, "CO2 As Feedstock," *Chem. Eng. News,* vol. 86, no. 35, p. 13, 2008.

[226] O. Joo, K. Jung, I. Moon, A. Y. Rozovskii, G. I. Lin, S. : Han and S. Uhm, "Carbon Dioxide Hydrogenation To Form Methanol via a Reverse-Water-Gas-Shift Reaction (the CAMERE Process)," *Ind. Eng. Chem. Res.,* vol. 38, pp. 1808-1812, 1999.

[227] Chemicals-technology.com, "George Olah CO2 to Renewable Methanol Plant, Reykjanes, Iceland," 2016. [Online]. Available: http://www.chemicals-technology.com/projects/george-olah-renewable-methanol-plant-iceland/. [Accessed 1 March 2016].

[228] N. Tsubaki, M. Ito and K. Fujimoto, "A New Method of Low-Temperature Methanol Synthesis," *J. Catal.,* vol. 197, pp. 224-227, 2001.

[229] R. S. Sapienza, W. A. Slegeir, T. E. O'Hare and D. Mahajan, "Low temperature catalysts for methanol production". United States of America Patent US4614749A, 30 September 1986.

[230] D. Mahajan, R. S. Sapienza, W. A. Slegeir and T. E. O'Hare, "Homogeneous catalyst formulations for methanol production". United States of America Patent US4935395A, 19 June 1990.

[231] Z. Liu, J. W. Tierney, Y. T. Shah and I. Wender, "Methanol synthesis via methylformate in a slurry reactor," *Fuel Process. Technol.,* vol. 23, no. 2, pp. 149-167, 1989.

[232] V. M. Palekar, "Alkali compounds and copper chromite as low-temperature slurry phase methanol catalysts," *Appl. Catal., A,* vol. 103, no. 1, pp. 105-122, 1993.

[233] Y. Zhao, L. Bai, Y. Hu, B. Zhong and S. Peng, "Catalytic performance of CuCr/CH3ONa used for low temperature methanol synthesis in slurry phase," *J. Nat. Gas Chem.,* vol. 8, no. 3, pp. 181-187, 1999.

[234] W. Chu, T. Zhang, C. He and Y. Wu, "Low-temperature methanol synthesis (LTMS) in liquid phase on novel copper-based catalysts," *Catal. Lett.,* vol. 79, pp. 129-132, 2002.

[235] M. Marchionna, L. Basini, A. Aragno, M. Lami and F. Ancillotti, "Mechanistic studies on the homogeneous nickel-catalyzed low temperature methanol synthesis," *J. Mol. Catal.,* vol. 75, no. 2, pp. 147-151, 1992.

[236] E. S. Lee and K. Aika, "Low-temperature methanol synthesis in liquid-phase with a Raney Nickel–alkoxide system: effect of Raney Nickel pretreatment and reaction conditions," *J. Mol. Catal. A: Chem.,* vol. 141, pp. 241-248, 1999.

[237] S. Ohyama, "Low-temperature methanol synthesis in catalytic systems composed of nickel compounds and alkali alkoxides in liquid phases," *Appl. Catal., A,* vol. 180, pp. 217-225, 1999.

[238] X. Liu, Y. Wu, S. Luo, Y. Yang, Z. Jia, S. Li, W. Chen and Z. Yu, "Concurrent synthesis of methanol and methyl formate catalyzed by copper-based catalysts: II. Influences of solvents and H2/CO mole ratios," *J. Nat. Gas Chem.,* vol. 8, no. 3, pp. 203-210, 1999.

[239] V. M. Palekar, H. Jung, J. W. Tierney and I. Wender, "Slurry phase synthesis of methanol with a potassium methoxide/copper chromite catalytic system," *Appl. Catal., A,* vol. 102, no. 1, pp. 13-34, 1993.

[240] W. Linghu, Z. Liu, Z. Zhu, J. Yang and B. Zhong, "Methanol synthesis in an integrated two-stage reactor," *Chem. Eng. Sci.,* vol. 54, pp. 3671-3675, 1999.

[241] K. Zhang, H. Song, D. Sun, S. Li, X. Yang, Y. Zhao and Z. W. Y. Huang, "Low-temperature methanol synthesis in a circulating slurry bubble reactor," *Fuel,* vol. 82, pp. 233-239, 2003.

[242] W. R. Brown, D. P. Drown and F. S. Frenduto, "Commercial-scale Demonstration of the Liquid Phase Methanol (LPMEOH) Process. Public Design Report.," 2000.

[243] E. C. Heydorn, B. W. Diamond and R. D. Lilly, "Commercial-scale Demonstration of the Liquid Phase Methanol (LPMEOH) Process. Final report.," 2003.

[244] U.S. Department of Energy, "Commercial-Scale Demonstration of the Liquid Phase Methanol (LPMEOH) Process. A DOE Assesment.," U.S. Department of Energy, National Energy Technology Laboratory, 2003.

[245] C. A. Huff and M. S. Sanford, "Cascade Catalysis for the Homogeneous Hydrogenation of CO2 to Methanol," *J. Am. Chem. Soc.,* vol. 133, pp. 18122-18125, 2011.

[246] S. Wesselbaum, T. vom Stein, J. Klankermayer and W. Leitner, "Hydrogenation of Carbon Dioxide to Methanol by Using a Homogeneous Ruthenium–Phosphine Catalyst," *Angew. Chem.,* vol. 124, pp. 7617-7620, 2012.

[247] Y. Chen, S. Choi and L. T. Thompson, "Low-Temperature CO2 Hydrogenation to Liquid Products via a Heterogeneous Cascade Catalytic System," *ACS Catal.,* vol. 5, pp. 1717-1725, 2015.

[248] B. Xu, R. Yang, F. Meng, P. Reubroycharoen, T. Vitidsant, Y. Zhang, Y. Yoneyama and N. Tsubaki, "A New Method of Low Temperature Methanol Synthesis," *Catal. Surv. Asia,* vol. 13, pp. 147-163, 2009.

[249] L. Fan, Y. Sakaiya and K. Fujimoto, "Low-temperature methanol synthesis from carbon dioxide and hydrogen via formic ester," *Appl. Catal., A,* vol. 180, pp. L11-L13, 1999.

[250] J. Zeng, K. Fujimoto and N. Tsubaki, "A New Low-Temperature Synthesis Route of Methanol: Catalytic Effect of the Alcoholic Solvent," *Energy Fuels,* vol. 16, pp. 83-86, 2002.

[251] P. Reubroycharoen, T. Yamagami, T. Vitidsant, Y. Yoneyama, M. Ito and N. Tsubaki, "Continuous Low-Temperature Methanol Synthesis from Syngas Using Alcohol Promoters," *Energy Fuels,* vol. 17, pp. 817-823, 2003.

[252] R. Yang, X. Yu, Y. Zhang, W. Li and N. Tsubaki, "A new method of low-temperature methanol synthesis on Cu/ZnO/Al2O3 catalysts from CO/CO2/H2," *Fuel,* no. 87, pp. 443-450, 2008.

[253] J. Bao, Z. Liu, Y. Zhang and N. Tsubaki, "Preparation of mesoporous Cu/ZnO catalyst and its application in low-temperature methanol synthesis," *Catal. Commun.,* vol. 9, pp. 913-918, 2008.

[254] T. Zhao, Y. Yoneyama, K. Fujimoto, N. Yamane, K. Fujimoto and N. Tsubaki, "Promotional Effect of Potassium Salt in Low-temperature Formate and Methanol Synthesis from CO/CO2/H2 on Copper Catalyst," *Chem. Lett.,* vol. 36, pp. 734-735, 2007.

[255] B. Hu and K. Fujimoto, "High-performance Cu/MgO–Na catalyst for methanol synthesis via ethyl formate," *Appl. Catal., A,* vol. 346, pp. 174-178, 2008.

[256] T. Zhao, K. Zhang, X. Chen, Q. Ma and N. Tsubaki, "A novel low-temperature methanol synthesis method from CO/H2/CO2 based on the synergistic effect between solid catalyst and homogeneous catalyst," *Catal. Today,* vol. 149, pp. 98-104, 2010.

[257] B. Hu, Y. Yamaguchi and K. Fujimoto, "Low temperature methanol synthesis in alcohol solvent over copper-based catalyst," *Catal. Commun.,* vol. 10, pp. 1620-1624, 2009.

[258] B. Hu and K. Fujimoto, "Promoting behaviors of alkali compounds in low temperature methanol synthesis over copper-based catalyst," *Appl. Catal., B,* vol. 95, pp. 208-216, 2010.

[259] R. Yang, Y. Fu, Y. Zhang and N. Tsubaki, "In situ DRIFT study of low-temperature methanol synthesis mechanism on Cu/ZnO catalysts from CO2-containing syngas using ethanol promoter," *J. Catal.,* vol. 228, no. 1, pp. 23-35, 2004.

[260] R. Yang, Y. Zhang and N. Tsubaki, "Dual catalysis mechanism of alcohol solvent and Cu catalyst for a new methanol synthesis method," *Catal. Commun.,* vol. 6, no. 4, pp. 275-279, 2005.

[261] R. Yang, Y. Zhang and N. Tsubaki, "Rideal-type reaction of formate species with alcohol: A key step in new low-temperature methanol synthesis method," *Catal. Commun.,* vol. 8, pp. 1829-1833, 2007.

[262] Y. Zhang, R. Yang and N. Tsubaki, "A new low-temperature methanol synthesis method: Mechanistic and kinetics study of catalytic process," *Catal. Today,* vol. 132, pp. 93-100, 2008.

[263] S. Cavallaro and S. Freni, "Ethanol Steam Reforming in a Molten Carbonate Fuel Cell. A preliminary kinetic investigation," *Int. J. Hydrogen Energy,* vol. 21, no. 6, pp. 465-469, 1995.

[264] J. Keuler, L. Lorenzen and S. Miachon, "The dehydrogenation of 2-butanol over copper-based catalysts: optimising catalyst composition and determining kinetic parameters," *Appl. Catal., A,* vol. 218, pp. 171-180, 2001.

[265] S. R. Segal, K. A. Carrado, C. L. Marshall and K. B. Anderson, "Catalytic decomposition of alcohols, including ethanol, for in situ H2 generation in a fuel stream using a layered double hydroxide-derived catalyst," *Appl. Catal., A,* vol. 248, pp. 33-45, 2003.

[266] T. Shinoki, K. Ota, Y. Sono, Y. Okuhigashi, J. Funaki and K. Hirata, "Hydrogen Production Using an Ethanol-Steam-Reforming Reactor with Cu/ZnO/Al2O3 and Ru/Al2O3 Catalysts," *Int. J. Energy Syst.,* vol. 5, no. 3, pp. 218-228, 2011.

[267] B. Lorenzut, T. Montini, L. De Rogatis, P. Canton, A. Benedetti and P. Fornasiero, "Hydrogen production through alcohol steam reforming on Cu/ZnO-based catalysts," *Appl. Catal., B,* vol. 101, pp. 397-408, 2011.

[268] S. Mostafa, J. R. Croy, H. Heinrich and B. Roldan Cuenya, "Catalytic decomposition of alcohols over size-selected Pt nanoparticles supported on ZrO2: A study of activity, selectivity, and stability," *Appl. Catal., A,* vol. 366, pp. 353-362, 2009.

[269] J. V. H. d'Angelo and A. Z. Francesconi, "Gas-Liquid Solubility of Hydrogen in n-Alcohols (1 <= n <= 4) at Pressures from 3.6 MPa to 10 MPa and Temperatures from 298.15 K to 525.15 K," *J. Chem. Eng. Data,* vol. 46, pp. 671-674, 2001.

[270] X. Gui, Z. Tang and W. Fei, "Solubility of CO2 in Alcohols, Glycols, Ethers, and Ketones at High Pressures from (288.15 to 318.15) K," *J. Chem. Eng. Data,* vol. 56, pp. 2420-2429, 2011.

[271] J. C. G. Hill, "Basic Concepts in Chemical Kinetics - Determination of the Reaction Rate Expression," in *An Introduction to Chemical Engineering Kinetics & Reactor Design*, John Wiley & Sons, Inc., 1977, pp. 24-76.

[272] Lappeenranta University of Technology, "REFLEX – Recycling carbon in a flexible competitive energy system," [Online]. Available: http://www.lut.fi/web/en/research/platforms/reflex. [Accessed 2 August 2016].

[273] J. Koponen and A. Kosonen, "Laboratory Setup for Hydrogen Production at LUT," [Online]. Available: http://www.neocarbonenergy.fi/wp-content/uploads/2016/02/14_Koponen-1.pdf. [Accessed 2 August 2016].

Appendix I: Calculation examples

Vapor pressure of the alcohols

The vapor pressures of the alcohols were calculated by the Antoine equation:

$$\log_{10} p = A - \frac{B}{C + T}$$

where p is the vapor pressure, T the temperature and A,B and C compound specific constants. For ethanol, the following values were used for the constants: $A = 7{,}68117$ $B = 1332{,}04$ and $C = 199{,}2$ [1]. These values apply for temperatures in centigrade. E.g. at 150 °C, the calculated vapor pressure is

$$p = 10^{(7{,}68117 - \left(\frac{1332{,}04}{199{,}2+150}\right))} = 9{,}81 \text{ bar}$$

For 2-butanol, the values used for the constants are $A = 4{,}19827$; $B = 1094{,}254$ and $C = -111{,}603$ [2]. These values are valid for absolute temperatures. At 150 °C, or 423.15 K, the calculated vapor pressure is

$$p = 10^{(4{,}19827 - \left(\frac{1094{,}254}{-111{,}603+423{,}15}\right))} = 4{,}85 \text{ bar}$$

Figures Figure A-37 and Figure A-38 show the calculated vapor pressures of ethanol and 2-butanol at the temperature range of 150 to 200 °C.

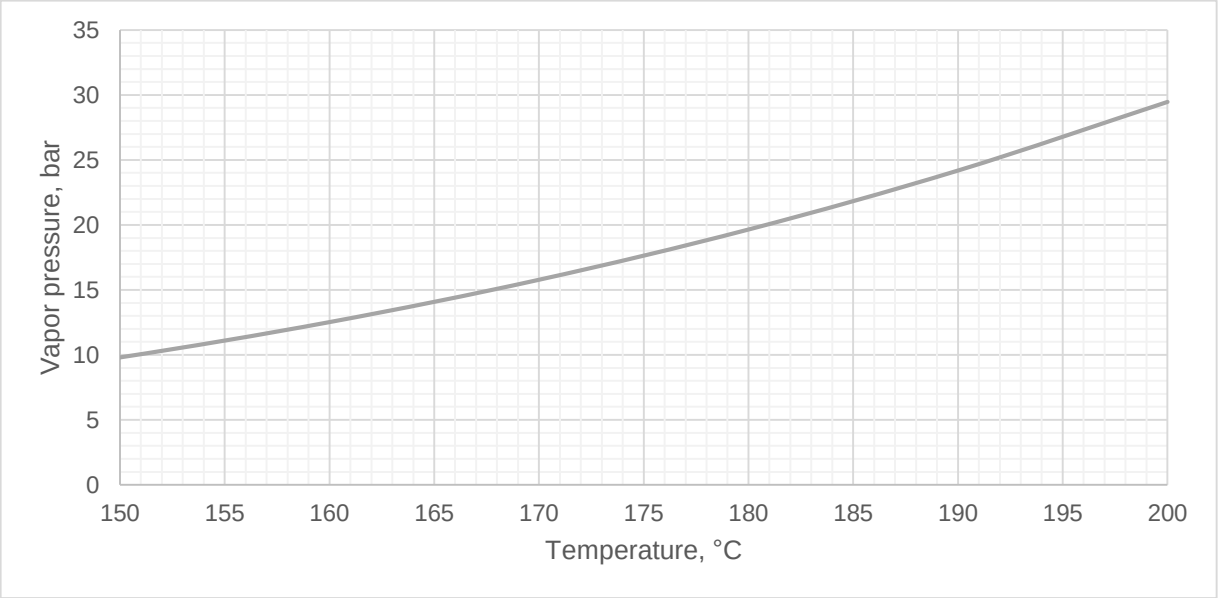

Figure A-37. Vapor pressure of ethanol calculated with the Antoine equation.

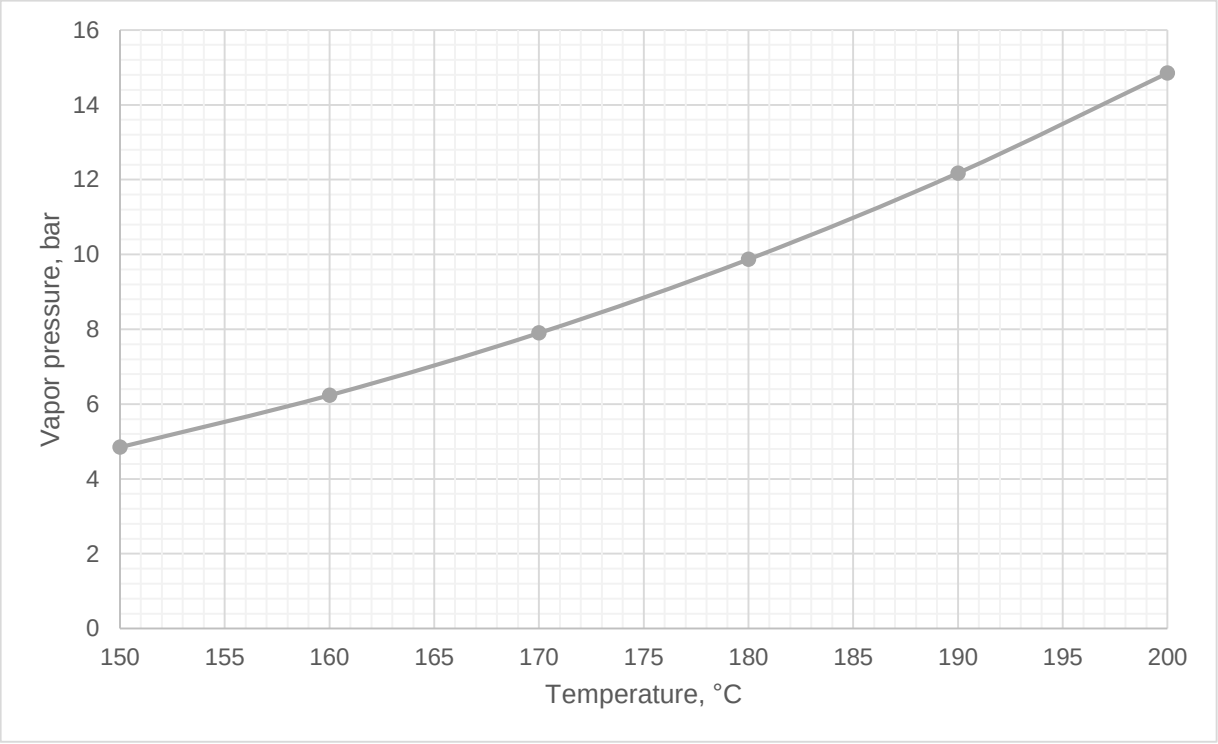

Figure A-38. Vapor pressure of ethanol calculated with the Antoine equation.

Catalyst and volume specific productivity of methanol

The specific productivity per catalyst mass measures the mass of methanol (g) produced per mass of catalyst (kg) per hour.

$$\frac{m_{MeOH}}{m_{catalyst} \cdot t} = \frac{\frac{c_{MeOH}}{1000} \cdot V_{solvent} \cdot \rho_{solvent}}{m_{catalyst} \cdot t}$$

m_{MeOH}	Mass of methanol produced, g
m_{catalyst}	Mass of catalyst used, kg
c_{MeOH}	Concentration of methanol, ppm (w/w) / mg/kg
V_{solvent}	Volume of the solvent, m^3
ρ_{solvent}	Density of the solvent, kg/m^3
t	Time, h

The batch experiment with 2-butanol and 10 g of catalyst at 180 °C and 60 bar of total pressure will be used as example. In this experiment, the concentration of methanol after 6 hours of reaction was 7891.5 ppm (w/w). A volume of 200 ml of 2-butanol was used. The density of 2-butanol is 806 kg/m^3 at room temperature.

$$\frac{m_{\mathrm{MeOH}}}{m_{\mathrm{catalyst}} \cdot t} = \frac{\frac{7891.5\ \mathrm{mg/kg}}{1000\ \mathrm{mg/g}} \cdot 200 \cdot 10^{-6}\ \mathrm{m^3} \cdot 806\ \mathrm{kg/m^3}}{0.01\ \mathrm{kg} \cdot 6\ \mathrm{h}} = 21.2\ \frac{\mathrm{g}}{\mathrm{kg} \cdot \mathrm{h}}$$

The specific productivity per volume measures the mass of methanol produced per volume of solvent per hour.

$$\frac{m_{\mathrm{MeOH}}}{V_{\mathrm{solvent}} \cdot t} = \frac{\frac{c_{\mathrm{MeOH}}}{1000} \cdot V_{\mathrm{solvent}} \cdot \rho_{\mathrm{solvent}}}{V_{\mathrm{solvent}} \cdot t}$$

Using the same experiment as example:

$$\frac{m_{\mathrm{MeOH}}}{V_{\mathrm{solvent}} \cdot t} = \frac{\frac{7891.5\ \mathrm{mg/kg}}{1000\ \mathrm{mg/g}} \cdot 806\ \mathrm{kg/m^3}}{6\ \mathrm{h}} = 1060.1 \frac{\mathrm{g}}{\mathrm{m^3 \cdot h}} = 1.06 \frac{\mathrm{g}}{\mathrm{l \cdot h}}$$

Conversion of feed gas

The batch experiment with 2-butanol and 10 g of catalyst at 180 °C and 60 bar of total pressure is used as example. At the reaction temperature, the calculated vapor pressure of 2-butanol is 9.9 bar. Thus, the partial pressure of feed gas (CO_2+H_2) is 50.1 bar at the start of reaction time.

At the end of the first 2 hour reaction time interval, the total pressure was 53.4 bar (see the pressure curve in Figure A-52, Appendix III: Pressure and composition data from the batch experiments). After subtraction of the vapor pressure of 9.9 bar, the partial pressure of feed gas is 43.5 bar at this stage. The conversion during this time interval is then calculated based on the relative decrease in partial pressure:

$$X = \frac{50.1\ \mathrm{bar} - 43.5\ \mathrm{bar}}{50.1\ \mathrm{bar}} \cdot 100\% = 13.2\%$$

Similarly, a conversion of 8.8% is calculated for the reaction time between 2 and 4 hours, and a conversion of 9.2% for the reaction time between 4 to 6 hours. Taking the average of these three values, an average degree of conversion of 10.4% is obtained for this experiment.

Kinetic model of methanol synthesis reaction

The concentration of methanol in the 30 bar partial pressure experiment in 2-butanol was 1623.1 ppm (w/w) after 2 hours of reaction time (Appendix IV: Composition data from the

semibatch experiments, Table A-XXX). As no methanol was present at 0 hours, the mass of the methanol formed during the first 2 hours was:

$$m_{\mathrm{MeOH}} = c_{\mathrm{MeOH}} \cdot V_{\mathrm{solvent}} \cdot \rho_{\mathrm{solvent}} = \frac{1623.1\,\frac{\mathrm{mg}}{\mathrm{kg}}}{1000\,\frac{\mathrm{mg}}{\mathrm{g}}} \cdot 200 \cdot 10^{-6}\ \mathrm{m^3} \cdot 806\,\frac{\mathrm{kg}}{\mathrm{m^3}} = 0.2616\ \mathrm{g}$$

The molar mass of methanol is 32.04 g/mol. Thus, 0.0082 mol of methanol was formed during this reaction time interval, corresponding to an average rate of 0.0041 mol/h, or $1.134 \cdot 10^{-6}$ mol/s of methanol formed. Similarly, an average reaction rate of $2.980 \cdot 10^{-6}$ mol/s was calculated for the 50 bar partial pressure experiment (Appendix IV: Composition data from the semibatch experimentsTable A-XXXII). The order of reaction was then calculated using equation (10):

$$m = \frac{\log\left(\frac{r_1}{r_2}\right)}{\log\left(\frac{p_1}{p_2}\right)} = \frac{\log\left(\frac{1.134\ \cdot\ 10 - 6\ \mathrm{mol/s}}{2.980\ \cdot\ 10 - 6\ \mathrm{mol/s}}\right)}{\log\left(\frac{30\ \mathrm{bar}}{50\ \mathrm{bar}}\right)} = 1.891$$

The rate constant was calculated by substituting the values of r and m into equation (8). Using $r_1$and p_1:

$$k = \frac{r_1}{p_1^m} = \frac{1.134\ \cdot\ 10^{-6}\ \mathrm{mol/s}}{(30\ \mathrm{bar})^{1.891}} = 1.825\ \mathrm{bar}^{-1.89}\ \mathrm{mol/s}$$

Using $r_2$and p_2 instead gives the same value. The temperature dependence was then evaluated based on equation (11). The values presented in Table A-XIV were calculated in order to generate the graph based on this equation.

$$\frac{d\ln k}{d\left(\frac{1}{T}\right)} = -\frac{E_a}{R} \qquad (11)$$

Table A-XIV. The values calculated for creating the graph based on equation (11), used for the determination of the activation energy. The resulting graph is shown in Figure A-39.

T, °C	T, K	r, mol/s	p, bar	k, $bar^{-1.89}$ mol/s	1/T, K^{-1}	ln k
160	433.15	$8.51816 \cdot 10^{-7}$	40	$7.9488 \cdot 10^{-10}$	0.002309	-20.9528
170	443.15	$1.24278 \cdot 10^{-6}$	40	$1.15971 \cdot 10^{-9}$	0.002257	-20.5751
190	463.15	$3.05279 \cdot 10^{-6}$	40	$2.84874 \cdot 10^{-9}$	0.002159	-19.6764
200	473.15	$3.4872 \cdot 10^{-6}$	40	$3.25411 \cdot 10^{-9}$	0.002113	-19.5433

Figure A-39 shows the resulting graph. The average reaction rates were calculated for the 0-2 hours of reaction time as described above. The concentration data for the experiments can be found in Tables Table A-XXXVI to Table A-XXXIX in Appendix IV: Composition data from the semibatch experimentsThe slope of the fitted curve gives $-\frac{E_a}{R}$, according to equation (11). Using the value of $R = 8.314 \frac{\mathrm{J}}{\mathrm{mol \cdot K}}$, we get the activation energy of $E_a = 63470.74 \frac{\mathrm{J}}{\mathrm{mol}} \approx 63.5\ \mathrm{kJ/mol}$.

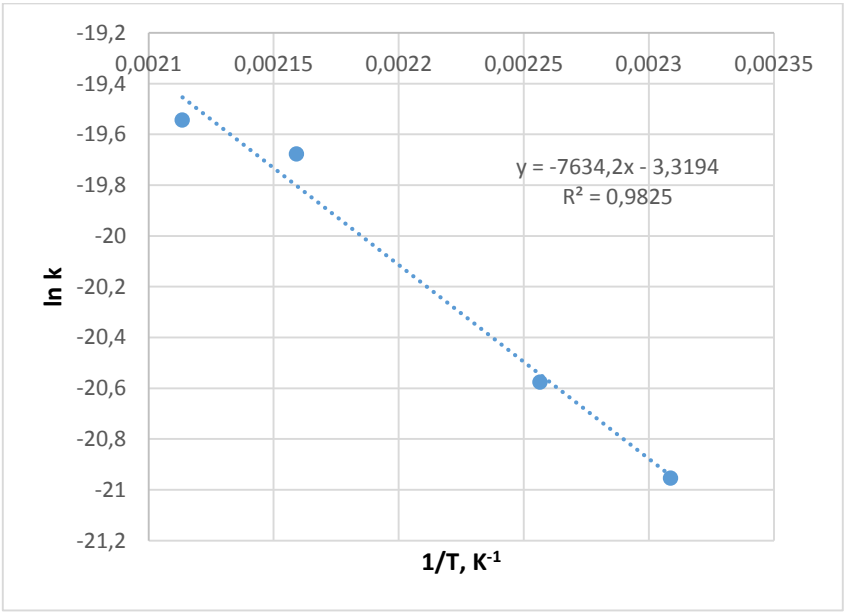

Figure A-39. The graph based on equation (11), used for the determination of the activation energy.

The pre-exponential factor was then calculated by substituting the activation energy and the values of k corresponding to each temperature (see Table A-XIV) into the Arrhenius equation (9). For example, using the data from the 160 °C experiment:

$$A = \frac{k}{e^{-E_a/RT}} = \frac{7.9488 \cdot 10^{-10}\ \mathrm{bar}^{-1.89}\ \mathrm{mol/s}}{\mathrm{e}^{-\frac{63470.74\ \mathrm{J/mol}}{8.314\frac{\mathrm{J}}{\mathrm{molK}} \cdot 433.15\ \mathrm{K}}}} = 0.0359\ \mathrm{bar}^{-1.89}\ \mathrm{mol/s}$$

Using the data from the other experiments, A gets the values 0.0352 (170 °C), 0.0410 (190 °C) and 0.0331 (200 °C). Taking the average of the four values, we get $A = 0.0363\ \mathrm{bar}^{-1.89}\ \mathrm{mol/s}$

Sizing of reactor

The maximum catalyst specific productivity in the experiments was found to be 40.2 g/(kg·h). We find that 23.8 kg of the catalyst is required to maintain the methanol production rate of 0.95 kg/h:

$$m_{\mathrm{cat}} = \frac{950\ \mathrm{g/h}}{40\ \mathrm{g/kgh}} = 23.75\ \mathrm{kg}$$

A mass fraction of 20% is assumed for the catalyst in the slurry. Thus, the total mass of the slurry is:

$$m_{\mathrm{sl}} = 23.75\ \mathrm{kg} \cdot \left(\frac{1}{0.2}\right) = 118.75\ \mathrm{kg}$$

The mass of 2-butanol is then:

$$m_{\mathrm{alc}} = (1 - 0.2) \cdot 118.75\ \mathrm{kg} = 95\ \mathrm{kg}$$

As the density of 2-butanol is 806 kg/m^3 (NTP), the volume of the liquid-phase is:

$$V_l = \frac{95\ \mathrm{kg}}{806\ \mathrm{kg/m^3}} = 0.118\ \mathrm{m^3} = 118\ \mathrm{l}$$

The total reactor volume is assumed to be double the liquid volume, or 236 l. The height of the cylindrical reactor is identical to the diameter. Thus, the diameter of the reactor is 0.67 m:

$$A_r = \pi \cdot \left(\frac{0.67\ \mathrm{m}}{2}\right)^2 \cdot 0.67\ \mathrm{m} = 0.236\ \mathrm{m^3}$$

Appendix II: Analysis of liquid samples by GC

The chromatogram shown in Figure A-40 was obtained for the mixed solution containing equal parts of methanol, ethanol, 2-butanol, 2-butanone and water. The retention times of each of the compounds were used for identification of the compounds in the actual samples.

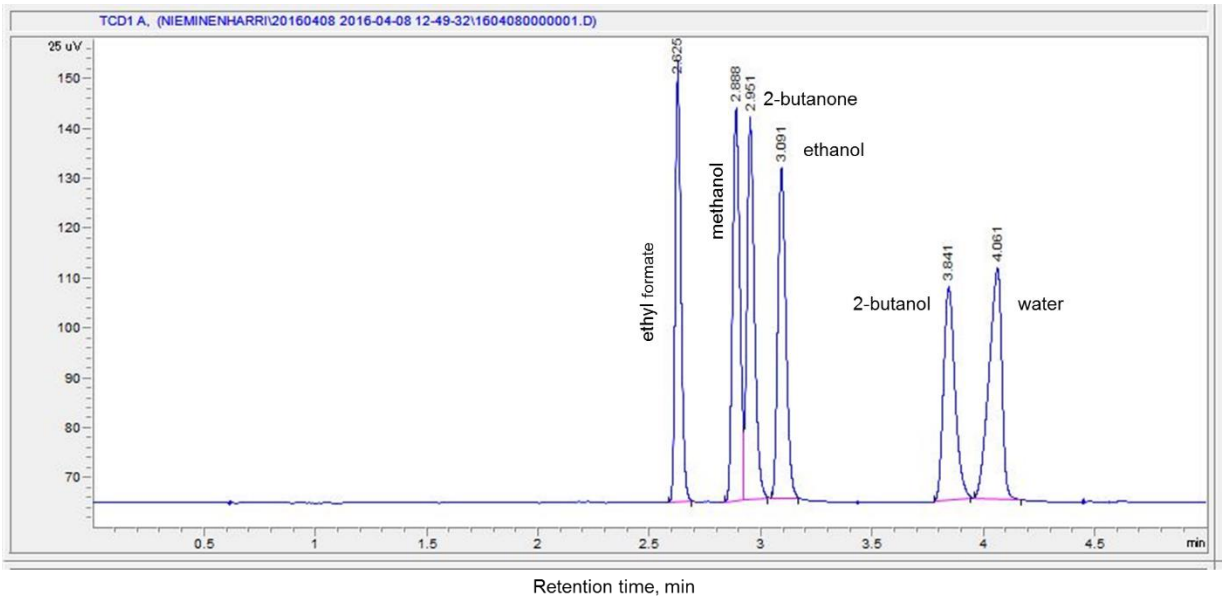

Figure A-40. Chromatogram of a mixed solution containing equal parts of methanol, ethanol, 2-butanol, 2-butanone and water.

The retention time of acetaldehyde was obtained by analyzing a mixture of acetaldehyde and ethanol. The chromatogram is shown in Figure A-41.

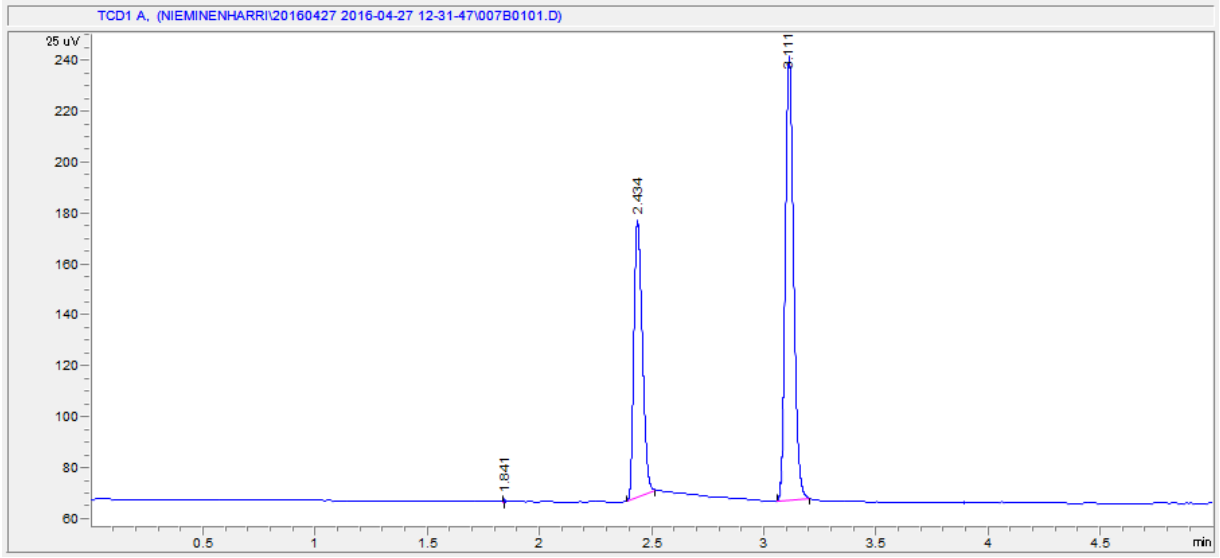

Figure A-41. Chromatogram of a mixture of acetaldehyde in ethanol.

The retention time of each compound is listed in Table A-XV.

Table A-XV. Retention times of the analyzed compounds in mixed solutions.

Compound	Retention time, min
Acetaldehyde	2,434
Ethyl formate	2,625
Methanol	2,888
2-butanone	2,951
Ethanol	3,091
2-butanol	3,841
Water	4,061

Calibration curves were prepared using standard solutions prepared in the relevant concentration range for each compound, i.e. at high concentrations for the solvents ethanol and 2-butanol and small concentrations for the expected reaction products. No calibration curve was prepared for acetaldehyde due to difficulties in preparing accurate standard solutions. Instead, the calibration curve of ethyl formate was (arbitrarily) used to give rough estimates of the concentration of acetaldehyde in the samples. The calibration curves with equations are shown in Figure A-42.

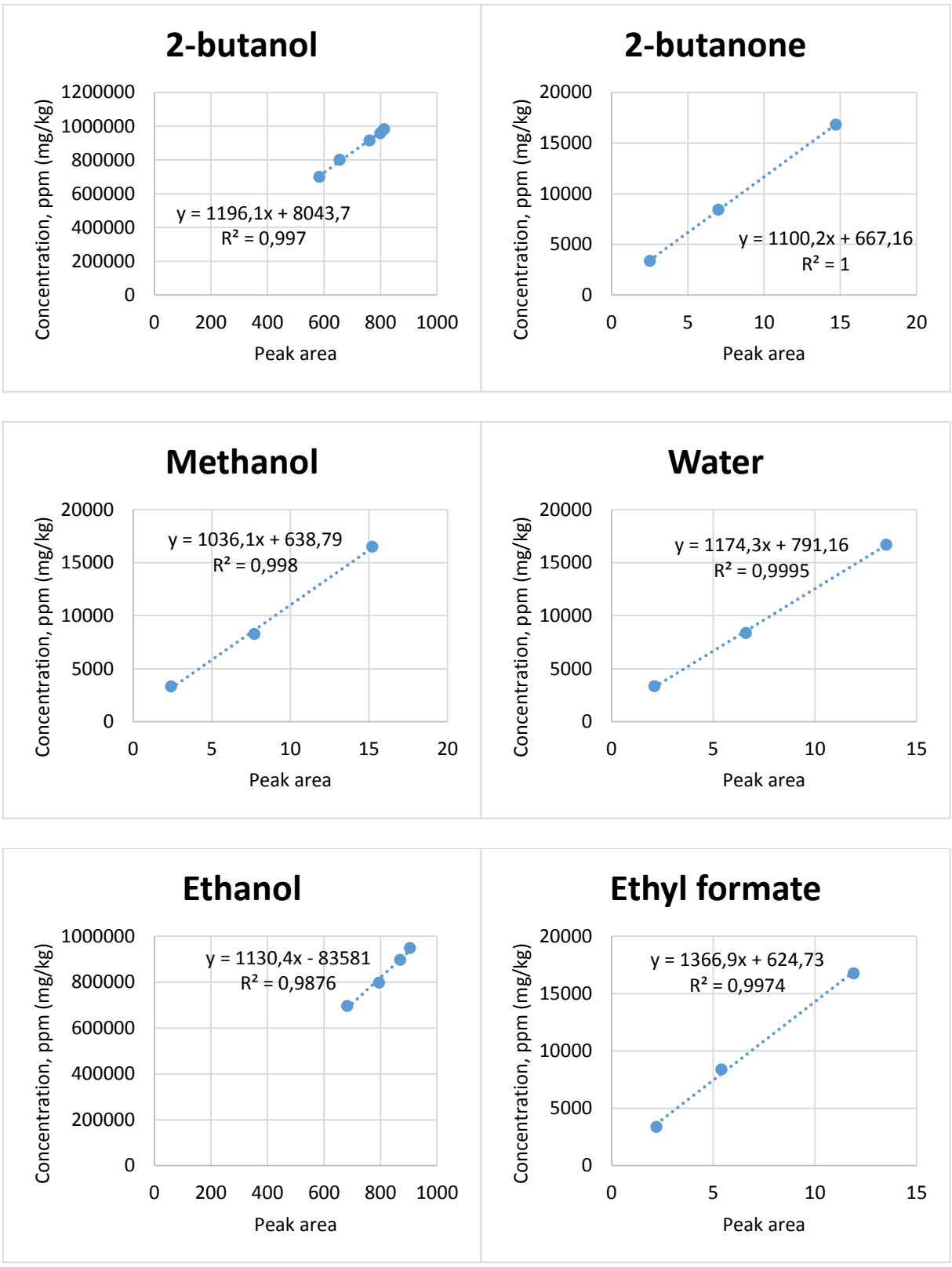

Figure A-42. GC calibration curves and equations for the analyzed compounds.

The accuracy of the calibration equations was tested by using the equations to calculate the concentrations in the same standard solutions that the equations were first prepared with. For example, Table A-XVI compares the measured (weighed) concentrations of methanol in three standard solutions to the concentrations calculated from the GC peak areas obtained for the same solutions, using the calibration equation for methanol. Tables Table A-XVII, Table A-XVIII andTable A-XIX show similar comparisons for 2-butanone, water and ethyl formate.

The deviation between the measured and calculated concentrations is the most significant for methanol and ethyl formate, at the low end of the calibration concentration range. Resultantly, systematic error caused by the inaccuracy of the calibration equations are expected for these compounds. However, the error caused by the calibration equations is judged to be small compared to the various potential sources of error in the experimental and analysis procedure.

Table A-XVI. The comparison of the weighed concentration of methanol and the methanol concentration calculated with the calibration equation, in three standard solutions.

Standard solution	ppm, weighed	ppm, calculated	Deviation
1	3324.7	3125.4	-6 %
2	8276.3	8616.8	4 %
3	16528.0	16387.5	-1 %

Table A-XVII. The comparison of the weighed concentration of 2-butanone and the 2-butanone concentration calculated with the calibration equation, in three standard solutions.

Standard solution	ppm, weighed	ppm, calculated	Deviation
1	3383.6	3417.7	1 %
2	8423.0	8368.6	-1 %
3	16820.9	16840.1	0 %

Table A-XVIII. The comparison of the weighed concentration of water and the water concentration calculated with the calibration equation, in three standard solutions.

Standard solution	ppm, weighed	ppm, calculated	Deviation
1	3361.7	3257.2	-3 %
2	8368.5	8541.5	2 %
3	16712.1	16644.2	0 %

Table A-XIX. The comparison of the weighed concentration of ethyl formate and the ethyl formate concentration calculated with the calibration equation, in three standard solutions.

Standard solution	ppm, weighed	ppm, calculated	Deviation
1	3371.8	3631.9	7 %
2	8393.7	8006.0	-5 %
3	16762.3	16890.8	1 %

Chromatograms of the samples taken from two experiments are presented next as examples. The chromatograms shown in Figures Figure A-43 to Figure A-46 are from the batch experiment in ethanol, with 10 g of catalyst at 180 °C and 60 bar of total pressure. The chromatograms in Figures Figure A-47 to Figure A-50 are from the batch experiment in 2-butanol, with 20 g of catalyst at 180 °C and 60 bar of total pressure. See the retention times in Table A-XV for identification of the peaks. The peak at approximately 2.2 min was present in all of the samples but could not be identified.

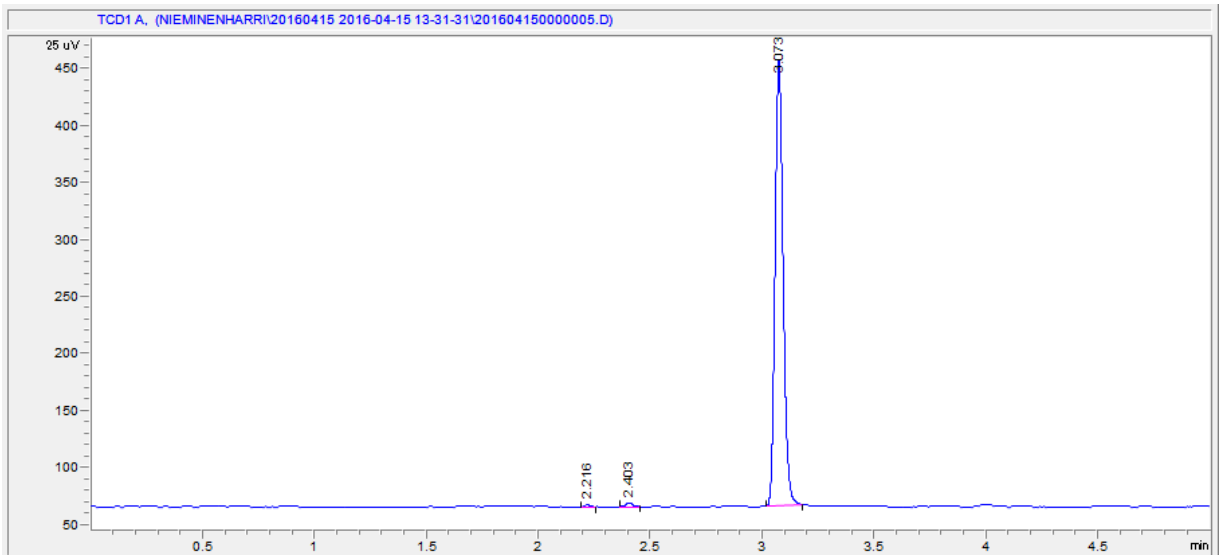

Figure A-43. GC chromatogram of the sample taken after heating of the reaction mixture, prior to introduction of the feed gas. From the batch experiment in ethanol, with 10 g of catalyst at 180 °C and 60 bar of total pressure.

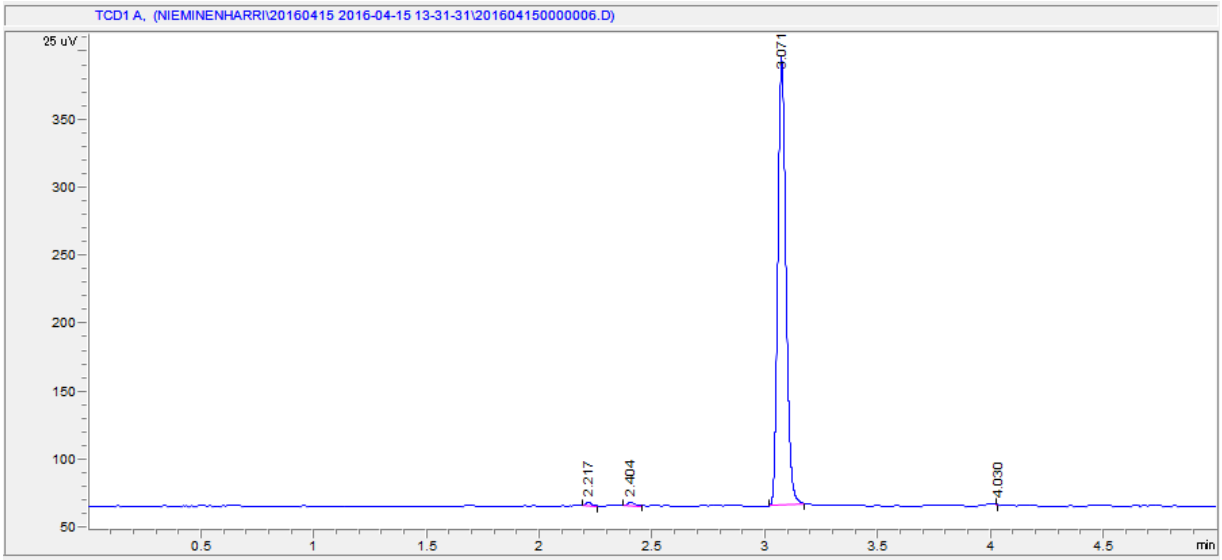

Figure A-44. GC chromatogram of the sample taken after 2 hours of reaction time. From the batch experiment in ethanol, with 10 g of catalyst at 180 °C and 60 bar of total pressure.

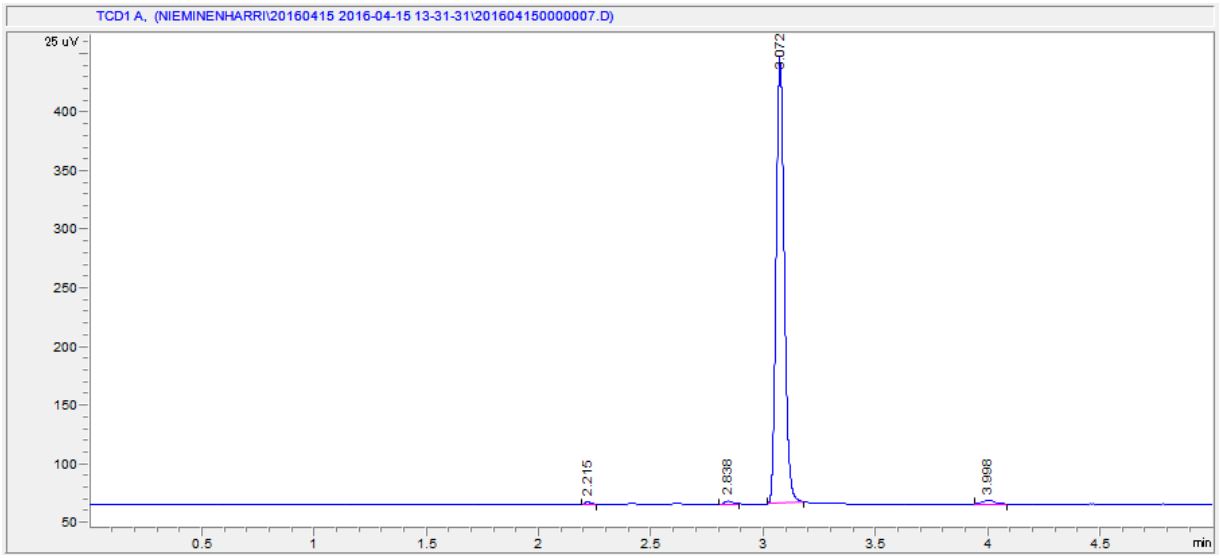

Figure A-45. GC chromatogram of the sample taken after 4 hours of reaction time. From the batch experiment in ethanol, with 10 g of catalyst at 180 °C and 60 bar of total pressure.

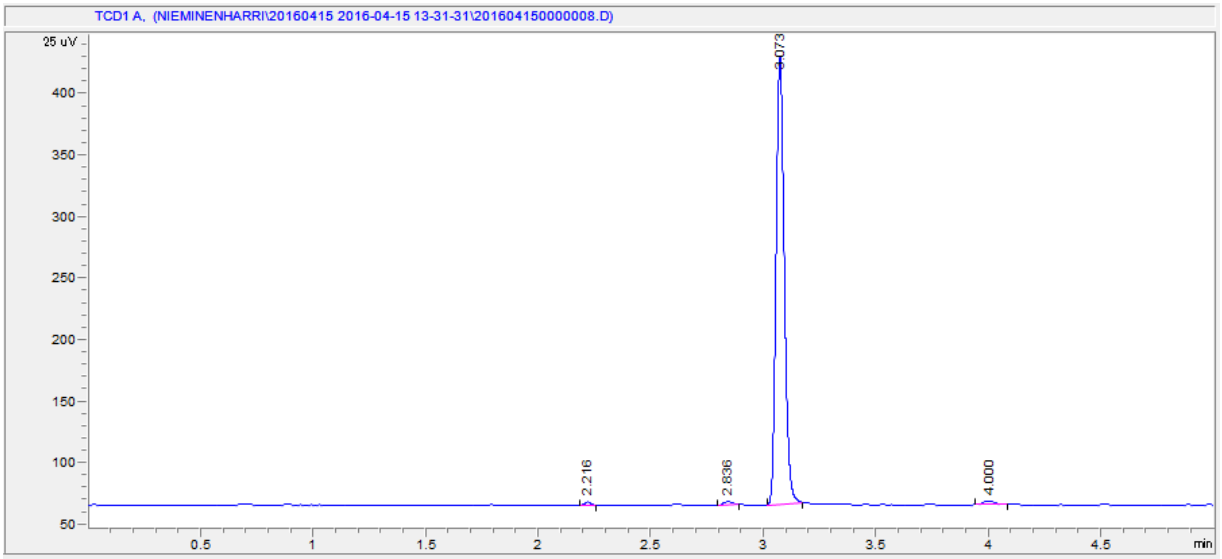

Figure A-46. GC chromatogram of the sample taken after 6 hours of reaction time. From the batch experiment in ethanol, with 10 g of catalyst at 180 °C and 60 bar of total pressure.

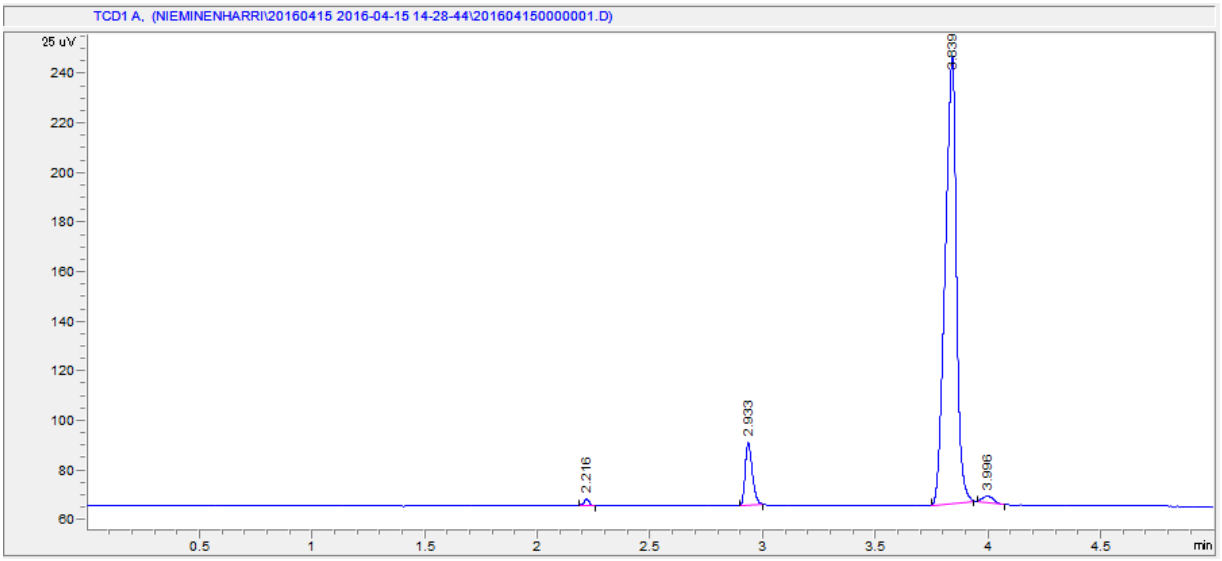

Figure A-47. GC chromatogram of the sample taken after heating of the reaction mixture, prior to introduction of the feed gas. From the batch experiment in 2-butanol, with 20 g of catalyst at 180 °C and 60 bar of total pressure.

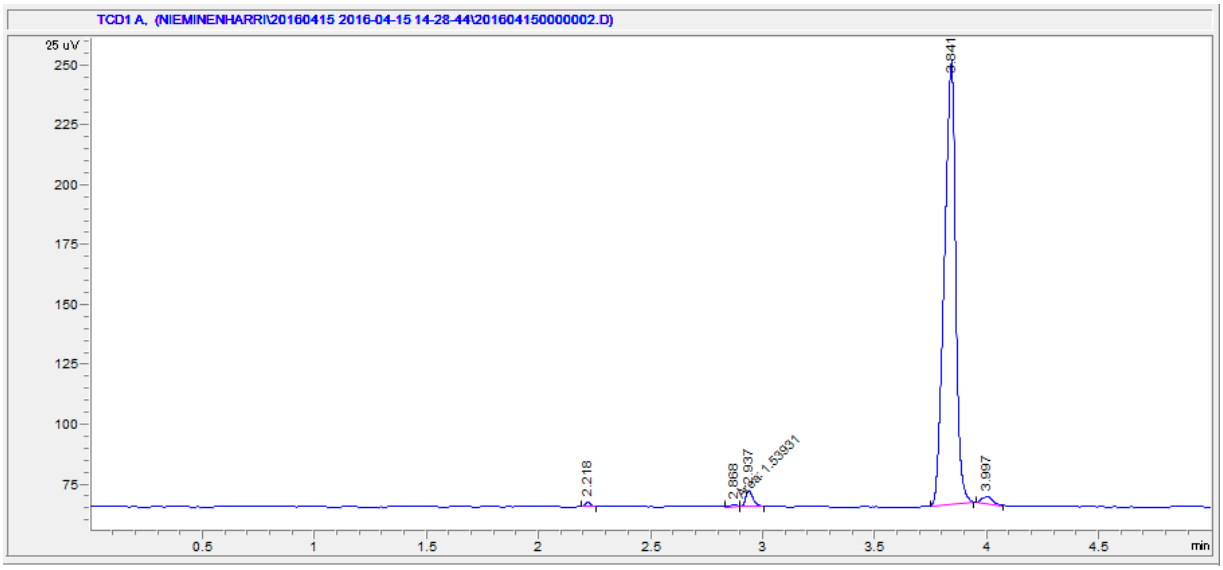

Figure A-48. GC chromatogram of the sample taken after 2 hours of reaction time. From the batch experiment in 2-butanol, with 20 g of catalyst at 180 °C and 60 bar of total pressure.

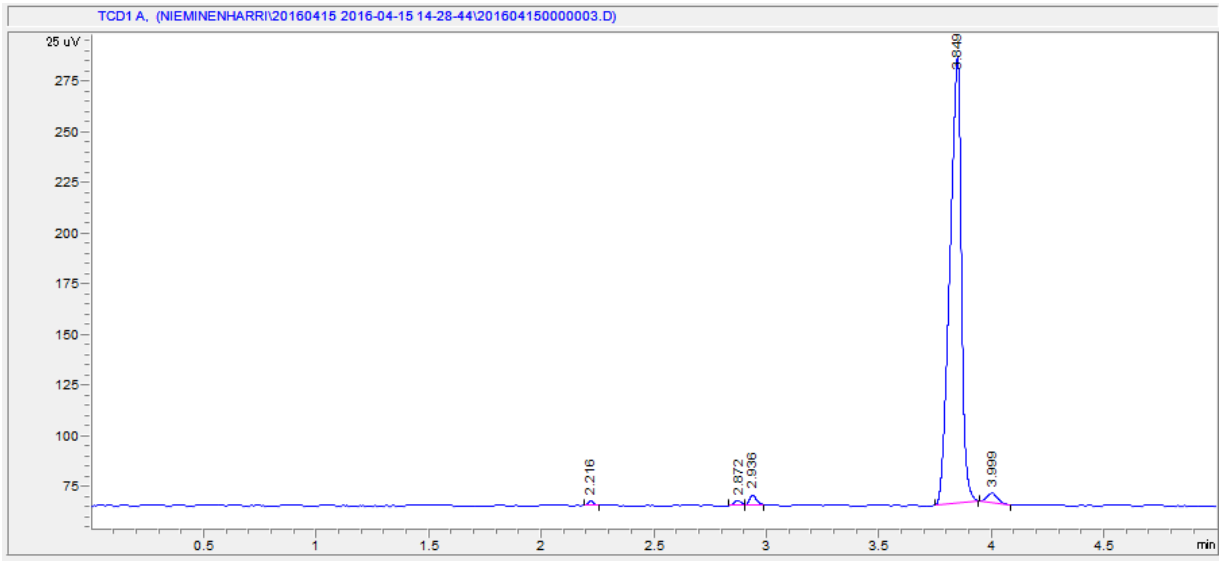

Figure A-49. GC chromatogram of the sample taken after 4 hours of reaction time. From the batch experiment in 2-butanol, with 20 g of catalyst at 180 °C and 60 bar of total pressure.

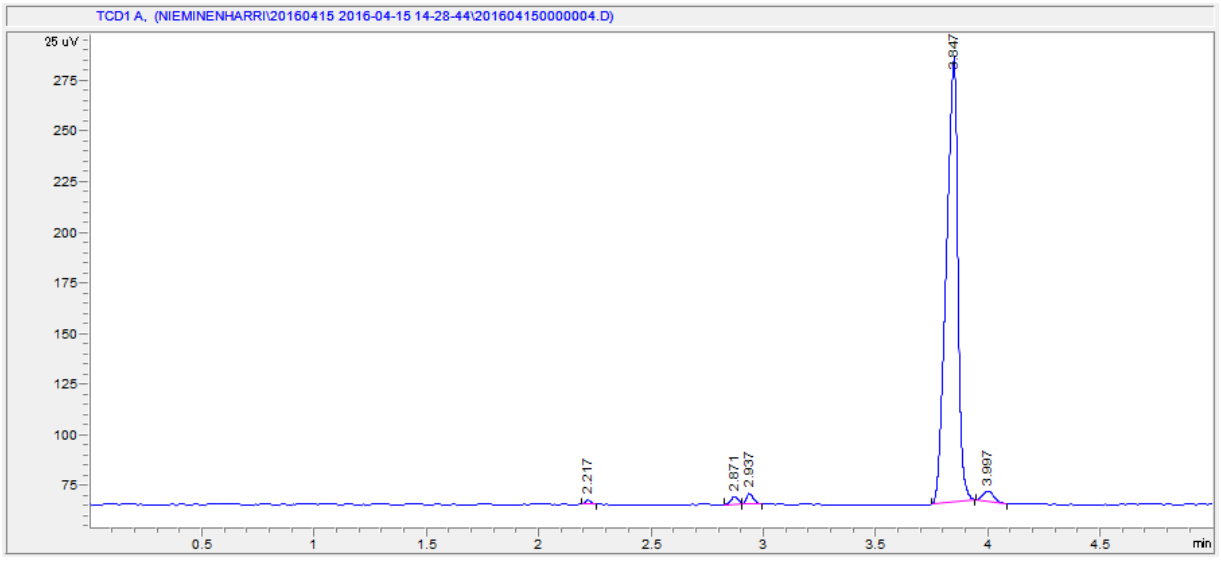

Figure A-50. GC chromatogram of the sample taken after 6 hours of reaction time. From the batch experiment in 2-butanol, with 20 g of catalyst at 180 °C and 60 bar of total pressure.

Appendix III: Pressure and composition data from the batch experiments

Note that reliable temperature and pressure curves were not available from all of the experiments.

Table A-XX. 2-butanol, 10 g of catalyst, 180 °C, 30 bar total pressure.

Reaction time, h	Concentration, ppm (mg/kg)	
	2-butanone	Water
0	65909.0	6545.2
2	49736.1	6192.9
4	38074.0	7837.0
6	33783.2	7367.2

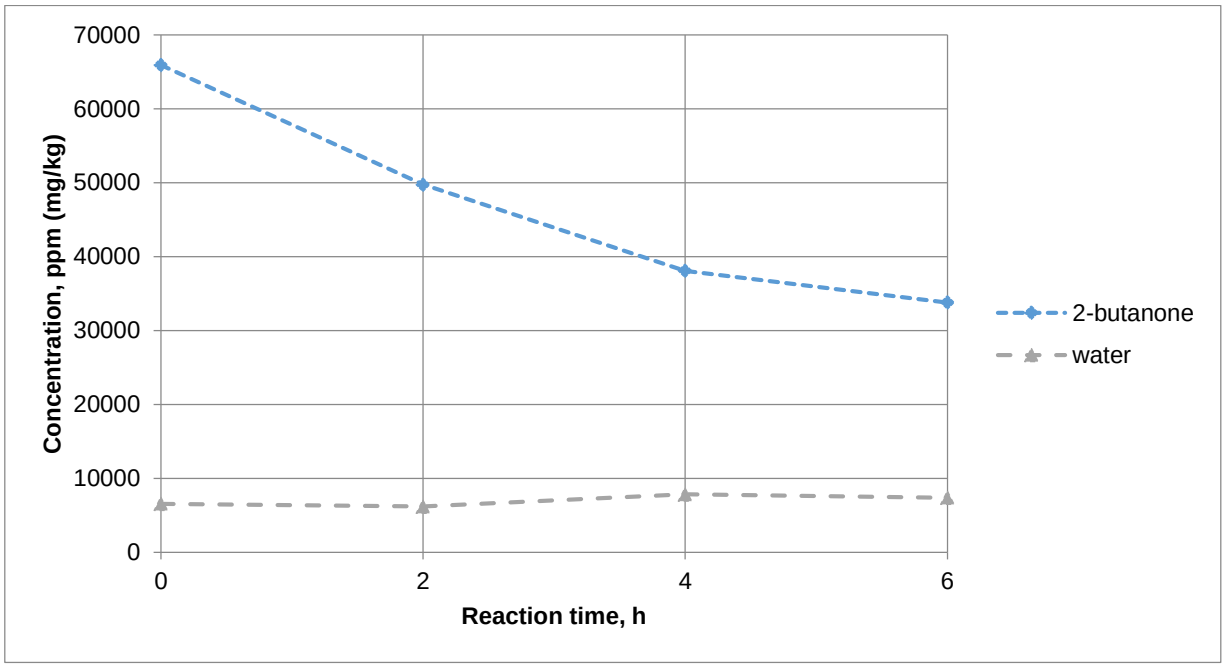

Figure A-51. 2-butanol, 10 g of catalyst, 180 °C, 30 bar total pressure.

Table A-XXI. 2-butanol, 10 g of catalyst, 180 °C, 60 bar total pressure.

Reaction time, h	Concentration, ppm (mg/kg)		
	2-butanone	Methanol	Water
0	47095.6	0.0	3624.2
2	16290.0	0.0	7602.1
4	10458.9	4576.0	8189.3
6	11559.1	7891.5	11829.6

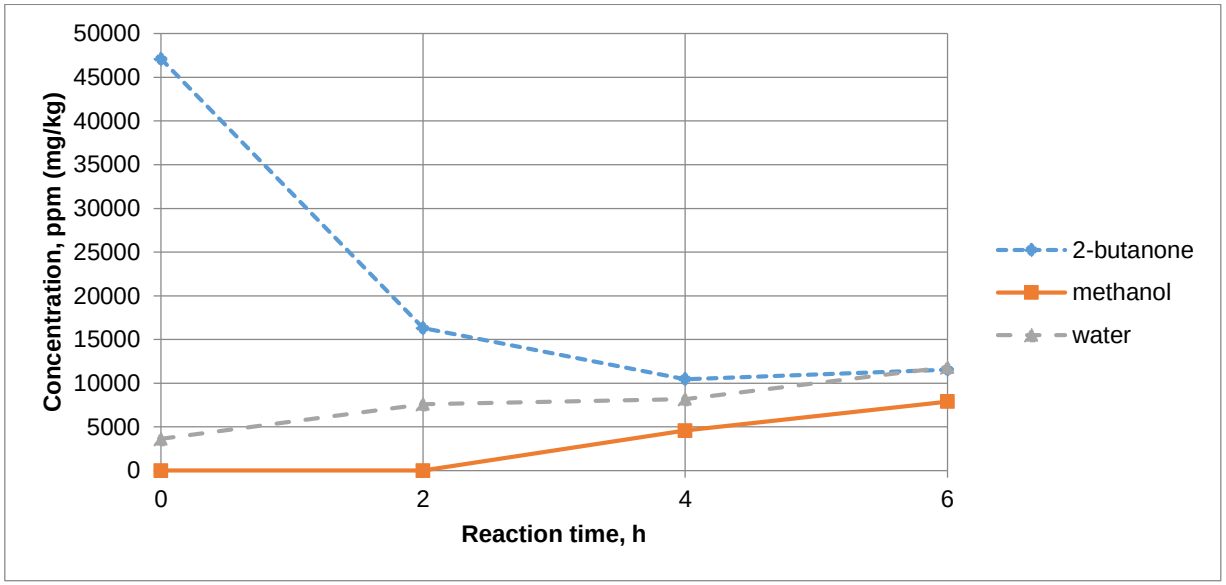

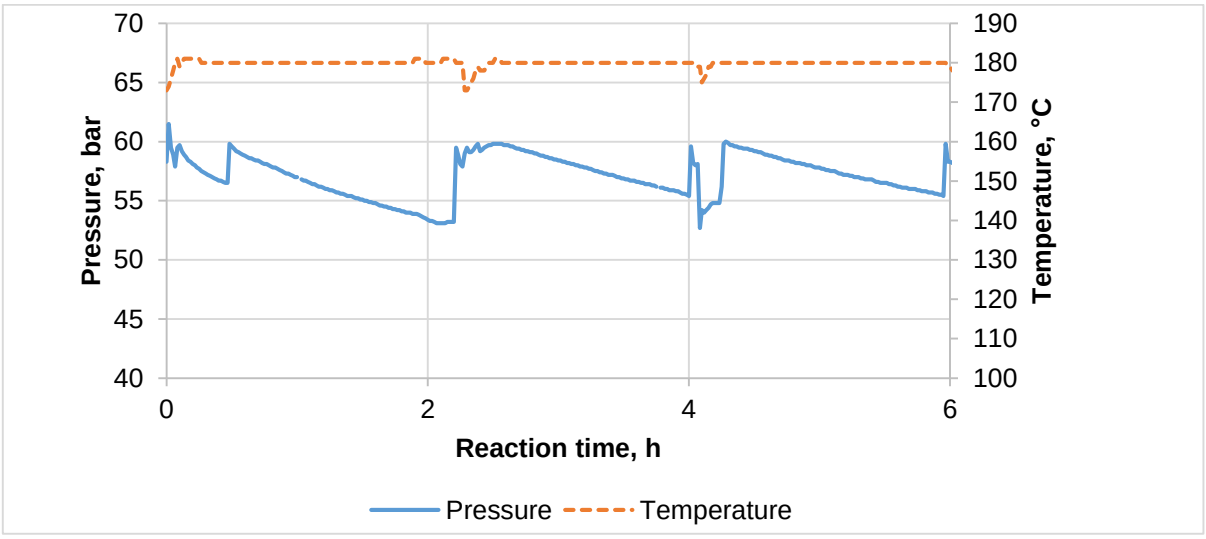

Figure A-52. 2-butanol, 10 g of catalyst, 180 °C, 60 bar total pressure.

Table A-XXII. 2-butanol, 20 g of catalyst, 180 °C, 60 bar total pressure.

Reaction time, h	Concentration, ppm (mg/kg)		
	2-butanone	Methanol	Water
0	61838.3	0.0	11125.0
2	16840.1	2192.9	12886.5
4	14199.6	6337.3	18170.8
6	13979.6	10067.3	19580.0

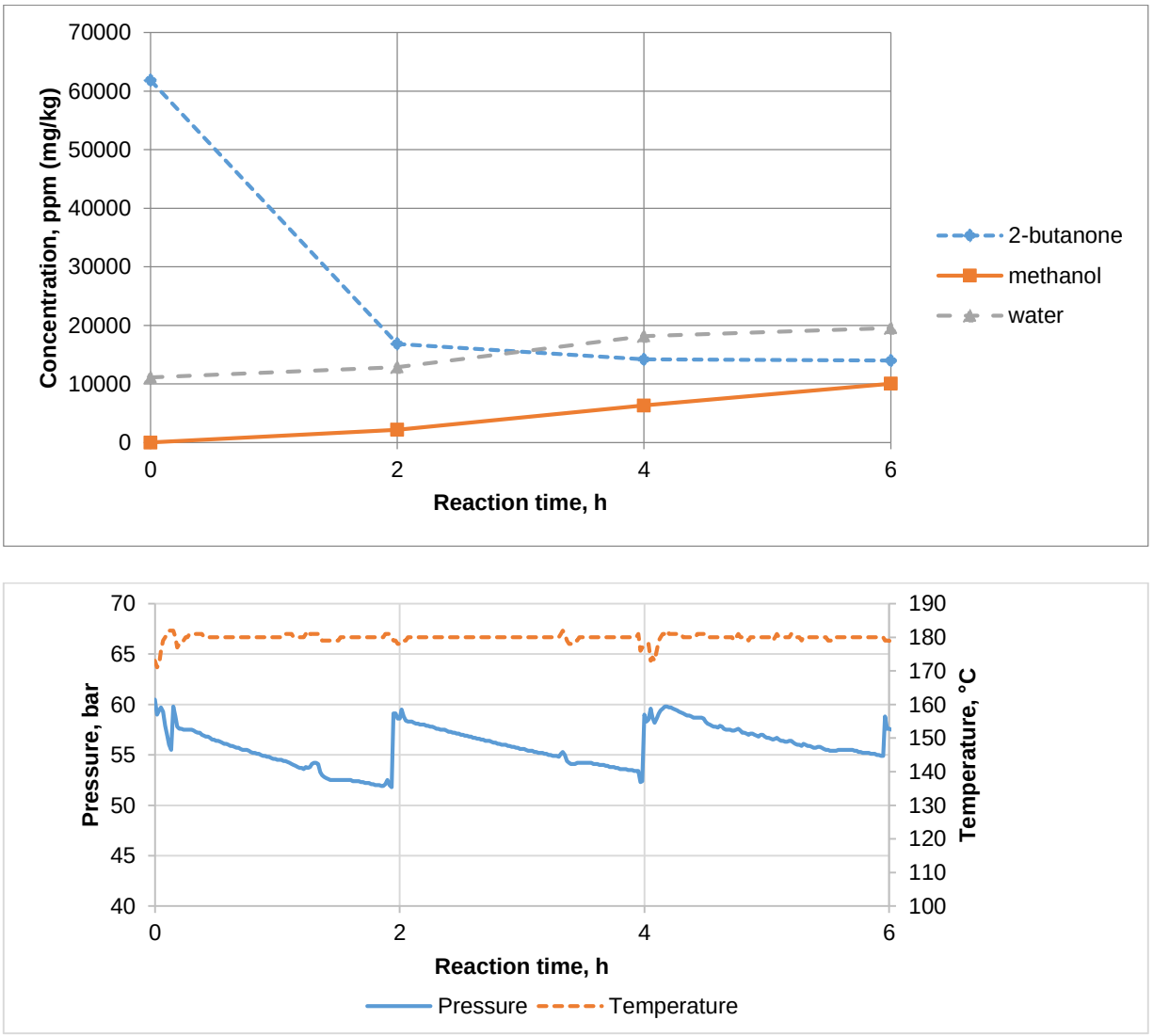

Figure A-53. 2-butanol, 20 g of catalyst, 180 °C, 60 bar total pressure.

Table A-XXIII. 2-butanol, 20 g of catalyst, 160 °C, 60 bar total pressure.

Reaction time, h	Concentration, ppm (mg/kg)		
	2-butanone	Methanol	Water
0	21350.9	0.0	3961.8
2	9578.8	0.0	12886.5
4	5398.0	1571.3	15235.1
6	5728.1	2296.6	15469.9

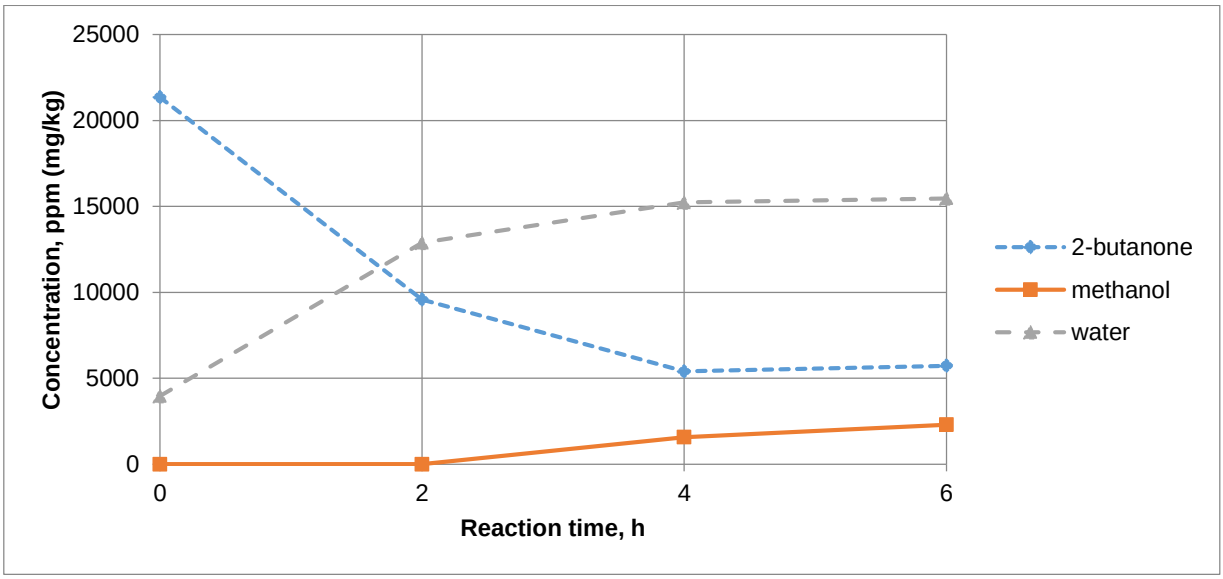

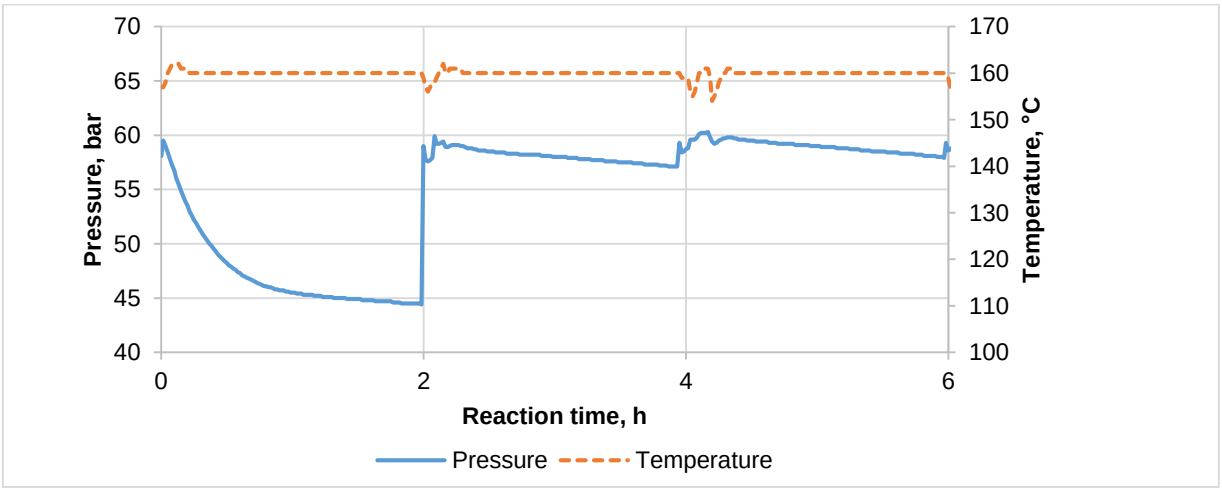

Figure A-54. 2-butanol, 20 g of catalyst, 160 °C, 60 bar total pressure.

Table A-XXIV. Ethanol, 10 g of catalyst, 180 °C, 30 bar total pressure.

Reaction time, h	Concentration, ppm (mg/kg)		
	Acetaldehyde	Methanol	Water
0	8006.0	0.0	7249.8
2	4452.1	4783.2	9246.1
4	1485.9	9445.6	11712.2
6	1567.9	12139.5	11242.4

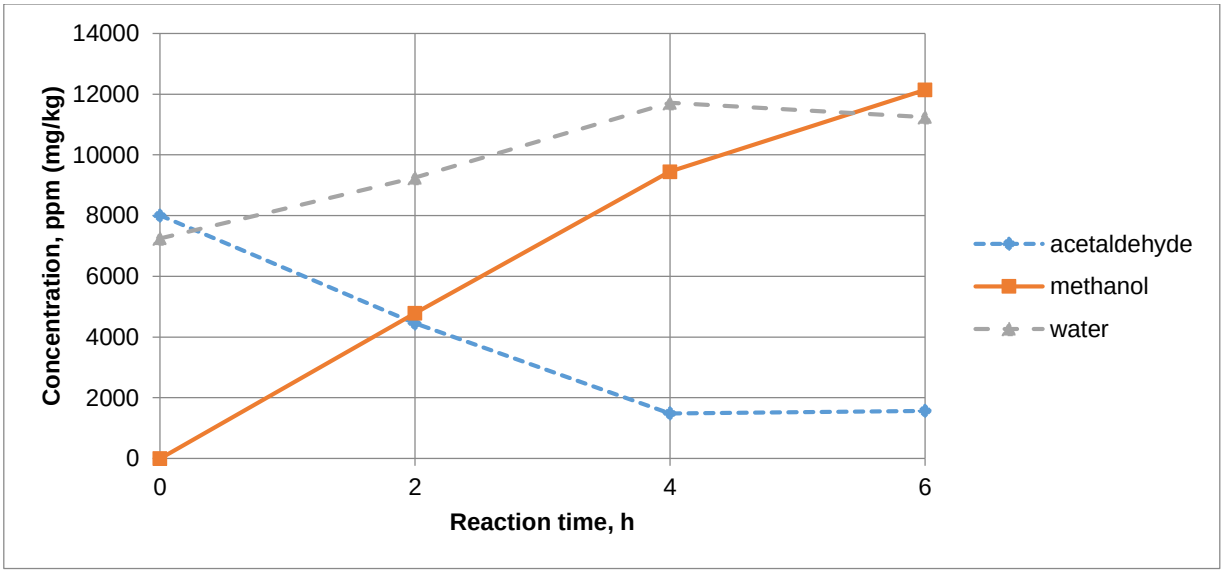

Figure A-55. Ethanol, 10 g of catalyst, 180 °C, 30 bar total pressure.

Table A-XXV. Ethanol, 10 g of catalyst, 180 °C, 60 bar total pressure.

Reaction time, h	Concentration, ppm (mg/kg)			
	Acetaldehyde	Ethyl formate	Methanol	Water
0	9783.0	0.0	0.0	10303.0
2	7732.6	0.0	0.0	7602.1
4	0.0	1991.6	7062.6	14647.9
6	0.0	1663.6	8098.7	14413.0

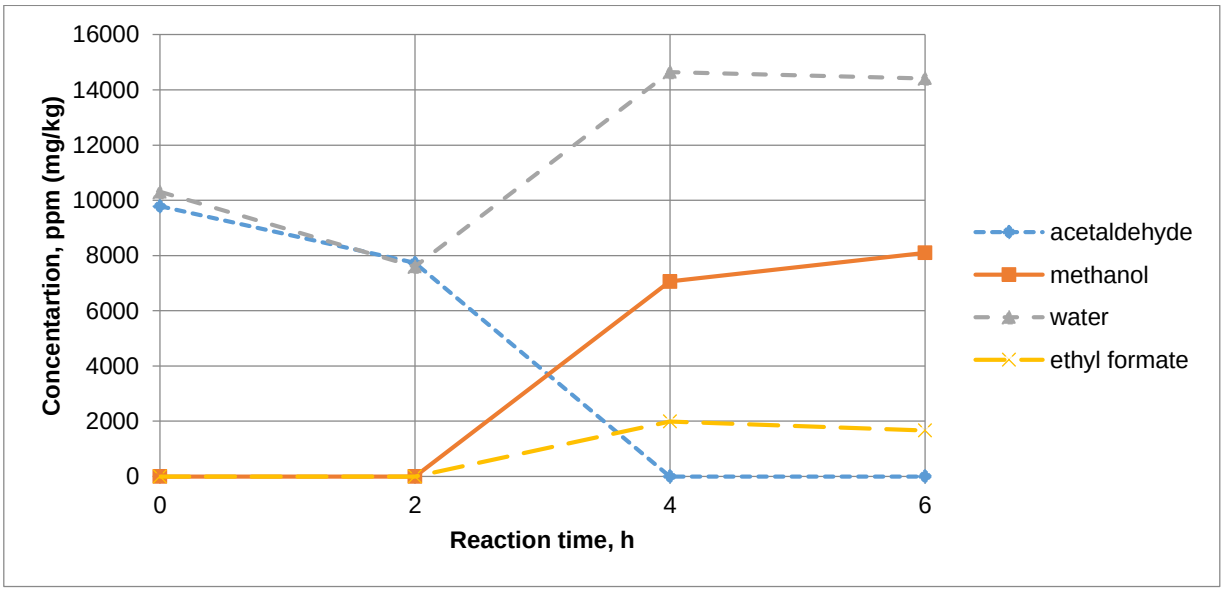

Figure A-56. Ethanol, 10 g of catalyst, 180 °C, 60 bar total pressure.

Table A-XXVI. Ethanol, 20 g of catalyst, 160 °C, 60 bar total pressure.

Reaction time, h	Concentration, ppm (mg/kg)		
	Ethyl formate	Methanol	Water
0	0.0	0.0	1965.5
2	2128.3	0.0	19345.1
4	3221.8	3332.7	23924.9
6	2811.8	6130.1	26038.6

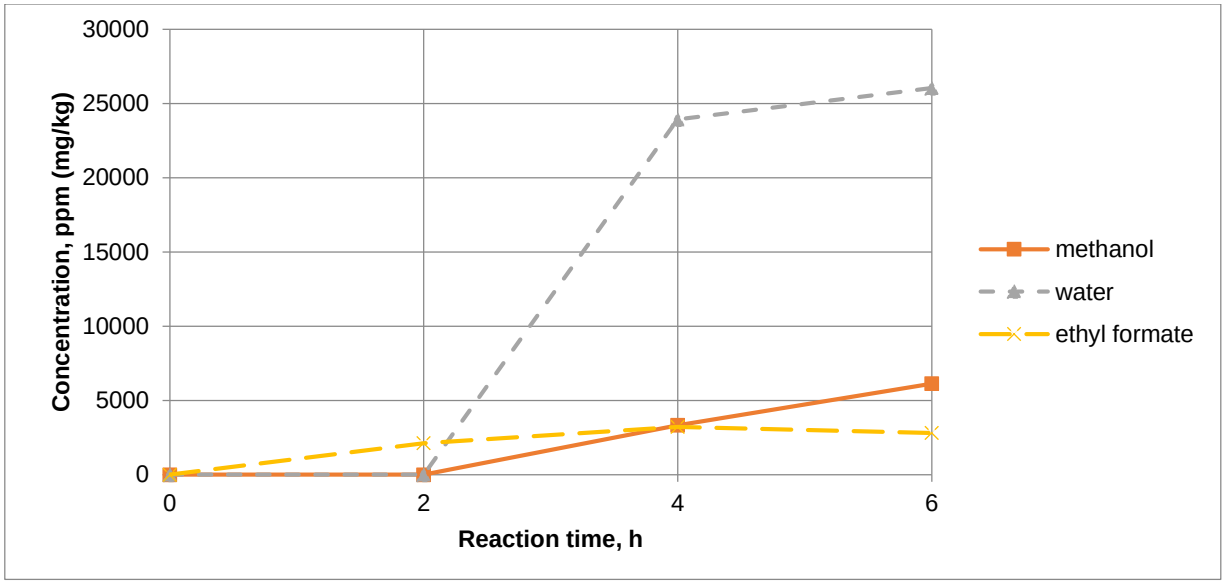

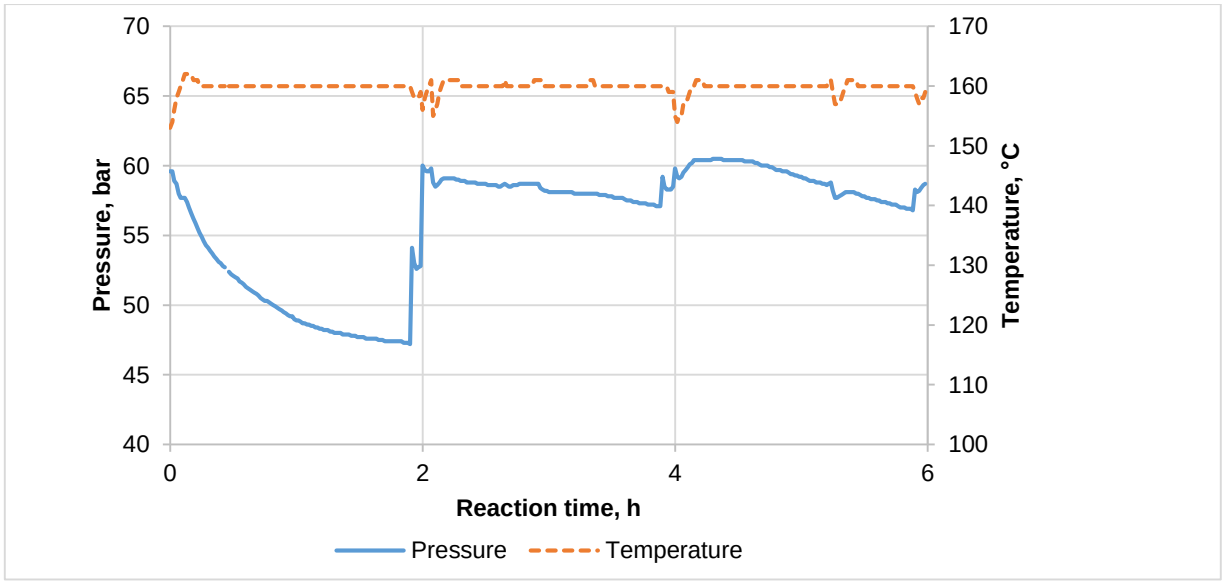

Figure A-57. Ethanol, 20 g of catalyst, 160 °C, 60 bar total pressure.

Table A-XXVII. Ethanol, 20 g of catalyst, 180 °C, 60 bar total pressure.

Reaction time, h	Concentration, ppm (mg/kg)			
	Acetaldehyde	Ethyl formate	Methanol	Water
0	8552.8	0.0	0.0	10420.4
2	7185.9	0.0	3332.7	12416.7
4	0.0	1827.6	10378.1	23572.6
6	0.0	0.0	12035.9	22163.4

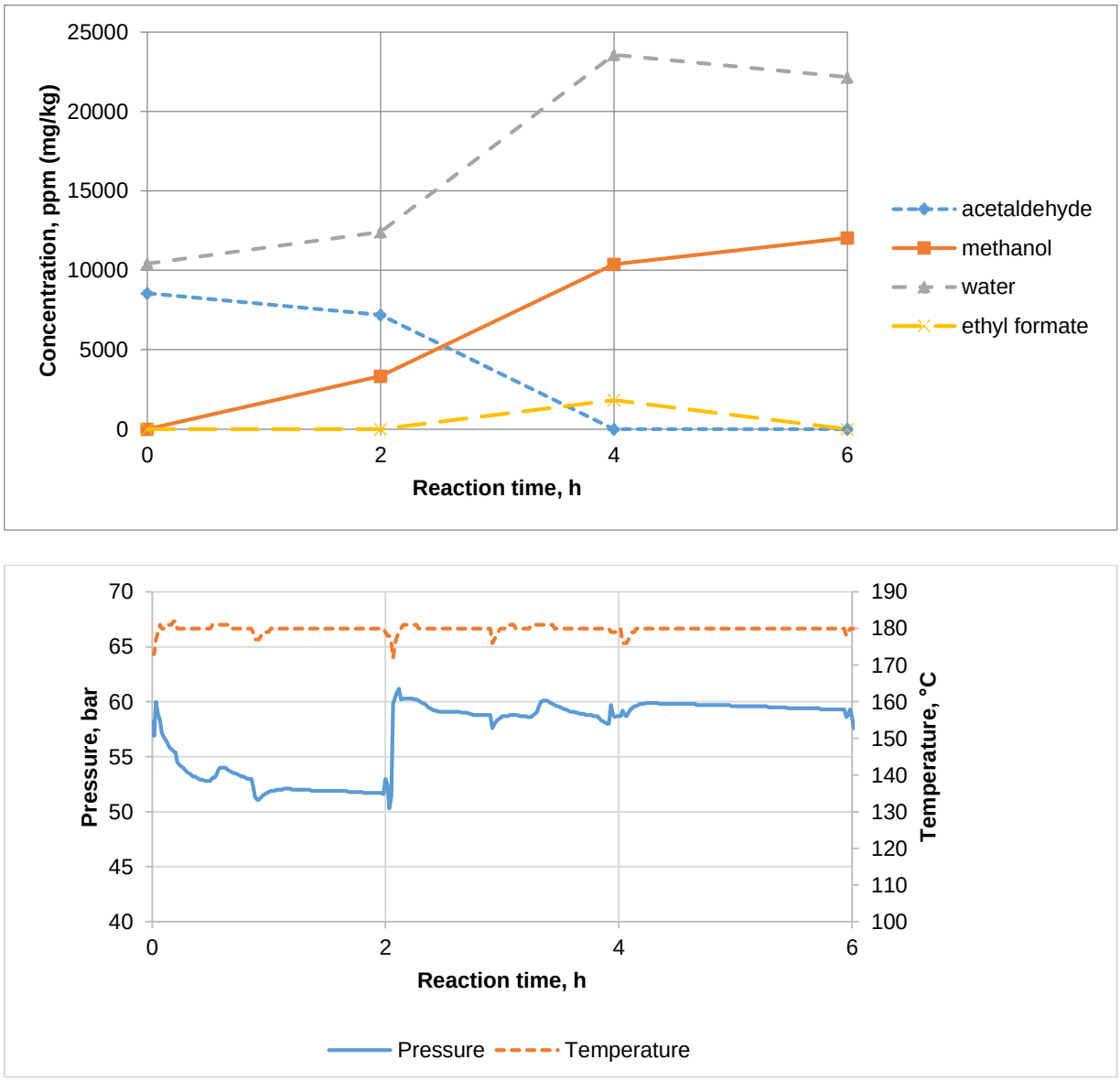

Figure A-58. Ethanol, 20 g of catalyst, 180 °C, 60 bar total pressure.

Table A-XXVIII. 2-butanol + 5 g water, 10 g of catalyst, 180 °C, 60 bar total pressure.

Reaction time, h	Concentration, ppm (mg/kg)		
	2-butanone	Methanol	Water
0	19150.5	0.0	25803.8
2	14419.7	0.0	33319.3
4	11779.2	1177.6	31440.4
6	10679.0	2089.3	32145.0

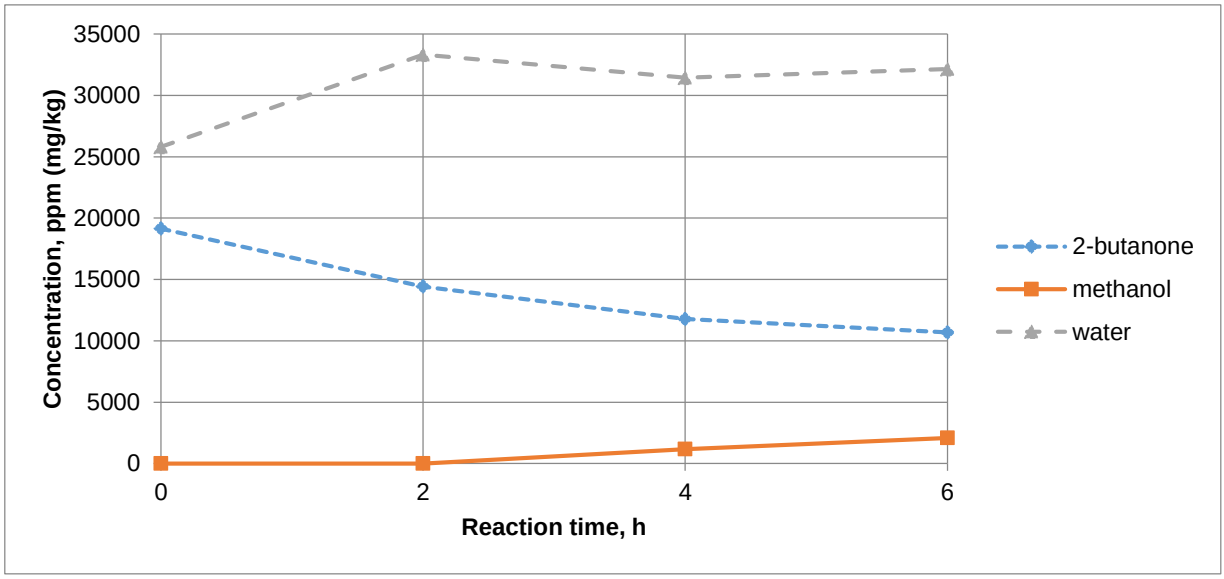

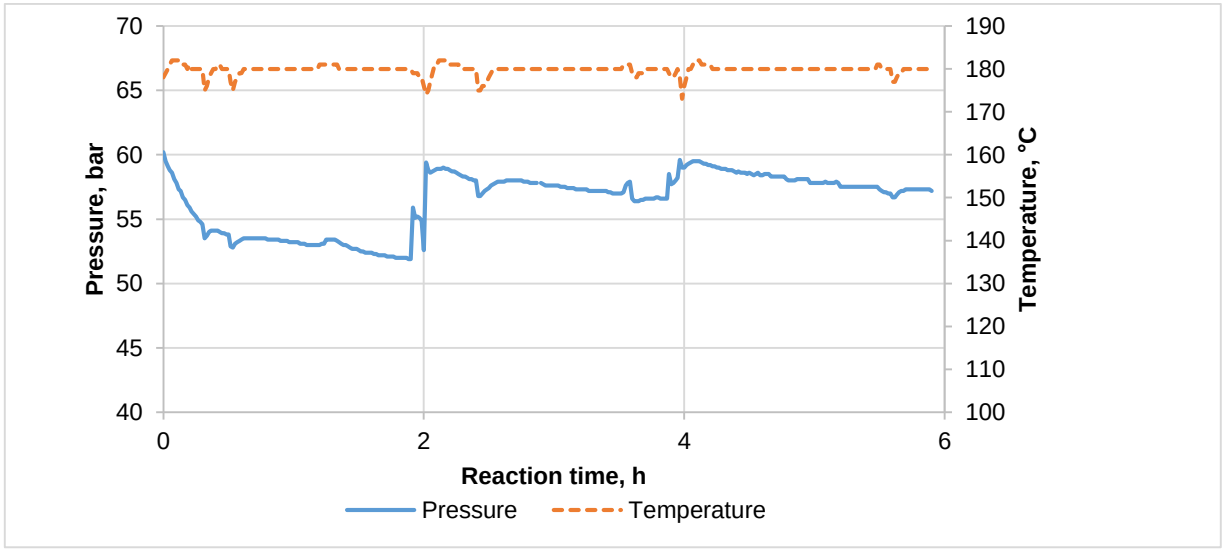

Figure A-59. 2-butanol + 5 g water, 10 g of catalyst, 180 °C, 60 bar total pressure.

Table A-XXIX. 2-butanol + 20 g 3Å molecular sieve, 10 g of catalyst, 180 °C, 60 bar total pressure.

Reaction time, h	Concentration, ppm (mg/kg)		
	2-butanone	Methanol	Water
0	40934.5	0.0	1190.4
2	30592.6	2814.6	2082.9
4	20690.8	8616.8	3139.8
6	17720.3	13590.0	5253.5

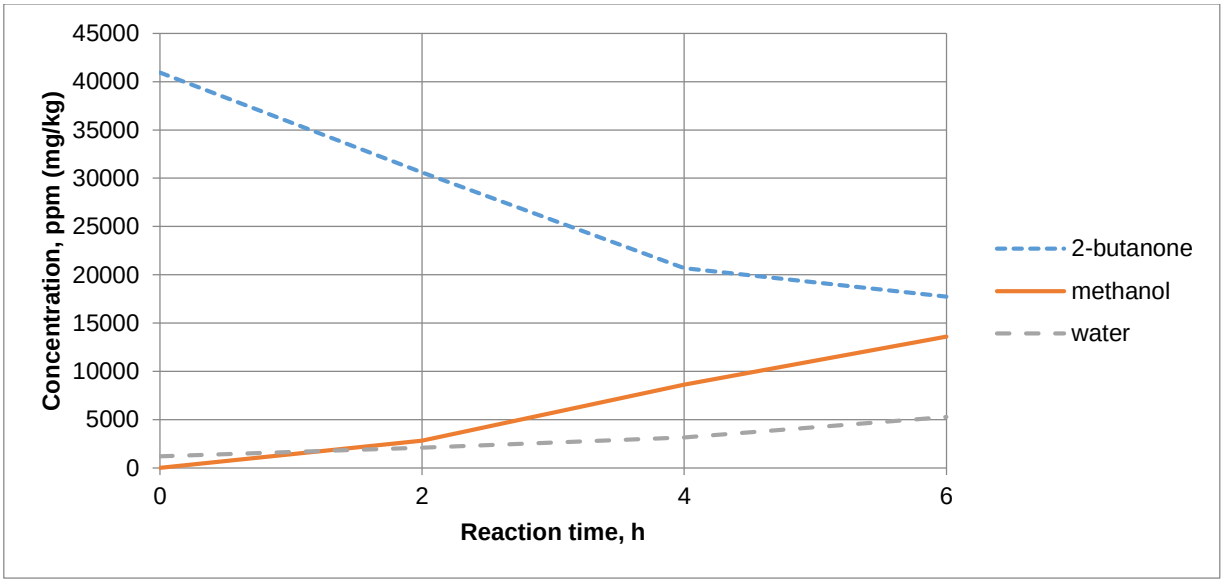

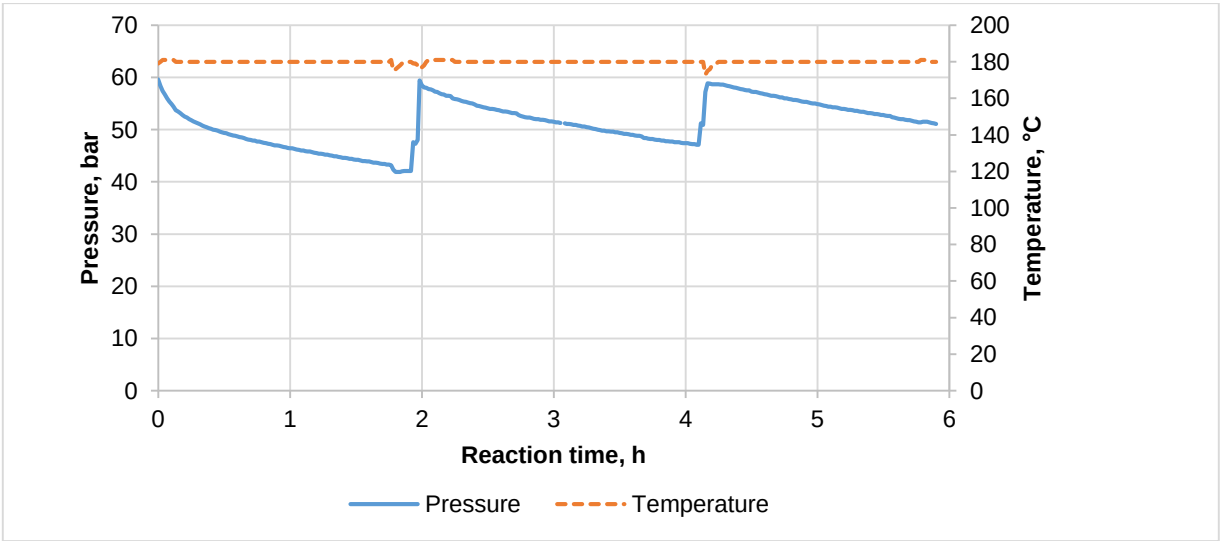

Figure A-60. 2-butanol + 20 g 3Å molecular sieve, 10 g of catalyst, 180 °C, 60 bar total pressure.

Appendix IV: Composition data from the semibatch experiments

Table A-XXX. 2-butanol, 10 g of catalyst, 180 °C, 30 bar partial pressure, 39.9 bar total pressure.

Reaction time, h	Concentration, ppm (mg/kg)		
	2-butanone	Methanol	Water
0	56117.2	0.0	5958.0
2	24211.4	1623.1	6897.5
4	19700.6	3332.7	6545.2
6	19590.6	4990.4	8071.8

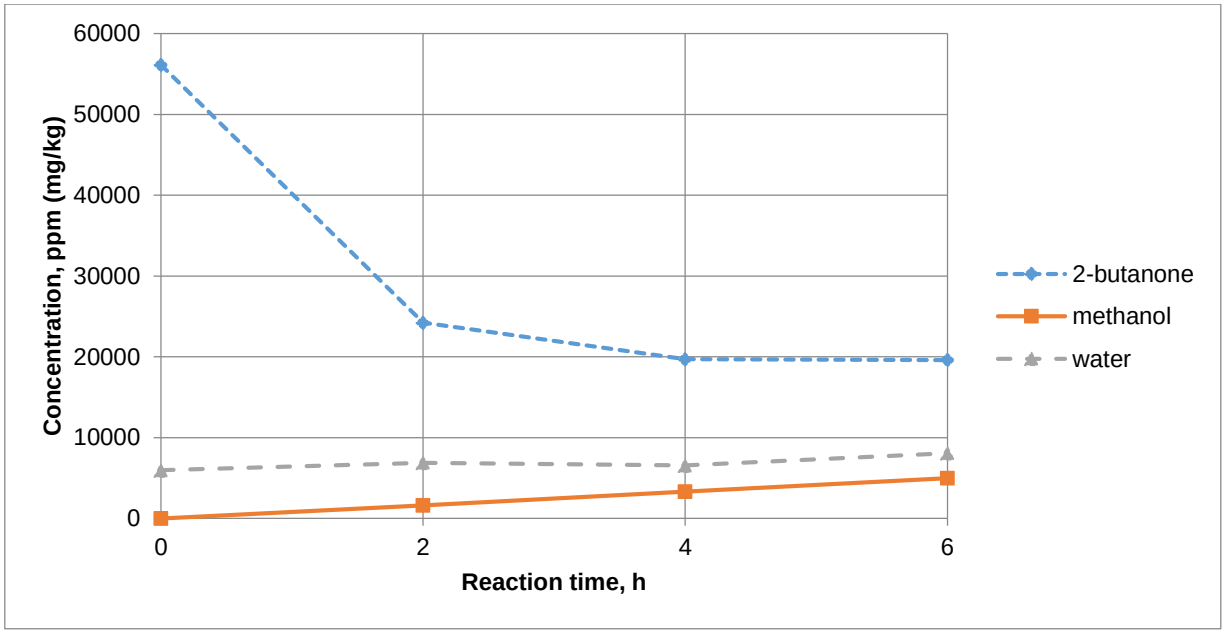

Figure A-61. 2-butanol, 10 g of catalyst, 180 °C, 30 bar partial pressure, 39.9 bar total pressure.

Table A-XXXI. 2-butanol, 10 g of catalyst, 180 °C, 40 bar partial pressure, 49.9 bar total pressure.

Reaction time, h	Concentration, ppm (mg/kg)		
	2-butanone	Methanol	Water
0	31802.8	0.0	8189.3
2	15079.8	0.0	7367.2
4	13649.5	3747.1	8541.5
6	13319.5	5715.7	10655.3

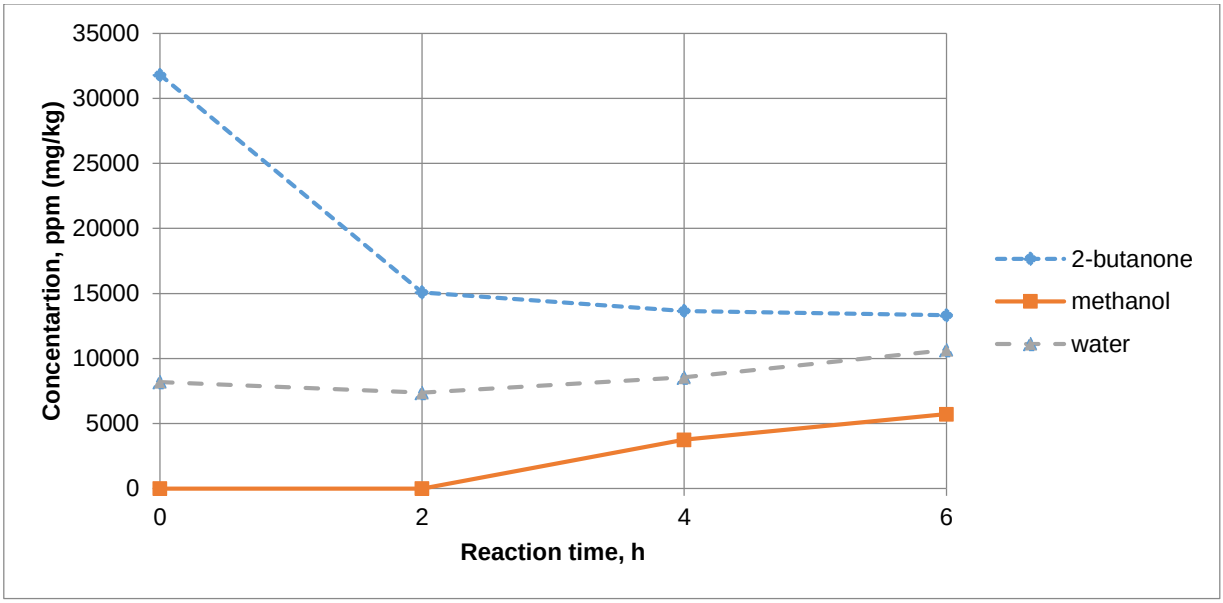

Figure A-62. 2-butanol, 10 g of catalyst, 180 °C, 40 bar partial pressure, 49.9 bar total pressure.

Table A-XXXII. 2-butanol, 10 g of catalyst, 180 °C, 50 bar partial pressure, 59.9 bar total pressure.

Reaction time, h	Concentration, ppm (mg/kg)		
	2-butanone	Methanol	Water
0	32462.9	0.0	6192.9
2	16180.0	4265.1	8659.0
4	11449.1	88234.0	10655.3
6	11009.0	12553.9	12651.6

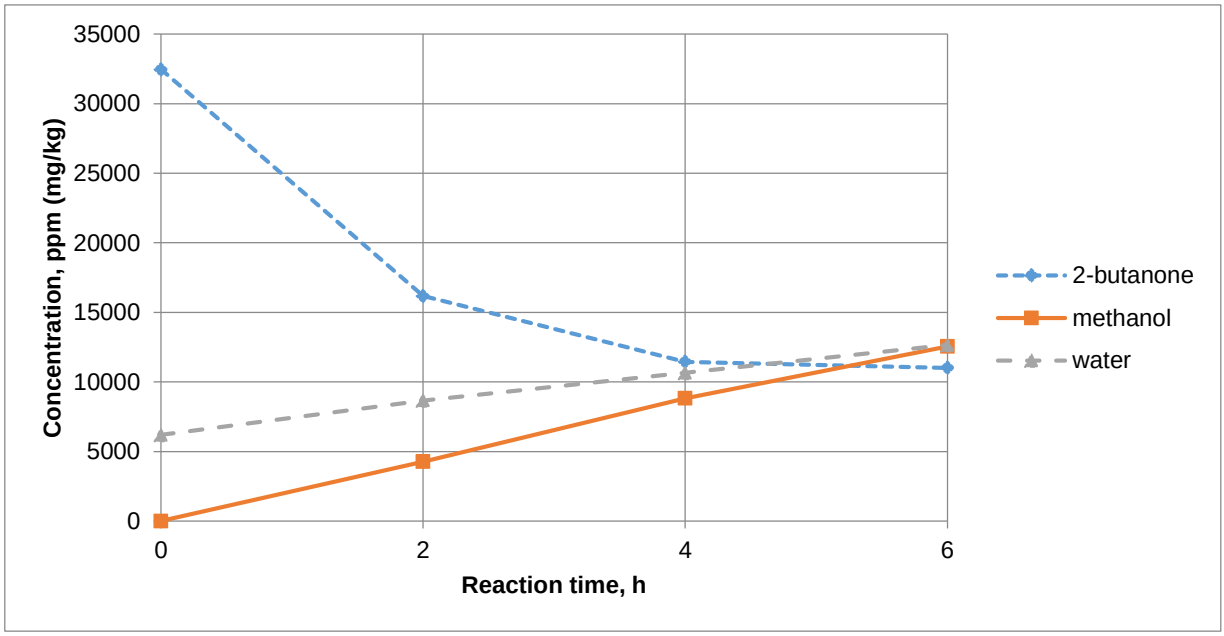

Figure A-63. 2-butanol, 10 g of catalyst, 180 °C, 50 bar partial pressure, 59.9 bar total pressure.

Table A-XXXIII. Ethanol, 10 g of catalyst, 180 °C, 20 bar partial pressure, 39.6 bar total pressure.

Reaction time, h	Concentration, ppm (mg/kg)		
	Acetaldehyde	Methanol	Water
0	1595.2	0.0	7484.7
2	0.0	4265.1	9833.3
4	0.0	8098.7	10537.9
6	0.0	10481.7	11125.0

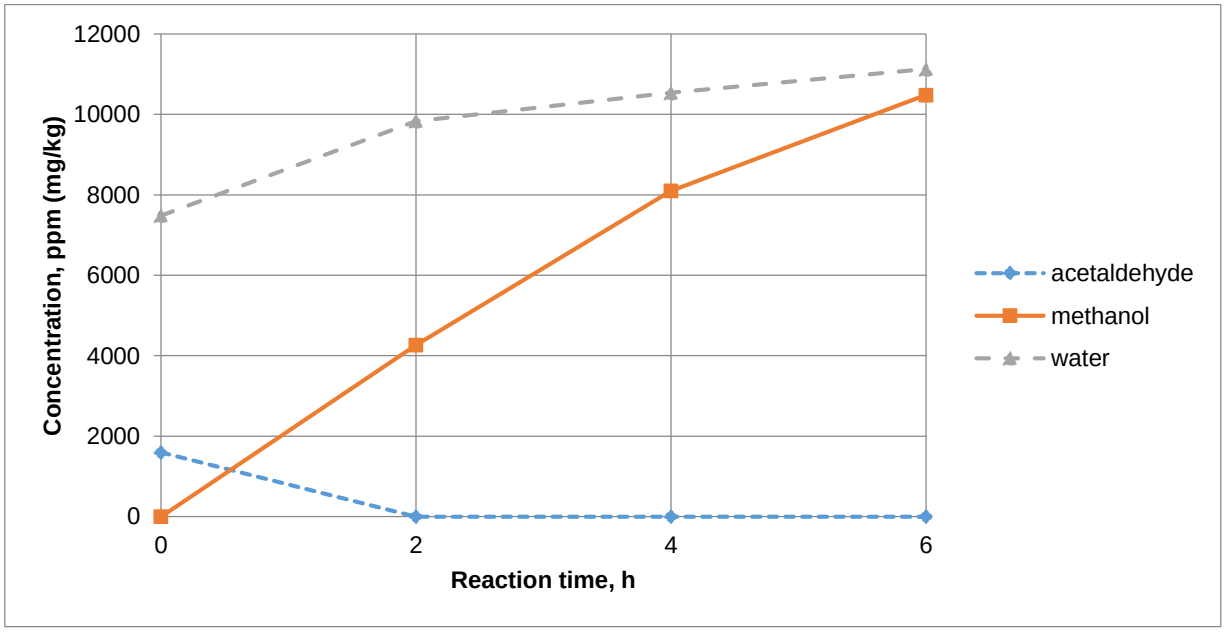

Figure A-64. Ethanol, 10 g of catalyst, 180 °C, 20 bar partial pressure, 39.6 bar total pressure.

Table A-XXXIV. Ethanol, 10 g of catalyst, 180 °C, 30 bar partial pressure, 49.6 bar total pressure.

Reaction time, h	Concentration, ppm (mg/kg)			
	Acetaldehyde	Ethyl formate	Methanol	Water
0	1677.2	0.0	0.0	10890.1
2	0.0	0.0	3125.4	101856.
4	0.0	0.0	5819.3	11712.2
6	0.0	1280.8	7684.3	12181.9

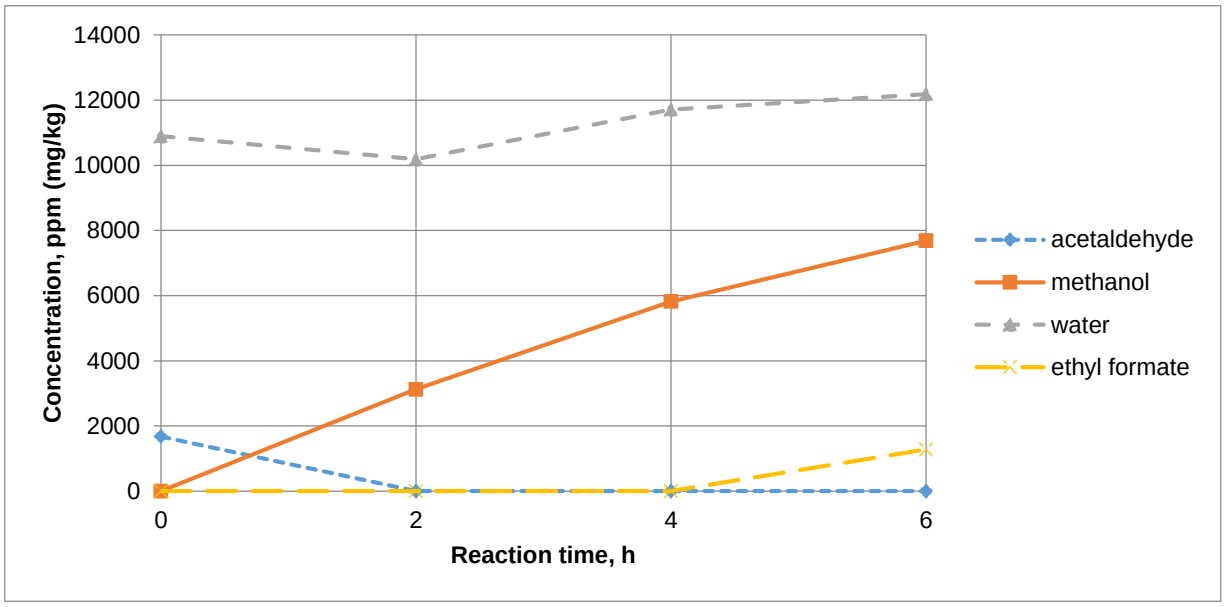

Figure A-65. Ethanol, 10 g of catalyst, 180 °C, 30 bar partial pressure, 49.6 bar total pressure.

Table A-XXXV. Ethanol, 10 g of catalyst, 180 °C, 40 bar partial pressure, 59.6 bar total pressure.

Reaction time, h	Concentration, ppm (mg/kg)			
	Acetaldehyde	Ethyl formate	Methanol	Water
0	1513.2	0.0	1882.1	9246.1
2	0.0	2538.4	4368.8	9950.7
4	0.0	1909.6	7891.5	12769.0
6	0.0	1786.6	10896.2	14060.8

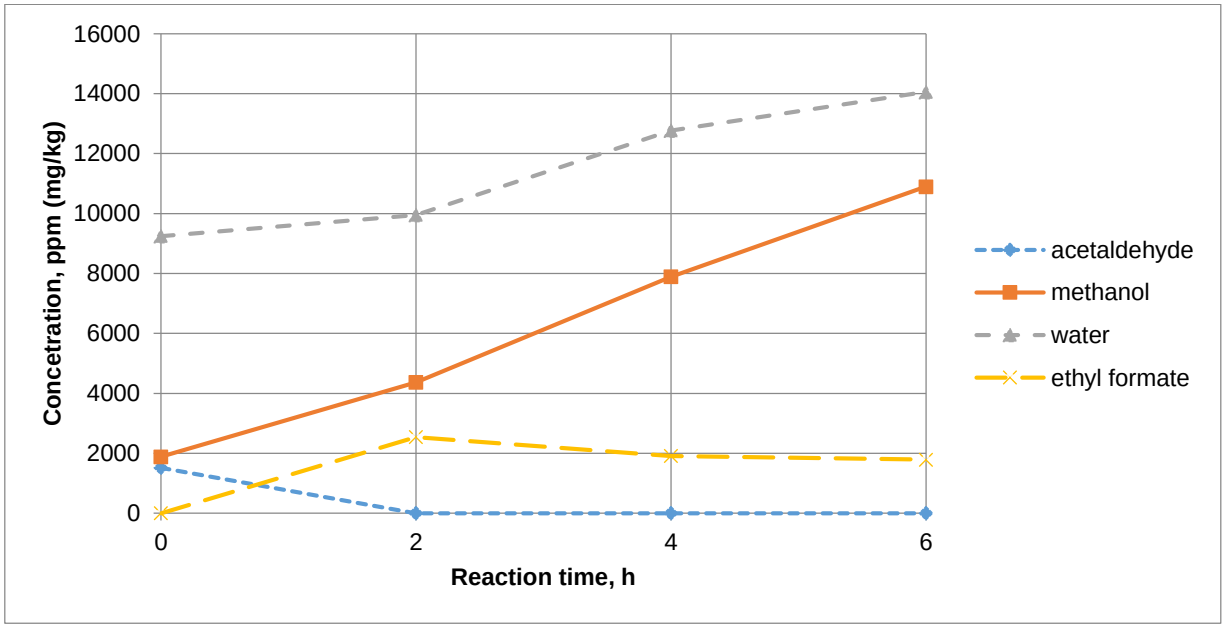

Figure A-66. Ethanol, 10 g of catalyst, 180 °C, 40 bar partial pressure, 59.6 bar total pressure.

Table A-XXXVI. 2-butanol, 10 g of catalyst, 160 °C, 40 bar partial pressure, 46.2 bar total pressure.

Reaction time, h	Concentration, ppm (mg/kg)		
	2-butanone	Methanol	Water
0	10128.9	0.0	2552.6
2	7268.4	1219.0	5253.5
4	6608.2	2089.3	5723.2
6	6388.2	3125.4	7015.0

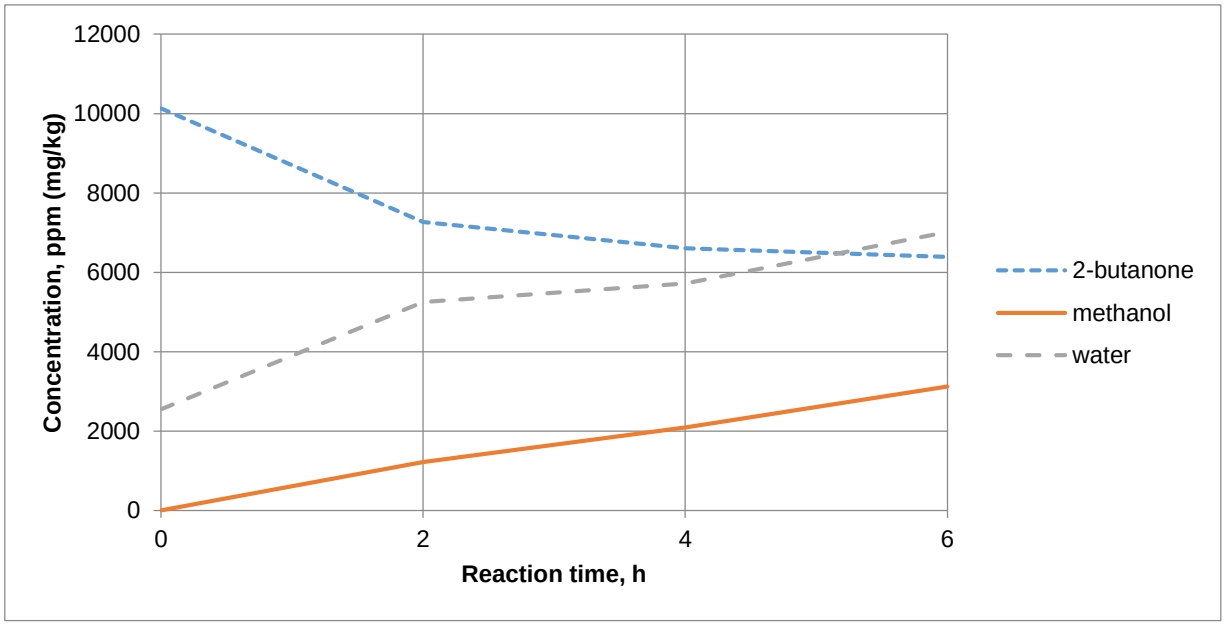

Figure A-67. 2-butanol, 10 g of catalyst, 160 °C, 40 bar partial pressure, 46.2 bar total pressure.

Table A-XXXVII. 2-butanol, 10 g of catalyst, 170 °C, 40 bar partial pressure, 47.9 bar total pressure.

Reaction time, h	Concentration, ppm (mg/kg)		
	2-butanone	Methanol	Water
0	26961.9	0.0	13591.0
2	12439.3	1778.5	14295.6
4	10018.9	3539.9	18992.8
6	10128.9	5301.2	18758.0

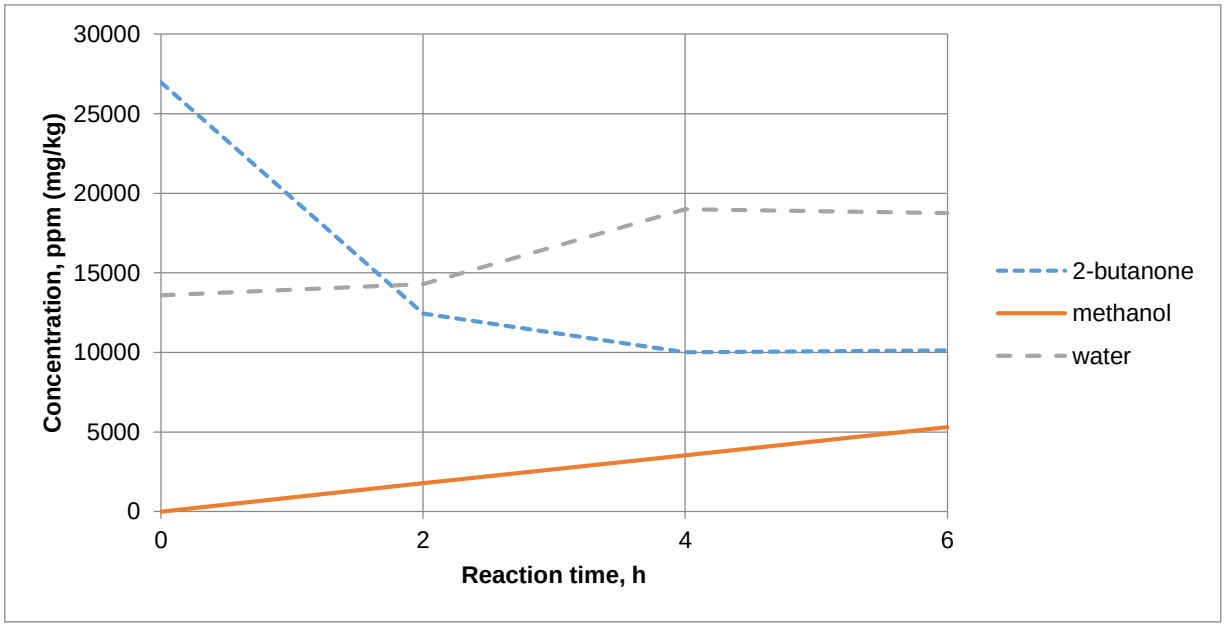

Figure A-68. 2-butanol, 10 g of catalyst, 170 °C, 40 bar partial pressure, 47.9 bar total pressure.

Table A-XXXVIII. 2-butanol, 10 g of catalyst, 190 °C, 40 bar partial pressure, 52.2 bar total pressure.

Reaction time, h	Concentration, ppm (mg/kg)		
	2-butanone	Methanol	Water
0	38514.0	0.0	13473.6
2	23881.4	4368.8	16879.1
4	20800.8	8305.9	20284.5
6	20800.8	11621.5	23102.9

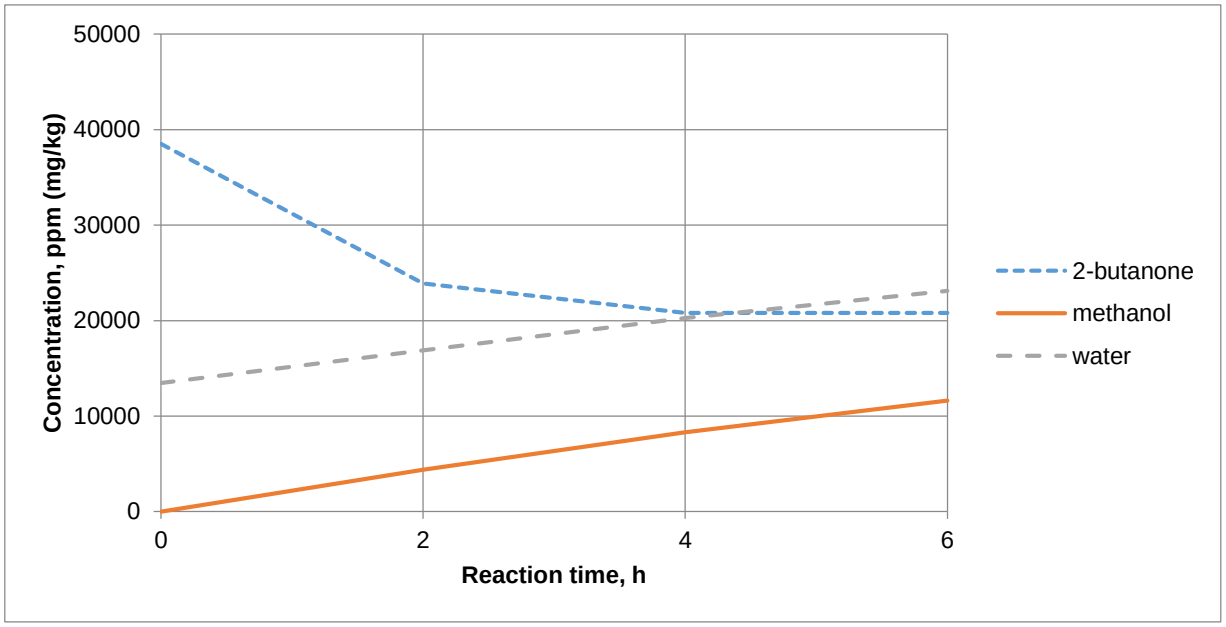

Figure A-69. 2-butanol, 10 g of catalyst, 190 °C, 40 bar partial pressure, 52.2 bar total pressure.

Table A-XXXIX. 2-butanol, 10 g of catalyst, 200 °C, 40 bar partial pressure, 54.8 bar total pressure.

Reaction time, h	Concentration, ppm (mg/kg)		
	2-butanone	Methanol	Water
0	53146.7	0.0	5605.8
2	33013.0	4990.4	20167.1
4	29052.3	9860.1	22868.0
6	28502.2	14108.1	25921.2

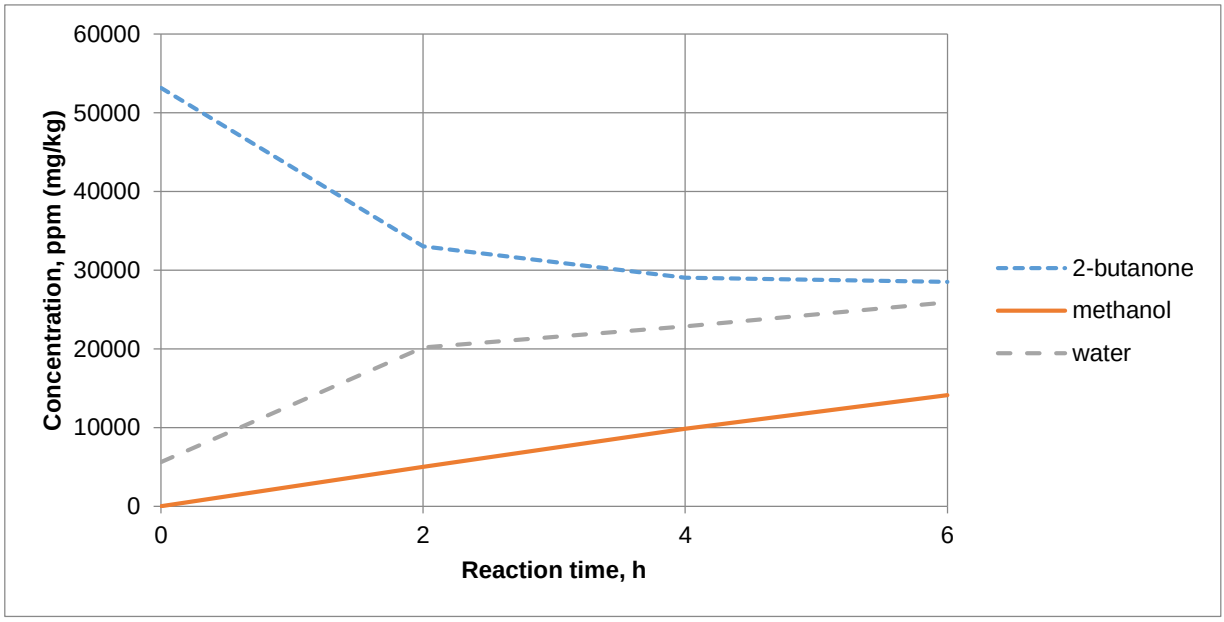

Figure A-70. 2-butanol, 10 g of catalyst, 200 °C, 40 bar partial pressure, 54.8 bar total pressure.

Table A-XL. 2-butanol, 5 g of catalyst, 180 °C, 40 bar partial pressure, 49.9 bar total pressure.

Reaction time, h	Concentration, ppm (mg/kg)		
	2-butanone	Methanol	Water
0	27182.0	0.0	1953.7
2	18160.3	2192.9	4196.6
4	14089.6	5197.6	4431.5
6	14199.6	7477.1	5840.7

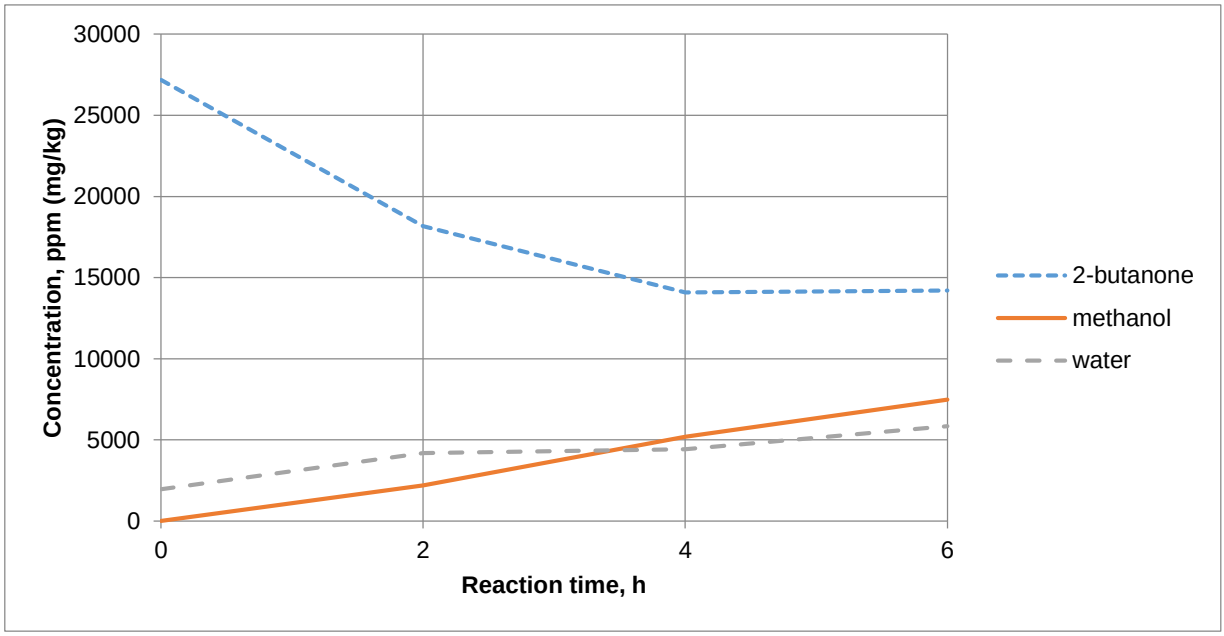

Figure A-71. 2-butanol, 5 g of catalyst, 180 °C, 40 bar partial pressure, 49.9 bar total pressure.

References in Appendices

[1] DDBST GmbH, "Saturated Vapor Pressure," [Online]. Available: http://ddbonline.ddbst.com/AntoineCalculation/AntoineCalculationCGI.exe. [Accessed 6 June 2016].

[2] NIST, "2-butanol," 2016. [Online]. Available: http://webbook.nist.gov/cgi/cbook.cgi?ID=C78922&Mask=4&Type=ANTOINE&Plot=on. [Accessed 6 June 2016].